

**Metabolic balance during protein production
with recombinant *Escherichia coli***

**Von der Naturwissenschaftlichen Fakultät
der Gottfried Wilhelm Leibniz Universität Hannover**

zur Erlangung des Grades

Doktor der Naturwissenschaften

Dr. rer. nat

genehmigte Dissertation

von

M. Eng. Zhaopeng Li

geboren am 02.09.1980, in Beijing, China

2013

Referent: Prof. Dr. Ursula Rinas

Korreferent: Prof. Dr. Thomas Scheper

Datum der Promotion: 23. November 2012

Erklärung

Ich versichere, dass ich diese Dissertation selbstständig und nur unter Verwendung der angegebenen Hilfsmittel und Quellen durchgeführt habe. Diese Arbeit wurde nicht als Diplomarbeit oder ähnliche Prüfungsarbeit verwendet.

Hannover, September 2012

Zhaopeng Li

Acknowledgments

It is a pleasure to thank the many people who made this thesis possible.

I would like to express my great gratitude Prof. Dr. Ursula Rinas for being an outstanding advisor and excellent supervisor. Her constant encouragement, support, and invaluable suggestions made this work successful.

I would also like to give my sincere appreciation to Prof. Dr. Thomas Scheper, who kindly provided me the opportunity to continue my research in the Institute for Technical Chemistry.

I am grateful to Prof. Dr. Bernd Hitzmann, whom I considered to be my co-advisor, for valuable suggestion and discussion during the completion of the project.

My sincere thanks go to Dr. Manfred Nimtz for the cherished teaching, instruction, discussion and help on protein identification and characterization by mass spectrometry.

Special thanks are also given to Dr. Konrad Büssow for valuable suggestions which greatly helped me to establish the protein labeling protocols.

I would like to acknowledge Dr. Christoph Kaleta for his valuable help and discussion on the proteome data processing and evaluation.

I am happy to acknowledge my debt to Dr. Joop van den Heuvel for his generous guidance and suggestion and support.

I would also like to thank many members from the two institutes, The Recombinant Protein Expression (RPEX) at Helmholtz Centre for Infection Research (HZI) and Institute for Technical Chemistry (TCI) at Leibniz University of Hanover (LUH), where I carried out my research work.

The support from FORSYS Partner Project “Dynamics and regulation of the metabolic balance in *Escherichia coli*” is greatly acknowledged.

Lastly, and most importantly, unspeakable gratitude and thank to my wife, Xiaoming Zhai, for the selfless support and encouragement. And also thank to the most precious gift of my life, my daughter, for all the laughing, smiling and even crying.

Abstract

In this thesis, a set of defined media was developed for a novel strategy to produce recombinant proteins using an autoinduction method and for an innovative protocol to generate recombinant proteins with specific labels.

A novel defined autoinduction medium was developed using a mixture of glucose, glycerol, and lactose as carbon substrates and ammonium as the sole nitrogen source. This medium was tested in 96-well microtiter plates, test tubes, shake flasks and 15 liter bioreactor for the production of different proteins achieving an average yield of 500 mg L⁻¹ product.

Based on the developed defined medium, a simple protocol for producing heavy isotope labeled proteins was developed. Label incorporation into the target protein reached 99%, 97% and about 75% for ¹⁵N, ¹³C, and ²H, respectively. This protocol is also applicable for selenomethionine (Se-Met) labeling, leading to Se-Met incorporation of 70% or 90% using prototrophic or methionine auxotrophic *E. coli* strains, respectively.

The cultivation performances, e.g. target protein solubility and productivity, in defined and complex media are different. Subsequently, proteomic analyses were performed to reveal the physiological differences between *E. coli* grown in defined and complex media to reveal the hidden bottleneck of recombinant protein production.

The regulation basis of acetate overflow metabolism under nutrient-rich conditions was first investigated: when precursors and reducing equivalents generated by the central metabolic pathways (CMPs) are sufficient for the cell growth, *E. coli* will simultaneously reduce the synthesis of proteins in the tricarboxylic acid cycle (TCA cycle) to decrease the generation of reducing equivalents and precursors. This leads to the increased formation of acetate.

Insufficient nutrient triggers a self-protection mechanism: the transport systems and by-products assimilation pathways are elevated for absorbing the limited nutrient in the environment. Many degradation processes are up-regulated to recycle the intracellular components that are no longer required. The proteins involved in eliminating the reactive oxygen species (ROS) and DNA protection are greatly increased. Conversely, proteins in transcription and translation processes are down-regulated, which can provide extra resources towards fine-tuning the whole proteome for long term starvation.

This self-protection mechanism breaks down completely when *E. coli* is forced to overproduce recombinant protein: chaperones are up-regulated simultaneously. The relative amounts of transcription and translation related proteins remain constant. The transport systems, CMPs, by-product metabolism, proteins for degradations, eliminating ROS and DNA protection, are down-regulated. This causes an overall breakdown in cellular regulation and physiology.

Keywords: *Escherichia coli*, Recombinant protein production, Proteomics

Zusammenfassung

In dieser Arbeit wurde eine neue Strategie entwickelt, um rekombinante Proteine in definierten Medien zu produzieren. Diese Methode basiert auf der Nutzung von autoinduzierenden Medien und einem neuen innovativen Protokoll, um spezifisch markierte rekombinante Proteine zu erzeugen.

Das neu entwickelte definierte Medium besteht aus Glukose, Glycerol und Laktose als Kohlenstoffquelle, sowie Ammonium als einziger Stickstoffquelle. Das Medium wurde in 96-well Mikrotiterplatten, Reagenzglasern, Schüttelkolben und in 15 Liter Bioreaktoren auf die effiziente Produktion unterschiedlicher Proteine getestet und es wurden durchschnittliche Produktkonzentrationen von 500 mg L^{-1} erzielt.

Basierend auf dem entwickelten Medium wurde des Weiteren ein einfaches Protokoll zur Produktion von mit schweren Isotopen markierten Proteinen erstellt. Dabei wurde eine Ausbeute an markiertem Zielprotein von 99 %, 97 % und um die 75 % bei ^{15}N , ^{13}C , und ^2H erreicht. Das Protokoll findet außerdem Anwendung bei der Produktion von mit Selenomethionin (Se-Met) markierten Proteinen mit Ausbeuten von 70 % oder 90 % in prototrophen oder Methionin-auxotrophen *E. coli* Stämmen.

Die Ergebnisse der Proteinproduktion, z.B. Löslichkeit des Zielproteins und Produktivität im definierten und komplexen Medium, sind unterschiedlich. Um die physiologischen Unterschiede vom Wachstum von *E. coli* im definierten und komplexen Medium aufzuklären und versteckte Engpässe der rekombinanten Proteinproduktion zu enthüllen, wurde eine Proteomanalyse durchgeführt.

Die Regulierung des Acetat-Überflussmetabolismus („Crabtree-Effekt“) unter nährstoffreichen Bedingungen wurde bei *E. coli* untersucht. Unter diesen Bedingungen können Vorläufermoleküle und reduzierende Äquivalente in den zentralen Stoffwechselwegen in ausreichender Menge generiert werden. Daraus folgend reduziert *E. coli* die Synthese von Proteinen aus dem Tricarbonsäurezyklus und reduziert somit auch die Generierung von Vorläufermolekülen und reduzierenden Äquivalenten.

Unzureichende Nährstoffversorgung führt zu einem Selbstschutzsystem; Proteine aus den Transportsystemen und zum Abbau von Nebenprodukten sind erhöht, um die limitierende Nährstoffversorgung aus der Umwelt zu kompensieren. Viele Abbauprozesse sind hochreguliert, um intrazelluläre Komponenten zu recyceln, welche nicht länger benötigt werden. Die Synthese der Proteine, die an der Eliminierung von reaktiven Sauerstoffspezies (z.B. Sauerstoffradikalen) und dem Schutz der DNA beteiligt sind, ist stark erhöht. Auf der anderen Seite sind Proteine, die in Transkriptions- und Translationsprozessen eine Rolle spielen, herunterreguliert, wodurch zusätzliche Ressourcen für das *fine tuning* des Proteoms in Hinsicht auf eine lange Hungerperiode zur Verfügung stehen.

Eine weitere Proteomanalyse zeigt, dass Selbstschutzmechanismen komplett ausgehebelt werden, wenn *E. coli* zur Überexpression von rekombinantem Protein gezwungen wird: Chaperone werden gleichzeitig hochreguliert. Die relative Menge der an der Transkription und Translation beteiligten Proteine bleibt dagegen konstant. Hingegen werden Proteine die für den Transport und die zentralen Stoffwechselwege, die Bildung und den Abbau von Nebenprodukten und andere Degradationsproteine, sowie Proteine für den Abbau reaktiver Sauerstoffspezies und den Schutz der DNA herunter reguliert. Diese Tatsache führt zu einem Zusammenbruch der Regulation des Stoffwechsels und der Physiologie.

Stichwörter: *Escherichia coli*, Rekombinante Proteinproduktion, Proteomik

Table of Contents

1	Introduction	1
1.1	Thesis objective.....	1
1.2	Thesis structure	2
1.3	Theoretical background.....	3
1.3.1	Recombinant protein production by autoinduction method	3
1.3.2	Specifically labelled recombinant proteins	4
1.3.3	Defined and complex medium	5
1.3.4	Acetate overflow metabolism.....	6
1.3.5	Self-protection response of <i>E. coli</i> against starvation	7
1.3.6	The metabolic burden during recombinant protein production	8
1.3.7	<i>E. coli</i> proteome analysis	8
2	Novel defined modular media to produce recombinant proteins	10
2.1	Introduction	10
2.2	Simple defined autoinduction medium for high-level recombinant protein production using T7-based <i>Escherichia coli</i> expression systems	11
2.2.1	Abstract	11
2.2.2	Introduction	12
2.2.3	Materials and methods	13
2.2.3.1	Strains and plasmids.....	13
2.2.3.2	Medium preparation	14
2.2.3.3	Analysis of cell growth	15
2.2.3.4	Analysis of protein concentration.....	16
2.2.3.5	Cultivation conditions	16
2.2.4	Results	17
2.2.4.1	Choice of reporter proteins.....	17
2.2.4.2	The influence of temperature and carbon substrate composition on protein production using autoinduction.....	18
2.2.4.3	The influence of nitrogen content on protein production using autoinduction.....	21
2.2.4.4	The influence of oxygen supply on protein production using autoinduction.....	22
2.2.4.5	Test of general applicability of S-DAB (HNC) for T7-based production systems	23
2.2.4.6	Test of applicability of S-DAB (HNC) for screening studies in 96-well microtiter plates.....	23
2.2.4.7	Test of applicability of S-DAB (HNC) for large-scale cultivation.....	26

2.2.5	Discussion	26
2.2.6	Acknowledgements.....	26
2.3	Optimized procedure to generate heavy isotope and selenomethionine-labeled proteins for structure determination using <i>Escherichia coli</i> -based expression systems .	27
2.3.1	Abstract.....	27
2.3.2	Introduction.....	28
2.3.3	Materials and methods	29
2.3.3.1	Strains and plasmids.....	29
2.3.3.2	Medium composition and preparation	29
2.3.3.3	Cultivation conditions.....	29
2.3.3.4	Analysis of cell growth and protein production.....	29
2.3.3.5	Heavy isotope and selenomethionine labeling efficiency determination	30
2.3.4	Results.....	32
2.3.4.1	General considerations for developing media for heavy isotope and selenomethionine labeling.....	32
2.3.4.2	Heavy isotope labeling.....	33
2.3.4.3	Selenomethionine labeling.....	37
2.3.5	Discussion	41
2.3.6	Acknowledgements.....	41
2.4	Summary and conclusion	42
2.5	Outlook	42
3	A comprehensive proteomic study of <i>Escherichia coli</i>	43
3.1	Introduction.....	43
3.2	A comprehensive proteomic study I. Regulation of acetate overflow metabolism in <i>Escherichia coli</i> under nutrient-rich condition	43
3.2.1	Abstract.....	43
3.2.2	Introduction.....	44
3.2.3	Materials and methods	45
3.2.3.1	Strain, media and cultivation conditions.....	45
3.2.3.2	Two-dimensional gel electrophoresis.....	45
3.2.3.3	Protein identification and classification	46
3.2.4	Results.....	46
3.2.4.1	Growth kinetics in defined and complex media.....	46
3.2.4.2	Systematic and comparative proteome analysis.....	48
3.2.4.3	Central carbon metabolism	50
3.2.4.4	By-product metabolism.....	52

3.2.4.5	TCA cycle.....	52
3.2.4.6	Connection between glycolysis and TCA cycle	53
3.2.4.7	Oxidative phosphorylation	55
3.2.4.8	Amino acid and nucleotide metabolism	55
3.2.4.9	Lipid, lipopolysaccharide and other cellular component biosynthesis....	56
3.2.5	Discussion	57
3.2.6	Acknowledgements	58
3.3	A comprehensive proteomic study II. Global response of <i>Escherichia coli</i> to nutrient deficiency and depletion	59
3.3.1	Abstract	59
3.3.2	Introduction	59
3.3.3	Materials and methods	60
3.3.3.1	Strain, media and cultivation conditions	60
3.3.3.2	Two-dimensional gel electrophoresis and protein spot identification	60
3.3.4	Results	61
3.3.4.1	Growth kinetics in defined and complex media.....	61
3.3.4.2	Systematic and comparative proteome analysis.....	61
3.3.4.3	(Metabolite) degradation	63
3.3.4.4	Sugar transport	63
3.3.4.5	Amino acid and peptide transport	64
3.3.4.6	Other transport proteins.....	64
3.3.4.7	RNA polymerases and binding proteins.....	65
3.3.4.8	Ribosomal proteins and associated proteins.....	65
3.3.4.9	Aminoacyl-tRNA synthetases	67
3.3.4.10	Elongation factors	67
3.3.4.11	RNA degradation.....	67
3.3.4.12	Isomerases	68
3.3.4.13	Chaperones	68
3.3.4.14	Proteases.....	68
3.3.4.15	Cell redox balance.....	69
3.3.4.16	DNA protection and repair	70
3.3.4.17	Transcription factors, unclassified and uncharacterized proteins.....	71
3.3.5	Discussion	73
3.3.6	Acknowledgements	74

3.4	A comprehensive proteome study III. Global metabolic response in <i>Escherichia coli</i> during recombinant protein overproduction.....	75
3.4.1	Abstract.....	75
3.4.2	Introduction.....	75
3.4.3	Materials and methods.....	76
3.4.3.1	Strain, media and cultivation conditions.....	76
3.4.3.2	Analysis of cell growth, acetate and glucose concentration, and protein production.....	77
3.4.3.3	Two-dimensional gel electrophoresis.....	77
3.4.3.4	Protein identification and classification.....	78
3.4.4	Results.....	78
3.4.4.1	hFGF-2 overexpression in <i>E. coli</i> using defined and complex media.....	78
3.4.4.2	Proteome analysis during recombinant protein production.....	80
3.4.4.3	Transportation system.....	82
3.4.4.4	Central carbon metabolism.....	82
3.4.4.5	By-product metabolism.....	86
3.4.4.6	TCA cycle and oxidative phosphorylation.....	87
3.4.4.7	Biomass block biosynthesis.....	87
3.4.4.8	Intracellular degradation processes.....	88
3.4.4.9	Cell redox balance and DNA protection.....	89
3.4.4.10	Transcription and translation.....	89
3.4.4.11	Protein folding and degradation.....	90
3.4.5	Discussion.....	91
3.4.6	Acknowledgements.....	93
3.5	Summary and conclusion.....	94
3.6	Outlook.....	94
4	References.....	95
5	Appendix.....	A-1
5.1	Detailed experimental procedures of <i>E. coli</i> proteome analysis.....	A-1
5.1.1	Protocol of 2D gel electrophoresis.....	A-1
5.1.1.1	Harvest <i>E. coli</i> culture.....	A-1
5.1.1.2	Cell pellet washing.....	A-1
5.1.1.3	BugBuster treatment.....	A-1
5.1.1.4	Chloroform/Methanol precipitation.....	A-2
5.1.1.5	Resolubilization of protein pellet.....	A-2
5.1.1.6	Beginning of isoelectric focusing (IEF).....	A-2

5.1.1.7	Preparation of SDS equilibration buffer.....	A-3
5.1.1.8	IPG strip equilibration.....	A-3
5.1.1.9	Transfer the IPG strips to the SDS-PAGE electrophoresis.....	A-4
5.1.1.10	Placement of cassettes into the DALT tank.....	A-4
5.1.1.11	Ending second-dimension SDS-PAGE electrophoresis	A-4
5.1.2	Protocol of MALDI identification.....	A-5
5.1.2.1	Trypsin digestion protocol for MALDI.....	A-5
5.1.2.2	Sample preparation for MALDI using Prespotted AnchorChip target ..	A-6
5.1.2.3	Sample preparation for MALDI using ZipTips (C18).....	A-7
5.1.3	Buffers and solutions for 2D gel electrophoresis and MALDI MS identification	A-8
5.2	Supplementary material for Chapter 2 - Novel defined modular media to produce recombinant proteins.....	A-13
5.2.1	Supplementary figures.....	A-13
5.2.2	Supplementary tables	A-16
5.3	Supplementary material for Chapter 3 - A comprehensive proteomic study of <i>Escherichia coli</i>	A-21
5.3.1	Supplementary figures.....	A-21
5.3.2	Supplementary tables	A-46
	Suppl. Table 5.3.1 Proteome data of <i>E. coli</i> BL21 (DE3) growing in different media	A-47
	Suppl. Table 5.3.2 Summary of proteome data of <i>E. coli</i> BL21 (DE3) growing in different media	A-72
	Suppl. Table 5.3.3 Sigma and transcription factors of the glycolysis and TCA cycle proteins	A-74
	Suppl. Table 5.3.4 Amino acids feedback inhibition.....	A-79
	Suppl. Table 5.3.5 Proteome data of hFGF-2 production in <i>E. coli</i> BL21 (DE3) using defined and complex media	A-81
	Suppl. Table 5.3.6 Summary of proteome data of hFGF-2 production in <i>E. coli</i> BL21 (DE3) using defined and complex media.....	A-107
5.3.3	Suppl. Methods - Determination of NADPH turn-over involved in amino acid biosynthesis	A-110
5.4	Chemicals.....	A-111
5.5	List of Abbreviations.....	A-113
	Curriculum Vitae	A-115
	Publications.....	A-116

1 Introduction

1.1 Thesis objective

Recombinant DNA techniques combined with bioprocess engineering allows many therapeutic and diagnostic proteins to be produced in large quantities in genetically modified microorganisms. The gram-negative bacterium *Escherichia coli* is the most popular choice and is widely used in pharmaceutical industries and academic institutions.

This thesis deals with the following objectives: first a set of novel easy-to-use defined media was developed to produce recombinant protein by an autoinduction method and to generate recombinant proteins with specific labels; secondly two proteomic analyses were performed to reveal the molecular differences of *E. coli* grown in defined and complex media under protein production and non-production conditions. Based on the proteomic comparisons, three fundamental cellular reactions were investigated: the regulation of acetate overflow metabolism in *E. coli* under nutrient-rich conditions; the global response of *E. coli* to nutrient deficiency and depletion; and the global metabolic response in *E. coli* during recombinant protein overproduction.

Inducible *E. coli* expression systems, e.g. isopropyl β -D-1-thiogalactopyranoside (IPTG) [1]-, arabinose [2]-, temperature [3]- inducible systems, are commonly used to produce recombinant proteins. Operational procedures of the conventional inducible protein expression systems are often complicated and tedious: cultivation is always performed in two phases (the growth phase and production phase); and the induction must be employed at an appropriate growth stage. Development of a single batch cultivation by autoinduction without monitoring the cell growth and starting induction will significantly reduce the manual handling during recombinant protein production.

E. coli expression systems provide a platform for the production of specifically labeled proteins for structure determination [4, 5]. An efficient and simple protocol for generating labeled proteins is very important for structural biologists. So there is great demand for protein labeling protocols which are easy to implement and lead to sufficient amount of protein with high-label incorporation at an acceptable cost.

Recombinant protein production is mainly performed in complex medium [6-11] and defined (minimal) medium [12, 13]. Both media have their unique qualities which are suitable for different applications. Clearing the physiological differences of *E. coli* grown in complex and defined media will greatly help researchers to choose the appropriate medium for their specific tasks and may reveal the hidden bottleneck of recombinant protein production.

When *E. coli* grows at a high rate, acetate is the major by-product [14-16]. Since it has a negative impact on cell growth and protein production [17-21], clarification of the

molecular mechanism of acetate overflow metabolism is of great importance.

The investigation of the metabolic burden observed during overexpression of heterologous genes has been extensively studied from the macroscopic view [22-24], but from the microscopic view (particularly at the proteome level) it is still ambiguous. A comprehensive proteomic analysis would significantly help to understand the global metabolic response during recombinant protein overproduction.

1.2 Thesis structure

The experimental work of this thesis is divided into two chapters (Chapter 2 and 3) as shown in Fig. 1.1

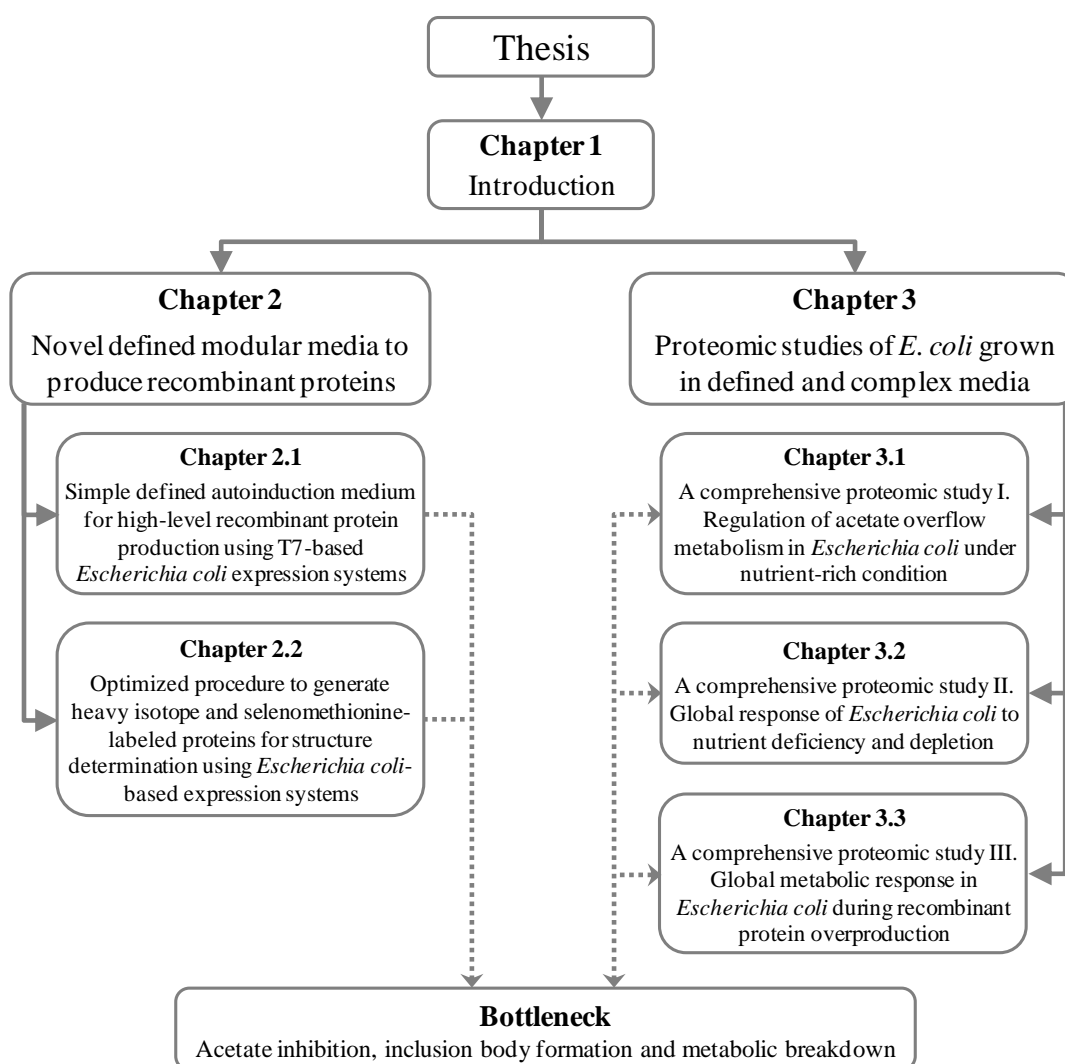


Fig. 1.1 Thesis structure

Chapter 2 consists of two sections: in the first section, a simple defined autoinduction medium for high-level recombinant protein production using T7-based *E. coli* expression systems is developed. In the second section, based on the defined medium, an optimized procedure to generate heavy isotope and selenomethionine-labeled proteins for structure determination is established using *E. coli*-based expression systems.

Chapter 2 observes that the use of defined medium elicits several advantages, e.g. higher biomass and better reproducibility. However there is a small increase in inclusion body formation and a prolonged production time compared with the cultivation in complex medium. Subsequently, chapter 3 shows two proteomic analyses, using two-dimensional gel electrophoresis and mass spectrometry. These were performed to reveal the physiological differences of *E. coli* grown in defined and complex media under recombinant protein production and non-production conditions.

In chapter 3, three fundamental biological mechanisms in *E. coli* were investigated. In the first section, the molecular mechanism of acetate overflow metabolism under nutrient-rich condition is clarified. In the second section, the global self-protection machinery in response to nutrient deficiency and depletion conditions is disclosed. In the third section the global metabolic response during recombinant protein overproduction is elaborated upon.

1.3 Theoretical background

1.3.1 Recombinant protein production by autoinduction method

The idea of autoinduction in the *lac* operon based *E. coli* expression system was introduced by Studier [25]. It presents an easy and convenient way to perform recombinant protein production. Cultivation using the autoinduction method contains only two steps, inoculation and harvest, which makes the whole procedure easy, economical and reproducible. Autoinduction omits the procedure of adding inducer to start production at a particular growth stage. This places the switch from cell growth to recombinant protein production under metabolic control of the host cell [26] (as indicated in Fig. 1.2).

Nowadays, there are several complex autoinduction media available: such as the medium described by Studier [25] or even commercial media, e.g. Overnight Express™ Autoinduction System from Novagen and MagicMedia™ from Invitrogen. All these media contain complex nutrients such as tryptone and yeast extract, which make the media expensive, and not compatible for protein labeling with heavy isotopes or selenomethionine, or similar labling methods.

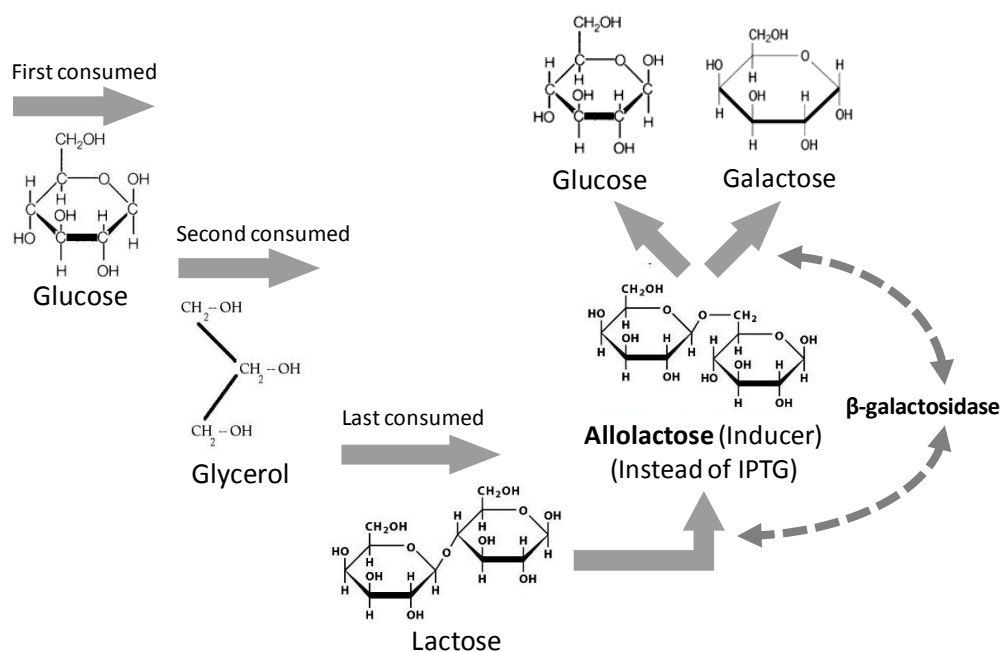


Fig. 1.2 Control of carbon source consumption in autoinduction cultivation

Based on Studier's protocol [25], several chemically defined autoinduction media were developed [26-30]. However, the composition of these media are complex; they contain several different amino acids, vitamins and trace elements, and so far only a limited number of reports are available on the universal applicability of these media [31-33]. Development of a defined autoinduction medium using a mixture of glucose, glycerol, and lactose as carbon substrates and NH_4^+ as the sole nitrogen source will significantly reduce the manual handling during recombinant protein production and will improve the heavy isotope labeling process.

1.3.2 Specifically labelled recombinant proteins

For heavy isotope labeling in *E. coli*, a chemically defined medium is the most important requirement; the recombinant protein production is performed in a defined medium supplied with stable heavy isotope labeled substrates. That is, ^{13}C -carbon, ^{15}N -nitrogen or deuterium oxide (D_2O). For Se-Met labeling, when the protein synthesis is carried out in a defined medium supplied with Se-Met instead of methionine (Met), the Met in the target protein will be replaced or partially replaced by Se-Met.

Stable heavy isotopes (^{15}N , ^{13}C and ^2H) and selenomethionine (Se-Met) labeled proteins are commonly used for protein structure determination through NMR spectroscopy [4] and X-ray crystallography [5], respectively. The generation of isotope-enriched protein samples is a prerequisite for carrying out structural studies using NMR spectroscopy [34-36]; and incorporation of Se-Met into proteins considerably helps protein structure determination by X-ray crystallography [37, 38].

An efficient and simple procedure for the generation of labeled material is very important for protein structure determination. Protocols described in literature are mainly based on M9 minimal medium [5, 39-43] leading to very poor final biomass concentrations (OD₆₀₀ of 1~2), and consequently, low yields of labeled proteins. Some improvements have been obtained by establishing carbon limited fed-batch processes [44, 45], or by optimizing the minimal medium [25, 27, 28, 46].

Despite the improvements, some of cultivation performances when using defined medium, e.g. final biomass, yield and productivity of proteins of interest, are still worse than the cultivation using traditional Luria-Bertani and Terrific Broth media. Clarification of the physiological and molecular differences between the recombinant protein production in defined and complex media may offer helpful advice and suggestions to improve the cultivation performance in defined media specifically for the labeling application.

1.3.3 Defined and complex medium

Two groups of media are mainly used in laboratory study and industrial production: the complex medium with unknown composition (e.g. Luria-Bertani broth or Terrific Broth which contains tryptone, a pancreatic digest of casein, and yeast extract, the water soluble portion of autolyzed yeast), or defined medium with chemically defined ingredients, e.g. M9 medium or Defined Non-inducing Broth (DNB) [13], in which glucose, NH₄⁺, PO₄³⁻ and SO₄²⁻ are the sole carbon, nitrogen, phosphorus and sulfur sources, respectively.

The use of chemically defined media is gaining more and more popularity [12], because the lot-to-lot variation of raw materials (e.g. yeast extract, peptone or tryptone) used in complex medium results in very poor reproducibility [25, 47]. When compared with cultivation in defined medium, it was found that when growing at maximum growth rate in complex medium *E. coli* produces more acetate [7, 16, 21], which inhibits cell growth and also protein production [17-20].

Despite many advantages, the culture performance in defined medium is normally “poorer” (e.g. more inclusion body formation, lower productivity and reduced product titer) than when using complex medium. When *E. coli* grows in defined or complex medium, the cell physiology shows big differences in growth kinetics [6-8] and the transcriptome [9-11]. So far there are only a few reports on the proteome differences. Clearing the physiological differences at the proteome level will help a lot towards choosing the appropriate conditions for the specific applications, and for improving recombinant protein production.

1.3.4 Acetate overflow metabolism

Acetate is the major by-product when *E. coli* metabolizes substrates at high rates even under well-aerated conditions [14-16]. The acetate has resulted in many negative effects on recombinant protein production [17-21]. It is found that when the loads and fluxes surpass the level of NADH turnover rate or the capacity of the TCA cycle, switching to acetate overflow can be predicted [48].

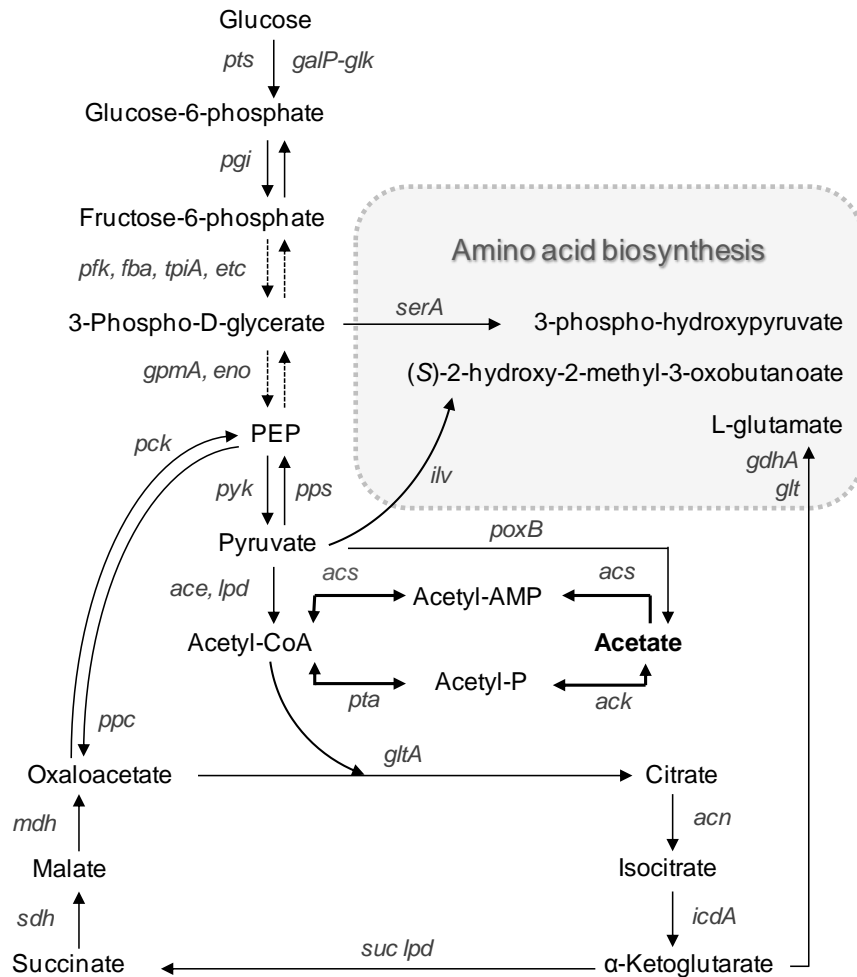


Fig. 1.3 Central metabolic pathways of *E. coli*

Acetate is located at the centre of the central metabolic pathways (CMPs) as shown in Fig. 1.3. The monomers (e.g. amino acids) for the cellular macromolecules (e.g. proteins) are made from a relatively small group of precursors that are the products of the CMPs, indicating a direct relation between acetate overflow metabolism and biomass building block biosynthesis [49]. Another important factor is that reducing equivalents [NAD(P)H], generated by CMPs are also required for monomer synthesis, especially for the amino acid biosynthesis [50], which implies a direct association between biomass building block biosynthesis and the NADH turnover rate. Since NADH and NADPH can be converted into each other through reversible transfer of reducing equivalents between NAD and

NADP by the two native *E. coli* transhydrogenases (PntAB and UdhA) [51-53], they are regarded as equal in this thesis.

The Arc two component system [Aerobic respiration control protein (ArcA) and its sensor protein (ArcB)] has been proved to be the mediator between the NADH turnover rate and the TCA cycle activity [54-58], which will in turn influence the acetate overflow metabolism. It was observed that the *arcA* deletion mutant showed a higher TCA cycle activity and a lower acetate formation rate [59, 60]. Due to the complexity of the intracellular metabolic network and also the extracellular environment, the understanding of the synergetic regulation of CMPs, oxidative phosphorylation, biomass building block biosynthesis and acetate overflow metabolism is still ambiguous.

The experimental observation of acetate formation and re-assimilation [61] suggests that acetate is probably one of the last utilized carbon substrates; and that after the re-assimilation of acetate, *E. coli* may face nutrient starvation and enter the stationary phase.

1.3.5 Self-protection response of *E. coli* against starvation

When essential nutrients are exhausted, the bacteria enter the stationary phase [62]. The organisms adapt to the starvation condition and survive in the absence of nutrients [63]. The cell's metabolism must be redirected to maintenance; endogenous energy reserves must be mobilized; and the cell must survive in the absence of reproduction. These changes require noticeable physiological and structural changes in the cells [64].

Proteins produced early during starvation play very important roles in the cell's survival [64-66]. For example, the synthesis of many proteins with specific roles in protecting the cell against external stresses is highly up-regulated during stasis survival [67-69]. It was found that many functions induced during stationary phase are also induced when the cells were grown at a low growth rate [63], so the inducible property of the stationary phase may also be important for growth under poor nutrient supply conditions.

When the concentration of nutrients decreases, cell growth and metabolic processes gradually slow down. Analysis at the proteome level would be an appropriate procedure for the investigation of the molecular response to nutrient starvation. It is clear that *E. coli* can establish a self-protection mechanism in response to nutrient starvation. Among the proteomic reports [65, 68, 70-73] the number of identified proteins is limited, which does not give a comprehensive overview of the stationary phase physiology.

So far, there is no report showing the relation between the self-protection response to nutrient deficiency and depletion, and the metabolic response during recombinant protein production in *E. coli*. In this thesis, it is found that clarification of the self-protection mechanism helps a lot in understanding the global metabolic response during recombinant protein overproduction.

1.3.6 The metabolic burden during recombinant protein production

Under the control of strong promoters (e.g. T7 promoter), heterologous proteins are typically produced at high levels in *E. coli*, which causes a physiological stress known as metabolic burden. The investigation of the metabolic burden caused by the overproduction of recombinant protein has been extensively studied at the macroscopic view [22-24]. This is shown to lead to a decrease of specific growth rate [74-78] and biomass yield [76-78]; and results in an increase of maintenance energy coefficient [74], respiratory activity [77, 79, 80], overflow metabolism of by-products [76] and inclusion bodies formation [81-86]. Apart from the production of the target protein, the simultaneously enhanced chaperones [77, 87, 88] and proteases [89, 90] also contribute to the metabolic burden.

Owing to the complexity of metabolic networks and production conditions, the molecular mechanism of the metabolic burden is still ambiguous. Proteomic analyses could significantly help in the understanding of the underlying mechanism in *E. coli*, however, among the published proteomic reports [76-79, 88, 91-96], the identified proteins are often limited, which may increase the probability of misinterpretation. Therefore, there is still a huge demand for comprehensive proteomic analysis to understand the metabolic burden during recombinant protein overproduction.

Ostensibly, there is no direct link between the cellular self-protection response to nutrient deficiency and depletion, and the metabolic burden during recombinant protein production in *E. coli*. In this thesis, the systemic proteomic analysis clearly revealed that the self-protection mechanism is significantly disturbed when cells are forced to overproduce recombinant protein.

1.3.7 *E. coli* proteome analysis

E. coli is probably the best understood of all the simple model organisms, with a fully sequenced genome which makes it accessible for proteomic analysis using mass spectrometry [97]. For comprehensive proteomic studies, both the more recent liquid chromatography based- [98, 99] and the traditional two-dimensional gel electrophoresis based- [97, 100] approaches have their strengths and limitations; and the choice of one or the other approach depends on the questions to be answered. Liquid chromatography-mass spectrometry (LC-MS) combines physical separation using liquid chromatography with mass spectrometry. Proteolytic peptides are separated by chromatography. When eluted from the column, they enter the mass spectrometer where the final analysis is performed.

In this thesis, the two-dimensional gel electrophoresis (2-DE) based proteomic platform was chosen to provide the relative abundance of each protein in the whole cell for the cross comparison between different growth conditions. 2-DE is a form of gel electrophoresis commonly used to analyze proteins [101]. It separates proteins in two steps, according to

two independent properties: the first dimension is isoelectric focusing (IEF), which separates proteins according to their isoelectric point (pI); the second dimension is sodium dodecyl sulfate polyacrylamide gel electrophoresis (SDS-PAGE), which separates proteins according to their molecular mass. With this method, complex mixtures consisting of thousands of different proteins can be resolved and the relative amount of each protein can be determined.

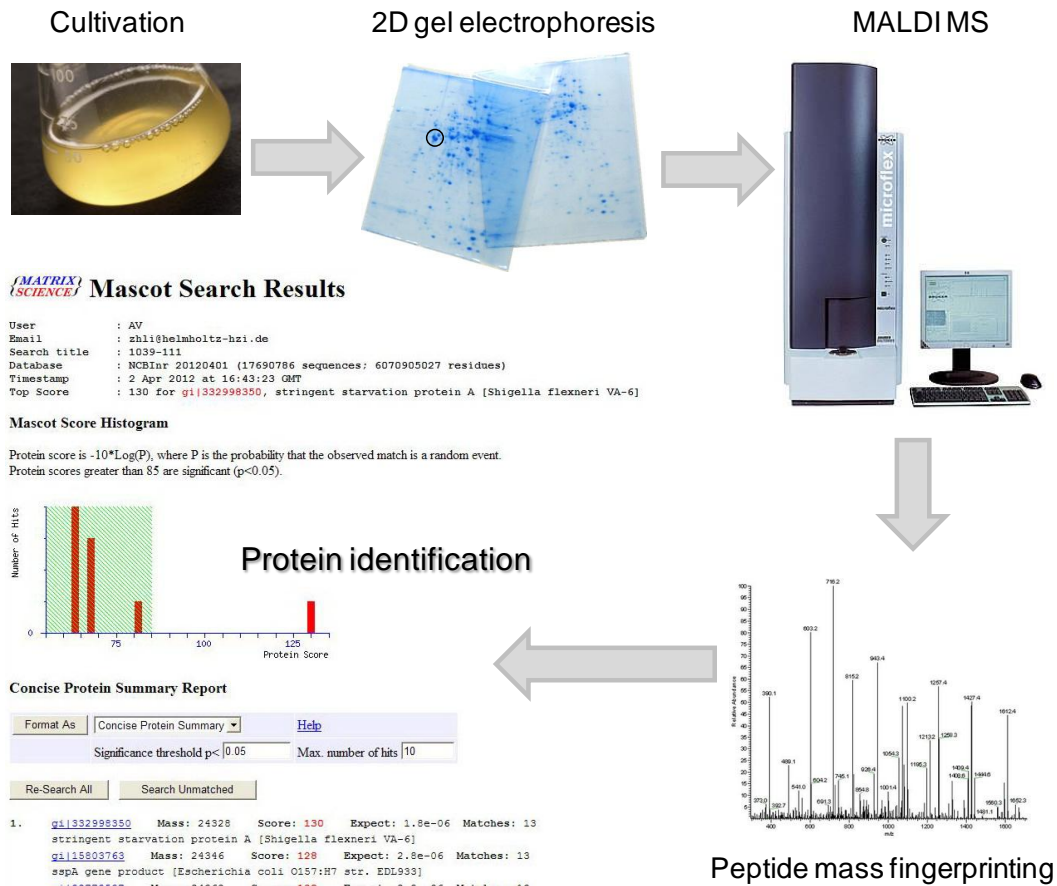


Fig. 1.4 Flowchart of *E. coli* proteome analysis

Matrix-assisted laser desorption/ionization-time of flight mass spectrometry (MALDI-TOF MS) [102] is a relatively novel technique in which a co-precipitate of an UV-light absorbing matrix and a biomolecule is irradiated by a nanosecond laser pulse. The ionized biomolecules are accelerated in an electric field and enter the flight tube. During the flight in this tube, different molecules are separated according to their mass to charge ratio. In this way each molecule yields a distinct signal. This method is used for detection and characterization of biomolecules, such as peptides, oligosaccharides and oligonucleotides.

2-DE and MALDI-TOF-MS are the workhorses for proteomics as shown in Fig. 1.4. For organisms whose genome sequence is known, the identification of “interesting” protein spots from a 2-D gel is routine. Protein spots are excised and digested with a specific protease, e.g. trypsin, and the fragments measured by MALDI-TOF-MS. This peptide mass fingerprint then can be used to search databases to identify the protein [103].

2 Novel defined modular media to produce recombinant proteins

2.1 Introduction

In this chapter, a simple defined autoinduction medium for recombinant protein production using T7-based *E. coli* expression systems with high product yields and good universal applicability is described. Based on the developed simple defined autoinduction medium, a protocol to generate heavy isotope and selenomethionine labeled proteins with high label incorporation and easy handling has been set up.

The present chapter is based on two articles:

Zhaopeng Li, Wolfgang Kessler, Joop van den Heuvel, Ursula Rinas. Simple defined autoinduction medium for high-level recombinant protein production for T7-based *Escherichia coli* expression systems, *Appl Microbiol Biotechnol*, 2011, 91(4), 1203-1213

Zhaopeng Li, Manfred Nimtz, Ursula Rinas. Optimized procedure to generate heavy isotope and selenomethionine-labeled proteins for structure determination using *Escherichia coli*-based expression systems, *Appl Microbiol Biotechnol*, 2011, 92(4), 823-833

2.2 Simple defined autoinduction medium for high-level recombinant protein production using T7-based *Escherichia coli* expression systems

Chapter 2.2 is an entire paper reprinted with the permission from Springer that was published in Applied Microbiology and Biotechnology in August 2011, Volume 91, Number 4, Page: 1203–1213

License Number: 2951820701925

License date: Jul 18, 2012

Licensed content publisher: Springer

Licensed content publication: Applied Microbiology and Biotechnology

Licensed content title: Simple defined autoinduction medium for high-level recombinant protein production using T7-based *Escherichia coli* expression systems

Licensed content author: Zhaopeng Li

Licensed content date: Jan 1, 2011

Volume number: 91

Issue number: 4

Type of Use: Thesis/Dissertation

2.2.1 Abstract

Protein production under the control of lac operon regulatory elements using autoinduction is based on diauxic growth of *Escherichia coli* on lactose after consumption of more preferred carbon substrates. A novel simple and cost-effective defined autoinduction medium using a mixture of glucose, glycerol, and lactose as carbon substrate and NH_4^+ as sole nitrogen source without any supplementation of amino acids and vitamins was developed for T7-based *E. coli* expression systems. This medium was successfully employed in 96-well microtiter plates, test tubes, shake flasks, and 15-L bioreactor cultivations for production of different types of proteins achieving an average yield of 500 mg L⁻¹ product. Cell-specific protein concentrations and solubility were similar as during conventional isopropyl β -D-1-thiogalactopyranoside induction using Luria-Bertani broth. However, the final yield of target proteins was about four times higher, as a higher final biomass was achieved using this novel defined autoinduction broth.

Keywords *Escherichia coli* · Recombinant protein production · Autoinduction · Defined medium

2.2.2 Introduction

The Gram-negative bacterium *Escherichia coli* is the most popular organism for recombinant protein production because of its well-characterized genetic background, its ability to grow to high cell densities, and the large number of available cloning vectors and optimized host strains. Among numerous *E. coli*-based expression systems, the bacteriophage T7 RNA polymerase-controlled system is currently the most popular protein production system [1]. The T7 RNA polymerase is usually under control of the lac operon, thus protein production initiated by the addition of isopropyl β -D-1-thiogalactopyranoside (IPTG).

The idea of autoinduction was introduced as a convenient way to perform recombinant protein production without inducer addition in small laboratory scale for lac operon-controlled expression systems [25]. Carbon substrate mixtures of glucose, glycerol, and lactose are used, where glucose as the preferred carbon substrate is utilized first, followed by glycerol and lactose which also acts as the inducer of lac operon-controlled protein production [26]. Autoinduction omits biomass monitoring for the correct timing of inducer addition and places the shift from growth to recombinant protein production under metabolic control of the expression host [26].

There are several complex autoinduction media currently available: the original medium described by Studier [25] and others from commercial sources (Overnight Express™ Autoinduction System from Novagen and MagicMedia™ from Invitrogen with unknown ingredients). The presence of complex medium compounds such as tryptone, yeast extract, and others renders these media expensive and also not compatible with protein labeling (selenomethionine or heavy isotope labeling). Thus, several defined autoinduction media have been described later, but all contain various amino acid and vitamin supplements [26-30]. For example, a defined autoinduction medium using an enhanced green fluorescent protein (GFP) as a reporter protein was announced which contains 18 different amino acids, 8 different vitamins, and 10 different trace elements, altogether 46 different compounds [26, 30]. This medium was successfully employed for screening studies in 96-well microtiter plates [104], but lower yields were achieved in larger-scale culture vessels [26]. Also, this medium has only been tested for a few proteins [31-33, 105] and, thus, has not been proven for universal applicability.

Here, we present a novel, simple-to-prepare defined autoinduction medium consisting of glucose, glycerol, and lactose as carbon substrate and NH_4^+ as sole nitrogen source. Supplementation of this medium with amino acids and vitamins is not required. This medium was developed using three target proteins with different properties (GFP, glutathione-S-transferase-tagged GFP, and human basic fibroblast growth factor) and optimized in test tube and shake flask cultures. Finally, it was successfully tested for production of various proteins in the molecular mass range of 18 to 90 kDa. Moreover, the

optimized autoinduction medium revealed the same efficacy for protein production in 96-well microtiter plates as well as in 15-L bioreactor cultivations leading to high final biomass concentrations ($OD_{600} > 20$) and average yields of 500 mg L^{-1} target protein.

2.2.3 Materials and methods

2.2.3.1 Strains and plasmids

Table 2.2.1 Strains, plasmids, and target proteins

Host strain	Plasmid	Target protein (MW)	Reference
<i>E. coli</i> BL21 (DE3)	pET-29c-hFGF-2	hFGF-2 (18 kDa)	[82]
<i>E. coli</i> BL21 (DE3)	pET-28c-His6-GFP	GFP (27 kDa)	This work
<i>E. coli</i> BL21 (DE3)	pET-15b-hPrP	hPrP (29 kDa)	[106]
<i>E. coli</i> BL21 (DE3)	pET-28a-PPAR γ	PPAR γ (33 kDa)	[107]
<i>E. coli</i> Rosetta 2 (DE3)	PGEX-6P-1-Rab1A and pETM30-SidM	Rab1A (50 kDa) and SidM (53 kDa)	[108]
<i>E. coli</i> BL21 CodonPlus (DE3) RIL	pETM30- Auto27-243-GST	Auto27-243-GST (52 kDa)	[109]
<i>E. coli</i> BL21 (DE3)	pETM30-His6-GST-GFP	GST-GFP (54 kDa)	[110]
<i>E. coli</i> BL21 (DE3)	PGEX-6P-1-YopO-GST	YopO-GST (90 kDa)	[111]

Strains and plasmids are described in Table 2.2.1. The construction of the plasmids pET-28c-His6-GFP and pETM30-His6-GST-GFP for production of different GFPs, His6-GFP (abbreviation: GFP), and His6-GST-GFP (abbreviation: GSTGFP) under the control of the T7 promoter was as follows. The plasmid pBAD-GFPuv (Clontech, Heidelberg, Germany) was used to generate pET-28c and pETM30 vector combinations for the C-terminal fusion of GFP to proteins of interest. Site-directed mutagenesis was used to remove the internal *Nco*I, *Nde*I, and *Bam*H1 sites from the coding sequence of GFPuv. The reaction was done using the Quickchange Kit of Stratagene as recommended by the supplier. In subsequent rounds of mutagenesis using the primer pairs GFPmut1 and mut2 (GFPmut1: 5'-GAAACTACCTGTTCCCTGGCCAACACTTGTC - 3', GFPmut2: 5' - TGA CAAGTGTGGCCAGGGAACAGGTAGTTTTTC-3'), GFPmut3 and mut4 (GFPmut3: 5'-CCGTTATCCGGATCACATGAAACGGCATGAC -3', GFPmut4: 5' -GTCATGCCGTTT CATGTGATCCGGATAACGG-3'), and GFPmut5 and mut6 (GFPmut5: 5'-CACAACTT GAAGATGGAAGCGTTCAACTAGCAGA-3', GFPmut6: 5'- TCTGCTAGTTGAACGCT TCCATCTTCAATGTTGTG-3'), respectively, the restriction sites were removed. An N-terminal adapter sequence was introduced to be able to generate in-frame fusions to genes of interest. The primer pair GFPfus1 and GFPfus2 (GFPfus1: 5'-CATGTGCCATGGGTCATATGTGTAACTGAGTAGGATCCGC TAGCGCT GGCTCCGCTGCTGGTTCTGGTA-3', GFPfus2: 5'-CTAGTACCAGAACCAGCAGCG GAGCCAGCGCTAGCGGATCCTACTCAGTTAACACATATGACCCATGGCA-3') was

annealed and ligated in pBADGFPmut digested with *NheI*. Correct linker integration concomitant to removal of the downstream *NheI* site was verified by sequencing. After selection of the correct clone, the vector was named pBADGFPFUS. The GFPFUS sequence was then cloned into pETM30 vector (EMBL, Heidelberg, Germany) using the *NcoI* site from the new linker and the downstream *EcoRI* site. The GFPFUS fragment was cloned into linearized pETM30 digested with *NcoI* and *EcoRI*. The positive clone was named pETM30GFPFUS. A similar clone pET-28c was generated by using the *NdeI*-*EcoRI* fragment of pBADGFPFUS cloned into the *NdeI* and *EcoRI* sites of pET-28c. This vector was named pET-28cGFPFUS. To create an in-frame fusion of GFP to His6- GST, the vector pETM30GFPFUS was digested with *NdeI* and *BamHI*. The ends were filled using Klenow polymerase and dNTPs, and thereafter, the vector was religated. The resulting vector was called pETM30-His6-GST-GFP. The pET-28cGFPFUS vector was used to create a His-tagged GFP fusion by digestion with *NheI* and religation. This vector was called pET-28c-His6-GFP. The His6-GST-GFP (abbreviation: GST-GFP) and His6-GFP (abbreviation: GFP) expression vectors were used as model systems to analyze the efficiency of recombinant gene expression.

2.2.3.2 Medium preparation

The composition of Luria-Bertani (LB) broth (low salts) was as follows: 10 gL⁻¹ tryptone, 5 gL⁻¹ yeast extract, and 5 gL⁻¹ NaCl. The pH was adjusted to 7 using 5 mol L⁻¹ NaOH before autoclaving. For solidification, 15 gL⁻¹ agar was added. The defined medium is based on methods described by Korz et al. [112]; details in composition are given in Table 2.2.2. Special instructions for medium preparation are given in the Supplementary Tables 5.2.1 and 5.2.2. Briefly, trace elements (CoCl₂ 6H₂O, MnCl₂ 4H₂O, CuCl₂ 2H₂O, H₃BO₃, Zn (CH₃COOH)₂ 2H₂O, and Titriplex III) were prepared as 2,000 times concentrated stock solution mixture, sterilized by filtration (0.2 μm), and stored at 4 °C. Na₂MoO₄ 2H₂O was prepared as 5,000 times concentrated stock solution, sterilized by filtration (0.2 μm), and stored separately at 4 °C to prevent coprecipitation with the other trace elements during long-term storage. Carbon sources and MgSO₄ (glucose, glycerol, lactose, and MgSO₄) were prepared together as a combined stock solution and sterilized by filtration (0.2 μm). For larger amounts, the combined glucose, glycerol, lactose, and MgSO₄ stock solution was heat-sterilized (121 °C, 20 min). After sterilization of the combined glucose, glycerol, lactose, and MgSO₄ stock solution, the 5,000 times concentrated Na₂MoO₄ 2H₂O stock solution can be added, and the mixture can be kept at room temperature for long-term storage (carbon source stock). Ammonium and phosphate salts additionally including citric acid and ferric citrate [(NH₄)₂HPO₄, KH₂PO₄, citric acid, and Fe(III) citrate] were prepared as combined stock solution. After adjusting the pH value to 6.8, the ammonium and phosphate salt stock solution can be heat-sterilized (121 °C, 20 min) or sterilized by filtration (0.2 μm). When the pH is adjusted by ammonium hydroxide (30%), filter sterilization is preferable. After sterilization, the ammonium and phosphate salts stock

solution can be mixed with the 2,000 times concentrated trace elements stock solution for long-term storage at room temperature (salt-trace stock). Directly before inoculation, the two major stock solutions (carbon source stock and salt-trace stock) were combined and supplemented with the appropriate antibiotics. Antibiotics working and stock solutions were prepared according to *Molecular Cloning: A Laboratory Manual (Third Edition)* [113]. For bioreactor cultures, the pH was adjusted to 6.8 with ammonium hydroxide after heat-sterilization.

Table 2.2.2 Carbon source matrix for autoinduction medium development

Experiment test tubes	Experiment shake flasks	Glucose (gL ⁻¹)	Glycerol (gL ⁻¹)	Lactose (gL ⁻¹)	Carbon source (gL ⁻¹)
T1		0	0	3.8	3.8
T2		0	4.0	3.8	7.8
T3	S1	0	7.4	3.8	11.2
	S3	0	7.4	7.6	15.0
	S3	0	11.1	3.8	14.9
	S4	0	11.1	7.6	18.7
T4		2.9	0	3.8	6.7
T5		2.9	4.0	3.8	10.7
T6	S5	2.9	7.4	3.8	14.1
	S6	2.9	7.4	7.6	17.9
	S7	2.9	11.1	3.8	17.8
	S8	2.9	11.1	7.6	21.6
T7		5.9	0	3.8	9.7
T8		5.9	4.0	3.8	13.7
T9	S9	5.9	7.4	3.8	17.1
	S10	5.9	7.4	7.6	20.9
	S11	5.9	11.1	3.8	20.8
	S12	5.9	11.1	7.6	24.6
IPTG	control	10.9	0	0	10.9

Except for the concentration of carbon substrate(s), the concentrations of the remaining components were identical and as follows: 4 gL⁻¹ (NH₄)₂HPO₄, 13.3 gL⁻¹ KH₂PO₄, 1.55 gL⁻¹ citric acid, 0.59 gL⁻¹ MgSO₄, 100.8 mg L⁻¹ Fe(III) citrate, 2.1 mg L⁻¹ Na₂MoO₄·2H₂O, 2.5 mg L⁻¹ CoCl₂·6H₂O, 15 mg L⁻¹ MnCl₂·4H₂O, 1.5 mg L⁻¹ CuCl₂·2H₂O, 3 mg L⁻¹ H₃BO₃, 33.8 mg L⁻¹ Zn(CH₃COOH)₂·2H₂O, and 14.1 mg L⁻¹ Titriplex III. The pH was adjusted with ~2.7 gL⁻¹ NaOH to pH 6.8

2.2.3.3 Analysis of cell growth

Cell growth was monitored by measurement of the absorbance at 600 nm (OD₆₀₀) and dry cell mass (DCM) as described [112]. One unit of OD₆₀₀ corresponds to 0.37 g dry cell mass per liter for *E. coli* BL21(DE3) [determined during growth in Defined Non-inducing Broth (DNB) at 30 °C].

2.2.3.4 Analysis of protein concentration

Culture samples were centrifuged at 17,000×g and 4 °C for 3 min. After removal of the supernatant, cell pellets were stored at –80 °C until further analysis. For preparation of cell extracts and determination of soluble and insoluble product fractions, cell pellets were disrupted by BugBuster™ Protein Extraction Reagent (Novagen, USA) with rLysozyme and Benzonase according to manufacturer's instructions. Soluble and insoluble cell fractions were separated by centrifugation at 17,000×g and 4 °C for 25 min. Sodium dodecyl sulfate-polyacrylamide gel electrophoresis (SDS-PAGE) analysis of total cell protein and soluble and insoluble protein fractions was performed using Criterion™ Tris–HCl Gel (8–16% polyacrylamide gel, 26-well) in Criterion™ Cell (Bio-Rad, USA) according to standard procedures [114] and manufacturer's instructions. Electrophoresis was carried out at constant voltage (160 V). After electrophoresis, SDS-PAGE gels were stained using colloidal Coomassie G-250 [115]. Destained wet gels were scanned using ScanMaker 9800XL (Microtek, Taiwan). Expression levels of target protein (in percentage of total cell protein) were determined by AIDA Image Analyzer (Raytest, Germany) from SDS-PAGE. Specific and volumetric product concentrations were calculated assuming a constant cell protein content of 550 mg protein per gram cell dry mass [116]. Fluorescence measurements were conducted in triplicate using Infinite™ M200 (Tecan, Switzerland) 96-well plate reader with 395 nm excitation and 510 nm emission filters as described [117] and according to equipment manufacturer's instructions.

2.2.3.5 Cultivation conditions

2.2.3.5.1 Test tube and shake flask cultivations

Test tubes with diameter of 10 mm, 100- or 250-ml Erlenmeyer flasks with three baffles, and 1.8-L Fernbach flask with three baffles were used with working volumes of 2, 10 or 25, and 200 ml, respectively. Glycerol stocks of recombinant *E. coli* strain were streaked on LB agar plates and incubated overnight at 37 °C. After overnight incubation, single colonies were picked and transferred to LB medium (2 ml in test tube or 10 ml in 100-ml shake flask). The cultures were shaken at 37 °C for 4~6 h until the OD600 reached about 1.0. Following, DNB medium in shake flasks were inoculated with LB medium pre-cultures to give a starting OD600 of 0.02. Cultures were shaken at 37 °C for 6~7 h until the OD600 reached 1.5~2.0. DNB medium pre-cultures were used to inoculate the main cultures (DNB or S-DAB) giving a starting OD600 of 0.02. The shaking speed was 180 and 140 rpm, respectively, for test tubes and shake flasks using a shaker with amplitude of 5 cm. The cultivation time using autoinduction medium was as follows: 18 h at 37 °C, 26 h at 30 °C, and 48 h at 23 °C. For IPTG-induced cultivation (in LB or DNB medium), the inoculated cultures were shaken at 37 °C until the OD600 reached 1.0 (LB medium) or 1.5 (DNB medium). Then, 0.25 mmol L⁻¹ IPTG was added to the culture to start protein production, and the temperature was reduced to 30 °C or 23 °C, depending on the required

induction temperature. The time of induction at 37 °C, 30 °C, and 23 °C was 4 h, 6 h, and overnight (about 16 h), respectively. Special attention should be paid to *E. coli* Rosetta 2 (DE3), which grows slower than *E. coli* BL21 (DE3). In this case, the starting OD600 value should be raised to 0.04 or the cultivation time prolonged. Test tube and shake flask cultivations were carried out in triplicate and duplicate, respectively. Mean values are given.

2.2.3.5.2 Bioreactor cultivations

For a 10-L autoinduction cultivation carried out in a 15-L bioreactor (Fermenter B10, Fa. Biologische Verfahrenstechnik, Switzerland), the following settings were chosen: starting OD600 of 0.02, temperature of 23 °C, starting pH of 6.8 (controlled at pH 6.8 by addition of ammonium hydroxide or non-controlled), air-flow rate of 1 vvm, and stirrer speed of 450 rpm. The conditions were kept constant during the entire cultivation. Off-gas analysis was performed using a BCproFerm system (BlueSens, Germany). The end of the cultivation was indicated by a sudden rise in the dissolved oxygen concentration indicating depletion of all carbon compounds.

2.2.3.5.3 Microtiter plate cultivations

For autoinduction cultivation carried out in 96 deep well plates (2 ml total volume per well), single colonies were transferred from LB agar plates to 0.5 ml LB broth (per well) and shaken at 1,000 rpm with an orbital amplitude of 2 mm at 37 °C for 7 h to reach stationary phase. Five microliters of these LB pre-cultures were inoculated to 0.5 ml DNB (per well) and cultivation carried out overnight (16 h) at 25 °C. After overnight cultivation, OD600 values of DNB pre-cultures were analyzed. Following, 0.5 ml of S-DAB (HNC) (per well) was inoculated with DNB grown pre-cultures to give a starting OD600 of 0.02. The cultures in 96 deep well plates were shaken at 25 °C for 40 h. All cultivations were carried out in triplicate. Mean values are given.

2.2.4 Results

2.2.4.1 Choice of reporter proteins

For the development of a universal production medium with a broad application range, three reporter proteins were chosen for medium optimization covering different protein properties, e.g., propensity to form inclusion bodies, size, biological activity, and post-translational oxidative fluorophore formation.

Two fluorescent proteins were employed. The amount of properly folded GFP can be easily accessed by fluorescence measurements rendering GFPs as the most popular reporter proteins [118, 119]. In addition to conventional GFP carrying an N-terminal His6 extension, a GFP fusion protein was chosen which additionally included the sequence of glutathione-S-transferase (GST) between the N-terminal His6 tag and GFP. The additional

presence of the GST tag increases the size of the protein from 27 to 54 kDa and also strongly increases the propensity to form inclusion bodies. The GST-GFP fusion protein only emits fluorescence when the entire fusion protein is correctly folded. As third reporter protein, human basic fibroblast growth factor (hFGF-2, 18 kDa) was employed. hFGF-2 can be produced as soluble active protein but also aggregates into non-active inclusion bodies. The expression level and the fraction of soluble active protein is strongly influenced by the culture conditions [3, 82, 83].

2.2.4.2 The influence of temperature and carbon substrate composition on protein production using autoinduction

Screenings were carried out in test tube and shake flask cultivations and not in microtiter plates to prevent potential inaccuracies during autoinduction medium development resulting from evaporation [26, 120].

The initial screening for temperature effects was carried out in test tube cultures using GFP and GST-GFP as reporter proteins. Both proteins were produced in test tube cultivations at 37 °C, 30 °C, and 23 °C employing a carbon source matrix with nine independent combinations of glucose, glycerol, and lactose (indicated as T1–T9 in Table 2.2.2) and using IPTG induction in DNB as control.

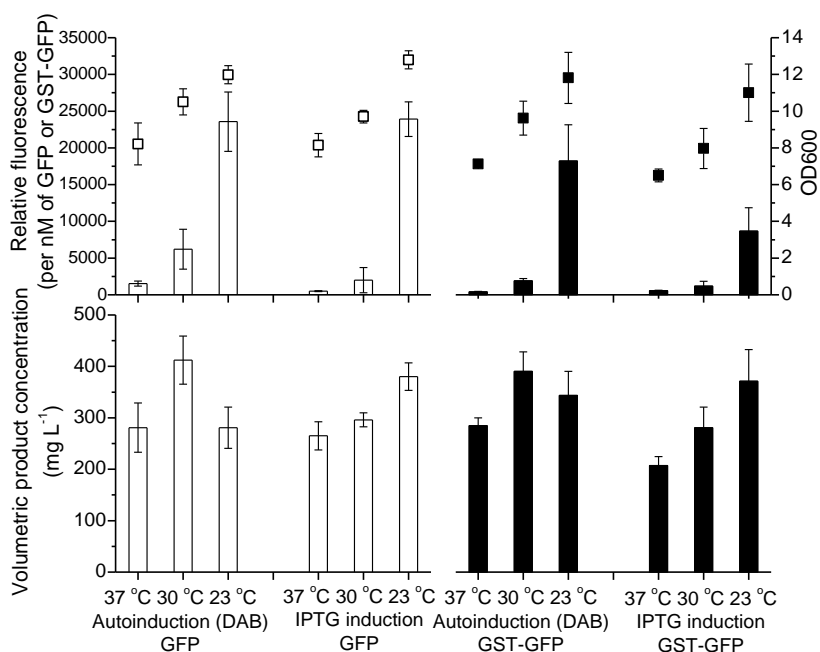


Fig. 2.2.1 Influence of temperature on protein production using autoinduction

Cells were grown in test tubes using autoinduction (T6, refer to Table 2.2.2), and production of GFP (*white columns*) and GST-GFP (*black columns*) followed using IPTG induction in defined medium (DNB) as control. Upper panel: relative fluorescence per nanomol of GFP (*white columns*) and GST-GFP (*black columns*). Final OD600 of GFP (*white squares*) and GST-GFP- (*black squares*) producing culture. Lower panel: volumetric concentration of GFP (*white columns*) or GST-GFP (*black columns*). Temperature and induction method are indicated below

A representative result showing the temperature effect on protein production using Defined Autoinduction Broth (DAB) is shown in Fig. 2.2.1. The volumetric product concentrations were not significantly affected by the temperature; however, the amount of correctly folded protein (indicated as fluorescence per nanomolar of GFP or GST-GFP) increased dramatically for both proteins with decreasing temperature. Thus, further experiments for optimizing the medium composition were carried out at 23 °C.

To obtain a general optimized autoinduction medium, the carbon source matrix from test tube cultivations was complemented by a matrix including 12 different carbon source combinations employed in shake flask cultivations (S1–S12) resulting in 18 different combinations of glucose, glycerol, and lactose and containing three combinations which were tested both in test tube and shake flask cultures (Table 2.2.2). The carbon source combination screening was performed with the two fluorescent proteins and hFGF-2.

The results revealed that each protein has its unique optimal carbon source combination (Fig. 2.2.2). For example, the highest volumetric fluorescence of GFP was obtained in autoinduction medium without glucose. Increasing glucose concentrations were accompanied with decreasing volumetric fluorescence of GFP in agreement with previously reported results [26]. However, the best production of the GST-GFP fusion protein was achieved in the presence of $\sim 3 \text{ gL}^{-1}$ glucose, and the best hFGF-2 production was obtained in the range of ~ 3 to 6 gL^{-1} glucose. Thus, the best medium composition for production of a new protein is determined as a compromise and might be used as a starting point for further optimization if repetitive or large-scale production is envisioned. For further studies, the combination of $\sim 3 \text{ gL}^{-1}$ glucose, $\sim 11 \text{ gL}^{-1}$ glycerol, and $\sim 7.5 \text{ gL}^{-1}$ lactose was chosen, and this medium was named “Smart”- DAB (S-DAB) (Table 2.2.3). It should be noticed that this autoinduction medium is superior to conventional IPTG induction in defined medium regarding the amount of properly folded protein (see GST-GFP as an example in Figs. 2.2.1 and 2.2.2). The complete dataset showing the influence of carbon source combination on protein production using autoinduction is shown in Supplementary Figs. 5.2.1 and 5.2.2.

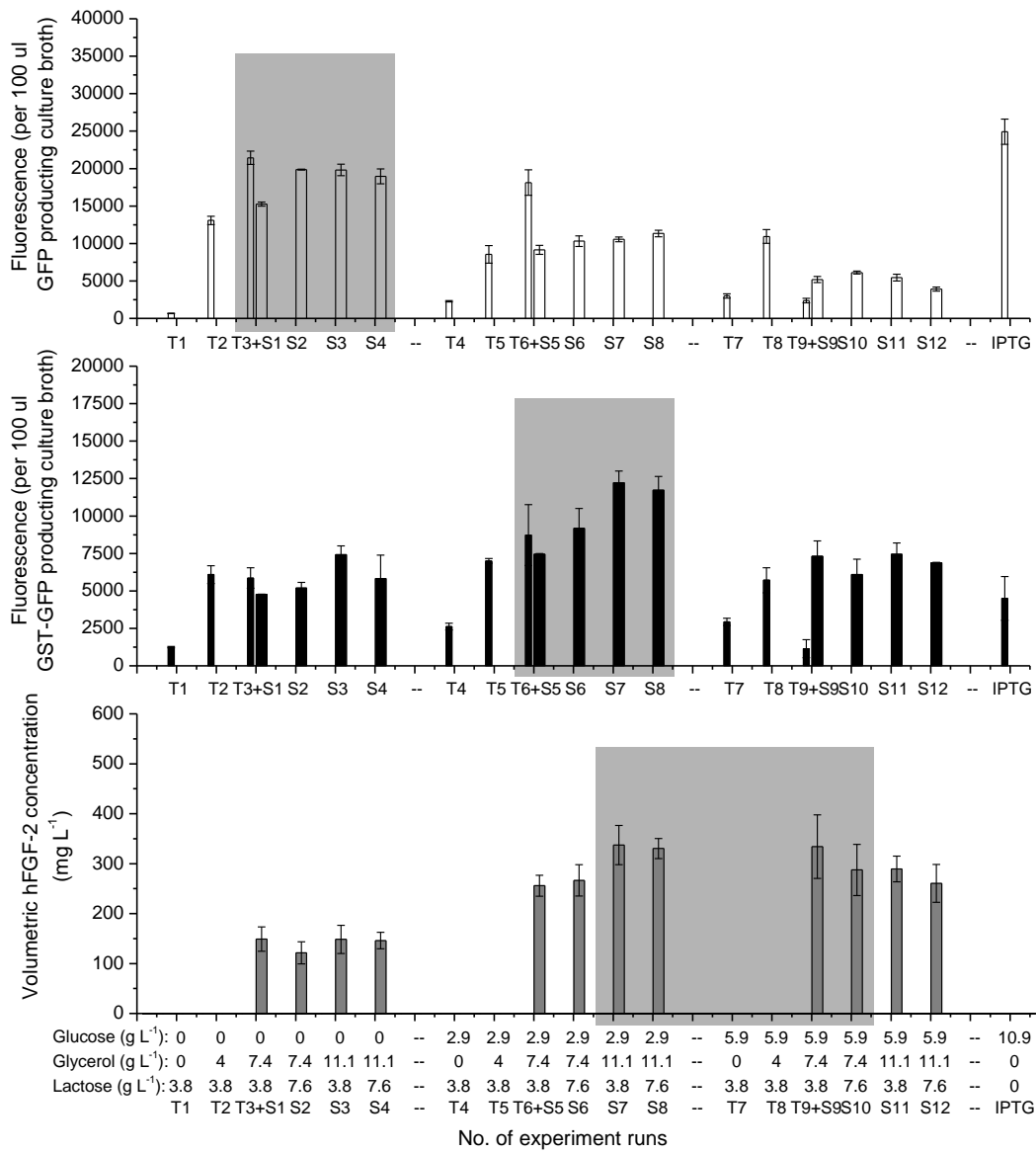


Fig. 2.2.2 Influence of carbon substrate composition on protein production using autoinduction

Cells were grown in test tube (*narrow column*) and shake flask (*broad column*). *Upper panel*: fluorescence per 100 µl of GFP-producing culture (*white columns*). *Middle panel*: fluorescence per 100 µl of GST-GFP-producing culture (*black columns*). *Lower panel*: volumetric hFGF-2 concentration (*gray columns*). The *light gray shadows* indicate the maximum product yield area. Test tube and shake flask run numbers and glucose, glycerol, and lactose concentrations are indicated below (refer to Table 2.2.2)

Table 2.2.3 Optimized defined (autoinduction) medium

Medium	Application	Carbon source(s)	pH adjustment
S-DAB (HNC): “smart”-defined autoinduction broth (high nitrogen content)	Cultivation with good oxygen supply	2.9 gL ⁻¹ glucose 11.17 gL ⁻¹ glycerol 7.6 gL ⁻¹ lactose	about 4.5 ~5 ml L ⁻¹ NH ₃ H ₂ O (~30 %) to reach pH 6.8
S-DAB: “smart”-defined autoinduction broth	Cultivation with intermediate oxygen supply	2.9 gL ⁻¹ glucose 11.17 gL ⁻¹ glycerol 7.6 gL ⁻¹ lactose	
DAB: defined autoinduction broth	Cultivation with poor oxygen supply	2.9 gL ⁻¹ glucose 7.4 gL ⁻¹ glycerol 3.8 gL ⁻¹ lactose	about 2.7 gL ⁻¹ NaOH to bring final pH to 6.8
DNB: defined non-inducing broth	IPTG induction or pre-culture	10.9 gL ⁻¹ glucose	

Except for the concentration of carbon substrate(s) and method of pH adjustment, the concentrations of remaining components were as in Table 2.2.2

2.2.4.3 The influence of nitrogen content on protein production using autoinduction

The pH of the medium can be adjusted either by sodium or ammonium hydroxide, which increases either the salt (sodium) or the nitrogen content of the medium, respectively. When pH adjustment of S-DAB was carried out with ammonium instead of sodium hydroxide, the ammonium content increased from 60 to 120 mmol L⁻¹, decreasing the C/N ratio from 12 to 6 (C-mol/N-mol), respectively.

Adjusting the pH with ammonium instead of sodium hydroxide resulted in higher final cell densities and higher final volumetric product concentrations (Fig. 2.2.3). Moreover, for GFP and GST-GFP, also a slight increase in the specific product concentration was observed, while no changes were found for hFGF-2 (Supplementary Fig. 5.2.3). The percentage of soluble target protein was unaffected for GFP and hFGF-2, but for GST-GFP, a substantial increase in inclusion body formation occurred when the medium pH was adjusted with ammonium hydroxide (Fig. 2.2.3). However, the volumetric concentration of correctly folded GST-GFP (also shown as GFP fluorescence per culture volume) was unaffected as the decreased solubility was compensated by the higher final volumetric GST-GFP concentration (Fig. 2.2.3). Thus, it is recommended to adjust the pH by using ammonium hydroxide. The corresponding medium has a higher nitrogen content (HNC) and, thus, is named S-DAB (HNC) (Table 2.2.3).

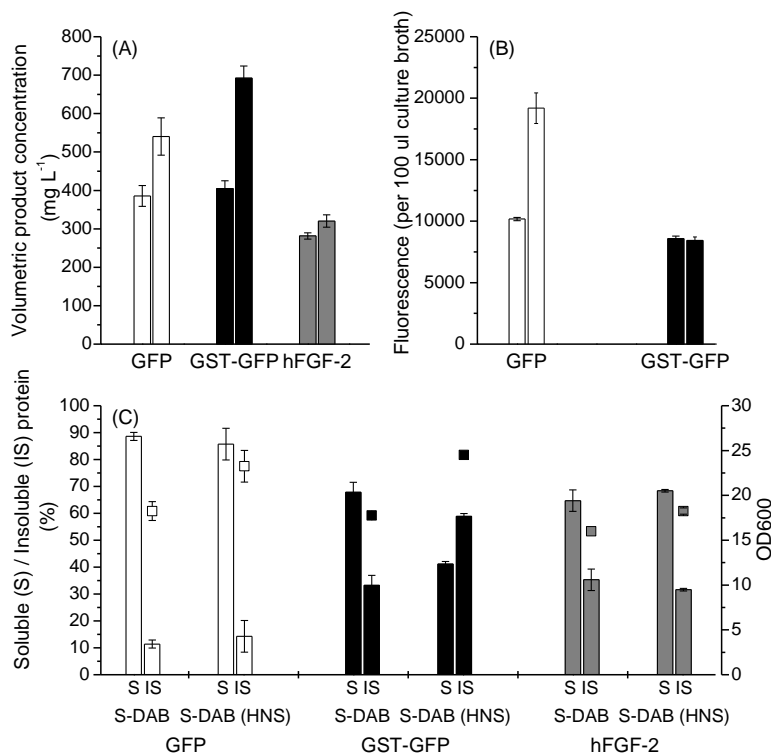


Fig. 2.2.3 The influence of nitrogen content on protein production using autoinduction

The nitrogen content of S-DAB was increased by using ammonium hydroxide [S-DAB (HNC)] for pH adjustment instead of sodiumhydroxide (S-DAB). (A) Volumetric concentrations of GFP (*white columns*), GST-GFP (*black columns*), and hFGF-2 (*gray columns*) in S-DAB (*left column*) and S-DAB (HNC) (*right column*). (B) Fluorescence per 100 µl of GFP (*white columns*) and GST-GFP-producing culture (*black columns*) in S-DAB (*left column*) and S-DAB (HNC) (*right column*). (C) Percentage of soluble (*left column*) and insoluble (*right column*) product amounts and final cell densities, respectively, of GFP (*white columns, white squares*), GST-GFP (*black columns, black squares*), and hFGF-2- (*gray columns, gray squares*) producing cultures in S-DAB and S-DAB (HNC)

2.2.4.4 The influence of oxygen supply on protein production using autoinduction

The oxygen supply in simple culture vessels can be improved by increasing the shaking speed and/or the culture surface to volume ratio. The analysis of oxygen supply on the production of GFP and hFGF-2 in S-DAB (HNC) clearly showed an increase in final cell density and volumetric product concentration for both proteins with increasing oxygen supply (Fig. 2.2.4). Moreover, better oxygenation also strongly decreased the formation of inclusion bodies during hFGF-2 production (Supplementary Fig. 5.2.4). Thus, protein production using autoinduction should be carried out under conditions which provide the best oxygenation. However, if sufficient oxygen cannot be supplied (e.g., growth in test tubes at 37 °C), glycerol and lactose concentrations can be reduced (to ~7.5 and 4 gL⁻¹, respectively). The resulting DAB can be pH adjusted with sodium hydroxide (Table 2.2.3).

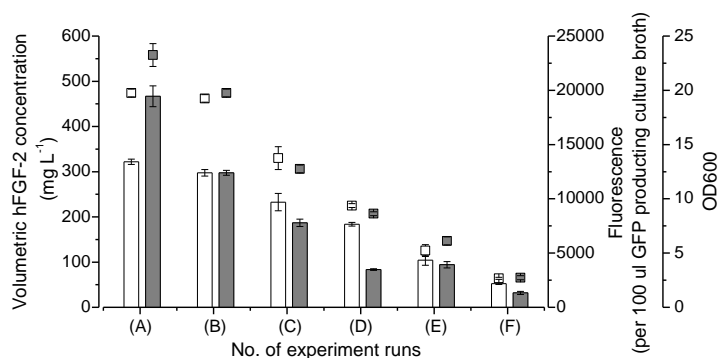


Fig. 2.2.4 The influence of oxygen supply on protein production using autoinduction

Fluorescence per 100 µl of GFP-producing culture (*white columns*) and volumetric hFGF-2 concentration (*gray columns*) and final cell densities of the GFP (*white squares*) and hFGF-2- (*gray squares*) producing culture using S-DAB (HNC). The experimental conditions were as follows: **(A)** 10 ml in 100-ml shake flask at 140 rpm, **(B)** 25 ml in 100-ml shake flask at 140 rpm, **(C)** 10 ml in 100-ml shake flask at 80 rpm, **(D)** 50 ml in 100-ml shake flask at 140 rpm, **(E)** 25 ml in 100-ml shake flask at 80 rpm, and **(F)** 50 ml in 100-ml shake flask at 80 rpm

2.2.4.5 Test of general applicability of S-DAB (HNC) for T7-based production systems

The general applicability of S-DAB (HNC) medium was tested for the production of eight different proteins involving three different T7-based host strains (Table 2.2.1). Production using autoinduction in S-DAB (HNC) was compared to production in conventional LB medium using IPTG for induction of protein synthesis. This comparison revealed in general similar specific product concentrations using either S-DAB (HNC) or LB, but final yields of target proteins were significantly higher in S-DAB (HNC) as about four times higher final biomass concentrations were reached (Fig. 2.2.5). However, it should be noted that the actual attainment is specific to the target protein. For example, in case of the protein Auto27-243-GST, the utilization of S-DAB (HNC) instead of LB not only resulted in six times higher cell densities but also significantly improved the specific product concentration and the solubility of the target protein. In most cases, the improvement was less spectacular, and in some cases, a slight decline in specific product concentration or solubility was observed. Thus, S-DAB (HNC) can be used for the production of different types of proteins with usual excellent results; moreover, it can also be used for T7-based host strains, which show poor growth characteristics such as *E. coli* Rosetta 2 (DE3).

2.2.4.6 Test of applicability of S-DAB (HNC) for screening studies in 96-well microtiter plates

The availability of a medium which omits inducer addition would greatly facilitate screening in 96-well microtiter plates for best production clones. Thus, the production of eight different proteins involving three different T7-based host strains (Table 2.2.1) was tested in 96 deep well plates using S-DAB (HNC) (Fig. 2.2.6). In all cases, the specific protein concentration was similar or even higher compared to production in shake flask

cultures (refer to Fig. 2.2.5). Moreover, in all cases, higher final cell densities were obtained presumably as a result of evaporation. In summary, it can be concluded that S-DAB (HNC) is very well suited for screening studies employing 96-well microtiter plates.

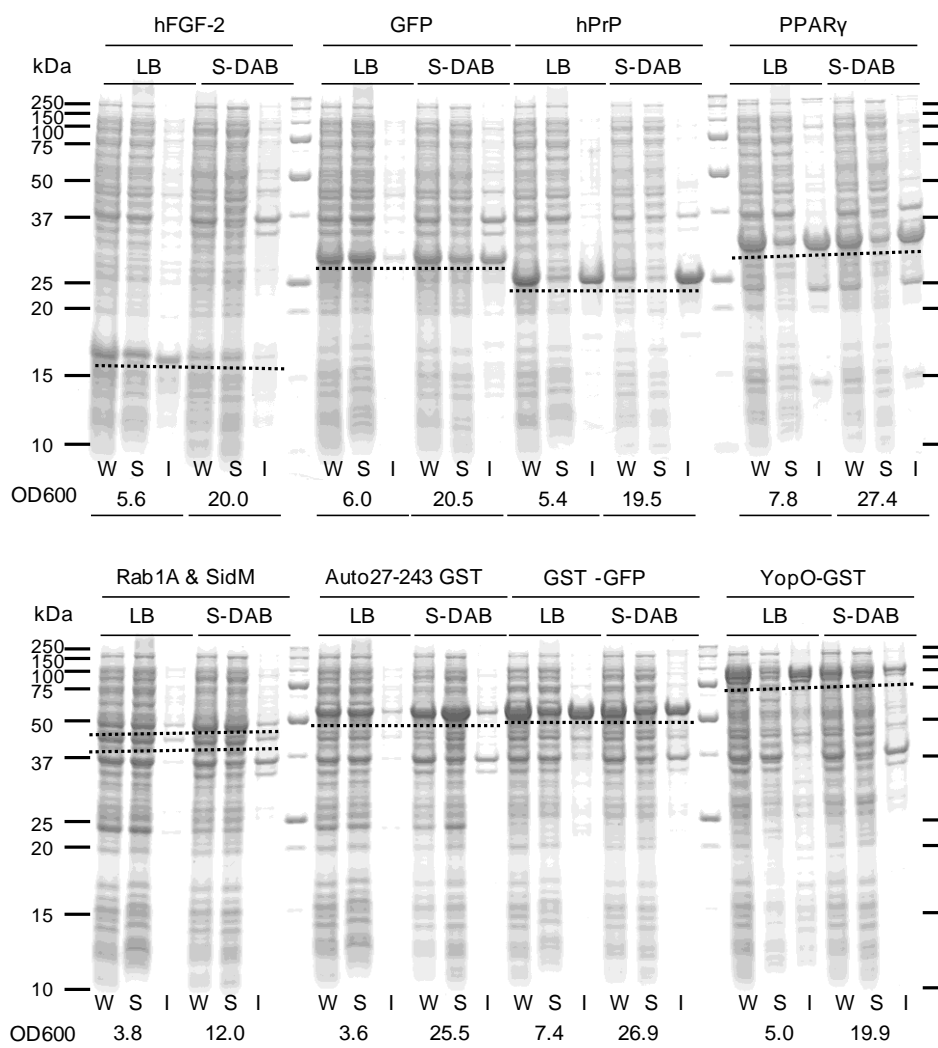


Fig. 2.2.5 Test of general applicability of S-DAB (HNC) for T7 based production systems

Production of various proteins using different T7-based expression systems was carried out in Fernbach flasks using S-DAB (HNC) or IPTG-induction in Luria Bertani broth as control. Produced target proteins (refer to Table 2.2.1) and media are indicated above. Below are indicated the cell fraction analyzed by SDS-PAGE (*W*: whole cell protein, *S*: soluble part and *I*: insoluble part of whole cell protein) and the final cell densities (OD600)

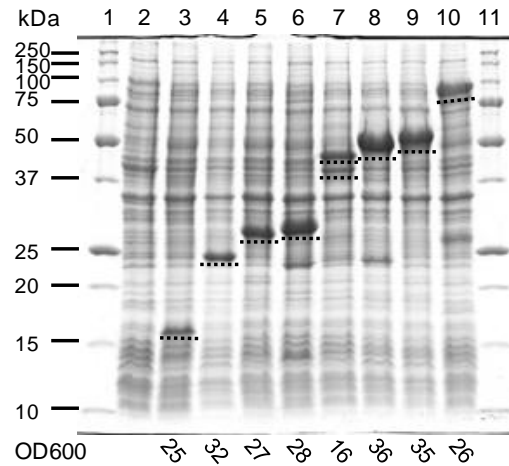


Fig. 2.2.6 Test of applicability of S-DAB (HNC) for screening studies in 96-well microtiter plates

The following proteins (refer to Table 2.2.1) were produced in deep-well plates and the total cell protein analyzed by SDS-PAGE: hFGF-2 (lane 3), hPrP (lane 4), GFP (lane 5), PPAR γ (lane 6), co-production of Rab1A and SidM (lane 7), Auto27-243-GST (lane 8), GST-GFP (lane 9), and YopO-GST (lane 10). Protein standard (lanes 1 and 11) and plasmid free *E. coli* BL21 (DE3) are included as control (lane 2). The final cell densities are indicated below

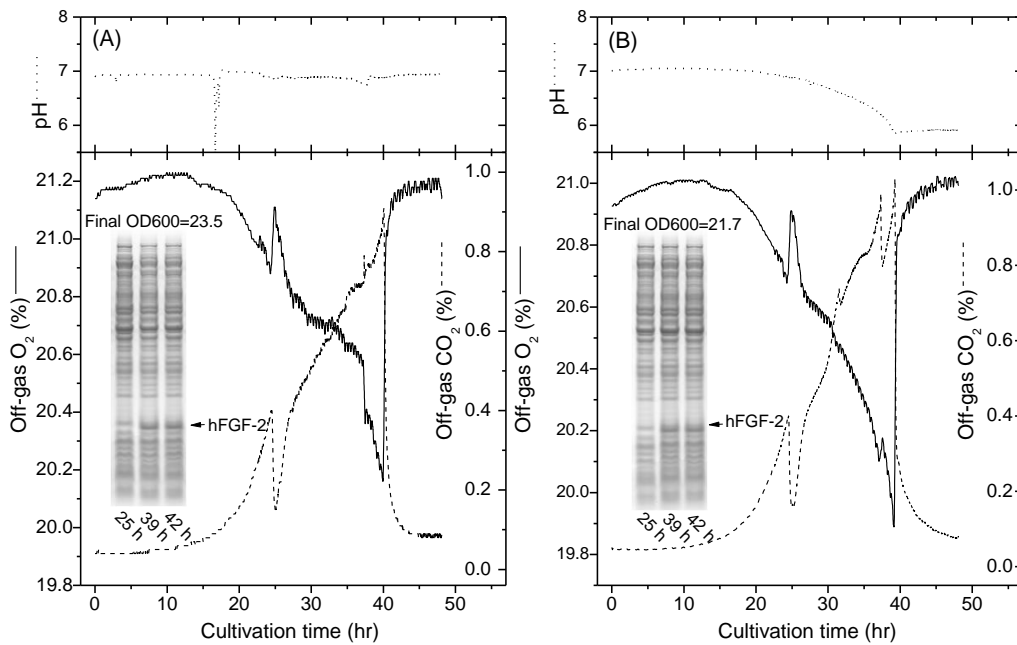


Fig. 2.2.7 Test of applicability of S-DAB (HNC) for large-scale cultivation

hFGF-2 was produced in 15-L bioreactors (A) with pH control (pH 6.8) and (B) without pH control. All other culture variables were identical in both cultures. The concentrations of oxygen (solid line) and carbon dioxide (dashed line) in the exhaust gas and the pH of the culture broth (dotted line) are shown. The inserts show SDS-PAGE analysis of whole cell protein from samples taken at indicated time points and final cell densities

2.2.4.7 Test of applicability of S-DAB (HNC) for large-scale cultivation

The applicability of S-DAB (HNC) for large-scale cultivation was analyzed in 15-L bioreactors for the production of hFGF-2. Cultivations were carried out as pH-controlled batch process and also in the absence of pH control while keeping other culture variables identical. Both conditions were leading to nearly identical final cell densities and expression levels as were obtained in well-aerated shake flask cultures (Fig. 2.2.7 and refer to Fig. 2.2.5). The final pH in the non-pH controlled culture reached pH 5.9, indicating an excellent buffering capacity of S-DAB (HNC) and its applicability for large-scale cultivation without pH control.

2.2.5 Discussion

A simple defined autoinduction medium was developed with general applicability for production of proteins with diverse properties using T7-based host strains with different growth characteristics. It can be employed in micro- as well as in macro-scale culture vessels leading to high final biomass concentrations ($OD_{600} > 20$) and average yields of 500 mg L^{-1} target protein. As there is no need for pH control and inducer addition, this defined medium represents a very convenient way for protein production. The final product levels are in average four times higher than can be reached in complex LB broth through IPTG-induced protein production. The well-balanced composition of SDAB (HNC) also becomes evident as the medium C/N ratio is close to the C/N ratio of the *E. coli* cell [121] and the biomass yield coefficient close to the one at best attainable, e.g., 0.5 and 0.43 gg^{-1} for glucose and glycerol, respectively [112, 122]. Moreover, the defined composition only including basic compounds and no vitamin and amino acid supplements also renders it suitable for production of labeled proteins. However, special attention should be given to provide sufficient oxygen, e.g., growth at low temperature and high surface-to-volume ratio of culture broth. Under conditions of poor oxygen supply, glycerol and lactose concentrations can be reduced.

2.2.6 Acknowledgements

Special thanks are given to Wolf-Dieter Schubert, Torsten Lührs, and Konrad Büsow for providing recombinant *E. coli* strains for testing general medium applicability. Partial support of the FORSYS Partner Project “Dynamics and regulation of the metabolic balance in *Escherichia coli*” is greatly acknowledged. We also thank Antonio Villaverde for “smart” suggestions.

2.3 Optimized procedure to generate heavy isotope and selenomethionine-labeled proteins for structure determination using *Escherichia coli*-based expression systems

Chapter 2.3 is an entire paper reprinted with the permission from Springer that was published in Applied Microbiology and Biotechnology in November 2011, Volume 92, Number 4, Page: 823–833

License Number: 2951820800709

License date: Jul 18, 2012

Licensed content publisher: Springer

Licensed content publication: Applied Microbiology and Biotechnology

Licensed content title: Optimized procedure to generate heavy isotope and selenomethionine-labeled proteins for structure determination using *Escherichia coli*-based expression systems

Licensed content author: Zhaopeng Li

Licensed content date: Jan 1, 2011

Volume number: 92

Issue number: 4

Type of Use: Thesis/Dissertation

2.3.1 Abstract

Generating sufficient quantities of labeled proteins represents a bottleneck in protein structure determination. A simple protocol for producing heavy isotope as well as selenomethionine (Se-Met)-labeled proteins was developed using T7-based *Escherichia coli* expression systems. The protocol is applicable for generation of single-, double-, and triple-labeled proteins (^{15}N , ^{13}C , and ^2H) in shaker flask cultures. Label incorporation into the target protein reached 99% and 97% for ^{15}N and ^{13}C , respectively, and 75% of (non-exchangeable) hydrogen for ^2H labeling. The expression yields and final cell densities (OD₆₀₀ ~16) were the same as for the production of non-labeled protein. This protocol is also applicable for Se-Met labeling, leading to Se-Met incorporation into the target protein of 70% or 90% using prototrophic or methionine auxotrophic *E. coli* strains, respectively.

Keywords *Escherichia coli* · Recombinant protein production · Stable heavy isotope labeling · Selenomethionine labeling · Autoinduction · Defined medium

2.3.2 Introduction

Stable heavy isotope (^{15}N , ^{13}C , and ^2H) and selenomethionine (Se-Met)-labeled proteins are commonly used for protein structure determination through NMR spectroscopy [4] and X-ray crystallography [5], respectively. The generation of isotope-enriched protein samples is a prerequisite for carrying out structural studies using NMR spectroscopy [34-36]. Also, incorporation of Se-Met into proteins considerably improves protein structure studies by X-ray crystallography through phase determination by multi-wavelength anomalous diffraction [37, 38].

As labeling experiments are usually costly, an efficient and simple protocol for generating labeled proteins is of crucial importance to structural biologists. Current protocols for production of heavy isotope and Se-Met-labeled proteins using *Escherichia coli* expression systems are mainly based on M9 minimal medium [5, 39-43] leading to very poor final biomass concentrations (OD600 of 1~2) and, consequently, low yields of labeled proteins. Some improvements have been obtained by optimizing the minimal medium [46] or by using autoinduction medium for the generation of ^{15}N and/or ^{13}C or Se-Met-labeled proteins [25, 27, 28]. Moreover, carbon-limited fed-batch processes have been developed for production of ^{15}N and ^{13}C [44] or Se-Met labeled proteins [45] which lead to higher final biomass concentrations (OD600 of ~6 or ~11 for heavy isotope or Se-Met-labeled proteins, respectively) and, thus higher labeled target protein yields. However, the establishment of carbon-limited fed-batch processes usually requires the availability of more sophisticated technical equipment and, more importantly, the availability of dedicated staff. Thus, there is still a great need for protein labeling protocols which are easy to implement and lead to sufficient protein amounts with high-label incorporation at acceptable costs.

The production of deuterated (^2H -labeled) proteins is even more difficult and very costly with current protocols as multiple adaptation steps of *E. coli* to pure D_2O are required to generate protein with high-label content [123]. Even after adaptation, cell densities reached in D_2O did not increase above OD600 ~5 [123, 124]. As alternative, cells can be grown in the presence of 75% D_2O to avoid the strong inhibitory effect of pure D_2O on growth and protein production; however, the reduced D_2O content also reduces the deuteration efficiency of the target protein [125]. Furthermore, for all labeling methods, different protocols are currently employed, all with their unique stock solutions and procedures, making the production of highly labeled proteins tedious, more costly than necessary and most often the bottleneck of protein structure determination.

In this work, we present a unified protocol based on a modular system which can be used to efficiently produce heavy isotope (mono- or multiple-incorporations of ^2H , ^{13}C , and ^{15}N) as well as Se-Met-labeled proteins with high-label content using the T7-based *E. coli* expression system. Special attention is given to the production of deuterated proteins.

2.3.3 Materials and methods

2.3.3.1 Strains and plasmids

E. coli BL21 (DE3) (Novagen, Germany) and the methionine auxotrophic strain T7 Express Crystal (New England Biolabs, USA) were used. The plasmid pET-15b-hPrP encoding the human prion protein (hPrP, residues 23–231) under control of the T7 promoter is described elsewhere [106]. Details concerning the plasmids pET-29c-hFGF-2 and pET-28c-His6-GFP encoding human basic fibroblast growth factor (hFGF-2) and His6-tagged green fluorescent protein (GFP) are found elsewhere [82, 110].

2.3.3.2 Medium composition and preparation

The composition of the Luria-Bertani (LB) medium was as follows: 10 g L⁻¹ tryptone, 5 g L⁻¹ yeast extract, 5 g L⁻¹ NaCl and 15 g L⁻¹ agar added for medium solidification, the final pH was adjusted to pH 7 before autoclaving. The composition and preparation of the defined labeling medium are based on the defined high cell-density cultivation medium [112] and the defined autoinduction medium [110]. A general scheme for the usage and composition of the defined labeling medium including medium abbreviations are given in Table 2.3.1. Detailed instructions for medium preparation are provided in the Supplementary Tables 5.2.1 and 5.2.2. Appropriate antibiotics were added to the medium for plasmid maintenance (pET-15b-hPrP, 100 mg L⁻¹ ampicillin, pET-29c-hFGF-2 and pET-28c-His6-GFP, 50 mg L⁻¹ kanamycin). D-glucose (U-¹³C6, 99%), ammonium chloride (¹⁵N, 99%), and deuterium oxide (D, 99.9%) used for labeling experiments were purchased from Cambridge Isotope Laboratories Inc. (Andover, MA, USA). L-selenomethionine was purchased from Sigma-Aldrich (Munich, Germany).

2.3.3.3 Cultivation conditions

Two different cultivation strategies for different labeling purposes were employed (for details, refer to Fig. 2.3.1). In principle, autoinduction was performed for non-labeled protein production (control run), and for ¹⁵N and ²H labeling. For ¹³C labeling (or combined with ²H or ¹⁵N labeling) and for selenomethionine labeling, medium exchange was applied (spin down pre-cultures and resuspend cell pellets in labeling medium). Cultivations were carried out in duplicate using 250 mL shake flasks with three baffles containing 25 mL medium at 180 rpm (using a shaker with an amplitude of 5 cm). Mean values are given.

2.3.3.4 Analysis of cell growth and protein production

Cell growth was monitored by measurement of the absorbance at 600 nm (OD₆₀₀). For protein production analysis, culture samples were centrifuged at 17,000×g and 4 °C for 3 min. After removal of supernatant, cell pellets were stored at -80 °C until further analysis.

SDS-PAGE analysis was performed in PROTEAN II xi (Bio-Rad, USA) according to standard procedures [114] and instructions from the manufacturer. BugBuster™ Protein Extraction Reagent (Novagen, USA) was used to generate cell extracts and to prepare soluble and insoluble fractions according to the instructions from the manufacturer. After electrophoresis, proteins on SDS-PAGE gels were visualized by colloidal Coomassie G-250 staining [115]. Stained wet gels were scanned by ScanMaker 9800XL (Mikrotek, Taiwan).

2.3.3.5 Heavy isotope and selenomethionine labeling efficiency determination

The heavy isotope or Se-Met labeling efficiency was analyzed by matrix-assisted laser desorption ionization time-of-flight mass spectrometry (MALDI-TOF MS). Protein bands were excised manually from the SDS-PAGE gels. After washing, reduction, and alkylation, in-gel digestion was carried out by incubation with sequencing grade-modified trypsin (Promega, USA). Obtained peptides were extracted and purified with reversed-phase C18 ZipTips (Millipore, USA). Desalted peptide solutions were mixed with a saturated matrix solution and spotted onto a 384 MTP target and dried at room temperature. A Bruker Ultraflex time-of-flight mass spectrometer (Bruker Daltonics GmbH, Germany) was employed to obtain peptide mass fingerprints. Details of the protocol have been described previously [126, 127].

The mass fingerprint spectra of proteins with different labeling methods were analyzed using the software flexAnalysis™ (Bruker Daltonics GmbH, Germany). The theoretical mass fingerprint spectra of the proteins were generated by PeptideCutter in ExPASy Proteomics Server (<http://www.expasy.org/tools/peptidecutter/>). The formula of each peptide was calculated by ProtParam in ExPASy Proteomics Server (<http://www.expasy.org/tools/protparam.html>). The theoretical peptide isotopic distributions with the different isotope abundances were calculated using IsoPro 3.0 MS/MS software and matched with the experimental mass spectra to determine the isotopic labeling efficiency. The numbers of non-exchangeable and exchangeable hydrogen atoms in the proteins were determined according to the amino acid sequence as described previously [128]. The theoretical isotopic distribution of the peptides with methionine replaced by Se-Met was calculated by IsoPro 3.0 MS/MS software and compared with the experimental mass spectra to help locate the position of peptides containing Se-Met in the experimental mass spectra. The area below the mass spectrum of a peptide containing methionine or Se-Met was integrated. The Se-Met labeling efficiency for each individual peptide was calculated according to the literature [129]. Average heavy isotope or Se-Met labeling efficiency of trypsin digested peptides in the experimental MS fingerprint was used to determine the approximate overall labeling efficiency of the protein.

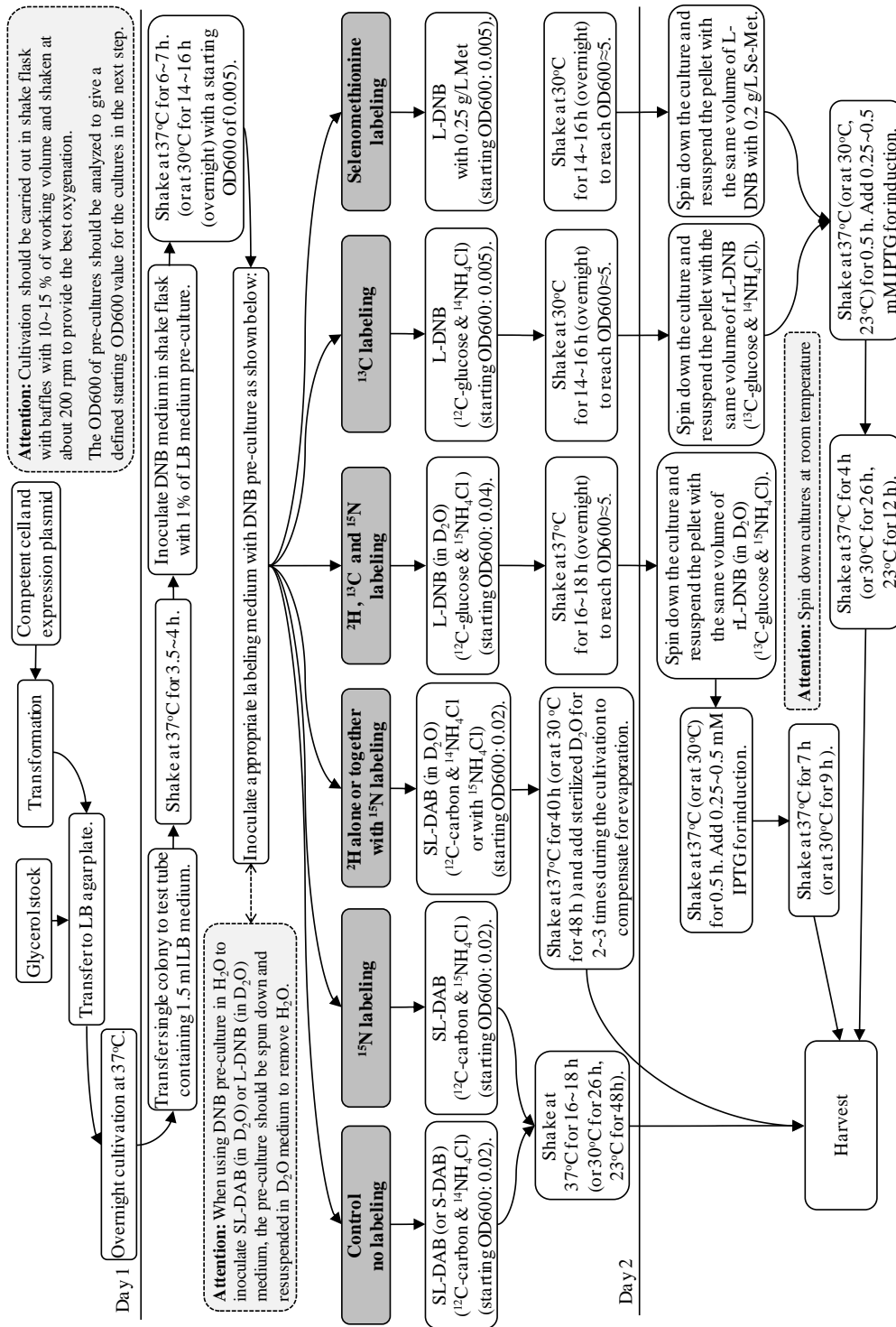


Fig. 2.3.1 Cultivation strategies for different labeling purposes

2.3.4 Results

2.3.4.1 General considerations for developing media for heavy isotope and selenomethionine labeling

Two different types of defined media were developed for generating labeled proteins based on the two methods used for induction of protein production: autoinduction and isopropyl β -D-1-thiogalactopyranoside (IPTG) induction (for details refer to Table 2.3.1).

Special attention was given to generate media recipes where labeled substrates of the lowest price can be used. For example, $^{15}\text{NH}_4\text{Cl}$ is much cheaper than $(^{15}\text{NH}_4)_2\text{HPO}_4$, thus NH_4Cl was used as the sole nitrogen source in labeling medium instead of $(\text{NH}_4)_2\text{HPO}_4$. Usually, ammonium phosphate is the better nitrogen source in defined media as it contributes to a better buffering capacity for pH maintenance and additionally provides the required phosphate for cell growth. When replacing $(\text{NH}_4)_2\text{HPO}_4$ in the medium (e.g., in the defined non-inducing broth [DNB]) by NH_4Cl (e.g., in the labeling defined non-inducing broth [L-DNB]), the labeling medium contains in addition 60.5 mmol L^{-1} NaCl, which is introduced by pH adjustment using NaOH (instead of NH_4OH). This higher salt content causes a decrease of the specific growth rate by 13% of *E. coli* BL21 (DE3) at $37 \text{ }^\circ\text{C}$ in L-DNB compared to DNB.

If possible, autoinduction was used as a very convenient method for generating labeled proteins as it omits biomass monitoring for the correct timing of inducer addition and places the shift from growth to recombinant protein production under metabolic control of the expression host [110]. Using autoinduction, a mixture of glucose, glycerol, and lactose is used as carbon substrate. However, the prices of ^{13}C -labeled glycerol and lactose are beyond the budget of most research groups and much higher compared to ^{13}C -glucose. Thus, employing the autoinduction method for generating ^{13}C -labeled proteins is not advised. In this case, the utilization of ^{13}C -labeled glucose as sole carbon source in combination with IPTG induction is the better choice. To reduce labeling costs, cells are pregrown on non-labeled glucose prior to simultaneous addition of IPTG and ^{13}C -glucose. For high-label incorporation, it is recommended to remove unlabelled carbon substrates and potentially toxic by-products such as acetic acid prior to adding IPTG and the labeled substrate. Thus, it is recommended to exchange the medium with fresh medium containing the IPTG and labeled glucose.

Another point to consider is the toxicity of labeled substrates. For example, Se-Met is a very toxic compound and *E. coli* BL21 (DE3) is not able to grow in autoinduction medium with more than 50 mg L^{-1} Se-Met leading to low label incorporation into the target protein (data not shown). Thus, IPTG induction combined with medium exchange is the best approach for generating Se-Met-labeled proteins. A general summary of the specific medium properties for specific labeling purposes is given in Table 2.3.1.

Table 2.3.1 General scheme for the usage and composition of the defined labeling medium

Name of medium	Solvent	General usage	Induction method	Carbon(s) (g L ⁻¹)	Nitrogen (g L ⁻¹)	KH ₂ PO ₄ (g L ⁻¹)
S-DAB (HNC)	H ₂ O	Non-labeled protein production	Auto-induction	2.9 glucose, 11.1 glycerol, 7.6 lactose	4.0 (NH ₄) ₂ HPO ₄	13.3
S-DAB	H ₂ O	Non-labeled protein production	Auto-induction	2.9 glucose, 11.1 glycerol, 7.6 lactose	4.0 (NH ₄) ₂ HPO ₄	13.3
DNB	H ₂ O	Pre-cultures and IPTG induction	IPTG	10.9 glucose	4.0 (NH ₄) ₂ HPO ₄	13.3
SL-DAB	H ₂ O	For ¹⁵ N labeling	Auto-induction	2.9 glucose, 11.1 glycerol, 7.6 lactose	3.2 ¹⁵ N-NH ₄ Cl	17.4
SL-DAB (in D ₂ O)	D ₂ O	For ² H and ¹⁵ N* labeling	Auto-induction	2.9 glucose, 11.1 glycerol, 7.6 lactose	3.2 ¹⁵ N-NH ₄ Cl	17.4
rL-DNB	H ₂ O	For ¹³ C and ¹⁵ N* labeling	IPTG	6.5 ¹³ C-glucose	2.6 ¹⁵ N-NH ₄ Cl	17.4
rL-DNB (in D ₂ O)	D ₂ O	For ² H, ¹³ C and ¹⁵ N* labeling	IPTG	6.5 ¹³ C-glucose	2.6 ¹⁵ N-NH ₄ Cl	17.4
L-DNB (in D ₂ O)	D ₂ O	Pre-culture of ¹⁵ N*, ¹³ C and ² H labeling	IPTG	10.9 glucose	3.2 ¹⁵ N-NH ₄ Cl	17.4
L-DNB	H ₂ O	Pre-cultures and Se-Met labeling	IPTG	10.9 glucose	3.2 NH ₄ Cl	17.4

For selenomethionine labeling, the pre-culture and main culture were supplemented with 250 mg L⁻¹ methionine and 200 mg L⁻¹ selenomethionine, respectively. ¹⁵N*: the labeling of ¹⁵N is optional. If ¹⁵N labeling is not required, ¹⁵N-NH₄Cl can be replaced by normal NH₄Cl

Except for the concentrations of the carbon and nitrogen substrates, potassium phosphate and the method of pH adjustment, the concentrations of remaining components were identical and as follows: 1.55 g L⁻¹ Citric acid, 0.59 g L⁻¹ MgSO₄, 100.8 mg L⁻¹ Fe(III) citrate, 2.1 mg L⁻¹ Na₂MoO₄ · 2H₂O, 2.5 mg L⁻¹ CoCl₂ · 6H₂O, 15 mg L⁻¹ MnCl₂ · 4H₂O, 1.5 mg L⁻¹ CuCl₂ · 2H₂O, 3 mg L⁻¹ H₃BO₃, 33.8 mg L⁻¹ Zn(CH₃COO)₂ · 2H₂O, 14.10 mg L⁻¹ Titriplex III. Except for S-DAB (HNC), the final pH of all other media was adjusted to 6.8 by NaOH. Details for medium preparation are given in the supplementary material

S-DAB (HNC) smart-defined autoinduction broth (high nitrogen content) with pH adjustment by NH₄OH, *S-DAB* smart-defined autoinduction broth, *DNB* defined non-inducing broth, *SL-DAB* smart labeling-defined autoinduction broth, *rL-DNB* reduced labeling-defined non-inducing broth (with reduced concentrations of carbon and nitrogen substrates), *L-DNB* labeling-defined non-inducing broth

2.3.4.2 Heavy isotope labeling

A set of shake flask experiments was carried out at 37 °C for the production of single, double, and triple-labeled (¹⁵N, ¹³C and ²H) hPrP using *E. coli* BI21 (DE3) as expression host (details for production are given in Fig. 2.3.1). When labeling was performed in autoinduction medium (only ¹⁵N and/or ²H labeling) or by medium exchange and IPTG induction (¹³C labeling alone or in combination with ¹⁵N and/or ²H labeling), final OD values reached OD₆₀₀ ~16 or ~12, respectively (Fig. 2.3.2). The expression level and the final biomass yields were not affected by the different labeling strategies and the target protein reached ~21% of the total cell protein (Fig. 2.3.2). Even deuterium labeling did not cause a decrease in the expression level and final biomass yield although cells grew

considerably slower in D₂O compared to H₂O. For example, the growth rate of *E. coli* BL21 (DE3) decreased by 60% at 37 °C when the medium was prepared with D₂O instead of H₂O.

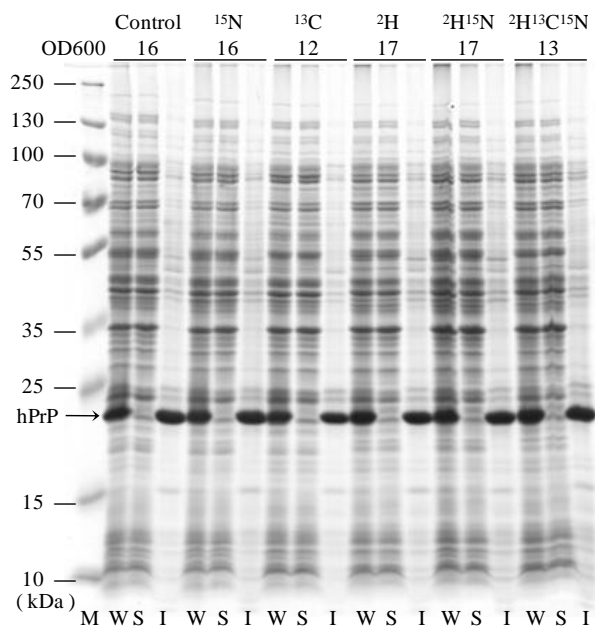


Fig. 2.3.2 Heavy isotope labeling of hPrP protein

Cells were grown at 37 °C in labeling medium and protein production analyzed by SDS-PAGE. The labeling strategies and final cell densities (OD600) are indicated on *top* of the figure. The analyzed cell fractions are indicated below (*W* whole cell protein, *S* soluble part, *I* insoluble part of whole cell protein, *M* Marker)

The overall labeling efficiency for the different isotopes and isotope combinations was determined from five peptides which cover 38% of the hPrP protein sequence (Table 2.3.2). Details of the isotopic distribution are shown in the mass spectrum of the most representative peptide (Fig. 2.3.3). For ¹⁵N labeling, 99% labeling was achieved using autoinduction. For ¹³C labeling, 97% labeling was achieved with medium exchange and IPTG induction. This slight reduction in ¹³C labeling efficiency was caused because cells were grown on non-labeled glucose before they were transferred into fresh labeling medium containing IPTG and ¹³C glucose. However, this overall high-label content also shows that the turnover of ¹²C-carbon from cells pre-grown on ¹²C glucose to the newly synthesized target protein was lower than 4%.

For mono ²H or combined ²H and ¹⁵N labeling, cells were grown in the presence of more than 98% D₂O using autoinduction medium. The overall labeling efficiency for deuterium was determined as 58% (Table 2.3.2). This seemingly low label incorporation was obtained because all analytical procedures after cell harvest were performed in H₂O instead of D₂O (e.g., SDS-PAGE, sample preparation for MALDI-TOF analysis). Deuterium at exchangeable hydrogen positions in deuterated proteins (peptides) will exchange to protium (¹H) in the presence of excess H₂O. Thus, the obtained overall labeling efficiency

of deuterium of 58% needs to be corrected to obtain the true labeling efficiency at non-exchangeable hydrogen positions (identical to the true labeling efficiency of all hydrogen positions directly after cell harvest before further sample processing). These corrections revealed a true labeling efficiency for deuterium of 75%. This lower labeling efficiency for deuterium compared to the other heavy isotopes was caused by the utilization of non-deuterated substrates (e.g., carbon substrates) which are incorporated into the biomass and target protein.

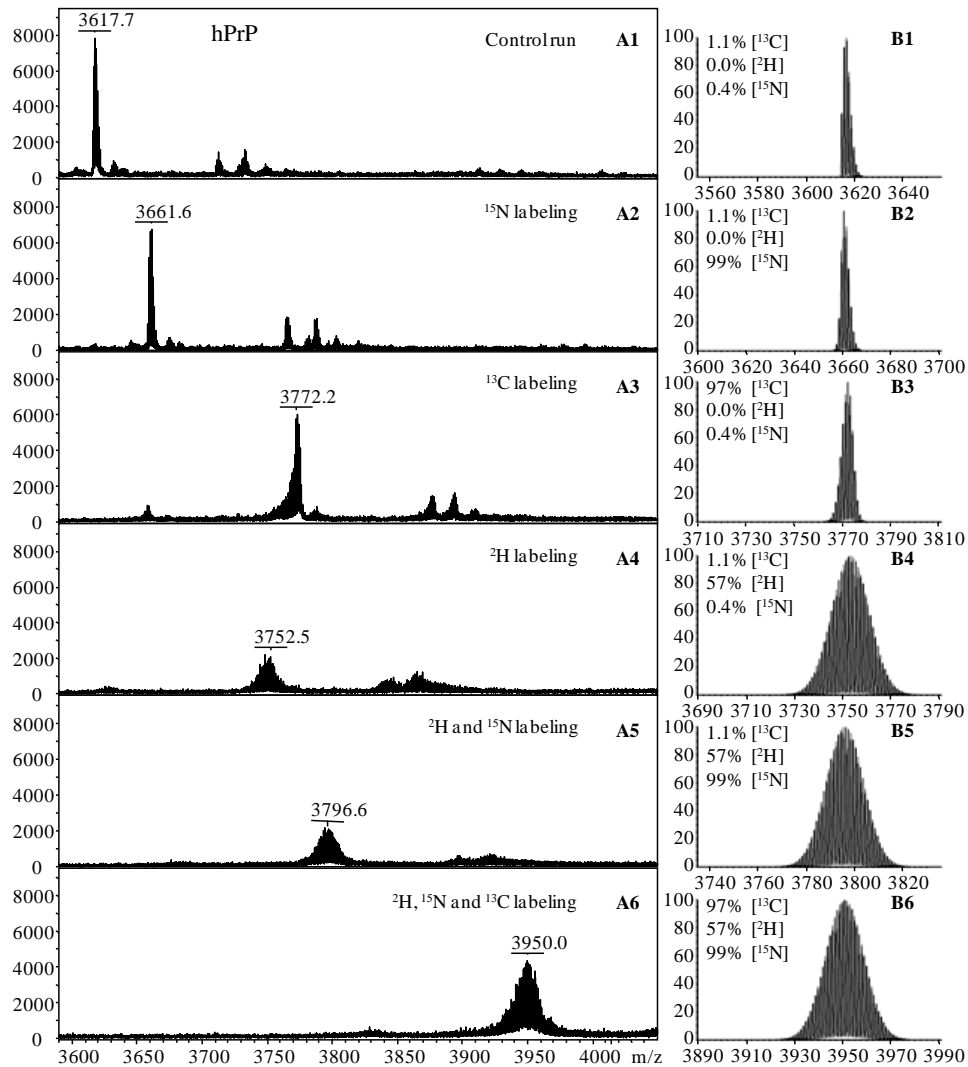


Fig. 2.3.3 Mass spectra of representative hPrP peptide after heavy isotope labeling

a Experimental mass spectra of the YPNQVYYRPVDQYNNQNNFVHDC_(CAM)VNITIK peptide resulting from different heavy isotope labeling strategies (indicated in the right upper corner of each panel). **b** Theoretical mass spectra of the YPNQVYYRPVDQYNNQNNFVHDC_(CAM)VNITIK peptide (Formula: C₁₆₁H₂₃₆N₄₅O₄₉S₁) at different isotope abundances (indicated in the *left upper corner* of each panel). The y-axis of each panel indicates the relative abundance of MS peaks and the x-axis indicates the mass/charge (m/z) ratio. C_(CAM) carbamidomethyl cysteine

Table 2.3.2 Heavy isotope labeling efficiency of hPrP

Peptide fragment in hPrP	¹⁵ N	¹³ C	² H	² H and ¹⁵ N	² H, ¹⁵ N and ¹³ C			
	Labeling	Labeling	labeling	labeling	labeling			
	Labeling efficiency (%)							
	¹⁵ N	¹³ C	² H	² H	¹⁵ N	² H	¹⁵ N	¹³ C
YPGQGSPGGNR	99	98	54 ^a (75 ^b)	54 ^a (75 ^b)	99	54 ^a (75 ^b)	99	98
YPNQVYYR	99	98	54 ^a (70 ^b)	54 ^a (70 ^b)	99	54 ^a (70 ^b)	99	98
VVEQMCTTQYQK	99	97	59 ^a (77 ^b)	59 ^a (77 ^b)	99	59 ^a (77 ^b)	99	97
HMAGAAAAGAVVG GLGGYMLGSAMSR	99	98	63 ^a (79 ^b)	63 ^a (75 ^b)	99	63 ^a (75 ^b)	99	98
YPNQVYYRPVDQYN NQNNFVHDCVNITIK	99	97	57 ^a (75 ^b)	57 ^a (75 ^b)	99	57 ^a (75 ^b)	99	97
Overall hPrP (approximate)	99	97	58 ^a (75 ^b)	58 ^a (75 ^b)	99	58 ^a (75 ^b)	99	97

^a Labeling efficiency for deuterium as determined by MALDI-TOF MS

^b Corrected as true labeling efficiency at non-exchangeable hydrogen positions

For double- and triple-labeling, the labeling efficiency for each isotope was the same as for mono-labeling. However, for combined ¹³C and ¹⁵N labeling, cells should be pre-grown on ¹⁵NH₄Cl before they are transferred to fresh labeling medium containing IPTG, ¹⁵NH₄Cl and ¹³C glucose, otherwise the ¹⁵N labeling efficiency will decrease to 95%. The turnover of nitrogen from cells pre-grown on non-labeled nitrogen to the newly synthesized target protein is higher than the carbon turnover as nitrogen is always recycled and carbon partially lost as carbon dioxide.

The general applicability of this labeling approach was tested for the production of two more proteins using T7-based expression systems. Moreover, proteins were chosen which can be produced as soluble protein but also in form of inclusion bodies to examine if label incorporation is different in soluble and aggregated proteins (Fig. 2.3.4). The results of these studies revealed that the labeling efficiency was independent of the protein being produced and, moreover, identical in both the soluble and aggregated fraction (Table 2.3.3 and Fig. 2.3.5).

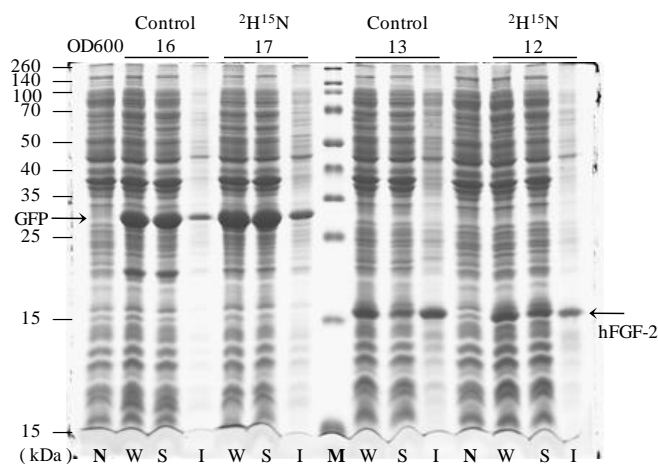


Fig. 2.3.4 Heavy isotope labeling of GFP and hFGF-2

Cells were grown at 30 °C in labeling medium and protein production analyzed by SDS-PAGE. The labeling strategies and final cell densities (OD600) are indicated on top of the figure. The analyzed cell fractions are indicated below (*W* whole cell protein, *S* soluble part, *I* insoluble part of whole cell protein, *M* marker, *N* non-induced negative control)

Table 2.3.3 Heavy isotope labeling efficiency of hFGF-2 and GFP

Peptide fragment in hFGF-2	^2H and ^{15}N labeling efficiency (%)		Peptide fragment in GFP	^2H and ^{15}N labeling efficiency (%)	
	^2H	^{15}N		^2H	^{15}N
YLAMKEDGR	63 ^a (82 ^b)	99	FEGDTLVNR	61 ^a (80 ^b)	99
IHPDGRVDGVR	64 ^a (81 ^b)	99	SAMPEGYVQER	60 ^a (77 ^b)	99
GVVSIKGVCANR	61 ^a (78 ^b)	99	AEVKFEGDTLVNR	61 ^a (79 ^b)	99
YTSWYVALKR	60 ^a (74 ^b)	99	GIDFKEDGNILGHK	59 ^a (76 ^b)	99
CVTDECFEER	59 ^a (75 ^b)	99	LEYNYNshNVYITADKQK	58 ^a (75 ^b)	99
Overall hFGF-2 (approximate)	61 ^a (78 ^b)	99	Overall GFP (approximate)	60 ^a (77 ^b)	99

^a Labeling efficiency for deuterium as determined by MALDI-TOF MS.

^b Corrected as true labeling efficiency at non-exchangeable hydrogen positions.

2.3.4.3 Selenomethionine labeling

Se-Met is toxic for *E. coli*, thus a similar labeling strategy with medium exchange was chosen as used for generating ^{13}C -labeled proteins. Cells were first grown on non-inducing medium which was supplemented with 250 mg L⁻¹ methionine to suppress the methionine biosynthesis pathway. Thereafter, cells were collected by centrifugation and resuspended in fresh medium containing IPTG, glucose as carbon substrate and Se-Met (experimental details are given in Fig. 2.3.1). Production of hPrP was studied in media supplemented with different Se-Met concentrations using the methionine prototrophic strain *E. coli* B121

(DE3) and the auxotrophic strain T7 Express Crystal (Fig. 2.3.6). The final cell densities and expression yields (OD600 ~10 and 22% hPrP of total cell protein) was independent on the Se-Met concentration (25–200 mg L⁻¹) for *E. coli* BL21 (DE3). However, for the auxotrophic strain T7 Express Crystal a strong influence of the Se-Met concentration on the final biomass yield and expression level was observed (Fig. 2.3.6). For this strain, the final biomass and the target protein expression level increased with increasing Se-Met concentration (up to 150 mg L⁻¹) reaching a maximum of OD600 ~20 and 17% hPrP of total cell protein, respectively. Compared to the methionine prototrophic stain *E. coli* BL21 (DE3), the methionine auxotrophic strain (T7 Express Crystal) exhibited a higher tolerance towards the toxic Se-Met by reaching higher cell densities; however, the target protein expression level was lower.

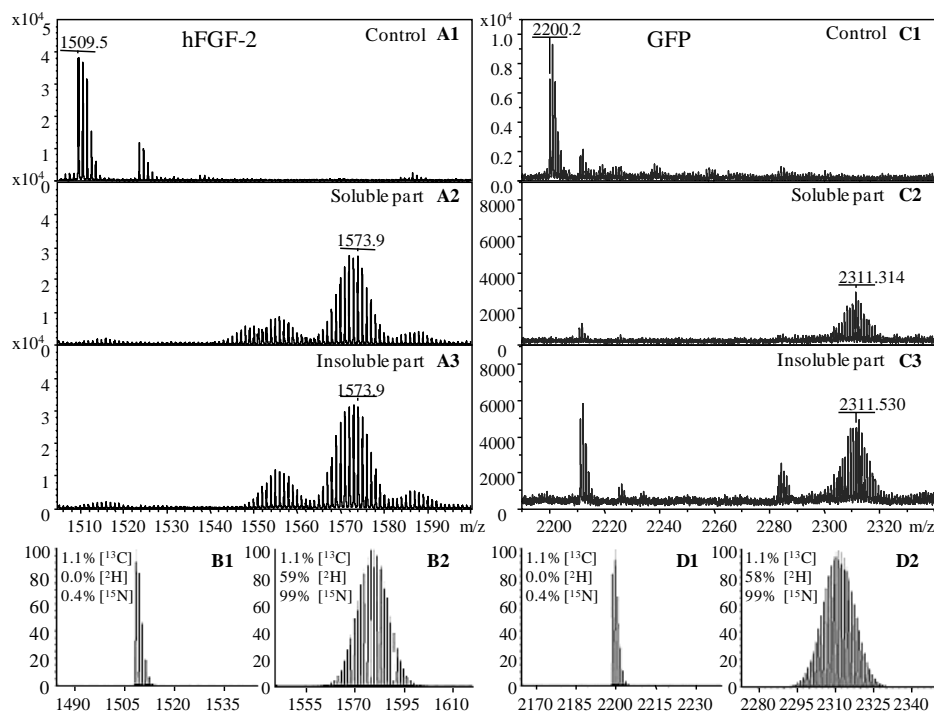


Fig. 2.3.5 Mass spectra of representative peptides of hFGF-2 and GFP after ²H and ¹⁵N double-labeling

a Experimental mass spectra of the C_(CAM)VTDEC_(CAM)FFFER peptide of hFGF-2: (A1) non-labeled hFGF-2, (A2) ²H-, and ¹⁵N-labeled in soluble and (A3) insoluble fraction of hFGF-2. **b** Theoretical mass spectra of the C_(CAM)VTDEC_(CAM)FFFER peptide (formula: C₆₂H₈₆N₁₄O₁₉O₂+ C₄H₆N₂O₂) of hFGF-2: (B1) non-labeling control and (B2) ²H- and ¹⁵N-labeled peptide. **c** Experimental mass spectra of the LEYNYNSHNVYITADKQK peptide of GFP: (C1) non-labeled GFP, (C2) ²H- and ¹⁵N-labeled in soluble and (C3) insoluble fraction of GFP. **d** Theoretical mass spectra of the LEYNYNSHNVYITADKQK peptide (formula: C₉₈H₁₄₆N₂₆O₃₂) of GFP: (D1) non-labeling control and (D2) ²H- and ¹⁵N-labeled peptide. The y-axis of each panel indicates the relative abundance of MS peaks and the x-axis indicates the mass/charge (m/z) ratio. C_(CAM) carbamidomethyl cysteine

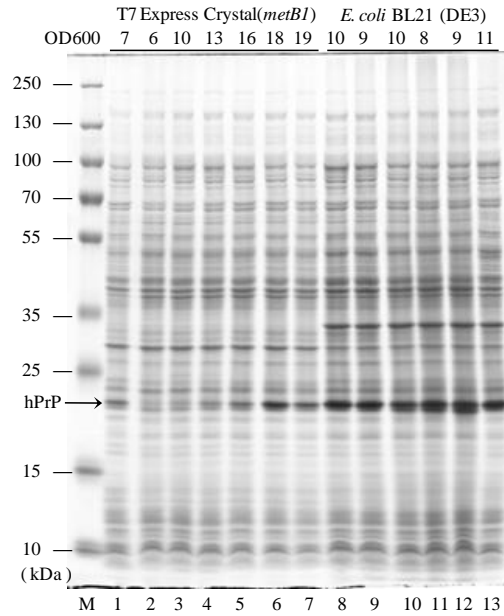


Fig. 2.3.6 Selenomethionine labeling of hPrP protein

Cells were grown at 37 °C in labeling medium and the whole cell protein analyzed by SDS-PAGE. The host strain and the final cell densities (OD600) are indicated on *top* of the figure. Lane numbers are indicated below. *M* marker; *lanes 1-7* hPrP produced in T7 Express Crystal (methionine auxotroph), *lane 1* positive control with 200 mg L⁻¹ methionine, *lane 2* negative control without methionine and Se-Met, *lane 3* 25 mg L⁻¹ Se-Met, *lane 4* 50 mg L⁻¹ Se-Met, *lane 5* 100 mg L⁻¹ Se-Met, *lane 6* 150 mg L⁻¹ Se-Met, *lane 7* 200 mg L⁻¹ Se-Met; *lanes 8-13* hPrP produced in *E. coli* BL21 (DE3), *lane 8* 25 mg L⁻¹ Se-Met, *lane 9* 50 mg L⁻¹ Se-Met, *lane 10* 100 mg L⁻¹ Se-Met, *lane 11* 150 mg L⁻¹ Se-Met, *lane 12* 200 mg L⁻¹ Se-Met, *lane 13* positive control with 200 mg L⁻¹ methionine

Table 2.3.4 Se-Met labeling efficiency of hPrP in *E. coli* BL21 (DE3)

Peptide fragment in hPrP	Se-Met labeling efficiency at different Se-Met concentration			
	50 mg L ⁻¹	100 mg L ⁻¹	150 mg L ⁻¹	200 mg L ⁻¹
VVEQM <u>C</u> TTQYQK	33%	50%	75%	70%
P <u>M</u> M <u>H</u> FGNDWEDRYR	56%	55%	77%	74%
H <u>M</u> AGAAAAGAVVGG <u>L</u> GGY <u>M</u> LGSAM <u>S</u> R	43%	62%	67%	70%
Overall hPrP (approximate)	45%	55%	70%	70%

Table 2.3.5 Se-Met labeling efficiency of hPrP in T7 Express Crystal

Peptide fragment in hPrP	Se-Met labeling efficiency at different Se-Met concentration			
	50 mg L ⁻¹	100 mg L ⁻¹	150 mg L ⁻¹	200 mg L ⁻¹
YYERN <u>M</u> NR	74%	68%	88%	95%
VVEQM <u>C</u> TTQYQK	74%	83%	81%	89%
P <u>M</u> M <u>H</u> FGNDWEDR	72%	69%	83%	86%
GENFTETDIK <u>I</u> MER	86%	91%	90%	92%
Overall hPrP (approximate)	75%	75%	85%	90%

The overall Se-Met labeling efficiency of hPrP produced in *E. coli* BL21 (DE3) and T7 Express Crystal was determined from three and four peptides, respectively, containing at least five of the nine methionines of hPrP (Tables 2.3.4 and 2.3.5, respectively). Details of the isotopic distribution are shown in the mass spectra of two representative peptides (Fig. 2.3.7). For *E. coli* BL21 (DE3), the Se-Met labeling efficiency increased from 45% to 70% with increasing Se-Met concentration reaching the maximum efficiency of 70% at 150 or 200 mg L⁻¹ Se-Met (Table 2.3.4). For *E. coli* T7 Express Crystal, higher labeling efficiencies were achieved, increasing from 75% to 90% with increasing Se-Met concentration and reaching the highest efficiency of 90% at 200 mg L⁻¹ Se-Met (Table 2.3.5).

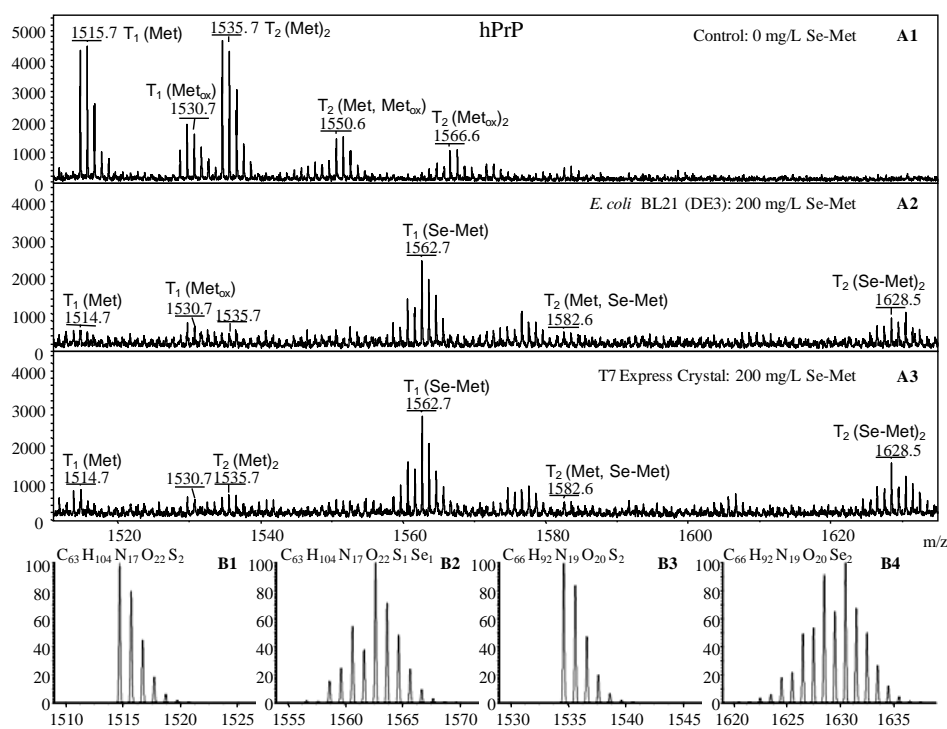


Fig. 2.3.7 Mass spectra of two representative hPrP peptides after Se-Met labeling

a Experimental mass spectra of T₁: “VVEQMC_(CAM)TTQYQK” and T₂: “PMMHFGNDWEDR” peptides.
b Theoretical mass spectra of the T₁ peptide: (B1) VVEQMC_(CAM)TTQYQK (m/z 1,515.7, T₁[Met]) and (B2) VVEQM_(Seleno)C_(CAM)TTQYQK (m/z 1,562.7, T₁[Se-Met]). Theoretical mass spectra of the T₂ peptide: (B3) PMMHFGNDWEDR (m/z 1,535.7, T₂[Met]₂) and (B4) PM_(Seleno)M_(Seleno)HFGNDWEDR (m/z 1,628.6, T₂[Se-Met]₂). The host strain and Se-Met concentrations in the labeling medium are indicated in the right upper corner of each panel. The y-axis of each panel indicates the relative abundance of MS peaks and the x-axis indicates the mass/charge (m/z) ratio. *Met* methionine, *Met*_{ox} oxidized methionine, *Se-Met* and *M*_(Seleno) Selenomethionine, *C*_(CAM) carbamidomethyl cysteine

2.3.5 Discussion

A unified protocol based on a modular system for production of labeled proteins using *E. coli*-based expression systems was developed. This protocol can be used to efficiently produce heavy isotope (mono- or multiple-incorporations of ^2H , ^{13}C , and ^{15}N) as well as Se-Met-labeled proteins with high-label content. The labeling efficiency reached 99% and 97% for ^{15}N and ^{13}C -labeling, respectively. The ^{13}C -labeling efficiency can be further increased when cells are pre-cultured on labeled glucose prior to induction of labeled protein production. The labeling efficiency for deuterated proteins was at least 75% with 80% as the theoretical maximal ^2H labeling efficiency when using non-deuterated carbon substrates. Incorporation of 99% deuterium can only be achieved when deuterated carbon substrates are used [40]. We also show that double- and triple-heavy isotope labeling did not change the labeling efficiency achieved by mono-labeling. Moreover, the labeling efficiency was independent of the target protein and identical for soluble and aggregated proteins. However, for the production of soluble proteins, it might be necessary to use lower culture temperatures during labeling. Labeling efficiency for Se-Met incorporation was 70% using the conventional *E. coli* strain BL21 (DE3) or increased to 90% using the methionine auxotrophic strain T7 Express Crystal. Incorporation of other labeled amino acids is possible by employing the appropriate labeled amino acid and the corresponding auxotrophic host strain. The target protein expression level as well as its solubility is characteristic for each protein; however, expression yields and solubility in labeling medium were not different from those obtained in non-labeling medium. Final cell densities and product titers for all labeling purposes were the most efficient so far reaching for deuterated proteins ~4 times higher levels as in previously published protocols.

2.3.6 Acknowledgements

We are most grateful to Thorsten Lührs who pointed our attention to the great need of the “protein structure community” for efficient protein labeling protocols and also for kindly providing the expression vector pET-15b-hPrP. Special thanks are also given to Thorsten Lührs and Konrad Büssow for valuable suggestions. Partial support of the FORSYS Partner Project: “Dynamics and regulation of the metabolic balance in *Escherichia coli*” is greatly acknowledged.

2.4 Summary and conclusion

A defined autoinduction medium was developed with very high final biomass concentrations (OD₆₀₀ >20). The expression level is similar as in LB medium with conventional IPTG induction. The universal applicability of the medium has been proved with different T7-based *E. coli* expression systems. Moreover, the application scalability has been successfully tested at different temperatures from 23 °C to 37 °C using microtiter plates, test tubes, shake flasks and bioreactors.

Following, a set of modular defined media for heavy isotopes as well as for Se-Met labeling was developed with easy experimental handling and high reproducibility. The methods have been tested for ²H, ¹³C, and ¹⁵N labeling leading to heavy isotope incorporation of ~75%, ~99%, and 99%, respectively, with three different target proteins. Se-Met labeling was proved to work both with methionine-auxotrophic and prototrophic *E. coli* leading to Se-Met incorporation of ~90% and ~70%, respectively.

2.5 Outlook

Two major bottlenecks for recombinant protein production in *E. coli* are the solubility of target protein and the final biomass, i.e. the final protein concentration. Current analyses indicate that the insoluble target protein (or inclusion body) formation during the cultivation using defined medium (S-DAB or DNB) is higher than using complex medium (LB medium). Conversely, the final biomass is much lower when using LB medium than using S-DAB or DNB medium.

The shortage of molecular chaperones and overflow metabolism of acetate (the growth-inhibiting by-product) are probably the reason for inclusion body formation and low final biomass yields, respectively. When the traditional process optimization reaches the bottleneck, there is a need for a deeper level of understanding of the molecular bottlenecks of recombinant protein production.

To reveal the corresponding bottlenecks at the molecular level, two comprehensive proteomic analyses of *E. coli* under recombinant protein production and non-production conditions in defined and complex media have been carried out as shown in the following chapter.

3 A comprehensive proteomic study of *Escherichia coli*

3.1 Introduction

In this chapter, two comprehensive proteomic analyses were carried out for *E. coli* grown in defined and complex media at exponential and stationary phases under recombinant protein production and non-production conditions.

Based on the first proteomic analysis under non-production condition, the regulatory basis of acetate overflow metabolism under nutrient-rich condition is shown first, and then the self-protection mechanism under insufficient nutrient condition is analyzed. The second proteomic analysis indicates that this self-protection mechanism breaks down when the cell is forced to overproduce a recombinant protein.

3.2 A comprehensive proteomic study I. Regulation of acetate overflow metabolism in *Escherichia coli* under nutrient-rich condition

3.2.1 Abstract

By the methods of two-dimensional gel electrophoresis and mass spectrometry, a comprehensive *Escherichia coli* proteomic analysis of the central metabolic pathways (CMPs), oxidative phosphorylation and synthesis of biomass building blocks, was performed for *E. coli* grown in defined and complex media, to understand the regulatory mechanism of acetate overflow metabolism under a nutrient-rich condition (i.e. growth in complex medium). During exponential growth in complex medium in the presence of excess nutrients (e.g., amino acids or peptides), precursors and reducing equivalents generated by the CMPs are sufficient for cell growth. *E. coli* spontaneously reduces the synthesis of enzymes of the tricarboxylic acid cycle (TCA cycle) to decrease the generation of reducing equivalents and precursors. Simultaneously, the lower glycolysis enzymes are up-regulated in the absence of catabolite repression by glucose. In this situation, the lower glycolytic pathway does not coincide with the TCA cycle capacity, which leads to the acetate overflow metabolism. At the transition into stationary phase facing nutrient depletion in the complex medium, the acetate can be completely re-assimilated through the up-regulated acetyl-coenzyme A synthetase (Acs) and TCA cycle enzymes.

Keywords *Escherichia coli* proteome · Central metabolic pathways · Overflow metabolism · Acetic acid · Two-dimensional gel electrophoresis · Defined medium · Complex medium

3.2.2 Introduction

Acetate is the major by-product, when *E. coli* is grown at a high rate of substrates consumption even in the presence of abundant oxygen [14-16]. For many years, it has been regarded as a negative effect in many fields of modern microbiology and biotechnology [17-21]. It was found that when loads are imposed and flux constraints exist either at the level of NADH turnover rate or the activity of TCA cycle, switching to acetate overflow is predicted [48]. The Arc two component system, the aerobic respiration control protein (ArcA) and its sensor protein (ArcB), has been proved to be the mediator between the NADH turnover rate and the TCA cycle activity [54-58]. It was observed that the *arcA* deletion mutant shows a higher TCA cycle activity, lower acetate formation rate [59, 60] and even a lower substrate yield coefficient for glucose compared to the wild-type strain [59]. These findings suggest that acetate may play a key role in keeping the balance of fast and efficient growth.

Acetate locates at the centre of central metabolic pathways (CMPs). The monomers, such as amino acids, for the synthesis of cellular macromolecules, such as proteins, are made from a relatively small group of precursors that are the products of the CMPs, indicating a direct relation between acetate overflow metabolism and synthesis of biomass building blocks [49]. Another important factor is that NAD(P)H generated by CMPs is also required for the monomers biosynthesis, especially for the amino acids [50], which implies an association between synthesis of biomass building blocks and NADH turnover rate. Owing to the complexity of intracellular metabolic networks and also the extracellular environment, the understanding of the synergetic regulation between CMPs, oxidative phosphorylation and biomass block biosynthesis is still ambiguous. As metabolic pathways are networks of enzymatic reactions, a comprehensive proteomic study will greatly help to disclose the corresponding regulatory mechanism of CMPs and the acetate overflow metabolism.

E. coli is probably the best understood of the simple model organisms, with fully sequenced genome which makes it accessible for comprehensive proteomic analysis [97-100]. Most of the modern proteomic studies were carried out with *E. coli* K-12 strains [97-100, 130-133]. But it was found that less acetate is produced by *E. coli* B strains compared to K-12 strains [134, 135] which could be explained by more active glyoxylate shunt, TCA cycle, and higher acetate uptake [136, 137]. In addition to the existing literature [93, 138-140], there is still a great need for a more detailed report on the global physiological analysis at the proteome level for the *E. coli* B strains.

It was found that when growing at maximum growth rate in complex medium *E. coli* produces more acetate than in defined medium [7, 16, 21]. For clarification, a comprehensive proteomic analysis was carried out for *E. coli* BL21 (DE3) grown in defined and complex media using 2-D gelelectrophoresis in combination with mass

spectrometry for protein identification. The molecular regulatory basis of the CMPs, oxidative phosphorylation and synthesis of biomass building blocks is investigated. Two major proteomic comparisons are explored: first, the proteomic difference between *E. coli* grown in defined and complex media at exponential phase (also referred to as log phase) is investigated to illustrate why acetate is produced in complex medium during exponential growth; secondly, the proteomic difference between *E. coli* grown at stationary and exponential phases in complex medium is used to show how acetate is re-assimilated at the early stationary phase.

3.2.3 Materials and methods

3.2.3.1 Strain, media and cultivation conditions

E. coli BL21 (DE3) (Novagen, Germany) was used. The composition of Luria-Bertani (LB) medium is as follows: 10 g L⁻¹ tryptone, 5 g L⁻¹ yeast extract, 5 g L⁻¹ NaCl. The composition of Terrific-Broth (TB) medium is as follows: 12 g L⁻¹ tryptone, 24 g L⁻¹ yeast extract, 5 g L⁻¹ glycerol, 2.31 g L⁻¹ KH₂PO₄, 12.54 g L⁻¹ K₂HPO₄. The composition of Defined Non-inducing Broth (DNB) is as follows: 10.91 g L⁻¹ glucose, 4 g L⁻¹ (NH₄)₂HPO₄, 13.3 g L⁻¹ KH₂PO₄, 1.55 g L⁻¹ Citric acid, 0.59 g L⁻¹ MgSO₄, 100.8 mg L⁻¹ Fe(III) citrate, 2.1 mg L⁻¹ Na₂MoO₄·2H₂O, 2.5 mg L⁻¹ CoCl₂·6H₂O, 15 mg L⁻¹ MnCl₂·4H₂O, 1.5 mg L⁻¹ CuCl₂·2H₂O, 3 mg L⁻¹ H₃BO₃, 33.8 mg L⁻¹ Zn(CH₃COOH)₂·2H₂O, 14.10 mg L⁻¹ Titriplex III. The pH of all media was adjusted to 6.8 by NaOH before sterilization. Cultivations were carried out in duplicate using 2 L Erlenmeyer flasks with three baffles containing 200 mL medium at 37 °C and 180 rpm (Multitron Cell, INFORS HT, Switzerland). Cell growth was monitored by measurement of the absorbance at 600 nm (OD₆₀₀) (WPA CO8000 Cell Density Meter, Biochrom, UK). Acetate was analyzed by an acetic acid kit (Cat. No. K-ACETRM, Megazyme, Ireland). Culture samples at exponential phase and stationary phase were centrifuged at 17,000 g and 4 °C for 3 min. After removal of the supernatant, cell pellets were stored at -80 °C until further analysis. Details about medium preparation and culture conditions have been described previously [110, 141].

3.2.3.2 Two-dimensional gel electrophoresis

Cell pellets were disrupted by BugBuster™ Protein Extraction Reagent (Novagen, USA) with rLysozyme and Benzonase according to manufacturer's instructions. Whole cell protein in the BugBuster suspension (without centrifugation) was precipitated as described previously [142]. The protein pellets were solubilized in rehydration solution with IPG buffer (GE Healthcare, UK). About 280 µg of each protein sample were loaded onto Immobiline DryStrip gels of pH 3-10 NL (GE Healthcare, UK). The first-dimension using isoelectric focusing (IEF) and second dimension using SDS-PAGE (10-15% gradient gel)

were run with the IPGphor™ Isoelectric Focusing System and Hoefer™ DALT System (GE Healthcare, UK), respectively. The detailed experimental conditions were according to manufacturer's instructions and as described before [126] (For details refer to section 5.1.1 in the Appendix). Coomassie stained gels [115] were analyzed using Proteomweaver™ 4.0 (Bio-Rad, USA) for protein spot detection, matching and quantification. For each sample, 2D gels were made in triplicate. The best two gels were analyzed by Proteomweaver™ 4.0. Each spot's intensity was normalized by the whole spots intensity on the same 2D gel. The corresponding average of the resulting percentage value from the duplicate gels was used for indication of the spot's protein portion (%) of the whole cell protein mass (WCPM). The total "WCPM %" of all spots representing the same protein was used for indicating the abundance of the corresponding protein.

3.2.3.3 Protein identification and classification

Protein spots were identified by matrix-assisted laser desorption ionization time-of-flight mass spectrometry (MALDI-TOF MS). Protein spots were excised manually from 2D gels. After washing, reduction and alkylation, in-gel digestion was carried out by incubation with sequencing grade trypsin (Promega, USA). Obtained peptides were extracted and purified with reversed-phase C18 ZipTips (Millipore, USA). Desalted peptide solutions were mixed with the saturated matrix solution and spotted onto a 384 MTP target and dried at room temperature. Bruker Ultraflex time-of-flight mass spectrometer (Bruker Daltonics GmbH, Germany) was employed to obtain peptide mass fingerprints. The detailed protocol was as described previously [126, 127] (For details refer also to section 5.1.2 in the Appendix). The MASCOT search program (Matrix Science, UK) was used for protein identification based on the annotated *E. coli* genome [Uniprot (<http://www.uniprot.org/>) serving as database]. All proteins with a Mowse score greater than 54 were regarded as significant ($p < 0.05$).

EcoCyc (<http://ecocyc.org/>) database [143] was mainly used for classification of identified proteins. The classification was confirmed by KEGG (<http://www.genome.jp/kegg/>) database [144]. The information on transcriptional regulation of identified proteins (genes) was mainly acquired from RegulonDB (<http://regulondb.ccg.unam.mx/>) database [145].

3.2.4 Results

3.2.4.1 Growth kinetics in defined and complex media

In complex medium (e.g. Luria-Bertani broth or Terrific-Broth which contains tryptone, a pancreatic digest of casein, and yeast extract, the water soluble portion of autolyzed yeast), different nutrients, e.g. sugars, alcohols, and organic acids, amino acids, peptides and nucleotides, will support a high growth rate of *E. coli*. Comparatively, defined medium (e.g. M9 or DNB medium, in which glucose, NH_4^+ , PO_4^{3-} and SO_4^{2-} are the sole carbon,

nitrogen, phosphorus and sulfur sources, respectively) requires *E. coli* to synthesize all cellular components.

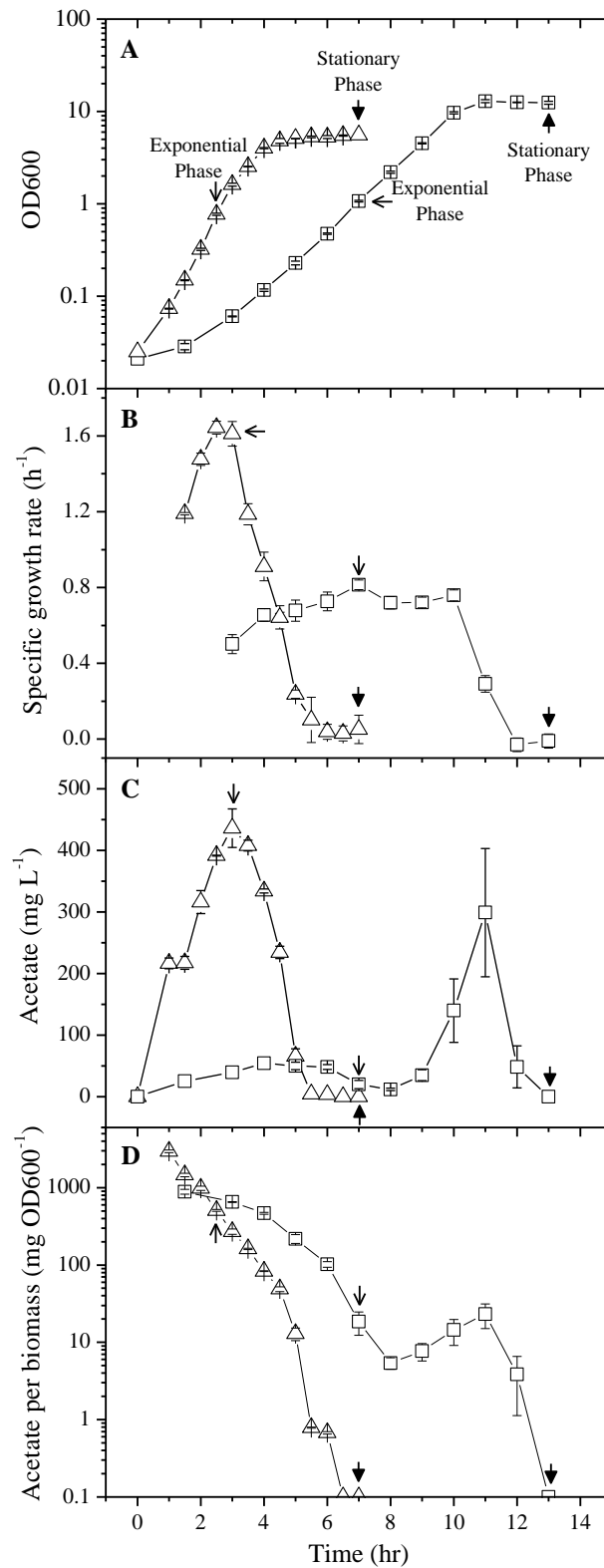


Fig. 3.2.1 Growth and acetate metabolism of *E. coli* BL21 (DE3)

Cultivations were carried out in shake flasks using DNB (square) and LB medium (triangle) at 37 °C. Samples for 2D gel electrophoresis analysis were taken at the time points indicated by arrows.

The growth of *E. coli* BL21 (DE3) at 37 °C in DNB and LB media is shown in Fig. 3.2.1A with maximum specific growth rates of 0.8 h⁻¹ and 1.5 h⁻¹, respectively (The growth in TB medium is shown in the Appendix). During growth in defined medium cells exhibited a nearly constant specific growth rate during the exponential phase. During growth in complex medium, the specific growth rate gradually decreased as shown in Fig. 3.2.1B. This occurs because *E. coli* reveals a sequential mode of substrate utilization in complex medium [9-11].

Excreted acetate concentration is shown in Fig. 3.2.1C. In LB medium acetate is produced during exponential growth of *E. coli*. The maximum acetate concentration is about 440 mg L⁻¹ when OD600 is 1.6. From the late exponential phase acetate starts to decrease to zero at early stationary phase. In LB medium no oxygen limitation was observed during the whole course of cultivation (i.e. dissolved oxygen did not drop below 30% of saturation; data not shown). In DNB medium at exponential phase, acetate remains at very low level (< 50 mg L⁻¹). During the transition from late exponential phase to early stationary phase, acetate increases to about 300 mg L⁻¹ when OD600 is 13. The excreted acetate decreases quickly to zero at stationary phase. In DNB medium, no oxygen limitation was observed at the exponential phase, but from late exponential phase to early stationary phase the dissolved oxygen dropped to zero for about 1 hour (data not shown). Fig. 3.2.1D shows that for *E. coli* growing in complex medium, the acetate excretion per biomass during exponential growth and the re-assimilation per biomass at the transition into stationary phase, are much higher than in defined medium.

3.2.4.2 Systematic and comparative proteome analysis

The whole cell proteome of *E. coli* BL21 (DE3) grown in defined (DNB) and complex (LB and TB) media at exponential and stationary phase was systematically analyzed. The proteomic data in LB and TB media are very similar, so an average from LB and TB media was used to represent a (unified) complex medium as shown in Suppl. Table 5.3.1. 516 spots were identified by MALDI-TOF MS representing 369 different proteins. These 369 proteins already cover approximately 80% of WCPM. All identified proteins were classified into 11 categories with 29 groups as shown in Suppl. Tables 5.3.1 and 5.3.2. Results of analysis were visualized and shown in Suppl. Figs 5.3.1-5.3.6. Annotated 2D gels are shown in the Suppl. Figs. 5.3.7-5.3.12. In this study, we focus on the proteomic differences in three functional categories at different growth stages and in defined and complex media: (I) carbohydrate metabolism (as shown in Fig. 3.2.2), (II) oxidative phosphorylation and (III) synthesis of biomass building blocks. Proteins involved in metabolite degradation, transportation, transcription, translation, protein folding and other processes are presented in chapter 3.3.

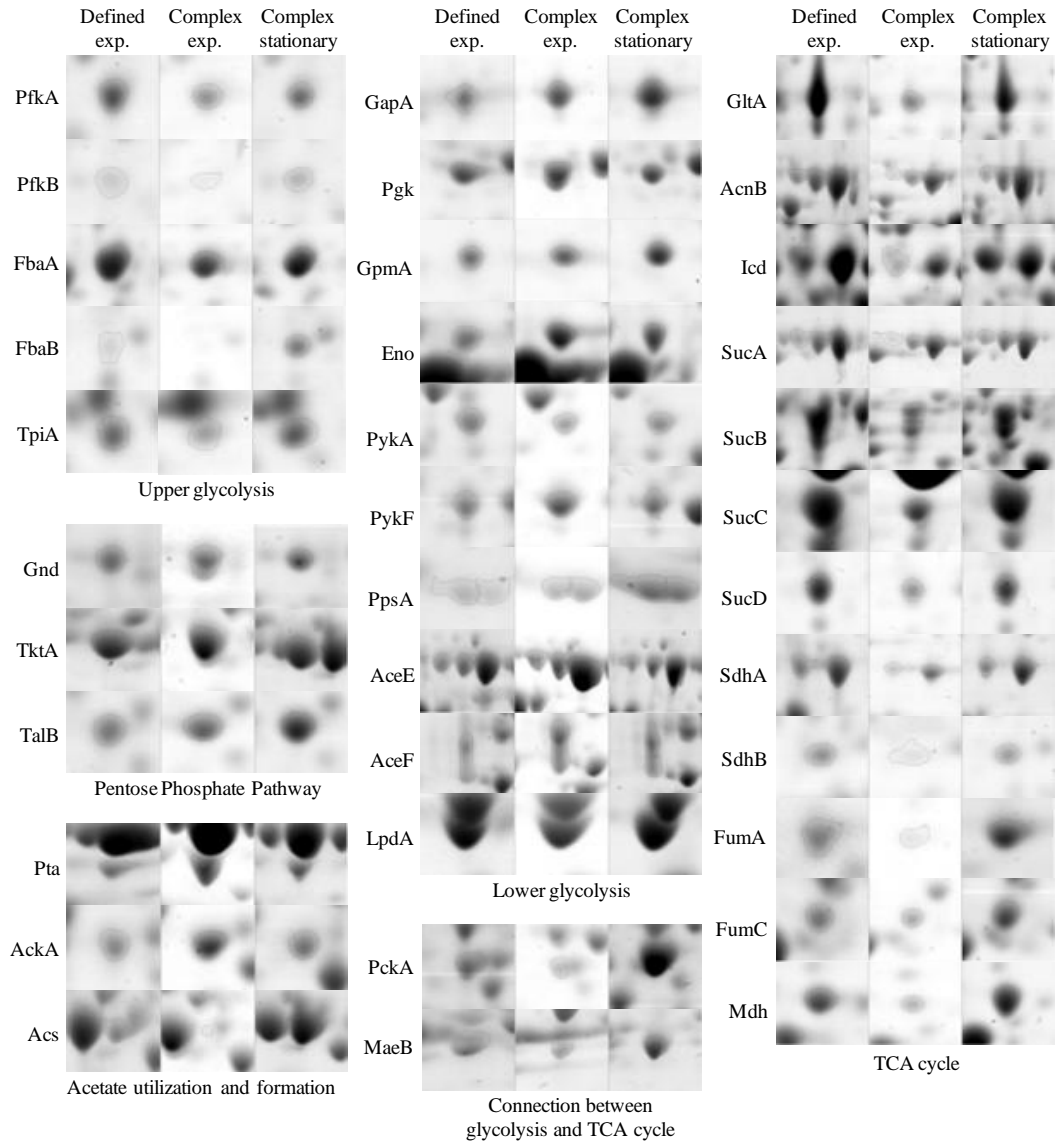


Fig. 3.2.2 Synthesis of central metabolic pathway related proteins at different conditions

Growth conditions are shown on the top: Defined exp., sample from cultivation in defined medium (DNB) at exponential phase; Complex exp., sample from cultivation in complex medium (LB) at exponential phase; Complex stationary, sample from cultivation in complex medium (LB) at stationary phase. Names of protein are marked at the left side. Pathway names are marked at the bottom. For details refer to Suppl. Figure 5.3.7-5.3.12.

3.2.4.3 Central carbon metabolism

At exponential phase, the synthesis of identified upper glycolysis proteins, PfkAB, FbaAB, and TpiA, is in general higher in defined medium than in complex medium, but for the 11 identified lower glycolysis proteins, nearly all of them are down-regulated in defined medium (as compared to complex medium) (Fig. 3.2.2 and 3.2.3A). In this study, the identified pyruvate dehydrogenase (AceEF) and dihydrolipoyl dehydrogenase (LpdA) are regarded as lower glycolysis proteins.

Gnd, TktAB, TalAB and Eda were identified from the pentose phosphate pathway (PPP). At exponential phase, except for TktB and TalA [which are isozymes of transketolase (TKT) and transaldolase (TAL), respectively], the rest of the identified proteins involved in PPP are all down-regulated in defined medium. In other words, proteins in PPP and lower glycolysis are higher in complex medium at exponential phase, which can lead to a higher level of carbon flux to the end of lower glycolysis (or before the TCA cycle, Fig. 3.2.4B) in complex medium.

When the cell reaches stationary phase, the identified proteins involved in glycolysis and PPP are generally up-regulated in all media (as compared to exponential phase) (Fig. 3.2.2, 3.2.3B and 3.2.3C).

The observed regulation of glycolysis proteins can be explained by the antagonistic regulation of two transcriptional regulators (Suppl. Table 5.3.3): catabolite repressor activator (Cra) [146] and cAMP receptor protein (CRP) [147]. Fructose-1-phosphate (F1P) or fructose-1,6-bisphosphate (FBP) inactivate Cra for relieving the repression of the majority of genes in glycolysis [148]. Glucose causes catabolite repression on many lower glycolysis genes by lowering the intracellular levels of CRP-cAMP [149].

At exponential phase in defined medium, the glucose concentration is high, which will lead to a high level of FBP (through the upper glycolysis pathway). The general up-regulation of upper glycolysis proteins in defined medium might be caused by relieving the catabolite repression exerted by Cra (Fig. 3.2.4A and 3.2.4B). At the same time, the catabolite repression by glucose, acting as an antagonist to the relieve of the catabolite repression by Cra, would be the reason for the down-regulation of lower glycolysis proteins in defined medium (Fig. 3.2.4A and 3.2.4B).

At stationary phase, the carbon sources are consumed. The catabolite repression by glucose is relieved. Simultaneously, Cra repression will be activated by the absence of inducers (F1P and FBP). But there is still another key factor controlling the regulation of glycolysis proteins at stationary phase: nearly all glycolysis genes are under the control of stationary phase sigma factor σ^S (Fig. 3.2.4C), as summarized in Suppl. Table 5.3.3. A general up-regulation of glycolysis proteins was clearly observed in stationary phase.

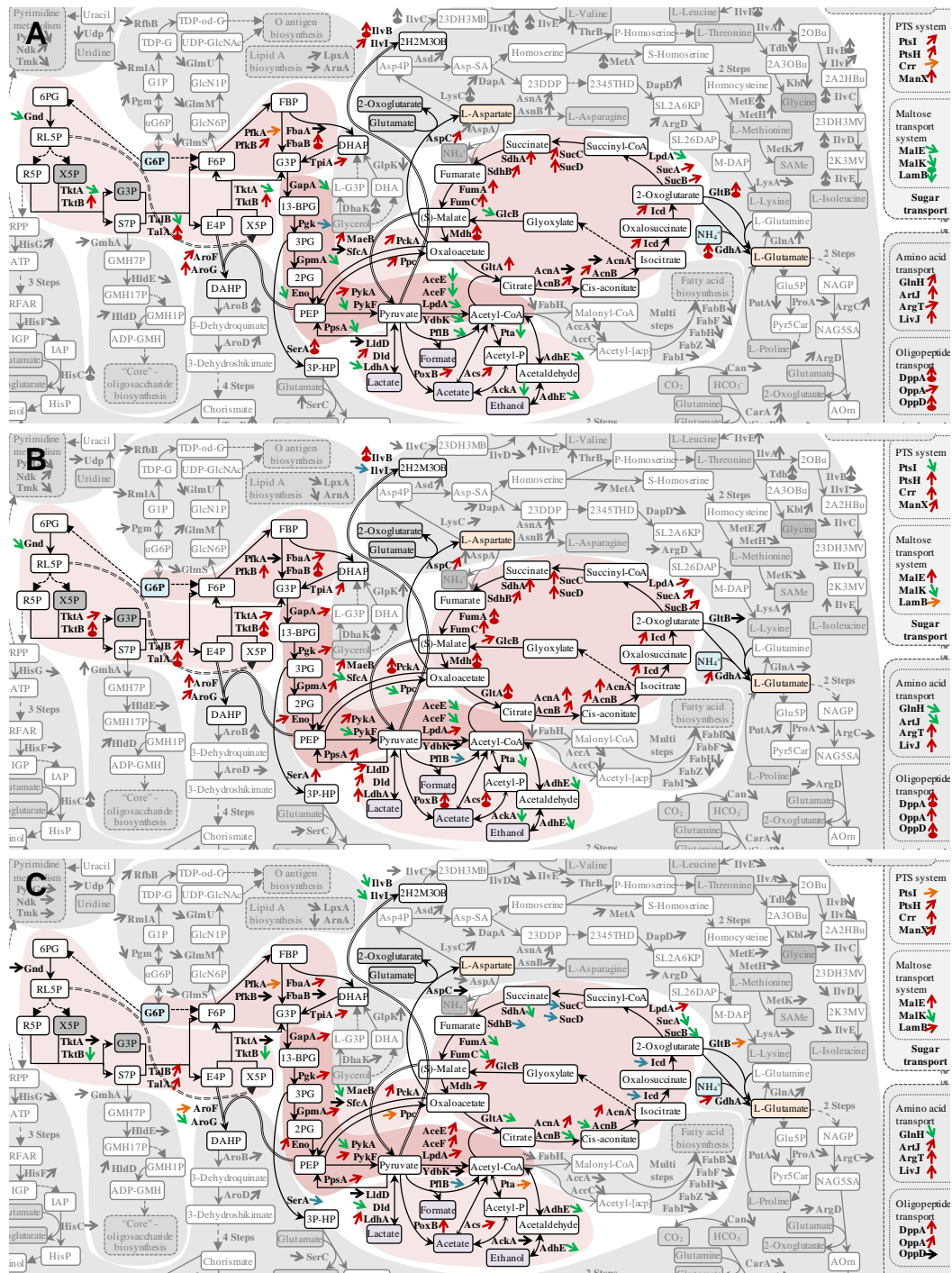


Fig. 3.2.3 Proteome comparison of *E. coli* grown in different conditions

A: Comparison between *E. coli* grown in defined/complex medium at exponential phase. B: Comparison between *E. coli* grown at stationary/exponential phase in complex medium. C: Comparison between *E. coli* grown at stationary/exponential phase in defined medium. Corresponding values of $\text{Log}_2(\text{defined/complex medium})$ at exponential phase (A), $\text{Log}_2(\text{stationary/exponential phase})$ in complex medium (B) and $\text{Log}_2(\text{stationary/exponential phase})$ in defined medium (C) as indicated by arrows are shown in Suppl. Table 5.3.1. DNB medium was employed to indicate the defined medium. An average of LB and TB media is calculated to represent complex medium. Figs. 3.2.3A, 3.2.3B and 3.2.3C are parts of Suppl. Figs. 5.3.1, 5.3.2 and 5.3.3, respectively. Abbreviations used in Fig. 3.2.3 are listed in Suppl. Abbreviation before Suppl. Figs. 5.3.1.

3.2.4.4 By-product metabolism

During growth of *E. coli*, acetate is produced as the the main by-product by PoxB or Pta-AckA pathway (Fig 1.3) [150]. The acetate can be converted back to Acetyl-CoA by Acs or by reversing the Pta-AckA pathway.

At exponential phase, Pta and AckA are down-regulated in defined medium (as compared to complex medium). At the same time, the PoxB is at very low level (less that 0.02% of WCPM), which is only about 5% of the amount of Pta and AckA. And the abundance of Acs is higher in defined medium than in complex medium at exponential phase (Fig. 3.2.3A).

When entering the stationary phase, the synthesis of Pta and AckA decreases in complex medium (Fig. 3.2.2, 3.2.3B and 3.2.3C). Simultaneously, Acs increases in all media. The proteomic results are compatible with the data shown in Fig. 3.2.2C: the Pta-AckA pathway (which is highly up-regulated in complex medium at exponential phase) functions primarily in a catabolic role, excreting acetate and generating ATP during aerobic growth on excess carbohydrates [137, 151]; in contrast, Acs (which is highly up-regulated at stationary phase) having a higher binding affinity towards acetate than AckA [152] mainly functions to metabolize extracellular acetate.

Ethanol can be produced by AdhE during anaerobic growth of *E. coli* [153]. AdhE is highly up-regulated in LB medium at exponential phase (no oxygen limitation was observed in the cultivation in LB medium; data not shown), which also indicates that the carbon flux exceeds the capacity of the CMPs in complex medium during exponential growth. Formate can be produced by PflB [154]. The regulatory pattern of PflB is similar to Pta and AckA. At exponential phase PflB is higher in complex medium. And it decreases in all media during entry into stationary phase. Fermentative lactate dehydrogenase can directly convert pyruvate to lactic acid [155]. At exponential phase the total amount of three identified lactate dehydrogenases (LldD, Dld and LdhA) is similar in all media, suggesting that in complex medium the excess of pyruvate is converted to acetate, formate and ethanol through acetyl-CoA by the higher level of AceEF, LpdA, Pta, AckA, AdhE and PflB. When *E. coli* reaches stationary phase, LldD, Dld and LdhA remain constant in defined medium but are up-regulated in complex medium, which could be caused by the reutilization of acetate in complex medium (discussed in the section 3.2.4.6).

3.2.4.5 TCA cycle

At exponential phase, the abundance level of 14 identified TCA cycle proteins is much higher in defined medium than in complex medium (Figs. 3.2.2 and 3.2.3A), which may be another important reason for the low- and high-level of acetate secretion in defined and complex media, respectively.

When bacteria reach stationary phase, nearly all of the TCA cycle proteins are highly up-

regulated in complex medium (Figs. 3.2.2, 3.2.3B and 3.2.3C). The reuse of formerly excreted acetate may play here an important role. But for *E. coli* grown in defined medium, TCA cycle proteins show a slight decrease at stationary phase.

The observed regulation of TCA cycle proteins can also be explained by the antagonistic regulation of two transcriptional regulators (Suppl. Table 5.3.3): phosphorylated-ArcA (P-ArcA) and CRP-cAMP. Oxidized forms of quinone electron carriers in the electron transport chain (oxidative phosphorylation) inhibit autophosphorylation of ArcB and therefore inhibit the transphosphorylation of ArcA. If quinones are present in the reduced form, ArcB undergoes autophosphorylation and then catalyzes the transphosphorylation of ArcA [54], which represses nearly all operons encoding TCA cycle proteins [156-159]. Glucose causes catabolite repression of most TCA cycle genes [158, 160-164] by decreasing the intracellular level of CRP-cAMP [149].

At exponential phase in complex medium (in which no glucose is supplied), the glucose-mediated catabolite repression does not occur, but synthesis of TCA cycle proteins is lower than in defined medium (with glucose as sole carbon source). This proteomic observation suggests that the repression by P-ArcA is stronger than the activation of CRP-cAMP (Fig. 3.2.4A and 3.2.4B).

The observed regulatory pattern of GatDZ, which are responsible for the degradation of galactitol into glyceraldehyde-3-phosphate (G3P) and dihydroxyacetone phosphate (DHAP) [165], and are also under the competitive control of P-ArcA [166] and CRP-cAMP [167], gives further evidence that it is the P-ArcA repression, not the CRP-cAMP activation, which determines synthesis of TCA cycle proteins. The synthesis of GatDZ is the same as TCA cycle proteins: they are up-regulated in defined medium compared to complex medium at exponential phase, and in complex medium at stationary phase compared to exponential phase.

3.2.4.6 Connection between glycolysis and TCA cycle

At exponential phase, the synthesis of 4 identified proteins (e.g. MaeB and PckA), which create bridges between glycolysis and TCA cycle, is up-regulated in defined medium compared to complex medium (Fig. 3.2.2 and 3.2.3A), which corresponds to the higher level of TCA cycle proteins and lower level of acetate excretion in defined medium.

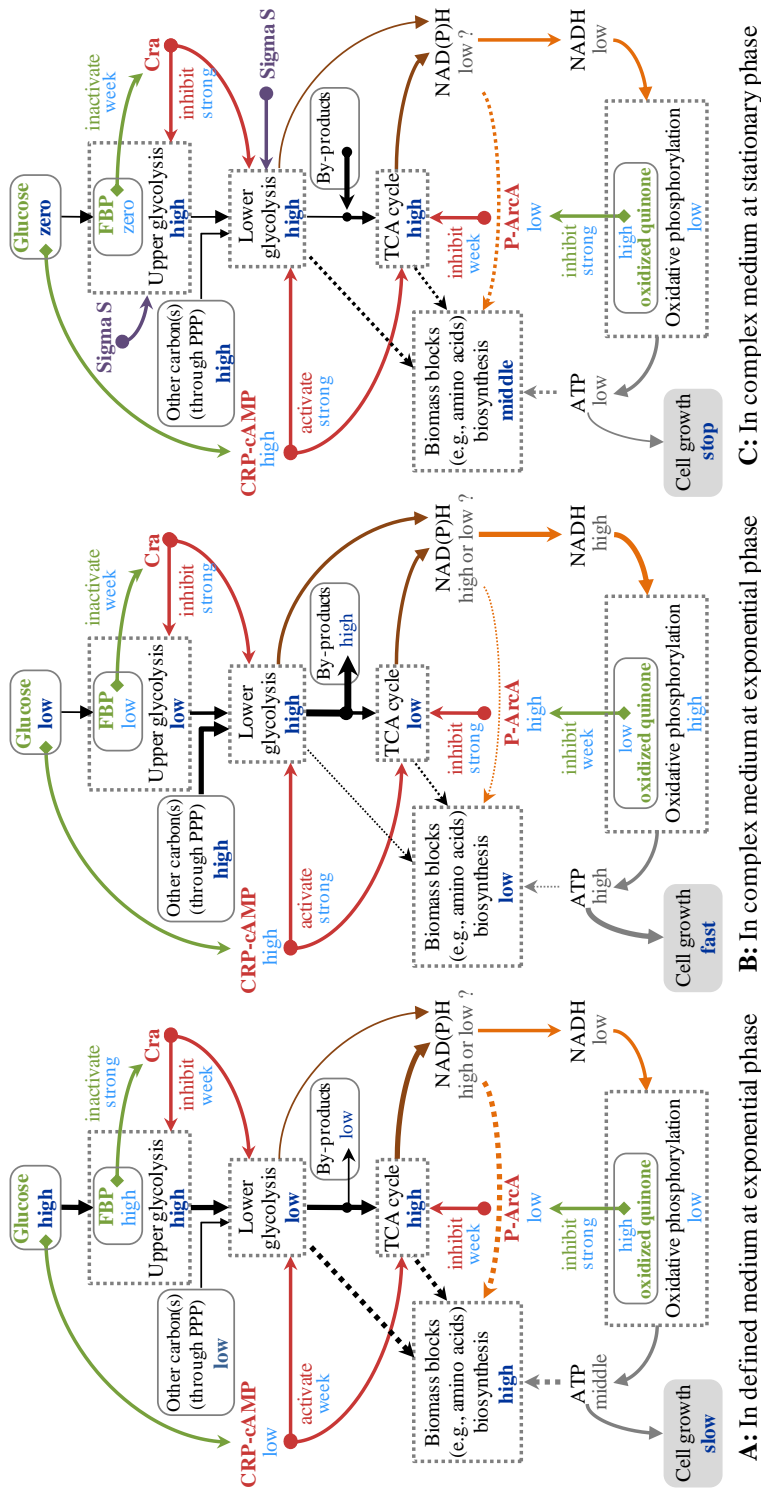


Fig. 3.2.4 Regulation of the CMPs, oxidative phosphorylation and biomass blocks biosynthesis

E. coli grown in defined medium at exponential phase (A) and in complex medium at stationary phase (C) is compared with *E. coli* grown in complex medium at exponential phase (B). The relative high or low levels of pathway components, which are indicated by *dark blue*, are current experimental observations. The relative high, low, week or strong values of components or transcriptional regulators, which are marked by *light blue*, are deduced from the experimental observation. The relative high or low levels of NAD(P)H, which are represented by *gray* color, are hypothetical. *Green* color indicates the (de)activation of transcriptional regulators, CRP-cAMP, Cra and P-ArcA, by glucose, FBP and oxidized quinone, respectively. *Red* color denotes the effect of transcriptional regulators (CRP-cAMP, Cra and P-ArcA) on glycolysis and TCA cycle. *Purple* color indicates that glycolysis genes are under the control of stationary phase sigma factor σ^S . *Black* arrows indicate potential carbon flux according to the abundance of corresponding enzymes. *Brown* arrows are used to show the generation of NAD(P)H from glycolysis and TCA cycle. *Orange* arrows indicate the flux of NAD(P)H entering the oxidative phosphorylation or amino acid biosynthesis pathways. The dashed *black* arrows show the fluxes of reducing equivalents and precursors, entering amino acid biosynthesis pathways. The width of *black*, *brown*, *orange* and *gray* arrows represents the proposed carbon, NAD(P)H and ATP fluxes, respectively.

At stationary phase (Fig. 3.2.2 and 3.2.3B), the up-regulation of MaeB and PckA in complex medium suggests an increase of carbon flux in TCA cycle. During re-assimilation of acetate, acetyl-CoA will enter the TCA cycle. The carbon flux can be converted back to pyruvate through MaeB (or SfcA) or to PEP through PckA. Meanwhile the up-regulation of PpsA catalyzing the conversion of pyruvate to PEP, and lactate dehydrogenases (LldD, Dld and LdhA), which can temporally direct the excess pyruvate to lactic acid, also corresponds to the reuse of acetate in complex medium to generate PEP and pyruvate that can be further used by *E. coli* for growth and maintenance.

3.2.4.7 Oxidative phosphorylation

Four subunits of NADH dehydrogenase I (NuoBCFG) and three subunits of ATP synthase F1 complex (AtpADH) were identified, which catalyze the transfer of electrons from NADH to the oxidized quinone pool and produce ATP for cell growth, respectively. The regulation of NADH dehydrogenase and ATP synthase is not prominent. Only the synthesis of NuoBCFG decreases a little from exponential to stationary phase in defined medium, which matches the slight down-regulation of TCA cycle proteins at the same condition. The non-significant regulation of the oxidative phosphorylation proteins is consistent with literature reports [168-170], suggesting that the electron transfer chain may be the bottleneck of energy production. But inside of the electron transport chain, quinone acts as a redox signal for the P-ArcA system [54], which may create a feedback control loop on the major reducing equivalents [NAD(P)H] generation pathway, the TCA cycle (Fig. 3.2.4). Due to the fact that NADH and NADPH can be converted into each other through reversible transfer of reducing equivalents between NAD and NADP by transhydrogenase [51-53], they are regarded as equal in this study.

3.2.4.8 Amino acid and nucleotide metabolism

During exponential growth in defined medium all amino acids must be synthesized from glucose, NH_4^+ and SO_4^{2-} . In defined medium the total abundance of 68 identified amino acid metabolism proteins (appr. 18% of WCPM), is three times higher than the corresponding abundance in complex medium (appr. 6% of WCPM) with the rich supply of amino acids and peptides (Suppl. Figs 5.3.1 and Table 5.3.1). This can be explained by the fact that most of the amino acid biosynthesis pathways are regulated by feedback inhibitions (as summarized in Suppl. Table 5.3.4). At the same time in complex medium, several proteins (e.g. AstD, Tdh, Kbl and PutA) identified in arginine, threonine and tryptophan degradation pathways are up-regulated. This also suggests that the amino acid biosynthesis is strongly repressed during the exponential phase in complex medium. Since the strongly down-regulated amino acids synthesis pathways require low amounts of precursors and reducing equivalents (generated by the CMPs), their down-regulation may also contribute to the acetate overflow metabolism in complex medium at exponential phase (as indicated by the dashed arrows in Fig. 3.2.4B).

When *E. coli* reaches the stationary phase, the feedback inhibition is relieved in complex medium. Some enzymes involved in amino acid biosynthesis are up-regulated (Suppl. Fig 5.3.2 and Table 5.3.1), but the up-regulation of proteins, which are responsible for amino acids degradation (e.g. AstABD, Tdh, Kbl and PutA), becomes more prominent. Whereas in defined medium during the entry into stationary phase, the abundance of amino acid biosynthesis and degradation proteins does not change significantly.

Inosine monophosphate (IMP) is the most important intermediate in purine biosynthesis. At exponential phase, the total abundance of identified IMP biosynthesis proteins in defined medium is two times higher than in complex medium (Suppl. Fig 5.3.1 and Suppl. Table 5.3.1). The down regulation of IMP biosynthesis proteins in complex medium at exponential phase is due to feedback inhibitions (mediated by PurR repressor) by purine nucleotides in complex medium [171-173]. At exponential phase in defined medium IMP must be synthesized *de novo*, but in complex medium IMP can be synthesized through salvage pathways [174].

Other proteins identified belonging to purine and pyrimidine biosynthesis or nucleotides salvage pathways show a similar regulatory pattern: at exponential phase nearly all the proteins are up-regulated in complex medium as compared to defined medium. In complex medium, *E. coli* can produce nucleotides faster through salvage pathways with less consumption of carbon and nitrogen sources, which may also contribute to the acetate overflow metabolism.

When the culture reaches stationary phase, the feedback inhibition is relieved. In complex medium, the amount of some IMP biosynthesis proteins (e.g. PurCDT) increases, but other proteins for nucleotide biosynthesis decrease with the cessation of cell growth (Suppl. Fig 5.3.2).

3.2.4.9 Lipid, lipopolysaccharide and other cellular component biosynthesis

In addition to enzymes involved in amino acid and nucleotide metabolism, 7 proteins for lipid synthesis, 10 proteins for lipopolysaccharide biosynthesis and 16 proteins belonging to different biomass block biosynthesis pathways were identified. The total abundance of these proteins is not high. Their abundance is mainly related to the growth rate, but individual regulations still exist. The proteomic data suggest that the lipid, lipopolysaccharide and other cellular component biosynthesis may not be related to the acetate overflow metabolism (for details, refer to Suppl. Table 5.3.1 and Suppl. Figs. 5.3.1, 5.3.2 and 5.3.3).

3.2.5 Discussion

Based on the information of *E. coli* transcription regulation from RegulonDB [145] as summarized in Suppl. Table 5.3.3 and current proteomic data as shown in Suppl. Table 5.3.1, a general regulatory model of the CMPs, oxidative phosphorylation and synthesis of biomass building blocks (e.g. amino acids) is proposed to explain the acetate overflow metabolism under nutrient-rich conditions (Fig. 3.2.4). During aerobic exponential growth, the high levels of enzymes in the PPP and lower glycolysis, and the low levels of TCA cycle and amino acid biosynthesis enzymes in complex medium are the main reasons leading to the corresponding acetate overproduction.

Many transcriptional factors are involved in the regulation of CMPs, but the most predominant three are Cra, CRP-cAMP, and P-ArcA. The observed regulation of proteins in glycolysis and TCA cycle can be explained by the antagonistic regulation through these three transcriptional regulators. In general, active Cra inhibits the expression of glycolysis genes [146, 148], CRP-cAMP activates the expression of genes in the lower glycolysis [149] and TCA cycle [158, 160-164], and P-ArcA only inhibits the TCA cycle genes [156-159]. It is found that there are competitions between Cra vs. CRP-cAMP and P-ArcA vs. CRP-cAMP, controlling the synthesis of lower glycolysis and TCA cycle proteins, respectively.

The mechanism of competition between Cra and CRP-cAMP is easy to understand: under a condition without additional fructose, glucose will cause catabolite repression by lowering the intracellular level of CRP-cAMP, but fructose-1,6-bisphosphate (FBP), which is produced during the utilization of glucose in upper glycolysis, will inactivate Cra for relieving the catabolite repression. When glucose is not present, the situation is the other way round. The proteomic data in this study indicate that Cra is the weaker one: during exponential growth, most of the upper glycolysis proteins in complex medium (no glucose added) are lower than in defined medium ($\sim 10 \text{ g L}^{-1}$ glucose), but the majority of proteins in lower glycolysis are higher in complex medium.

To explain the mechanism of competition between CRP-cAMP and P-ArcA, the amino acid biosynthesis and NADH turnover in oxidative phosphorylation must be taken into consideration, because they can affect the transphosphorylation of ArcA. With the presence of yeast extract and tryptone, the amino acid biosynthesis pathways in complex medium are deeply down-regulated at exponential phase. The corresponding demand for the precursors and energy (ATP and reducing equivalents) are lower in complex medium. It is difficult to judge the production level of reducing equivalents during exponential growth in defined and complex media, but through calculation as described in Suppl. Methods (determination of NADPH turn-over involved in amino acid biosynthesis), about 80% of total NADPH is spent on the amino acid biosynthesis in defined medium. Then a hypothesis is made that during exponential growth the reducing equivalents entering

oxidative phosphorylation to produce ATP in complex medium is higher than in defined medium. The high level of NADH turnover rate will lead to a low level of oxidized quinones. Then the inhibition of transphosphorylation of ArcA imposed by oxidized quinones is weak. The P-ArcA will address strong inhibition on the expression of TCA cycle genes [59]. It was observed that the synthesis of TCA cycle proteins in complex medium is much lower than in defined medium. Furthermore, in defined medium and also in complex medium at stationary phase, low level of NADH entering oxidative phosphorylation, results in a large size of oxidized quinone pool, which will inhibit the phosphorylation of ArcA to relieve the repression of P-ArcA on TCA cycle genes. The up-regulation of TCA cycle proteins in these two conditions was clearly observed. The proteomic data suggest that P-ArcA is stronger than CRP-cAMP.

It is proposed that P-ArcA creates a feedback control loop on the major reducing equivalent generation pathway, the TCA cycle; when reducing equivalents are enough for high speed of growth, *E. coli* tends to reduce TCA cycle activity. Simultaneously, enzymes in lower glycolysis can not be down-regulated as a result of the competition between Cra- and CRP-cAMP-dependent regulations. At this situation, the carbon flux in glycolysis is not compatible with TCA cycle capacity, which results in a high level of by-product production. The enhanced by-product production may make the carbon sources utilization more efficient, because acetate can be re-assimilated after other nutrients are consumed. Moreover, the excreted acetate can also inhibit the growth of other competitors in the same milieu, which helps *E. coli* to win the competition against other microorganisms.

3.2.6 Acknowledgements

Support from the FORSYS Partner Project: "Dynamics and regulation of the metabolic balance in *Escherichia coli*" is greatly acknowledged.

3.3 A comprehensive proteomic study II. Global response of *Escherichia coli* to nutrient deficiency and depletion

3.3.1 Abstract

Through the techniques of two-dimensional gel electrophoresis and mass spectrometry, a systematic quantitative proteome analysis was carried out for *Escherichia coli* grown in defined and complex media. The global self-protection response of *E. coli* towards nutrient deficiency and depletion was analyzed. When cells enter stationary phase but also when cells are grown on nutrient-poor medium, the sugar, amino acid and peptide transport systems, by-products assimilation pathways (e.g. acetate) as well as the upper glycolysis pathway are up-regulated to absorb the limited nutrients in the environment; amino acid and certain metabolite degradation processes are also up-regulated to recycle the intracellular resources that are no longer required. Concurrently, the synthesis of proteins involved in the elimination of the reactive oxygen species and DNA protection is also highly increased. Conversely, proteins associated with transcription and translation processes, which represent a large amount of total cellular protein during fast exponential growth, are down-regulated with the decrease of the growth rate.

Keywords *Escherichia coli* proteome · Stationary phase · Starvation · Stress response · Two-dimensional gel electrophoresis · Defined medium · Complex medium

3.3.2 Introduction

In the natural environment bacteria seldom encounter conditions that permit continuous balanced growth. The biosphere in a given area always undergoes a cycle of “feast” and “famine”. When nutrients are insufficient for steady growth, bacteria face such demanding conditions by entering a state named stationary phase [62]. The organisms should adapt to nutrient starvation and survive for long periods in the absence of nutrients [63]. The cellular metabolism must be reoriented to maintenance. Endogenous energy reserves must be mobilized, and the cell must survive in the absence of reproduction. These changes require noticeable physiological and structural changes in the cells [64]. Proteins synthesized early during starvation are the likely candidates required for starvation survival [64-66]. For example, the synthesis of many proteins with specific roles in protecting the cell against external stresses, e.g. heat, oxidants, osmotic challenge, and exposure to toxic chemicals, is highly up-regulated in stationary phase for cell survival [67-69].

It was found that many functions induced during stationary phase are also induced when the cells are grown with a long doubling time [63]. So properties identified as stationary phase induced may be also important for growth under conditions of nutrient deficiency or poor nutrient availability, such as the growth in defined (minimal) medium.

The investigation of starving bacterial cells is not only of crucial importance in medicine, but also in many fields of modern biotechnology [175]. Owing to the arrested cell growth and reduced metabolic activity, a study on whole cell proteome, which performs the direct biological functions, will be the most suitable procedure to study how cells deal with “poor” nutrient availability. The fully sequenced *E. coli* genome makes it accessible for proteomic analysis using mass spectrometry [97]. But only a few proteomic analyses of stationary phase physiology [65, 68, 70-73] with very limited number of identified proteins have been reported.

The growth rates of microorganism are not constant when facing different environmental conditions. The influence of temperature, pH, dissolved oxygen and other environmental conditions, has been widely investigated for many years. But how different nutrients, especially different carbon and nitrogen sources, determine the specific growth rate is still ambiguous [14]. Generating comprehensive proteomic data will greatly facilitate to reveal the global regulation of cell growth.

Together with chapter 3.2, a systematic proteomic study using a 2D gel-based proteome analysis was carried out for *E. coli* BL21 (DE3) cells from exponential and stationary phase cultures grown in defined and complex media to reveal the cellular physiology when nutrients are insufficient. When comparing to the growth in complex medium, the nutritional condition in defined medium is described as nutrient deficiency. When comparing to the growth at exponential phase (also known as log phase), the nutritional condition at the stationary phase is defined as nutrient depletion. In the present study, two major proteomic comparisons are investigated: first the proteomic difference between defined and complex media at exponential phase is used to reveal the cellular response to nutrient deficiency; secondly the proteomic difference between stationary and exponential phases in complex medium is studied to show the cellular response to nutrient depletion.

3.3.3 Materials and methods

3.3.3.1 Strain, media and cultivation conditions

E. coli BL21 (DE3) (Novagen, Germany) was used in this study. The composition of Luria-Bertani (LB) medium, Terrific-Broth (TB) medium and Defined Non-inducing Broth (DNB) [110, 141], and cultivation conditions were described in chapter 3.2.3.

3.3.3.2 Two-dimensional gel electrophoresis and protein spot identification

Immobiline DryStrip gels of pH 3-10 NL (GE Healthcare, UK) and SDS-PAGE (10-15% gradient gel) were used for the first and second dimension of 2D gel electrophoresis. Coomassie stained gels were analyzed by using Proteomweaver™ 4.0 (Bio-Rad, USA) for protein spot detection, matching and quantification. Each spot's intensity was normalized by the whole spot intensity on the same 2D gel. The corresponding average value from the

duplicated gels was used indicating the spot's protein portion (%) of whole cell protein mass (WCPM). The sum "WCPM %" of spots representing the same protein was used for indicating the expression of the corresponding protein. Protein spots were identified by matrix-assisted laser desorption ionization time-of-flight mass spectrometry (MALDI-TOF MS). The MASCOT search program (Matrix Science, UK) was used for protein identification with the annotated *E. coli* genome [Uniprot (<http://www.uniprot.org/>) serving as database]. All proteins with a Mowse score greater than 54 were regarded as significant ($p < 0.05$). Detailed methods have been described previously [126, 127] and in section 5.1 in the Appendix.

EcoCyc (<http://ecocyc.org/>) [143] and KEGG (<http://www.genome.jp/kegg/>) databases [144] were used for classification of identified proteins. The transcriptional regulation of identified proteins was mainly acquired from the RegulonDB (<http://regulondb.ccg.unam.mx/>) database [145].

3.3.4 Results

3.3.4.1 Growth kinetics in defined and complex media

With the presence of tryptone and yeast extract, *E. coli* has a maximum specific growth rate of about 1.5 h^{-1} in complex medium ($37 \text{ }^\circ\text{C}$). But in defined medium, the maximum specific growth rate decreases to 0.8 h^{-1} ($37 \text{ }^\circ\text{C}$). It has also been observed that the acetate excretion during exponential growth and assimilation during entry into stationary phase, are much higher for *E. coli* grown in complex medium than in defined medium. Detailed growth and acetate production kinetics of *E. coli* in defined (DNB) and complex (LB) media were shown in the Fig. 3.2.1 in chapter 3.2. In this chapter, the defined medium was used to mimic the nutrient deficiency as compared to complex medium, and the stationary phase was used to simulate nutrient depletion compared with the exponential phase.

3.3.4.2 Systematic and comparative proteome analysis

The whole cell proteome of *E. coli* grown in defined and complex media at exponential and stationary phase was analyzed. 516 spots were identified by MALDI-TOF MS representing 369 different proteins. Results of analysis and annotated 2D gels are summarized in Suppl. Figs 5.3.1-5.3.12. The most representative 2D gels are shown in Fig. 3.3.1. All identified proteins are classified into 11 categories with 29 groups as shown in Suppl. Table 5.3.1 and 5.3.2. The first three categories: carbohydrate metabolism, oxidative phosphorylation and synthesis of biomass building blocks are thoroughly discussed in chapter 3.2. In the current chapter, we focus on the proteomic differences of the remaining categories: (IV) (Metabolite) degradation, (V) transportation, (VI) transcription and translation, (VII) protein folding and degradation, (VIII) cell redox balance, (IX) DNA protection and repair, (X) unclassified and (XI) uncharacterized proteins.

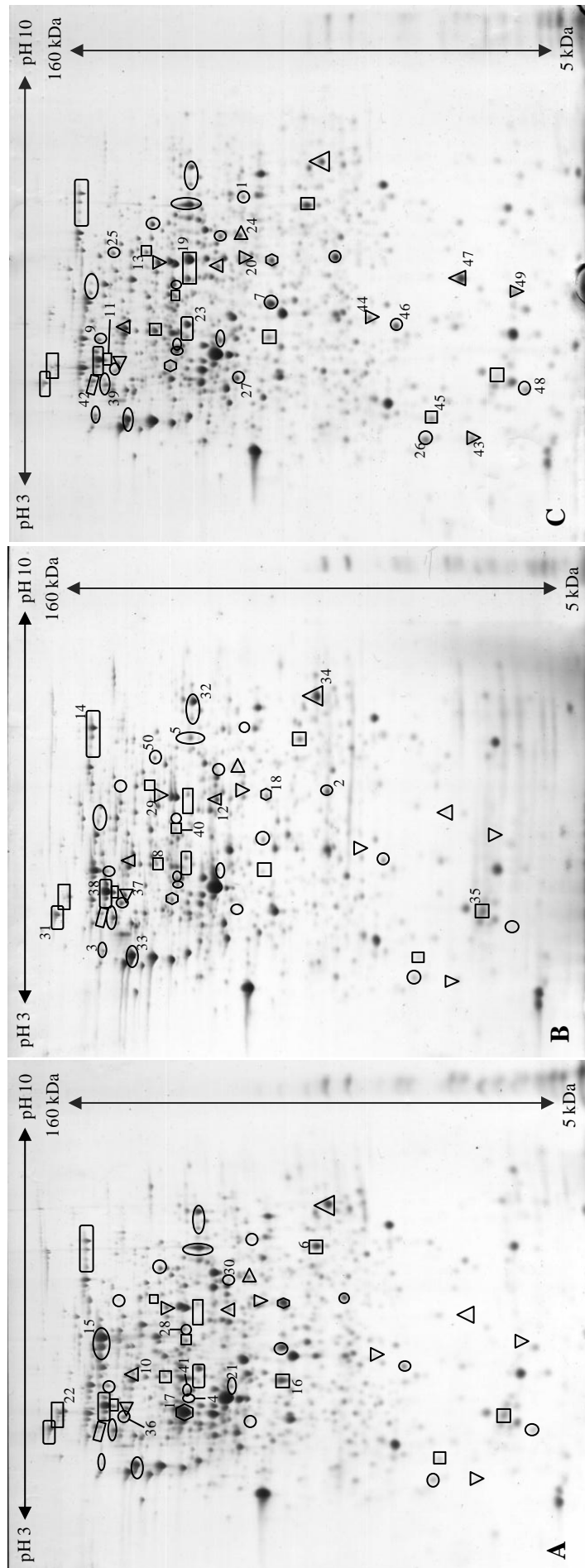


Fig. 3.3.1 *E.coli* proteome response towards nutrient deficient and depleted conditions

E. coli grown in defined medium at exponential phase (A) and in complex medium at stationary phase (C) is compared with cells grown in complex medium at exponential phase (B), respectively. 50 proteins with significant regulations are shown on the 2D gels: FbaB 1, GpmA 2, PpsA 3, GlpK 4, GltA 5, SucD 6, Mdh 7, PckA 8, MaeB 9, Acs 10, Pta 11, AckA 12, PoxB 13, AdhE 14, MetE 15, IlvE 16, IlvC 17, CysK 18, TnaA 19, Tdh 20, PurT 21, PurL 22, GatZ 23, GatD, 24, FadB 25, Ctr 26, MalE 27, DppA,28, OppA 29, TolB 30, RpoB 31, Rho 32, RpsA 33, RpsB 34, RpsF 35, TypA 36, GlyS 37, FusA 38, Pnp 39, PepQ 40, PepD 41, PepN 42, Bfr 43, WrbA 44, Tpx 45, SodB 46, Dps 47, UspA 48, YgaU 49, LfiI 50. DNB and LB media were used to represent the defined and complex media, respectively. Different geometric shapes (e.g. circle, rectangle and square) are used for helping to locate and cross-compare identified proteins. For other conditions and the rest of identified proteins please refer to Suppl. Figs. 5.3.7-5.3.12.

3.3.4.3 (Metabolite) degradation

During exponential growth, the total abundance of 19 identified proteins belonging to different metabolite degradation processes is at similar level in defined and complex media. But regulations of individual proteins are very different. Four proteins, MalPQ [176], TreC [177] and FadH [178] are highly up-regulated in complex medium at exponential phase indicating that different carbon sources, e.g. maltose, trehalose and even fatty acids, can be used during exponential growth of *E. coli*. Especially for maltose, the corresponding maltose transport systems are also up-regulated in complex medium (discussed in the next section).

During the transition from exponential to stationary phase, the proteins belonging to different metabolite degradation processes remain constant in defined medium, but greatly increase in complex medium. 11 proteins, which are involved in degradation pathways of galactitol_(GatZD) [165], trehalose_(TreA) [177], melibiose_(MelA) [179], 4-aminobutyrate_(GabDT) [180], putrescine_(Ptr) [181], nucleotides_(CpdB) [182], fatty acids_(FadB) [183], methylglyoxal_(DkgA) [184] and sialic acid_(NanA) [185], are highly up-regulated in complex medium at stationary phase as compared to exponential phase (Suppl. Table 5.3.1).

3.3.4.4 Sugar transport

At exponential phase, four identified proteins (PtsIH, Crr and ManX) belonging to the phosphotransferase system (PTS) are higher in defined medium (with glucose as sole carbon source) than in complex medium (in which no glucose is supplied) (Suppl. Fig 5.3.1). Meanwhile, the three identified maltose transport proteins (MalEK and LamB) are lower in defined medium than in complex medium. When *E. coli* reaches stationary phase, PtsH, Crr, ManX and MalE are highly up-regulated in all media (Suppl. Fig 5.3.2 and 5.3.3).

The proteomic data show that the sugar transport systems (especially PTS) are up-regulated in response to nutrient deficiency and depletion (Fig. 3.2.3 in chapter 3.2). The observed synthesis of PTS proteins can be explained by the antagonistic regulation of four transcription regulators (CRP-cAMP, Cra, NagC and Mlc). The mechanisms of regulation through CRP-cAMP and Cra were discussed in chapter 3.2. The repressing activity of NagC is induced by GlcNAc-6-P, the product of GlcNAc transport by the PTS [186]. And the repressing activity of Mlc is inactivated by binding to the dephosphorylated form of EIICB^{Glc} (PtsG), which is formed during the transport of glucose [187].

At exponential phase in defined medium, glucose is the sole carbon source. The repression of PTS genes by low level of CRP-cAMP (caused by the high glucose concentration) is strong. However, the inhibitions by Cra, Mlc and NagC are weak, which are caused by the high level of fructose-1,6-bisphosphate (FBP, produced during the utilization of glucose), the dephosphorylated form of PtsG (formed during the transport of glucose) and the

absence GlcNAc in defined medium, respectively. The observed up-regulation of PTS proteins suggests that the derepression of Cra, Mlc and NagC is stronger than the catabolite repression by glucose in defined medium at exponential phase.

At the transition into stationary phase with the depletion of carbon sources, the repression by glucose and NagC is relieved. But the repression by Mlc (caused by the cessation of glucose uptake through PTS) and Cra (caused by the absence of F1P and FBP) is activated. The derepression of CRP and NagC seem to win the competition: up-regulation of PTS proteins is observed in all media at stationary phase.

The observed synthesis of proteins of the maltose transport system can be explained by the co-regulation of CRP-cAMP [188] and MalT [189]. At exponential phase in complex medium, catabolite repression by glucose does not occur, and maltose or maltodextrin in the medium can induce MalT to activate the expression of the *malK-lamB-malM* and *malEFG* operons [189]. At exponential phase, up-regulation of maltose transport proteins is observed in complex medium. When cells enter stationary phase with the depletion of carbon sources, the MalT activation vanishes (which will suppress the expression of maltose transport genes), but the catabolite repression by glucose is relieved (which will activate the expression of maltose transport genes). The up-regulation of MalE and the down- and/or non-regulation of MalK and LamB, respectively, are observed.

3.3.4.5 Amino acid and peptide transport

The general regulation of the amino acid and peptide transport proteins is very similar to PTS proteins. At exponential phase, the synthesis of 7 identified proteins (GlnH, ArtJ, ArgT, LivJ, DppA and OppAD) is much higher in defined medium (Suppl. Fig 5.3.1), in which no amino acids are added. At the transition into stationary phase with the exhaustion of nutrients, except GlnH, strong up-regulation of the remaining 6 proteins was observed in both defined and complex media (Suppl. Fig 5.3.2 and 5.3.3).

3.3.4.6 Other transport proteins

14 identified proteins are assigned to the group of other transport proteins (for details refer to Suppl. Table 5.3.1), which altogether account for about 5% of WCPM. At exponential phase, the synthesis of the majority of them is slightly higher in complex medium as compared to defined medium, suggesting that the nonspecific diffusion channels, e.g. OmpA and OmpF, may be sufficient for rapid nutrient absorption to support the fast growth, when the concentration of nutrients is high in complex medium. During the transition into stationary phase, the nonspecific diffusion channels (OmpAF) in complex medium remain constant, but have an increase in defined medium. The synthesis of OmpAF can be explained by the control of CRP-cAMP [162, 190]. In defined medium, at exponential phase the high concentration of glucose represses the synthesis of OmpAF; whereas at stationary phase catabolite repression by glucose is relieved which allows the up-regulation

of OmpAF.

3.3.4.7 RNA polymerases and binding proteins

The regulation of the identified three subunits (RpoABC) of the core RNA polymerase (RNAP) is directly correlated with the growth rate. At exponential phase, the synthesis of RpoABC in defined medium is lower than in complex medium. When reaching stationary phase, RpoABC decreases in both defined and complex media.

RNAP-associated proteins bind to RNAP affecting various steps in the transcription cycle or RNAP assembly. At exponential phase, 7 identified RNAP binding proteins (RapA, NusAG, Rho, RpoD, SspA and DksA) are also generally down-regulated in defined medium as compared to complex medium. When *E. coli* reaches stationary phase, the total abundance of identified RNAP-associated proteins decreases in complex medium, but the corresponding total abundance remains constant in defined medium (Suppl. Table 5.3.2). There are only two identified RNAP binding proteins (SspA and DksA), which are up-regulated when *E. coli* enters stationary phase in all media. SspA is induced by starvation and increases with the decrease of growth rate [191] and is essential for cell survival during acid-induced stress [192]. DksA binds directly to RNA polymerase, affecting transcript elongation and augmenting the effect of the alarmone ppGpp [193], which causes a redirection of transcription so that genes important for starvation survival are favored at the expense of those required for growth and proliferation [194].

3.3.4.8 Ribosomal proteins and associated proteins

Ribosomes are responsible for synthesizing the proteins in the cell. In the current study, 5 ribosomal proteins (RplLI and RpsABF) were identified. Their synthesis is strictly correlated with the growth rate (growth rate dependent). At exponential phase, the synthesis of identified ribosomal proteins in defined medium is much lower than in complex medium (Fig. 3.3.2A). When *E. coli* enters stationary phase, the synthesis of 5 ribosomal proteins remains nearly constant (or decreases slightly) in defined medium, but in complex medium, significant down-regulations are observed (Fig. 3.3.2B and 3.3.2C).

8 ribosome-associated proteins were identified. At exponential phase, most of them are also lower in defined medium than in complex medium (Fig. 3.3.2A). When the culture reaches stationary phase, regulations are divided into two groups: EngAD, YcaO, TypA, HflX and Tig are generally down-regulated; Frr and RaiA are up-regulated (Fig. 3.3.2B and 3.3.2C). In the first group, four proteins (EngAD, TypA and HflX) have GTPase activity [195] providing energy for translation by the hydrolysis of GTP. The trigger factor (Tig) is a ribosome-associated chaperone guiding the initial steps of emerging nascent peptide chain folding [196, 197]. In the second group, Frr is important for the ribosome recycling and is also involved in preventing translation errors [198]. And RaiA was found likely to be involved in the stabilization and preservation of ribosomes in the stationary phase [199].

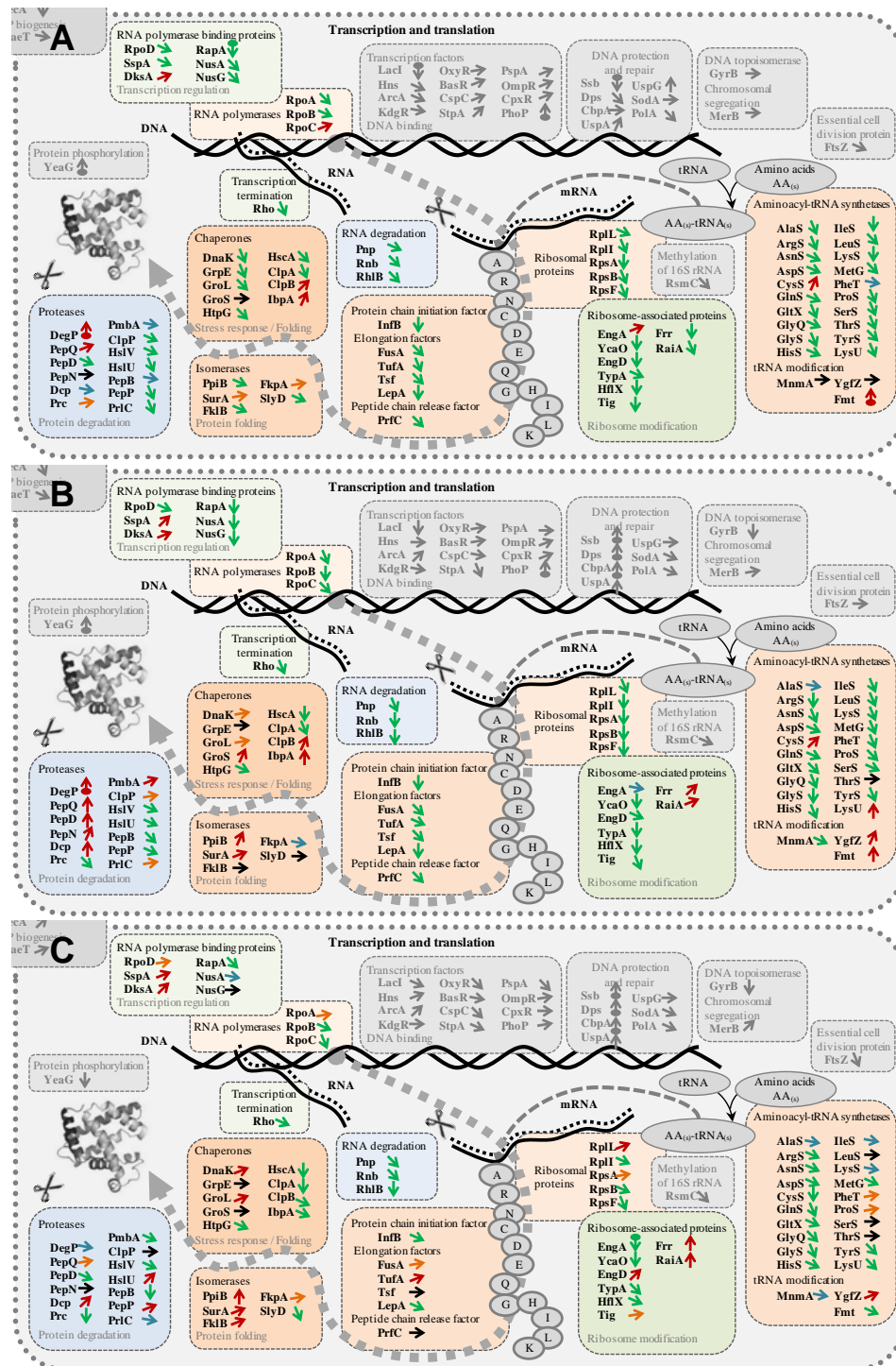


Fig. 3.3.2 Proteome comparison of transcription and translation processes of *E. coli* grown in different conditions

A: Proteome comparison of *E. coli* grown in defined/complex medium at exponential phase. **B:** Comparison of *E. coli* grown at stationary/exponential phase in complex medium. **C:** Comparison of *E. coli* grown at stationary/exponential phase in defined medium. Corresponding values of $\text{Log}_2(\text{defined/complex medium})$ at exponential phase (**A**), $\text{Log}_2(\text{stationary/exponential phase})$ in complex medium (**B**) and $\text{Log}_2(\text{stationary/exponential phase})$ in defined medium (**C**) as indicated by arrows are shown in Suppl. Table 5.3.1. DNB medium was employed as defined medium. An average of protein abundancies from cells grown in LB and TB media is calculated to represent the proteome of cells grown in complex medium. Figs 3.3.2A, 3.3.2B and 3.3.2C are parts of Suppl. Figs 5.3.1, 5.3.2 and 5.3.3, respectively. Abbreviations used in Fig 3.3.2 are listed in Suppl. abbreviation before Suppl. Fig 5.3.1.

3.3.4.9 Aminoacyl-tRNA synthetases

Aminoacyl-tRNA synthetases link amino acids to their specific tRNA molecules to generate aminoacyl-tRNAs which are substrates for translation [200]. 20 aminoacyl-tRNA synthetases, plus three proteins (Fmt, YgfZ and MnmA) which are responsible for the modification of aminoacyl-tRNAs, were identified. In general, the synthesis of all the aminoacyl-tRNA synthetases is directly related to the growth rate. At exponential phase, identified aminoacyl-tRNA synthetases are lower in defined medium than in complex medium (Fig. 3.3.2A). When entering stationary phase, general down-regulation of aminoacyl-tRNA synthetases in both defined and complex media is observed (Fig. 3.3.2B and 3.3.2C).

At exponential phase, Fmt is highly up-regulated during slow growth in defined medium. During the transition to stationary phase in complex media, its synthesis increases with the cessation of cell growth. The regulation of Fmt is consistent with its proposed biological function: Fmt attaches a formyl group only to the initiator Met-tRNA; the formyl group provides a positive determinant for the initiation factor IF2, which blocks the binding of the elongation factor [201]. YgfZ, involved directly in tRNA modification, may present a novel global regulatory system [202]. Its synthesis is up-regulated during stationary phase in all media.

3.3.4.10 Elongation factors

One protein chain initiation factor (InfB), four elongation factors (FusA, TufA, Tsf and LepA) and one peptide chain release factor (PrfC) were identified. At exponential phase, these six proteins are all down-regulated in the defined medium (with a slower growth rate) as compared to complex medium (Fig. 3.3.2A). When *E. coli* enters stationary phase, the abundance of the identified initiation, elongation and release factors remains constant in defined medium, but in complex medium they decrease greatly to a similar level as in defined medium (Figs. 3.3.2B and 3.3.2C).

The regulation pattern, which is very similar to the ribosomal proteins, is directly related to the growth rate with an exception during the transition into stationary phase in the defined medium. This indicates that the synthesis of ribosomal proteins and elongation factors may have reached the minimum level in defined medium at exponential phase.

3.3.4.11 RNA degradation

Three proteins (Rnb, Pnp and RhlB) responsible for RNA degradation were identified. The synthesis of Rnb, Pnp and RhlB, is strictly correlated with the growth rate: they are down-regulated at lower growth rate (in defined medium as compared to complex medium) and in stationary phase in all media (Fig. 3.3.2).

When cells grow at a faster rate, the total RNA synthesis rate increases with the increase of

growth rate [203], but mRNA half-lives do not decrease with the increase of growth rate [204]. A larger amount of “waste” tRNA and mRNA will be produced after translation at higher growth rate (e.g. during exponential growth in complex medium). The regulation of Rnb, Pnp and RhlB perfectly fits their biological responsibility for RNA degradation.

3.3.4.12 Isomerases

Peptidyl prolyl cis-trans isomerases (PPIases) catalyze the cis-trans isomerization of proline peptide bonds during protein folding [205, 206]. Five PPIases (PpiB, SurA, FklB, FkpA and SlyD) were identified. The total abundance of them is very low (only about 0.6% of WCPM). The regulation of nearly all proteins involved in transcription and translation is directly proportional to the growth rate. But the identified PPIases remain constant in different media and growth stages indicating that the PPIase may be a potential bottleneck for the protein folding after translation.

3.3.4.13 Chaperones

Within the current experimental setup, the majority of *E. coli* chaperones were identified as shown in Suppl. Table 5.3.1. The DnaK chaperone system and GroL-GroS chaperonin complex play the central role in the folding of nascent polypeptide chains and stress response [207, 208].

At exponential phase, most of the identified chaperones (e.g. DnaK, GrpE, GroL, HtpG, HscA and ClpA) are down-regulated in defined medium as compared to complex medium. Only two identified chaperones, IbpA and ClpB, which are able to bind to or resolubilize aggregated proteins [87, 209, 210], are up-regulated in nutrient deficient conditions (in defined medium as compared to complex medium) (Fig. 3.3.2A).

During the transition to stationary phase, the total abundance of chaperones remains constant in all media (Suppl. Table 5.3.1). But the regulations of individual proteins are very prominent. IbpA and ClpB are up-regulated during nutrient depletion in complex medium (Fig. 3.3.2B and 3.3.2C). The identified DnaK system (DnaK and GrpE) and GroL-GroS complex are slightly increased at the stationary phase. On the contrary, the synthesis of HtpG [211], ClpA [212], and HscA [213] is down-regulated in stationary phase in all media.

3.3.4.14 Proteases

Proteolysis in *E. coli* serves to rid the cell of abnormal and misfolded proteins and to limit the time and amounts of availability of critical regulatory proteins [214]. At exponential phase in complex medium, the higher synthesis of 13 identified proteases (e.g. HslU, PepP and PrlC as shown in Suppl. Table 5.3.1) corresponds to the hypothesis that in addition to the chaperones, proteases also play a very important role in the cellular system for the *de novo* folding and quality control of proteins [215]. In defined medium at exponential phase,

only DepP, which can degrade abnormal and aggregated proteins in the periplasm [216], is up-regulated.

Proteases are also very important for *E. coli* to survive during stationary phase [217-219]. The enhanced proteolysis can provide the starving cell with a source of amino acids for the synthesis of stationary phase proteins [64, 219]. As observed in this study, not all identified proteases are up-regulated during the transition to stationary phase. In complex medium, five identified proteases (DegP, PepQDN and Dcp) are highly up-regulated. And five (Prc, HslVU, PepBP) are down-regulated. In general, the total abundance of identified proteases increases during entry of *E. coli* into stationary phase in complex medium. But in defined medium under nutrient deficient conditions, no prominent up-regulation occurs. Correspondingly, proteome differences between exponential and stationary phase cells are much less prominent in defined medium than in complex medium (as indicated in Fig. 3.3.3).

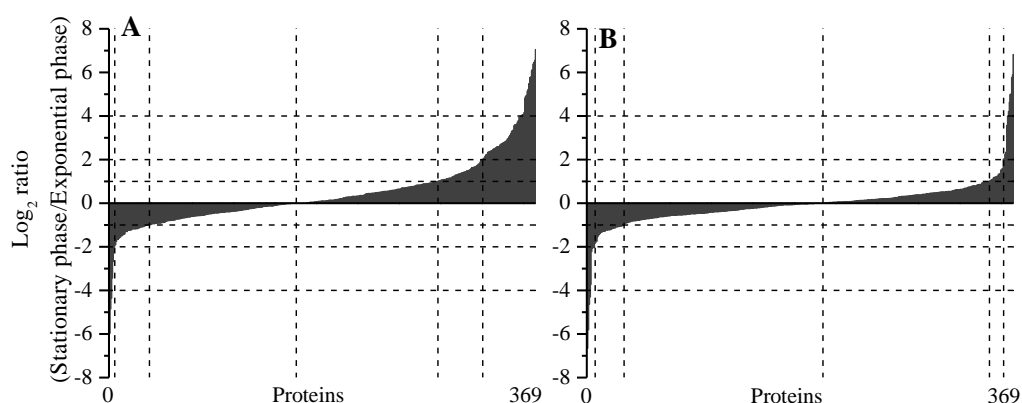


Fig. 3.3.3 Proteome comparison of *E. coli* during exponential and stationary phase

The \log_2 ratios of all identified proteins were plotted for *E. coli* grown at stationary phase versus exponential phase in complex medium (A) and in defined medium (B). Corresponding values of $\log_2(\text{stationary/exponential phase})$ in complex medium (A) and $\log_2(\text{stationary/exponential phase})$ in defined medium (B) are shown in Suppl. Table 5.3.1. DNB medium was employed as the defined medium. An average of protein abundancies from cells grown in LB and TB media is calculated to represent the proteome of cells grown in complex medium. Bar charts were generated with individual proteins plotted on the x axis and the \log_2 expression ratios plotted on the y axis.

3.3.4.15 Cell redox balance

The intracellular redox balance is tightly regulated in *E. coli*. At exponential phase, the synthesis of 9 identified proteins having dehydrogenase activity, 8 identified proteins with oxidoreductase activity, 5 hydroperoxide reductases and one superoxide dismutase are at same level (about 2.6% of WCPM) in different media (for details refer to Suppl. Table 5.3.1).

When *E. coli* reaches stationary phase, the proteins involved in maintaining cell redox balance show a general increase in both defined and complex media. But the regulation in defined medium is less prominent as compared to complex medium (Suppl. Table 5.3.1).

In the past decades, the oxidative damage caused by superoxide (O_2^-) and hydrogen peroxide (H_2O_2) was studied in *E. coli* [220, 221]. Hydroperoxidase I and II, lipid hydroperoxide peroxidase, superoxide dismutase and alkyl hydroperoxide reductase have been proven to play an important role in eliminating reactive oxygen species (ROS) [222, 223]. But the formation of ROS in *E. coli* is still obscure so far.

At exponential phase, the synthesis of identified hydroperoxide reductases (AhpFC, Tpx and KatG) and SodB is similar in defined and complex media (Suppl. Fig 5.3.1). When *E. coli* reaches stationary phase, except AhpF, the synthesis of AhpC, Tpx, KatG and SodB, is generally up-regulated in all media (Suppl. Fig 5.3.2 and 5.3.3), clearly indicating that the capacity of ROS degradation is higher at stationary phase. At the same time, the observed up-regulation of CueO, which can oxidize Fe(II) to Fe(III) [224], and Bfr, which greatly attenuates the production of hydroxyl radicals during Fe(II) oxidation by H_2O_2 [225], also corresponds to the increased capacity of scavenging ROS at stationary phase.

Based on the current observation, it could be speculated that the production of H_2O_2 and O_2^- is higher at stationary phase than during exponential growth, at least in complex medium. The reuse of formerly excreted acetate (as observed in chapter 3.2) may play an important role. It was found that a hydroperoxidase-deficient *E. coli* strain, that can grow with glucose or glycerol, cannot grow using acetate as sole carbon source [222], indicating that when *E. coli* metabolizes acetate, the ROS generation rate is higher.

The ratio between NADH and NADPH may be the potential “switcher” for the generation of intracellular ROS. During aerobic batch growth on glucose, only 55–70% of the NADPH is produced through the pentose phosphate pathway and tricarboxylic acid cycle (TCA cycle). The remaining part of NADPH is mostly generated from NADH by transhydrogenases [53]. But during acetate utilization, the situation is the other way round. Acetate will be firstly metabolized to acetyl-CoA. Acetyl-CoA will enter the TCA cycle, in where isocitrate dehydrogenase (Icd) is the major source for generation of NADPH. At stationary phase the enhanced synthesis of SthA; which is a transhydrogenase catalyzing the conversion of NADPH to NADH [53]; and WrbA which has NADPH-dependent redox activity and reduces quinones [226], corresponds to the potentially increased level of NADPH in complex medium. The high level of NADPH (produced by the utilization of acetate) may lead to the generation of ROS.

3.3.4.16 DNA protection and repair

The protection of DNA is crucial for *E. coli*. 7 proteins related to DNA protection and repair were identified (Suppl. Table 5.3.1). Three of them (Ssb, Dps, and CbpA) are non-sequence-specific DNA binding proteins. Ssb is involved in all aspects of DNA metabolism: replication, repair, and recombination [227]. Dps forming extremely stable complexes with DNA, plays an important role both in gene expression and DNA protection during stationary phase [228]. CbpA binds to curved DNA without sequence-specificity

[229]. The universal stress protein, UspA, is a member of all starvation and stress stimulons [230, 231]. It also plays a critical role for resistance to DNA damaging agents [232].

At exponential phase, the synthesis of Ssb, Dps, and CbpA is at very low level in all media (Suppl. Table 5.3.1). UspAG are up-regulated in defined medium as compared to complex medium. When *E. coli* reaches stationary phase, all three identified non-sequence-specific DNA binding proteins and the universal stress protein UspA are highly up-regulated in all media (Suppl. Fig 5.3.2 and 5.3.3), clearly indicating that DNA protection mechanisms are activated when *E. coli* responds to nutrient depletion.

PolA is required for several types of DNA repair. At exponential phase, the synthesis of PolA is higher in complex media indicating that higher level of proofreading capacity is required for the faster growth of *E. coli*. During the transition into stationary phase, the synthesis of PolA and SodA, which is more effective than SodB in preventing damage to DNA [233], does not increase. This may indicate that the oxidative damage to DNA at stationary phase is not significant in our experimental setup. The up-regulated hydroperoxide reductases and SodB can manage the oxidative stress before it causes real damage to DNA at stationary phase.

3.3.4.17 Transcription factors, unclassified and uncharacterized proteins

In this study 12 identified proteins are transcription factors, which bind to specific DNA sequences controlling the transcription of genetic information. The synthesis of them is nearly constant under different conditions (For details refer to Suppl. Table 5.3.1). However, their biological activities are generally regulated by post translation modification (e.g. phosphorylation of ArcA), which need more detailed study in the future.

7 proteins with different biological functions are assigned to the unclassified protein group. The corresponding regulations are generally correlated with growth rate. 13 proteins identified in this research are uncharacterized proteins or proteins with putative function. Many of them (e.g. YjgR, YdcJ, YcgB, YgaU, YfbU, LfiI and YhdH) show very strong up-regulation towards nutrient deficiency (exponential phase in defined medium) and/or nutrient depletion (stationary phase in complex medium). So there is a great requirement for further characterizations to reveal their underlying biological functions. For details of synthesis and regulation of unclassified and uncharacterized proteins, please refer to Suppl. Table 5.3.1.

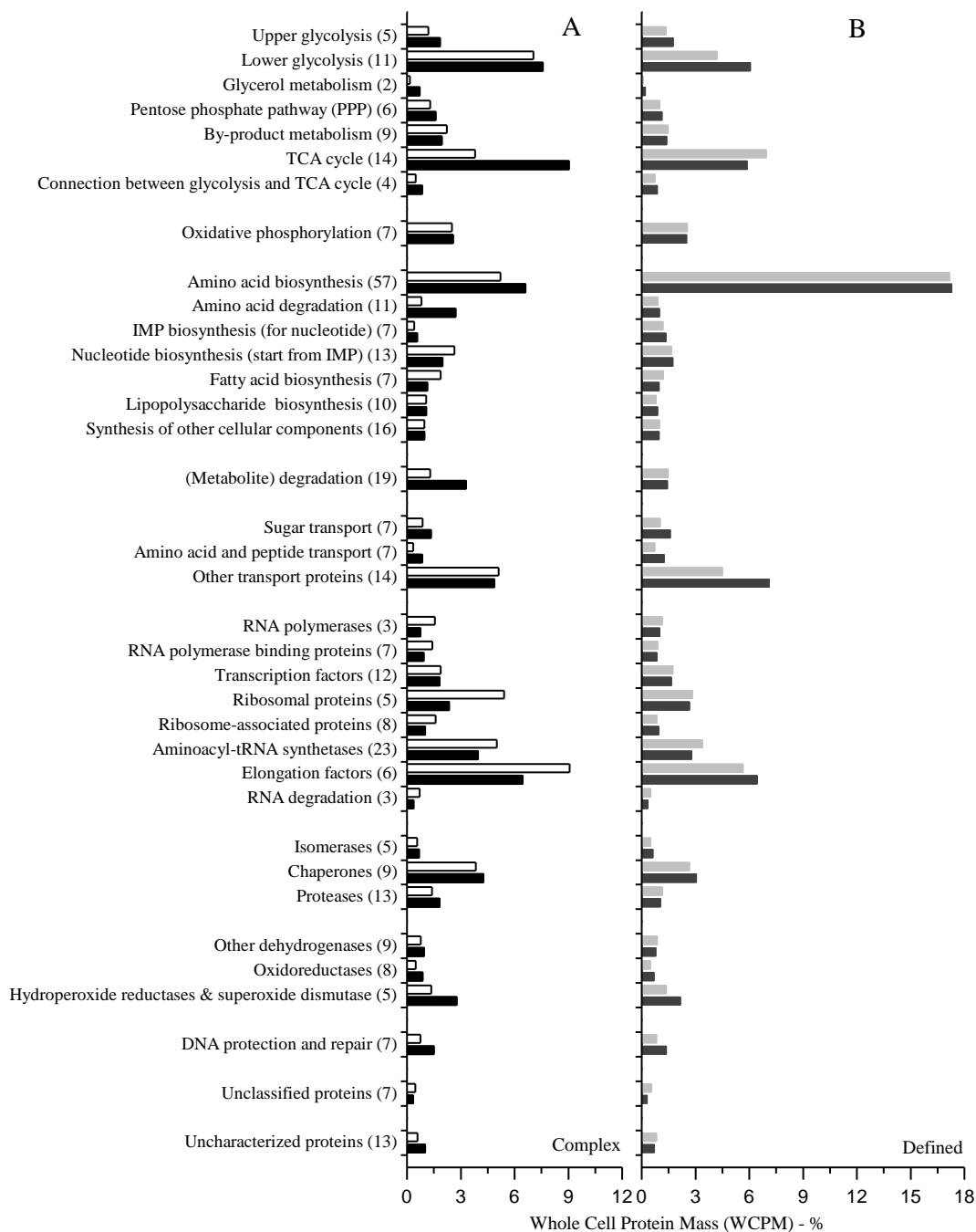


Fig. 3.3.4 Summary of proteome data of *E. coli* grown at different conditions

The number in the bracket after each category is the number of proteins that were identified belonging to the corresponding category. **A:** in complex medium at exponential phase (*white bar*) and at stationary phase (*black bar*). **B:** in defined medium at exponential phase (*gray bar*) and at stationary phase (*dark gray bar*). DNB medium was employed as the defined medium. An average of protein abundancies from cells grown in LB and TB media is calculated to represent the proteome of cells grown in complex medium. The entire data sets are shown in Suppl. Table 5.3.2.

3.3.5 Discussion

In complex medium supplied with yeast extract and tryptone, *E. coli* grows in a nutrient rich environment. Comparatively, when cultivated in defined medium with glucose and NH_4^+ as the sole carbon and nitrogen sources, respectively, the nutritional condition is defined as nutrient deficiency. The most apparent difference is the cell growth: the maximum growth rate at 37 °C in defined medium ($\sim 0.8 \text{ h}^{-1}$) is much lower than in complex medium ($\sim 1.5 \text{ h}^{-1}$). Simultaneously, during exponential growth in complex medium much more by-product, acetate, is produced and re-assimilated when cells reach stationary phase (Fig. 3.2.1).

Together with results revealed in chapter 3.2, the cellular responses towards nutrient deficiency and depletion are shown here in detail (Fig. 3.3.4 and Suppl. Figs. 5.3.1-5.3.6). When nutrient supplementation is poor, the PTS system for sugar transport and amino acid and peptide transport systems are highly up-regulated for a better assimilation of nutrients at low concentration or for scavenging remains from dying neighbors. But the maltose transport system and other transport proteins, e.g. OmpAFX and TolBC, do not show a strong regulation towards nutrient limitation. Corresponding to the enhanced level of proteins from the PTS system, proteins from carbohydrate metabolism, e.g. glycolysis, pentose phosphate pathway and TCA cycle, also show a general up-regulation. Interestingly, the proteins belonging to oxidative phosphorylation remain nearly constant.

Concerning the synthesis of biomass building blocks, only proteins from pathways for amino acid and IMP biosynthesis are up-regulated when nutrient supplementation is poor. The amounts of proteins from other pathways for biomass building block synthesis are generally proportional to the growth rate.

Proteins from amino acid biosynthesis pathways occupy more than 17% of the whole proteome during growth in defined medium, compared with only about 6% in complex medium. During the transition to stationary phase in complex medium, instead of greatly increasing the whole amino acid biosynthesis pathway, *E. coli* chooses a more efficient strategy: enzymes involved in amino acids degradation are highly up-regulated. Many identified proteins in the (metabolite) degradation category are also strongly up-regulated during the transition to stationary phase in complex medium. But for the growth in defined medium, the corresponding up-regulation is not significant.

Most of the proteins involved in transcription and translation, e.g. ribosomal proteins, aminoacyl-tRNA synthetases and elongation factors, are of high abundance and correlate in abundance with the growth rate. It is clear that when facing a “famine” environment, *E. coli* will greatly reduce the abundance of these proteins. For example, when cells reach stationary phase in complex medium, the total abundance of identified proteins involved in transcription and translation decreases from $\sim 27\%$ to $\sim 17\%$ of WCPM. In contrast, proteases and enzymes from amino acid degradation and (metabolite) degradation

pathways are highly up-regulated (Fig. 3.3.4).

Reducing the damage of cellular components, especially of DNA, is of crucial importance for *E. coli* to survive during starvation. Some oxidoreductases, nearly all hydrogen peroxide reductases and SodB for eliminating reactive oxygen species, are strongly up-regulated at stationary phase to prevent the cellular damage caused by superoxide or hydrogen peroxide. Non-sequence-specific DNA binding proteins for DNA protection are also highly up-regulated at stationary phase.

In complex medium, the difference in the composition of the proteome of cells in exponential and stationary phases is much more significant than in defined medium (as indicated by Fig. 3.3.3). This is a result of the re-assimilation of formerly excreted acetate and the possible scavenging of remains from proteins involved in transcription and translation which are no longer required and can be used to provide energy and resources for fine-tuning the proteome for survival during starvation.

In this chapter, a comprehensive quantitative proteomic profile of a self-protection mechanism employed by *E. coli* to cope with nutrient deficiency or depletion is presented: proteins from transport systems, glycolysis and by-products (e.g. acetate) assimilation pathways are up-regulated to absorb limited nutrients; the abundance of transcription and translation related proteins is greatly reduced; correspondingly, proteins involved in different degradation processes (e.g. amino acid degradation) are increased to salvage reusable materials; proteins for different stress responses (e.g. eliminating reactive oxygen species) and for the protection of DNA are also greatly enhanced. Furthermore, in the next chapter, it will be shown that this kind of self-protection mechanism collapses when *E. coli* is forced to overproduce recombinant protein.

3.3.6 Acknowledgements

Support from the FORSYS Partner Project: "Dynamics and regulation of the metabolic balance in *Escherichia coli*" is greatly acknowledged.

3.4 A comprehensive proteome study III. Global metabolic response in *Escherichia coli* during recombinant protein overproduction

3.4.1 Abstract

The global metabolic response during recombinant protein overproduction in *Escherichia coli* grown in defined and complex media has been analyzed using two-dimensional gel electrophoresis and mass spectrometry. During recombinant protein production, the proteome of *E. coli* shows a completely different regulation pattern as when facing nutrient deficiency and depletion. When *E. coli* is forced to overproduce a recombinant protein, chaperones are simultaneously highly up-regulated. Proteins from the transcription and translation processes remain at the same level as before induction. But proteins from the transport systems (e.g. the PTS, maltose, amino acid and peptide transport systems), the central metabolic pathways [e.g. glycolysis and tricarboxylic acid cycle (TCA cycle)], by-product (e.g. acetate) metabolism, and proteins for degradations, reactive oxygen species elimination and DNA protection are down-regulated, which causes an overall metabolic breakdown: in complex medium, the formerly excreted acetate cannot be efficiently re-assimilated; in defined medium, extracellular glucose cannot be utilized completely.

Keywords *Escherichia coli* proteome · Recombinant protein production · Stress response · Metabolic burden · Two-dimensional gel electrophoresis · Defined medium · Complex medium

3.4.2 Introduction

Recombinant DNA techniques with the combination of bioprocess engineering allowed many therapeutic and diagnostic proteins to be produced in large quantities in genetically modified microorganisms, such as *Escherichia coli*. Under the control of strong promoters, e.g. T7 promoter, heterologous proteins are typically produced at high levels in *E. coli*, which will address a physiological stress named metabolic burden. Then the proteins of interest tend to aggregate into inclusion bodies [81-86].

The metabolic burden caused by overexpression of heterologous genes has been extensively studied [22-24], it will lead to a decrease of specific growth rate [74-78] and biomass yield [76-78], and will result in an increase of maintenance energy coefficient [74], respiratory activity [77, 79, 80], and acetate overflow metabolism [76]. Besides the production of target protein, the simultaneously enhanced formation of chaperones [77, 87, 88] and proteases [89, 90] will also contribute to the metabolic burden.

Owing to the complexity of metabolic networks and different production conditions, e.g. temperature, growth rate and the dose of inducer, the molecular mechanism of the metabolic burden is still ambiguous. 2D gel electrophoresis seems to be the most suitable

techniques to disclose the underlying machinery. Among the proteomic studies [76-79, 88, 91-96] about recombinant protein production in *E. coli*, the numbers of identified proteins are often low, which may increase the probability of misinterpretation, so there is a great demand for a comprehensive proteomic analysis for helping to reveal the global metabolic response during recombinant protein overproduction.

Two groups of media are used in laboratory study and industrial production: complex and defined media [6-11]. The lot-to-lot variations of raw materials (e.g. yeast extract, peptone or tryptone) used in complex medium lead to poor production reproducibility [25, 47]. So the use of chemically defined medium is gaining more and more popularity [12, 110, 141]. Clearing the physiological differences of recombinant protein production in complex and defined media will help a lot towards choosing the appropriate conditions for the specific applications.

Previous proteomic analysis (as described in chapters 3.2 and 3.3) revealed that during nutrient deficiency and depletion, *E. coli* will activate a self-protection mechanism to enhance the amount of proteins from transport systems, central metabolic pathways (CMPs), by-product metabolism, and proteins involved in different degradation processes, for eliminating reactive oxygen species (ROS) and for DNA protection. Conversely, the transcription and translation related proteins will be greatly reduced.

In the present study, compared with non-induced controls, *E. coli* is forced to overproduce a recombinant protein (human basic fibroblast growth factor, hFGF-2, which serves as a model protein) in defined and complex media by the addition of isopropyl β -D-1-thiogalactopyranoside (IPTG). The major proteomic comparisons between production and non-production conditions are investigated to show that the self-protection mechanism, which is observed when *E. coli* faces nutrient deficiency and depletion (as shown in chapter 3.3), breaks down completely: proteins involved in transcription and translation remain constant; and the proteins from transport systems, CMPs, by-product metabolism, and proteins for degradations, eliminating ROS and DNA protection are down-regulated. This causes an overall metabolic breakdown.

3.4.3 Materials and methods

3.4.3.1 Strain, media and cultivation conditions

E. coli BL21 (DE3) with the plasmid pET-29c-hFGF-2 was used in this study [82]. The composition of Luria-Bertani (LB) medium is as follows: 10 g L⁻¹ tryptone, 5 g L⁻¹ yeast extract and 5 g L⁻¹ NaCl. The composition of Defined Non-inducing Broth (DNB) is as follows: 10.91 g L⁻¹ glucose, 4 g L⁻¹ (NH₄)₂HPO₄, 13.3 g L⁻¹ KH₂PO₄, 1.55 g L⁻¹ Citric acid, 0.59 g L⁻¹ MgSO₄, 100.8 mg L⁻¹ Fe(III) citrate, 2.1 mg L⁻¹ Na₂MoO₄·2H₂O, 2.5 mg L⁻¹ CoCl₂·6H₂O, 15 mg L⁻¹ MnCl₂·4H₂O, 1.5 mg L⁻¹ CuCl₂·2H₂O, 3 mg L⁻¹ H₃BO₃, 33.8

mg L⁻¹ Zn(CH₃COOH)₂·2H₂O, 14.10 mg L⁻¹ Titriplex III. The pH of all media was adjusted to 6.8 by NaOH before sterilization. After sterilization, 50 mg L⁻¹ kanamycin was added to the media. Details of the media preparation were described in previous reports [110, 141].

Cultivations were carried out in duplicate using 1.8 L Fernbach flasks with three baffles containing 200 mL medium at 30 °C and 180 rpm. When the culture reaches the mid-exponential phase, isopropyl β-D-1-thiogalactopyranoside (IPTG) was added to a final concentration of 0.25 mmol L⁻¹ for starting hFGF-2 production. The cells were harvested after 3.5h and 5h of IPTG induction in LB and DNB media, respectively. Culture samples were centrifuged at 17,000×g and 4 °C for 3 min. After removal of the supernatant, cell pellets were stored at -80°C until further analysis.

3.4.3.2 Analysis of cell growth, acetate and glucose concentration, and protein production

The cell growth was monitored by measuring the absorbance at 600 nm (OD₆₀₀). Acetate was analyzed by an acetic acid kit (Cat. No. K-ACETRM, Megazyme, Ireland). Glucose was determined by YSI 2300 STAT Plus (YSI Life Sciences, USA). For protein production SDS-PAGE analysis was performed in Mini-PROTEAN 3 Cell (Bio-Rad, USA) according to standard procedures [114] and instructions from the manufacturer. BugBuster™ protein extraction reagent with rLysozyme and Benzonase (Novagen, USA) was used to generate cell extracts and to prepare soluble and insoluble fractions according to the instructions from the manufacturer. After electrophoresis, SDS-PAGE proteins were visualized by Coomassie staining [115].

3.4.3.3 Two-dimensional gel electrophoresis

Cell pellets were disrupted by BugBuster™ protein extraction reagent. The whole cell protein in the BugBuster suspension was precipitated as described previously [142]. The protein pellets were re-solubilized in rehydration solution with IPG buffer (GE Healthcare, UK). About 280 µg protein for each sample was loaded onto Immobiline DryStrip gel (pH gradient 3-10NL, GE Healthcare, UK). The first-dimension using isoelectric focusing (IEF) and second dimension using SDS-PAGE (10-15% gradient acrylamide gel) were run with the IPGphor™ Isoelectric Focusing System and Hoefer™ DALT System (GE Healthcare, UK), respectively. The detailed protocol has been described previously [126] with reference to manufacturer's instructions (For details refer to section 5.1.1 in the Appendix). For each sample, 2D gels were made in triplicate. And the best two Coomassie stained gels [115] were analyzed by Proteomweaver™ 4.0 (Bio-Rad, USA) for protein spot detection, matching and quantification. Each spot's intensity was normalized by the whole spots intensity of the same 2D gel. An average of the resulting percentage values from the corresponding duplicated gels was taken indicating each spot's protein portion (%) of

whole cell protein mass (WCPM). The total “WCPM %” of all spots representing the same protein was used for indicating the abundance of the corresponding protein.

3.4.3.4 Protein identification and classification

Protein spots were identified by matrix-assisted laser desorption ionization time-of-flight mass spectrometry (MALDI-TOF MS). Protein spots were excised from the 2D gels. After washing, reduction and alkylation, in-gel digestion was carried out by incubation with sequencing grade trypsin (Promega, USA). Obtained peptides were extracted and purified with reversed-phase ZipTips C18 (Millipore, USA). The resulting peptide solutions were mixed with a saturated matrix solution (acetonitrile 40%, α -Cyano-4-hydroxycinnamic acid 1% and trifluoroacetic acid 0.06%) and spotted onto a 384 MTP target and dried at room temperature. A Bruker Ultraflex time-of-flight mass spectrometer (Bruker Daltonics GmbH, Germany) was used to obtain peptide mass fingerprints. Detailed experimental procedures have been described previously [126, 127] (For details refer to section 5.1.2 in the Appendix). The MASCOT search program (Matrix Science, UK) was used for protein identification with the annotated *E. coli* genome [Uniprot (<http://www.uniprot.org/>) serving as database]. All proteins with a Mowse score greater than 54 were regarded as significant ($p < 0.05$).

For classification of identified proteins the EcoCyc (<http://ecocyc.org/>) [143] and KEGG (<http://www.genome.jp/kegg/>) databases [144] were used as described chapter 3.2. The transcriptional regulation information was mainly obtained from the RegulonDB (<http://regulondb.ccg.unam.mx/>) database [145].

3.4.4 Results

3.4.4.1 hFGF-2 overexpression in *E. coli* using defined and complex media

hFGF-2 production was carried out in shake flasks at 30 °C with DNB and LB media. In the defined medium (DNB), all cellular components are exclusively synthesized from glucose, NH_4^+ , PO_4^{3-} , and SO_4^{2-} . But in complex medium (LB) with the presence of sugars, amino acids, peptides, nucleotides and other nutrients from yeast extract and tryptone, the growth rate is much higher, because less energy and resources are loaded into the corresponding biosynthetic processes (as shown in chapter 3.2). The maximum growth rate in complex medium during exponential growth before induction is much higher than in defined medium (Fig. 3.4.1.B1 and 3.4.1B2). But after induction, there is a significant decrease of growth rate in complex medium, especially during the first two hours after induction. SDS-PAGE analysis indicates (Fig. 3.4.2) that hFGF-2 production in complex medium is much faster than in defined medium, which triggers a higher level of inclusion body formation (Suppl. Figs 5.3.29 and 5.3.30).

In complex medium (LB) as indicated in Figs. 3.4.1C1 and 3.4.1D1, the excreted acetate (during exponential growth) can be re-assimilated in the control run, but in the hFGF-2 overproduction cultivation, the acetate is not completely re-assimilated. No oxygen limitation (i.e. dissolved oxygen did not drop below 30% of saturation; data not shown) was observed during the whole cultivation process in LB medium.

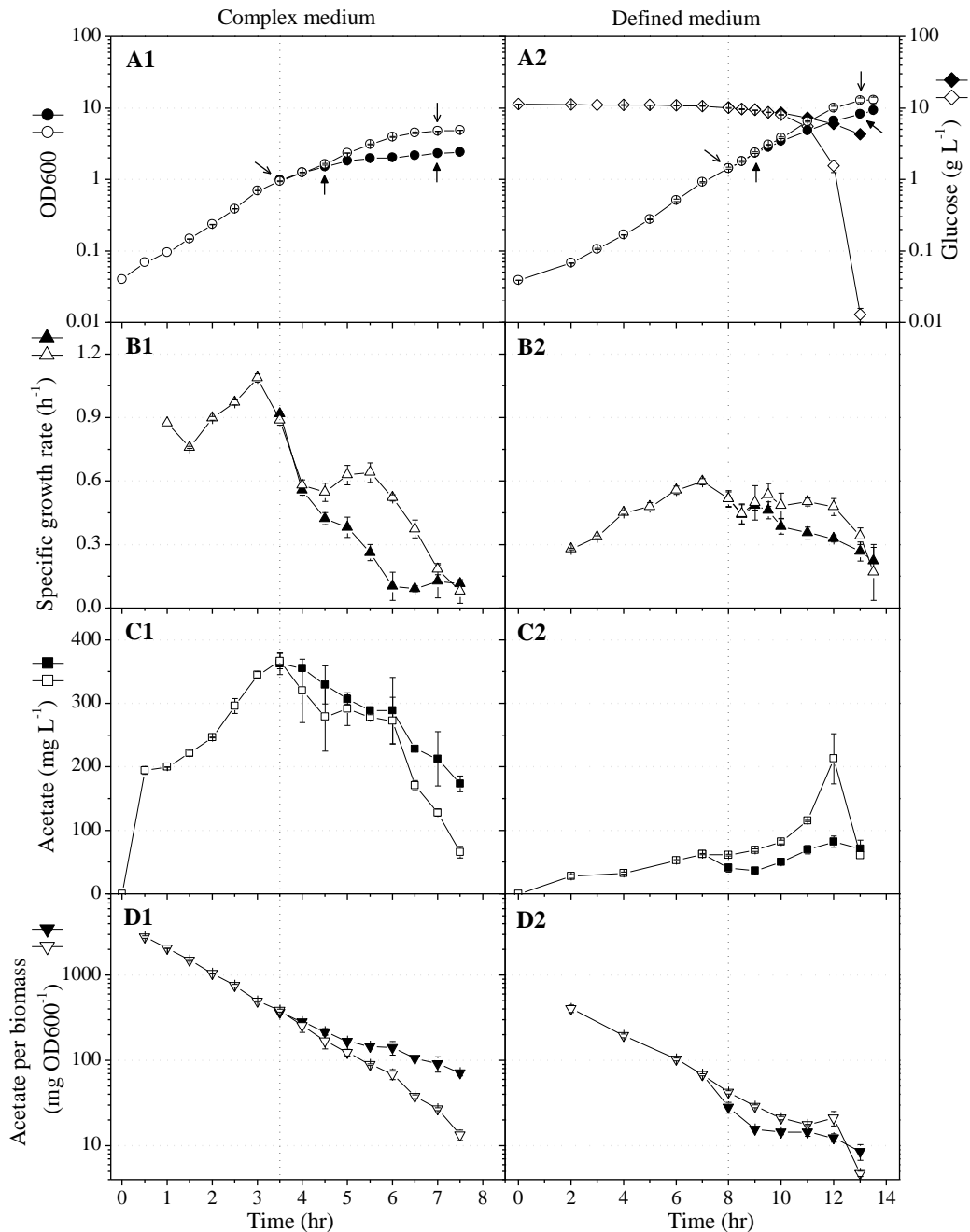


Fig. 3.4.1 Kinetics of growth, glucose utilization and acetate formation during hFGF-2 production

hFGF-2 production was carried out in shake flasks with LB medium as indicated in **A1-D1**, and DNB medium as indicated in **A2-D2**. 0.25 mM IPTG was added to the culture at 3.5 h for LB medium and 8 h for DNB medium. Control run without IPTG induction is marked using white symbols. hFGF-2 producing culture is marked with black symbols. Samples for 2D gel electrophoresis analysis were taken at the time points indicated by arrows.

In defined medium (DNB), acetate excretion was observed at early stationary phase in the control run, but was not found in the cultivation with hFGF-2 overproduction (Fig. 3.4.1C2). Correspondingly, in the control run an increased glucose utilization was observed also at early stationary phase, but during hFGF-2 production, glucose cannot be completely metabolized (Fig. 3.4.1A2). In the cultivation using DNB medium, oxygen limitations were observed at the early stationary phase for about 1.5 hours (data not shown).

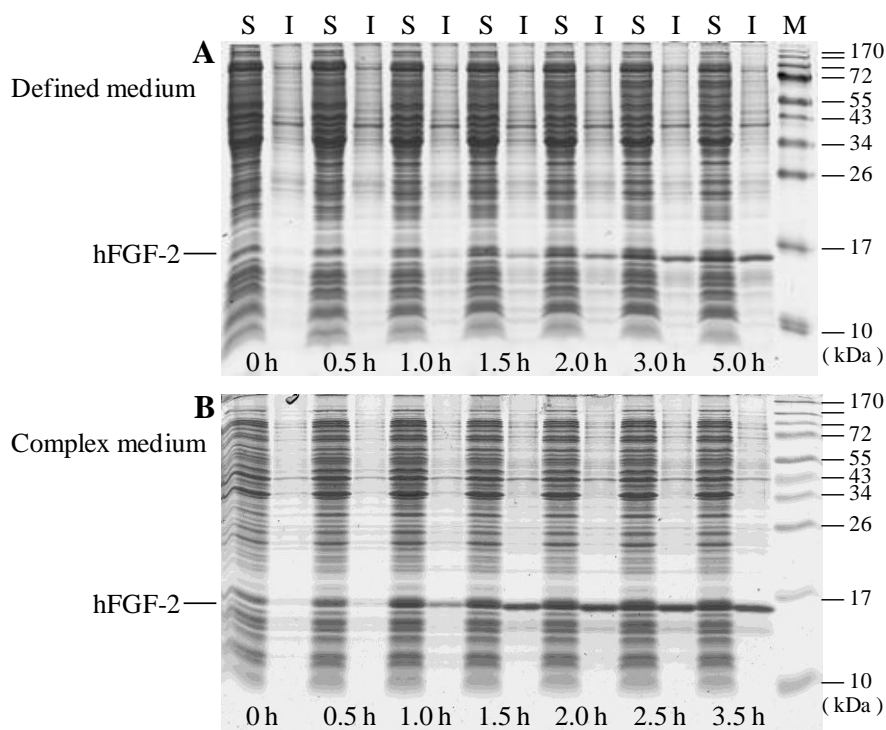


Fig. 3.4.2 Recombinant protein overproduction in defined and complex media

hFGF-2 production as analyzed by SDS-PAGE was carried out in DNB medium (A) and LB medium (B). The time after IPTG induction is indicated below the gel images. The analyzed cell fractions are indicated above (S: soluble part of whole cell protein, I: insoluble part of whole cell protein, M: marker)

3.4.4.2 Proteome analysis during recombinant protein production

Culture samples (as indicated in Fig. 3.4.1A1 and 3.4.1A2) from LB and DNB media at exponential phase before IPTG induction, 1h after IPTG induction, 3.5h (for LB medium) or 5h (for DNB medium) after IPTG induction, and stationary phase without IPTG induction were analyzed by 2D gel electrophoresis. More than 500 spots representing about 370 different proteins were identified by mass spectrometry. Spots on 2D gels were identified, matched, normalized and categorized (the most representative 2D gels are shown in Fig. 3.4.3). All identified proteins were classified into 11 categories with 29 groups as described in chapter 3.2 and 3.3. Results of analysis have been summarized in Suppl. Tables 5.3.5-5.3.6 and visualized in Suppl. Figs 5.3.13-5.3.20. Annotated 2D gels are shown in the Suppl. Figs 5.3.21-5.3.28.

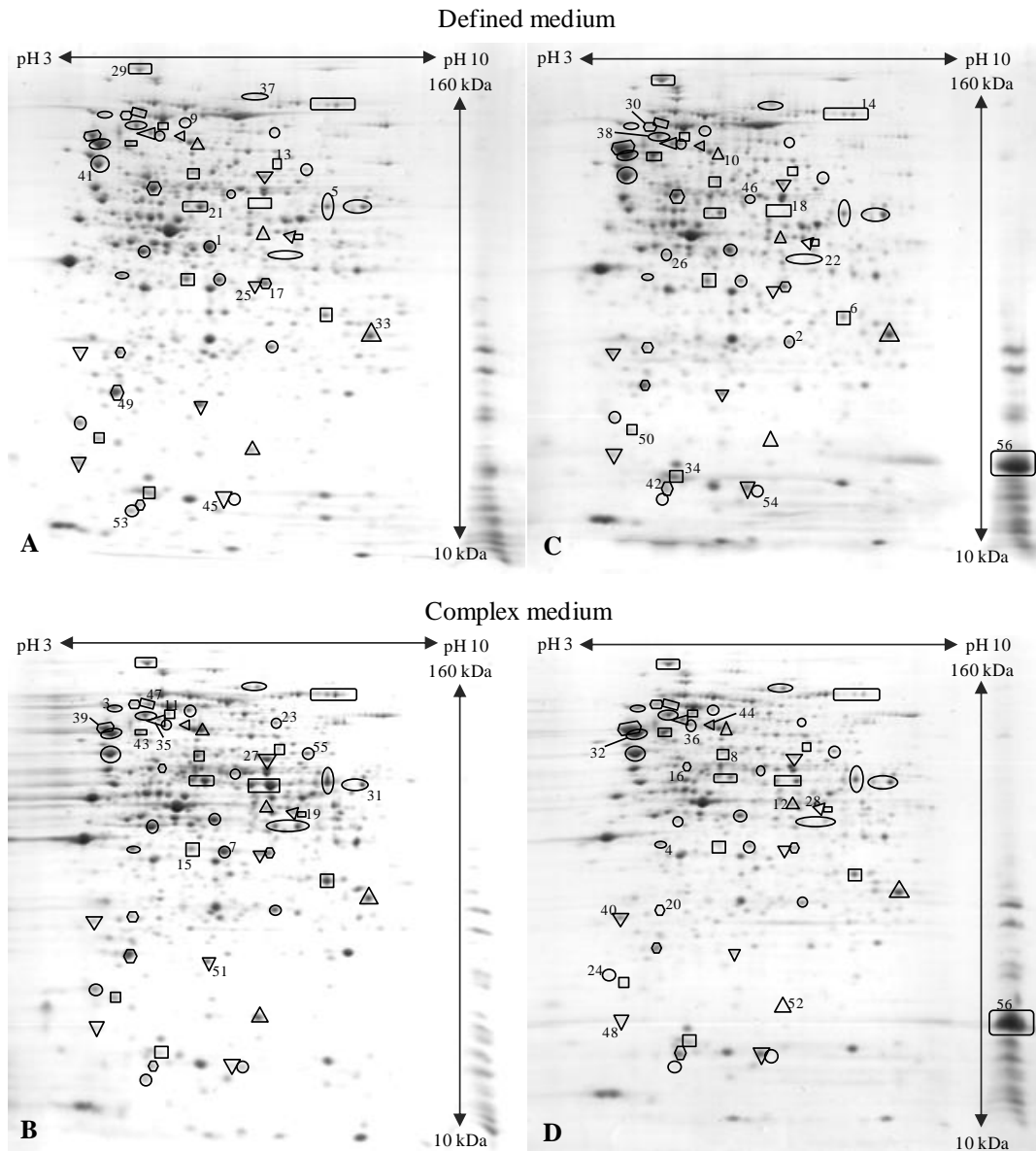


Fig. 3.4.3 *E. coli* proteome changes in response to hFGF-2 overproduction

The *E. coli* proteome of cells grown at stationary phase without IPTG induction in defined medium (**A**) and complex medium (**B**) is compared with the proteome of cells grown after 5h IPTG induction in defined medium (**C**) and 3.5 h IPTG induction in complex medium (**D**), respectively. 56 proteins with significant regulations are shown on the 2D gels: FbaA 1, GpmA 2, PpsA 3, TalB 4, GltA 5, SucD 6, Mdh 7, PckA 8, MaeB 9, Acs 10, Pta 11, AckA 12, PoxB 13, AdhE 14, IlvE 15, IlvC 16, CysK 17, TnaA 18, AstA 19, PurC 20, GatZ 21, GatD, 22, FadB 23, Crr 24, ManX 25, MalE 26, OppA 27, TolB 28, RpoB 29, RpoD 30, Rho 31, RpsA 32, RpsB 33, RpsF 34, TypA 35, GlyS 36, InfB 37, Pnp 38, Dnak 39, GrpE 40, GroL 41, GroS 42, HtpG 43, ClpB 44, IbpA 45, PepQ 46, PepN 47, Bfr 48, AhpC 49, Tpx 50, SodB 51, Dps 52, UspA 53, YgaU 54, LfiI 55, hFGF-2 56. Different geometric shapes (e.g. circle, triangle, rectangle and square) are used for helping to locate and cross-compare identified proteins. For other conditions and the rest of identified proteins, please refer to Suppl. Figs 5.3.21-5.3.28.

3.4.4.3 Transportation system

At the end of IPTG induction in both defined and complex media, proteins in transport systems are generally down-regulated as compared to the non-induced cultivation at stationary phase. The down-regulation of proteins in transport systems, such as phosphotransferase system (PTS) (PtsHI and Crr), maltose transport system (ManX, MalEK and LamB), amino acid (ArgT and LivJ) and peptide (DppA and OppAD) transport systems, which require energy during operation [e.g. adenosine triphosphate (ATP) or phosphoenolpyruvate (PEP)], is more significant than for transport proteins (e.g. CusB, FadL, OmpAF and TolC), which do not require energy during operation (Suppl. Table 5.3.5). The glucose in defined medium can not be completely utilized in the IPTG induced culture as shown in Fig. 3.4.1A2, which corresponds the proteomic observation (Fig. 3.4.4).

In defined medium at stationary phase, proteins in PTS and maltose transport systems are up-regulated as compared to the exponential phase (also known as log phase) (Fig. 3.4.4A), leading to an accelerated glucose uptake as shown in Fig. 3.4.1A2. Proteins in amino acid and peptide transport systems are also slightly up-regulated. In complex medium, the up-regulation of proteins from sugar, amino acid and peptide transport systems is even more significant during entry into stationary phase in the non-induced cultivation (Fig. 3.4.5A). Other transport proteins, such as FadL, OmpAFX and TolBC, remain relatively constant at exponential and stationary phases in both media (Suppl. Table 5.3.5).

It is found that when nutrients are not sufficient in the environment, the sugar, amino acid and peptide transport systems are up-regulated for a better absorption of the limited supply of nutrients in the environment. However, the increased nutrient uptake capacity at low nutrient concentrations is impaired by the overproduction of recombinant protein.

3.4.4.4 Central carbon metabolism

After 1h IPTG induction, the amount of glycolysis proteins catalyzing the reactions from glucose-6-phosphate (G6P) to PEP and proteins in the pentose phosphate pathway (PPP) is still the same as before induction. But the decrease of proteins (PykAF, AceEF and LpdA) for the conversion of PEP to Acetyl-CoA already starts (Suppl. Figs. 5.3.13 and 5.3.17), which potentially impairs the production of precursors (e.g. pyruvate, Acetyl-CoA and 2-oxoglutarate) or reducing equivalents, and the assimilation of non-fermentable carbon sources, e.g. acetate. At the end of the hFGF-2 production phase, most of proteins of the glycolysis and PPP are down-regulated as compared to the exponential phase (before induction) or the stationary phase (without IPTG induction).

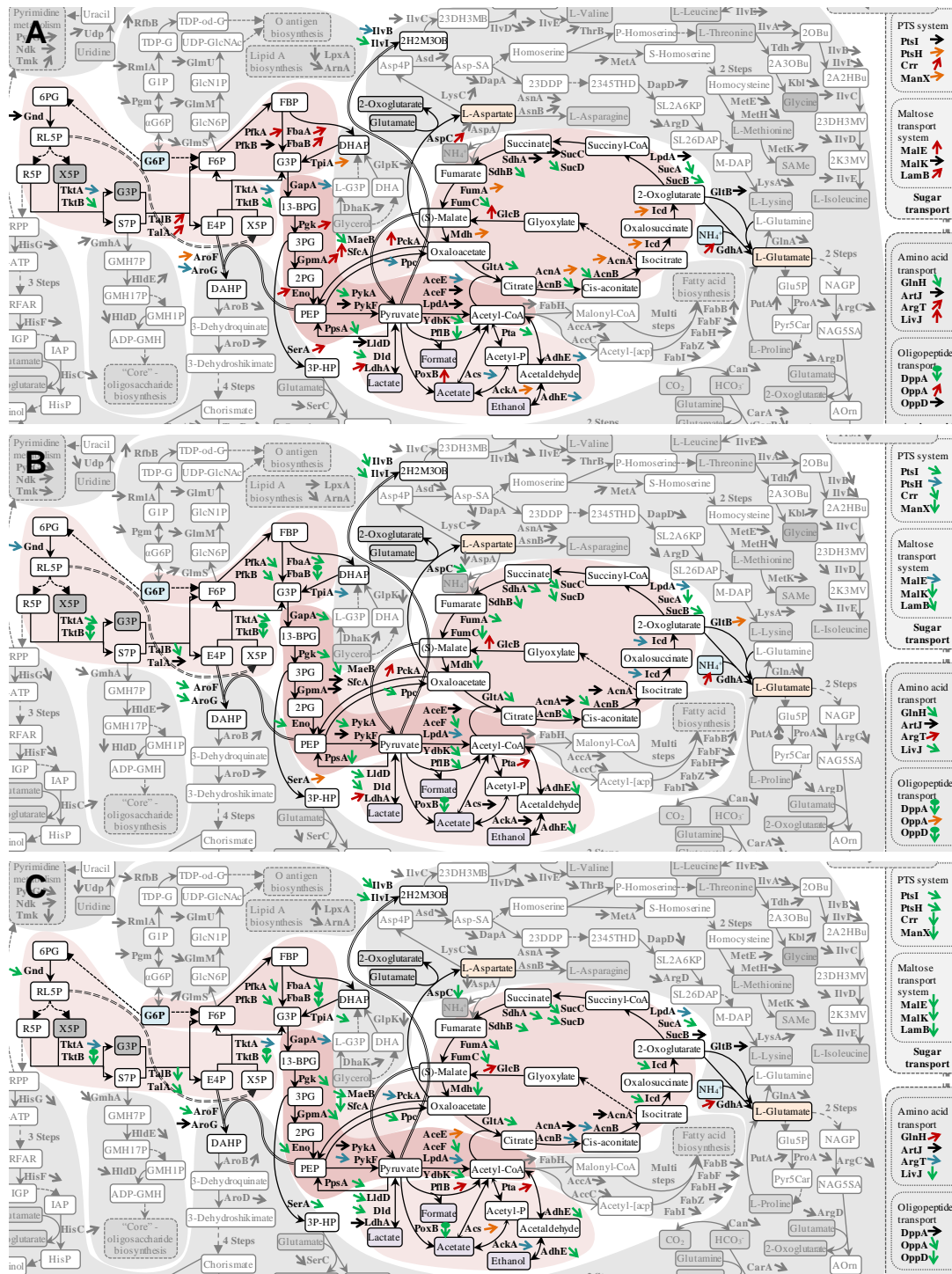


Fig. 3.4.4 Proteome changes during hFGF-2 production in defined medium (DNB)

A: Proteome comparison of *E. coli* growing at stationary/exponential phase without production. **B:** Proteome comparison 5 h after IPTG induction/exponential phase (before IPTG induction). **C:** Proteome comparison 5 h after IPTG induction/stationary phase without production. Corresponding values of $\text{Log}_2(\text{stationary/exponential phase})$ (A), $\text{Log}_2(5 \text{ h after IPTG induction/exponential phase})$ (B) and $\text{Log}_2(5 \text{ h after IPTG induction/stationary phase})$ (C) as indicated by arrows are shown in Suppl. Table 5.3.5. Fig 3.4.4A, 3.4.4B and 3.4.4C are parts of Suppl. Fig 5.3.16, 5.3.14 and 5.3.15, respectively. A comparison between 1 h after IPTG induction/exponential phase in defined medium is provided in Suppl. Fig 5.3.13.

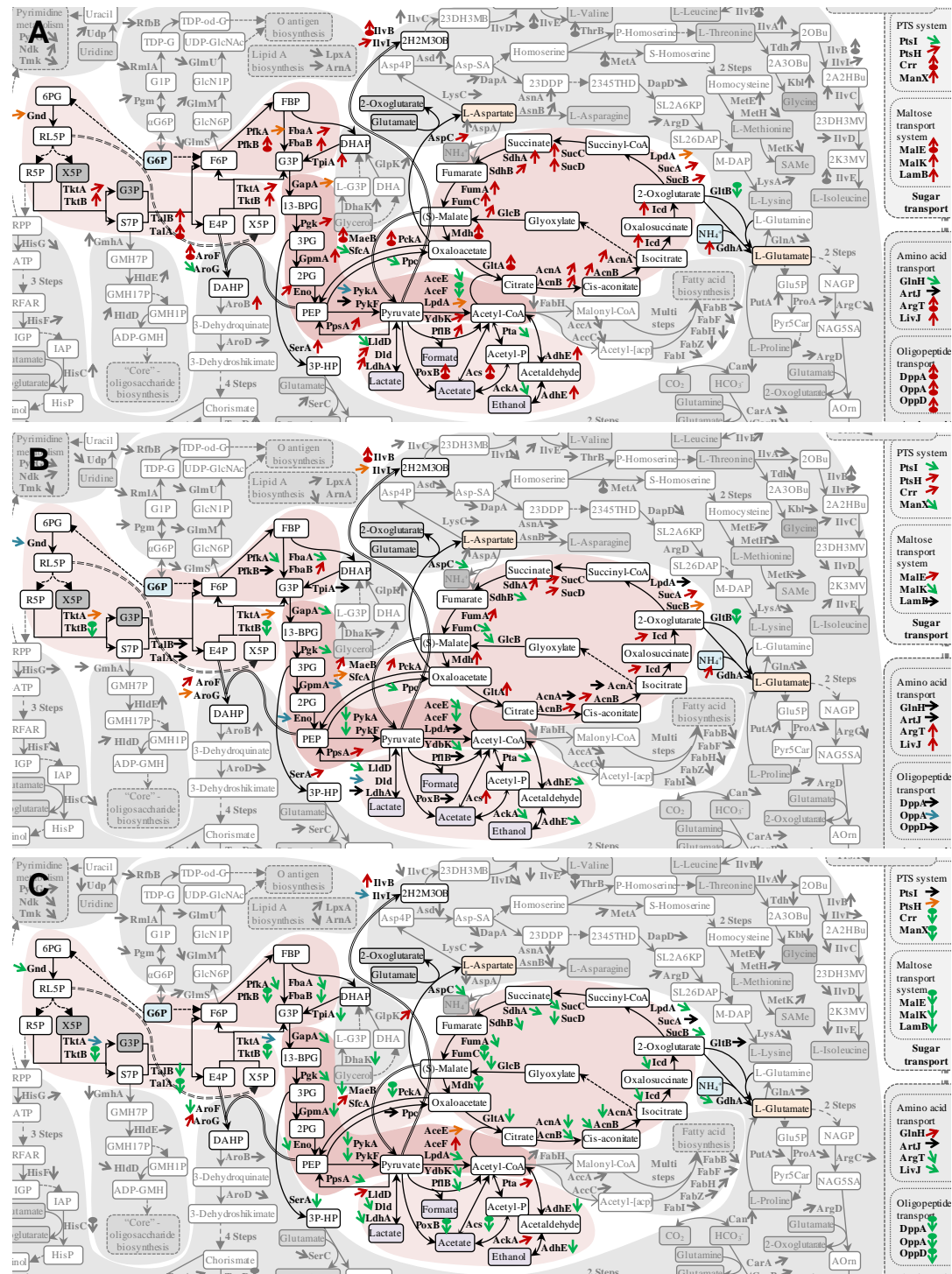


Fig. 3.4.5 Proteome changes during hFGF-2 production in complex medium (LB)

A: Proteome comparison of *E. coli* growing at stationary/exponential phase without production. **B:** Proteome comparison 3.5 h after IPTG induction/exponential phase (before IPTG induction). **C:** Proteome comparison 3.5 h after IPTG induction/stationary phase without production. Corresponding values of $\text{Log}_2(\text{stationary/exponential phase})$ (**A**), $\text{Log}_2(3.5 \text{ h after IPTG induction/exponential phase})$ (**B**) and $\text{Log}_2(3.5 \text{ h after IPTG induction/stationary phase})$ (**C**) as indicated by arrows are shown in Suppl. Table 5.3.5. Fig 3.4.5A, 3.4.5B and 3.4.5C are parts of Suppl. Fig 5.3.20, 5.3.18 and 5.3.19, respectively. A comparison between 1 h after IPTG induction/exponential phase in complex medium is provided in Suppl. Fig 5.3.17.

When *E. coli* enters stationary phase without induced protein production, enzymes in the glycolytic pathway catalyzing the reactions from G6P to PEP and the PPP are generally up-regulated, especially in complex medium (as shown in Figs. 3.4.4A and 3.4.5A) helping cells to respond better to nutrient depletion. Proteins in the lower glycolytic pathway catalyzing the conversion of PEP via pyruvate to Acetyl-CoA (PykAF, AceEF and LpdA) are slightly down-regulated in both media as compared to the exponential phase. The ability to increase the amount of enzymes in the glycolytic pathway during entry into stationary phase for a better assimilation of nutrients at low concentration is compromised when *E. coli* is forced to produce a recombinant protein (as shown in Fig. 3.4.4C and 3.4.5C).

The observed changes of enzymes from the glycolytic pathway can be explained by the regulation through two transcriptional regulators: the catabolite repressor activator (Cra) [146] and the cAMP receptor protein (CRP) [147]. Intracellular fructose-1,6-bisphosphate (FBP, which can be produced during glucose catabolism) and fructose-1-phosphate (F1P) will deactivate Cra for relieving the repression of the majority of glycolysis genes [146, 148]. High level of glucose causes catabolite repression on many lower glycolysis genes by lowering the intracellular levels of CRP-cAMP [147, 149].

In defined medium at the end of the production phase, the glucose concentration is higher than under non-production conditions (as shown in Fig. 3.4.1A2, caused by the down-regulated PTS system), thus, the catabolite repression on lower glycolysis genes by glucose will be stronger. At the same time under production conditions, the intracellular FBP will also be lower than at non-production conditions due to the down-regulated PTS system. The low level of FBP under production conditions will activate the catabolite repression by Cra on glycolysis genes. Thus, a decrease of glycolysis proteins is observed during recombinant protein production.

In complex medium (no glucose is added), the difference of catabolite repression by glucose between production and non-production conditions can be neglected. However, under production conditions, intracellular FBP and F1P can be lower than in the non-induced cells because of the down-regulated transport system, which may exert a stronger catabolite repression by Cra on glycolysis genes.

Another reason that causes the down-regulation of glycolysis proteins (under production condition) may be the stationary phase sigma factor σ^S . Nearly all glycolysis genes are under the control of sigma factor σ^S (as summarized in Suppl. Table 5.3.3), which can cause an increase of the synthesis of glycolysis proteins at stationary phase. The recombinant protein overproduction may influence its activity, leading to the down-regulation of glycolysis proteins after IPTG induction.

3.4.4.5 By-product metabolism

The mechanism of acetate overflow was analyzed for *E. coli* BL21 (DE3) growing at 37 °C (as described in chapter 3.2). When the temperature is decreased to 30 °C, no significant difference between 37 °C and 30 °C is observed without protein production: the extracellular acetate concentration (Fig. 3.4.1C) and synthesis of proteins involved in by-product metabolism (Fig. 3.4.4A and 3.4.5A) follow the same pattern.

After IPTG induction in complex medium, the synthesis of Acs (which mainly functions to metabolize extracellular acetate as discussed in chapter 3.2) is much lower than in the control cultivation without IPTG induction (Fig. 3.4.5C), and the synthesis of Pta-AckA (which function primarily in a catabolic role for excreting acetate and generating ATP) is higher than the corresponding value at stationary phase without induction. The regulatory pattern of Acs and Pta-AckA in complex medium after IPTG induction indicates that the acetate re-assimilation is compromised by the stress of recombinant proteins overproduction. Under non-production conditions in complex medium during the transition to stationary phase, the excreted acetate can be re-assimilated (Fig. 3.4.1C1) by the up-regulated Acs (Fig. 3.4.5A). Simultaneously, the Pta and AckA are down-regulated to decrease (or stop) the excretion of acetate. However, the acetate is not efficiently re-assimilated after IPTG induction (Fig. 3.4.1C1 and 3.4.1D1) due to the down-regulated Acs and up-regulated Pta-AckA.

PoxB, which is under control of the stationary phase sigma factor σ^S [234], catalyzes the oxidative decarboxylation of pyruvate to acetate and carbon dioxide [235]. In complex medium before and after IPTG induction, PoxB is not detectable in 2D gels. But it is found in cells growing in defined medium.

In defined medium 5h after IPTG induction, the synthesis of PoxB (together with proteins of the PTS system and glycolysis catalyzing the reactions from G6P to PEP) is down-regulated as compared to stationary phase without IPTG induction (Fig. 3.4.4C). In the absence of protein production at stationary phase (Fig. 3.4.4A), the up-regulation of PoxB (together with proteins of the PTS system and glycolysis catalyzing the reactions from G6P to PEP) and the slightly down-regulated TCA cycle proteins, may cause acetate excretion at early stationary phase (about 200 mg L⁻¹ as shown in Fig. 3.4.1C2). This kind of acetate excretion is not observed during protein production due to the down-regulated PoxB, PTS system and glycolysis proteins.

After IPTG induction, proteins involved in lactate (LldD, Dld and LdhA), formate (PflB) and ethanol (AdhE) metabolism are generally down-regulated as compared to the non-induced conditions (Fig. 3.4.4C and 3.4.5C). To achieve a better assimilation of lactate, formate or ethanol, the synthesis of them increases when other nutrients in growth media are insufficient. However, the increased assimilation capacities are hampered by the recombinant protein overproduction.

3.4.4.6 TCA cycle and oxidative phosphorylation

A major function of the TCA cycle is the generation of precursors for amino acid synthesis and reducing equivalents. In defined medium 5h after IPTG induction, the TCA cycle proteins together with the proteins connecting TCA cycle and glycolysis (e.g. Ppc and MaeB) are down-regulated as compared to the exponential phase before induction (Fig. 3.4.4B). In complex medium 3.5h after IPTG induction, the TCA cycle proteins together with the proteins connecting TCA cycle and glycolysis (e.g. PckA and MaeB) are up-regulated in relation to the exponential phase (Fig. 3.4.5B). However, when comparing with the stationary phases without production, several hours after IPTG induction, the synthesis of proteins in the TCA cycle and connecting pathways to glycolysis is much lower for both defined and complex media (Fig. 3.4.4C and 3.4.5C), clearly indicating that when *E. coli* is forced to overproduce a recombinant protein, the TCA cycle cannot properly perform its biological functions to generate precursors and reducing equivalents.

Under non-production condition when entering the stationary phase in complex medium, the proteins of the TCA cycle and connecting pathways to glycolysis are highly up-regulated leading to acetate re-assimilation (Fig. 3.4.1C1). However, during recombinant protein production in complex medium, the acetate is not completely re-assimilated because the proteins of the TCA cycle are down-regulated.

Oxidative phosphorylation is responsible for the transfer of electrons from NADH to the oxidized quinone pool to produce ATP for cell growth. When *E. coli* is induced to overproduce recombinant proteins, identified subunits of NADH dehydrogenase I (NuoBCFG) and ATP synthase F1 complex (AtpADH) are slightly down-regulated as compared to the control runs, especially in the cultivation using defined medium. But in the absence of protein production, the synthesis of proteins involved in oxidative phosphorylation remains nearly constant at different conditions, indicating that the energy-generating pathway (oxidative phosphorylation) is also compromised by the overproduction of the recombinant protein.

3.4.4.7 Biomass block biosynthesis

Amino acid biosynthesis pathways are important pathways in *E. coli* and are mainly controlled by the feedback inhibition (as described in chapter 3.2). The synthesis of amino acid biosynthesis proteins contributes to the biggest proteomic difference of *E. coli* grown in complex and defined media (as shown in Suppl. Table 5.3.5 and 5.3.6): when *E. coli* was grown at exponential phase, the total abundance of 57 identified amino acid biosynthesis proteins is much higher in defined medium (about 12% of WCPM) than in complex medium (about 4% of WCPM).

After 3.5h or 5h IPTG induction in complex or defined media, general down-regulations of amino acid biosynthesis proteins was observed compared to the stationary phase without

IPTG induction; the observed down-regulation in complex medium is more significant than in defined medium (Suppl. Figs 5.3.15 and 5.3.19). Specifically, during hFGF-2 production in complex medium extracellular amino acids and peptides decrease, which relieves the feedback inhibition, but the amino acid biosynthesis proteins are not up-regulated compared to the non-production control. The down-regulation of amino acid biosynthesis proteins could contribute to the down-regulation of other important proteins (e.g. proteins in glycolysis and TCA cycle).

The regulations of the majority of proteins of the nucleotide, lipopolysaccharide and other cellular component biosynthesis pathways [especially of the inosine monophosphate (IMP) biosynthesis pathway, which is an important intermediate of purine synthesis] are similar but less pronounced than the amino acid biosynthesis pathways (for details refer to Suppl. Table 5.3.5 and 5.3.6). At the end of hFGF-2 production, moderate down-regulations were observed when comparing to the stationary phase of the non-induced culture. The synthesis of biomass building blocks is impaired by the overproduction of recombinant protein, especially in the culture using complex medium.

The regulation of proteins which are responsible for the fatty acid biosynthesis is directly proportional to the growth rate at the non-induced condition, and the recombinant protein overproduction does not affect the regulatory pattern (Suppl. Table 5.3.5).

3.4.4.8 Intracellular degradation processes

When FGF-2 production is induced by IPTG in complex medium, the general regulation of identified proteins belonging to amino acid and different metabolite degradation processes (e.g. TnaA, AstABD and GatDZ) (groups 6.2 and 11 in Suppl. Table 5.3.6) is very similar to the corresponding pattern of TCA cycle proteins: the up-regulations of proteins at the end of the production (as compared to the exponential phase before induction) are less significant compared to stationary phase without production. At the end of production, the synthesis of proteins of degradation processes is down-regulated as compared to stationary phase without IPTG induction. Moreover, during production the down-regulation of proteins involved in different degradation processes is more significant in complex medium than in defined medium.

When entering stationary phase without protein production, proteins from different degradation processes are generally up-regulated to salvage the intracellular resources especially amino acids, which are no longer required. The up-regulation is less significant in defined medium (as shown in Suppl. Table 5.3.5). In complex medium, the salvage capacity is greatly impaired by the overproduction of recombinant protein due to the down-regulation of proteins from intracellular degradation pathways. In defined medium, this impairment still exists but to a lesser extent (Suppl. Figs 5.3.15 and 5.3.19).

3.4.4.9 Cell redox balance and DNA protection

Eliminating ROS and protecting DNA are crucial for *E. coli* to survive during starvation. At the end of production, the synthesis of critical proteins (groups 26 and 27 in Suppl. Table 5.3.6) for eliminating ROS (e.g. WrbA, SthA, CueO, Bfr, AhpFC, Tpx, KatG and SodB) and for protecting DNA (e.g. Ssb, Dps, UspA) are at the same or slightly lower level than before IPTG induction. But when comparing with the non-induced cultivation at stationary phase, the synthesis of the critical proteins is significantly lower (Suppl. Figs 5.3.15 and 5.3.19).

When entering stationary phase without protein production, this self-protection mechanism is activated (as described in chapter 3.3): proteins for eliminating ROS and protecting DNA are highly up-regulated (Suppl. Figs 5.3.16 and 5.3.20). But recombinant protein overproduction diminishes nearly all the up-regulations of these critical proteins. Moreover, when recombinant protein production is faster (as in complex medium), the down-regulation of these critical proteins (as compared to the stationary phase in the control run) is more significant as when the recombinant protein production is slower (as in defined medium)(Suppl. Table 5.3.5).

3.4.4.10 Transcription and translation

Identified proteins involved in transcription and translation (groups 15-22 in Suppl. Table 5.3.6), e.g. RNA polymerase, RNA polymerase binding proteins, ribosomal proteins, ribosome-associated proteins, aminoacyl-tRNA synthetases, elongation factors and RNA degrading enzymes, are mostly high abundance proteins in *E. coli*. Their synthesis is directly proportional to the growth rate under non-production conditions (as described in chapter 3.3).

After IPTG induction, the synthesis of transcription and translation related proteins does not change (or slightly decreases) as compared to the situation before induction in both defined and complex media. When comparing samples from the end of the cultivation with and without protein production, the amounts of RNA polymerases, ribosomal proteins, aminoacyl-tRNA synthetases and proteins for RNA degradation are higher in the producing culture in both defined and complex media.

In the absence of production in complex medium during the transition into stationary phase, a general down-regulation of these proteins is observed (Suppl. Fig 5.3.20). The decrease in transcription and translation related proteins can make allowance (or make proteome space) for the increase of stationary phase- or starvation induced-proteins, which helps *E. coli* to survive in the absence of sufficient nutrients. However, the general down-regulation is hindered by recombinant protein production in complex medium. The proteome data (as shown in Suppl. Table 5.3.5) clearly indicate that in complex medium during production, proteins required for translation and protein synthesis are high; *E. coli* cannot reduce the

transcription and translation related proteins for extra resources as it does when responding to nutrient depletion under non-producing conditions.

In defined medium when entering stationary phase, transcription and translation related proteins remain at nearly the same level as during exponential growth, which may be because the synthesis of these proteins have reached already the minimal level during exponential growth in defined medium (Suppl. Fig 5.3.16). Thus, during production in defined medium the unchanged (or slightly increased) amounts of RNA polymerases, ribosomal proteins, aminoacyl-tRNA synthetases, will not significantly disturb cellular metabolism.

3.4.4.11 Protein folding and degradation

After IPTG induction in both defined and complex media, the identified peptidyl prolyl cis-trans isomerases (PPIases) (PpiB, SurA, FklB, FkpA and SlyD, in group 23 in Suppl. Table 5.3.6) which could help protein folding [205, 206], are down-regulated as compared to the stationary phase without induction or exponential phase before induction. Moreover, the down-regulation is more pronounced in complex medium (with faster recombinant protein production). In non-induced cultures, the identified PPIases are generally up-regulated at stationary phase in both media. The proteomic data (as indicated in Suppl. Figs 5.3.15 and 5.3.19) suggest that the lack of isomerases may be a bottleneck for recombinant protein folding processes.

Chaperones are critical for protein folding. After several hours of IPTG induction, except HscA and ClpA, the identified chaperones, DnaK, GrpE, GroLS, HtpG, ClpB and IbpA, are highly up-regulated, and the up-regulation is much stronger and faster in complex medium. The total abundances of 9 identified chaperones increased from about 2% and 3% of WCPM at the exponential phase (before induction), to about 5% and 7% of WCPM at the end of production phase in defined and complex media, respectively. Under non-induced conditions, when *E. coli* grows to stationary phase, the identified chaperones remain at roughly the same level as during exponential growth. The proteomic analysis shows that in addition to the overproduction of recombinant protein, the up-regulated chaperones will also contribute to the metabolic burden.

Proteases are very important for the quality control of synthesized proteins [215] and also for surviving in stationary phase [217-219] (as described in chapter 3.3). At the end of production in both complex and defined media, the amounts of DegP, PepDQNP and PrlC are much lower than the corresponding amounts at stationary phase without protein production, which could explain the constant levels of proteins involved in amino acid degradation, transcription and translation during the production phase. Oppositely, under non-induced conditions when entering the stationary phase in defined and complex media, the proteases, e.g. DegP and PepDQP, are up-regulated, especially in complex medium, which corresponds to the general up-regulation of amino acid degrading proteins and also

the general down-regulation of proteins involved in transcription and translation at these conditions. The resource recycling systems have been compromised through recombinant protein overproduction.

At the end of the production phase, three proteases (Dcp and HslUV) are highly up-regulated in both media, and the up-regulation is not observed in the control cultivation, indicating that these three proteases may play important roles in folding and quality control of recombinant proteins.

3.4.5 Discussion

When nutrients are not sufficient, *E. coli* will construct a self-protection machinery (as described chapter 3.2 and 3.3) to elevate the transport and by-product assimilation pathways to absorb nutrients at low concentrations from the environment. Many degradation processes are up-regulated to salvage the intracellular components that are no longer required. The proteins involved in ROS elimination and DNA protection are also highly up-regulated. Conversely, proteins involved in transcription and translation are down-regulated, which can provide extra resources towards fine-tuning the whole proteome for long periods of starvation.

However, when *E. coli* is forced to overproduce a recombinant protein, this self-protection machinery is severely compromised. The present proteomic analysis (as shown in Fig. 3.4.6) also suggests that during faster recombinant protein production (i.e. production using complex medium), the damage to the self-protection machinery is more significant than during production at lower speed (i.e. production using defined medium).

The target protein normally amounts to about 10%-20% of WCPM. In response to the overproduction of the recombinant protein, the abundance of chaperones also increases to about 6% of WCPM. Simultaneously, proteins involved in transcription and translation, e.g. ribosomal proteins, aminoacyl-tRNA synthetases and elongation factors, do not change their abundance during the production phase. Thus, *E. coli* cannot relocate the resources from proteins involved in transcription and translation processes as it usually does in the absence of protein production in the stationary phase. Following, the resource recycling systems, such as certain proteases, proteins for amino acid or metabolite degradation, are not up-regulated at the end of recombinant protein production. The critical proteins for ROS elimination and protection of DNA also do not increase after IPTG induction, indicating that the cell is more vulnerable to oxidative damages and damage to genomic or plasmid DNA during recombinant protein production.

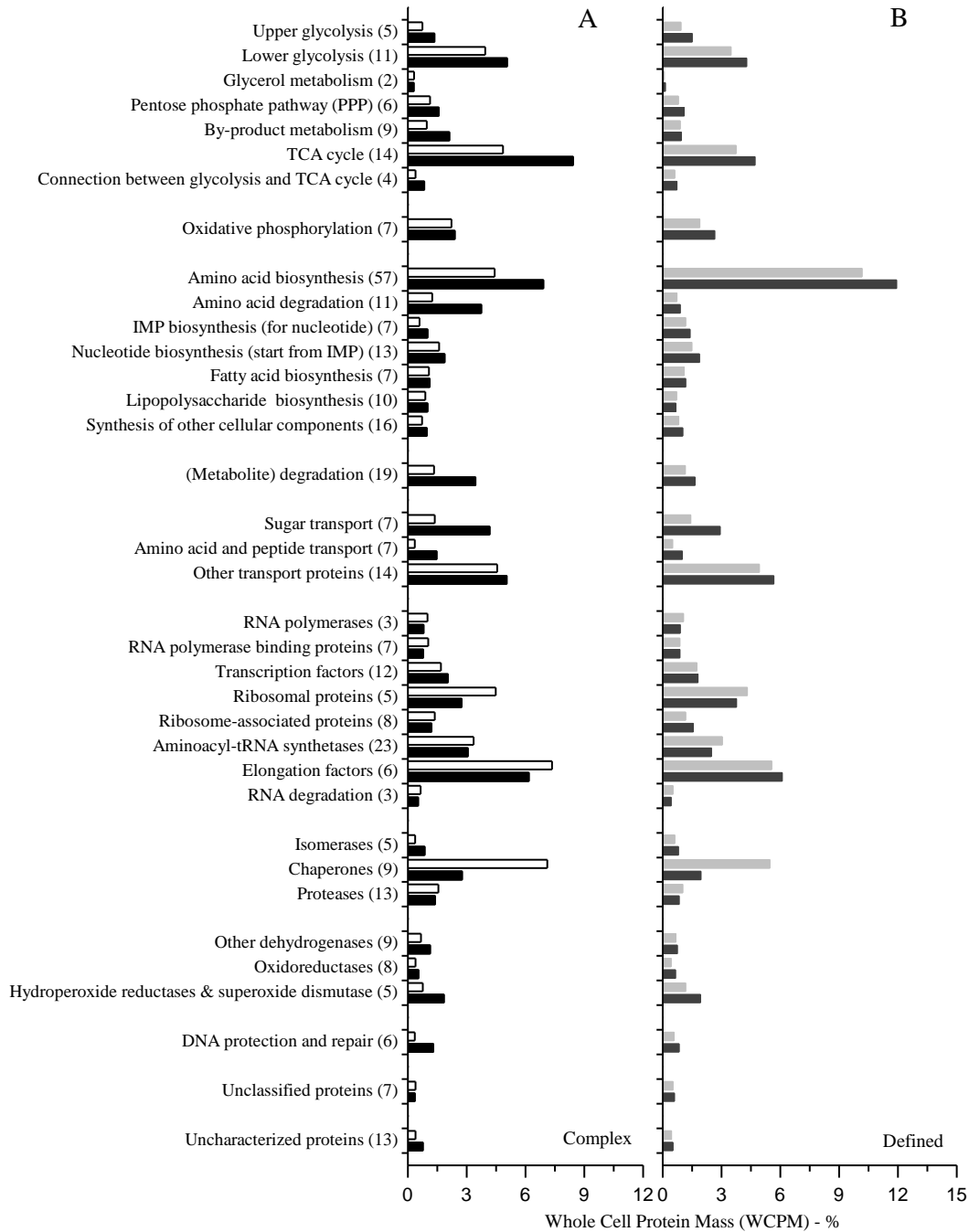


Fig. 3.4.6 Summary of proteome data of *E. coli* from stationary phase with and without protein production

Number in the bracket after each category is the number of proteins that were identified belonging to the corresponding category. **A:** in complex medium (LB) after 3.5h IPTG induction (*white bar*) and at stationary phase without induction (*black bar*). **B:** in defined medium (DNB) after 5h IPTG induction (*gray bar*) and at stationary phase without induction (*dark gray bar*). The entire data sets are shown in Suppl. Table 5.3.6.

Most importantly, nutrients decrease in the medium during the cultivation. This requires an up-regulation of proteins of different nutrient uptake pathways to increase substrate uptake efficiency. This up-regulation is hindered by the overproduction of recombinant proteins: at the end of the production phase, proteins of the glycolytic pathway and nutrient uptake systems, such as the PTS, maltose, amino acid, and peptide transport systems and proteins of the by-product assimilation pathways, show lower amounts than at stationary phase in the absence of protein production.

Acetate is the major growth-inhibiting by-product of *E. coli* and is produced during exponential growth in complex medium. During the transition into stationary phase, it is re-assimilated through the up-regulated Acs, TCA cycle proteins and proteins connecting TCA cycle and glycolysis. But when *E. coli* is forced to produce a recombinant protein, the up-regulation of Acs and proteins of the TCA cycle and pathways connecting TCA cycle and glycolysis is less prominent, which decreases the capability to metabolize acetate. The acetate is not completely re-assimilated during recombinant protein production.

In defined medium at the early stationary phase, acetate is produced because of the up-regulated PTS system (which leads to an accelerated glucose uptake), proteins from the glycolytic pathway (from G6P to pyruvate), PoxB and the slightly down-regulated TCA cycle proteins. But after 5h IPTG induction, proteins of the PTS and glycolytic pathway are down-regulated; glucose is consumed at lower rates. Thus, during protein production in defined medium, acetate excretion at the early stationary phase is lower than in the control cultivation without IPTG induction.

Although chaperones are strongly up-regulated, formation of inclusion bodies is still at a high level indicating that the capacity of the cellular protein folding support is not sufficient for the high speed of transcription and translation. Moreover, the reduced levels of isomerases may represent a bottleneck for protein folding. Trying to maintain the chaperones up-regulated and simultaneously reducing the amount of enzymes involved in translation and transcription seems to be the ultimate way to improve recombinant production in *E. coli*. A reduced capacity for translation and transcription would reduce the speed of protein synthesis before the folding process, and may also help to maintain a general metabolic balance or capacity for the synthesis of proteins required for e.g. glycolysis, TCA cycle, nutrient absorption and cell protection.

3.4.6 Acknowledgements

Support from the FORSYS Partner Project: "Dynamics and regulation of the metabolic balance in *Escherichia coli*" is greatly acknowledged.

3.5 Summary and conclusion

Two proteomic analyses were performed by the methods of 2D gel electrophoresis and mass spectrometry to reveal the physiological responses of *E. coli* to different conditions.

First, the regulation of the central metabolic pathways (CMPs), respiratory chain and biomass block biosynthesis was clarified: when precursors and reducing equivalents generated by the CMPs are sufficient for cell growth, *E. coli* simultaneously reduces the synthesis of proteins in the TCA cycle to decrease the generation of reducing equivalents and precursors for saving resources and energy. Simultaneously, enzymes of the lower glycolytic pathway are not down-regulated due to the absence of catabolite repression. This leads to an increased formation of the growth-inhibiting by-product acetate.

Second, a self-protection mechanism in response to insufficient nutrient supply was disclosed: proteins from transport and by-product assimilation pathways are elevated for absorbing the reduced amounts of nutrients in the environment. Degradation processes are enhanced to salvage the intracellular components that are no longer required. The proteins involved in eliminating the reactive oxygen species (ROS) and DNA protection are greatly enhanced. Conversely, proteins required for transcription and translation are down-regulated, which can provide extra resources towards fine-tuning the whole proteome for long term starvation.

Third, this self-protection mechanism cannot be activated when *E. coli* is forced to overproduce a recombinant protein: the relative amounts of transcription and translation related proteins remain constant. The proteins of transport systems, CMPs, by-product metabolism, and proteins for degradations, eliminating ROS and DNA protection, decrease in abundance. This causes a severe damage to the metabolic machinery (e.g. nutrients cannot be efficiently utilized).

3.6 Outlook

The proteomic profiles of *E. coli* grown in shaker flask cultures under different conditions were thoroughly studied. However, fed-batch cultivations are more practical for improving industrial production processes. Time-course proteomic data from fed-batch cultivations will help to understand cell physiology under industrially relevant conditions.

4 References

1. Studier, F.W. and Moffatt, B.A., Use of bacteriophage T7 RNA polymerase to direct selective high-level expression of cloned genes. *J Mol Biol*, 1986. 189(1): 113-30.
2. Guzman, L.M., Belin, D., Carson, M.J. and Beckwith, J., Tight regulation, modulation, and high-level expression by vectors containing the arabinose PBAD promoter. *J Bacteriol*, 1995. 177(14): 4121-30.
3. Hoffmann, F. and Rinas, U., Kinetics of heat-shock response and inclusion body formation during temperature-induced production of basic fibroblast growth factor in high-cell-density cultures of recombinant *Escherichia coli*. *Biotechnol Prog*, 2000. 16(6): 1000-7.
4. Gardner, K.H. and Kay, L.E., The use of ^2H , ^{13}C , ^{15}N multidimensional NMR to study the structure and dynamics of proteins. *Annu Rev Biophys Biomol Struct*, 1998. 27: 357-406.
5. Doublet, S., Preparation of selenomethionyl proteins for phase determination. *Methods Enzymol*, 1997. 276: 523-30.
6. Wang, C.H. and Koch, A.L., Constancy of growth on simple and complex media. *J Bacteriol*, 1978. 136(3): 969-75.
7. Reiling, H.E., Laurila, H. and Fiechter, A., Mass culture of *Escherichia coli*: Medium development for low and high density cultivation of *Escherichia coli* B/r in minimal and complex media. *J Biotechnol*, 1985. 2(3-4): 191-206.
8. Nancib, N., Branlant, C. and Boudrant, J., Metabolic roles of peptone and yeast extract for the culture of a recombinant strain of *Escherichia coli*. *J Ind Microbiol*, 1991. 8(3): 165-169.
9. Baev, M.V., Baev, D., Radek, A.J. and Campbell, J.W., Growth of *Escherichia coli* MG1655 on LB medium: determining metabolic strategy with transcriptional microarrays. *Appl Microbiol Biotechnol*, 2006. 71(3): 323-8.
10. Baev, M.V., Baev, D., Radek, A.J. and Campbell, J.W., Growth of *Escherichia coli* MG1655 on LB medium: monitoring utilization of amino acids, peptides, and nucleotides with transcriptional microarrays. *Appl Microbiol Biotechnol*, 2006. 71(3): 317-22.
11. Baev, M.V., Baev, D., Radek, A.J. and Campbell, J.W., Growth of *Escherichia coli* MG1655 on LB medium: monitoring utilization of sugars, alcohols, and organic acids with transcriptional microarrays. *Appl Microbiol Biotechnol*, 2006. 71(3): 310-6.
12. Zhang, J. and Greasham, R., Chemically defined media for commercial fermentations. *Appl Microbiol Biotechnol*, 1999. 51(4): 407-421.
13. Li, Z., Kessler, W., van den Heuvel, J. and Rinas, U., Simple defined autoinduction medium for high level recombinant protein production using T7-based *Escherichia coli* expression systems. *Appl Microbiol Biotechnol*, 2011.
14. Andersen, K.B. and von Meyenburg, K., Are growth rates of *Escherichia coli* in batch cultures limited by respiration? *J Bacteriol*, 1980. 144(1): 114-23.

References

15. Hollywood, N. and Doelle, H.W., Effect of specific growth rate and glucose concentration on growth and glucose metabolism of *Escherichia coli* K-12. *Microbios*, 1976. 17: 23-33.
16. Meyer, H.P., Leist, C. and Fiechter, A., Acetate formation in continuous culture of *Escherichia coli* K12 D1 on defined and complex media. *J Biotechnol*, 1984. 1: 355-358.
17. Luli, G.W. and Strohl, W.R., Comparison of growth, acetate production, and acetate inhibition of *Escherichia coli* strains in batch and fed-batch fermentations. *Appl Environ Microbiol*, 1990. 56(4): 1004-11.
18. De Mey, M., De Maeseneire, S., Soetaert, W. and Vandamme, E., Minimizing acetate formation in *E. coli* fermentations. *J Ind Microbiol Biotechnol*, 2007. 34: 689-700.
19. Nakano, K., Rischke, M., Sato, S. and Markl, H., Influence of acetic acid on the growth of *Escherichia coli* K12 during high-cell-density cultivation in a dialysis reactor. *Appl Microbiol Biotechnol*, 1997. 48(5): 597-601.
20. Eiteman, M.A. and Altman, E., Overcoming acetate in *Escherichia coli* recombinant protein fermentations. *Trends Biotechnol.*, 2006. 24: 530-536.
21. Han, K., Lim, H.C. and Hong, J., Acetic acid formation in *Escherichia coli* fermentation. *Biotechnol Bioeng*, 1992. 39(6): 663-71.
22. Gill, R.T., Valdes, J.J. and Bentley, W.E., A comparative study of global stress gene regulation in response to overexpression of recombinant proteins in *Escherichia coli*. *Metab Eng*, 2000. 2(3): 178-89.
23. Oh, M.K. and Liao, J.C., DNA microarray detection of metabolic responses to protein overproduction in *Escherichia coli*. *Metab Eng*, 2000. 2(3): 201-9.
24. DeLisa, M.P., Valdes, J.J. and Bentley, W.E., Quorum signaling via AI-2 communicates the "Metabolic Burden" associated with heterologous protein production in *Escherichia coli*. *Biotechnol Bioeng*, 2001. 75(4): 439-50.
25. Studier, F.W., Protein production by auto-induction in high density shaking cultures. *Protein Expr Purif*, 2005. 41(1): 207-34.
26. Blommel, P.G., Becker, K.J., Duvnjak, P. and Fox, B.G., Enhanced bacterial protein expression during auto-induction obtained by alteration of lac repressor dosage and medium composition. *Biotechnol Prog*, 2007. 23(3): 585-98.
27. Sreenath, H.K., Bingman, C.A., Buchan, B.W., Seder, K.D., Burns, B.T., Geetha, H.V., Jeon, W.B., Vojtik, F.C., Aceti, D.J., Frederick, R.O., Phillips, G.N., Jr. and Fox, B.G., Protocols for production of selenomethionine-labeled proteins in 2-L polyethylene terephthalate bottles using auto-induction medium. *Protein Expr Purif*, 2005. 40(2): 256-67.
28. Tyler, R.C., Sreenath, H.K., Singh, S., Aceti, D.J., Bingman, C.A., Markley, J.L. and Fox, B.G., Auto-induction medium for the production of [U-¹⁵N]- and [U-¹³C, U-¹⁵N]-labeled proteins for NMR screening and structure determination. *Protein Expr Purif*, 2005. 40(2): 268-78.
29. Sivashanmugam, A., Murray, V., Cui, C., Zhang, Y., Wang, J. and Li, Q., Practical protocols for production of very high yields of recombinant proteins using *Escherichia coli*. *Protein Sci*, 2009. 18(5): 936-48.
30. Fox, B.G. and Blommel, P.G., Autoinduction of protein expression. *Curr Protoc Protein Sci*, 2009. Chapter 5: Unit 5 23.

31. Sobrado, P., Goren, M.A., James, D., Amundson, C.K. and Fox, B.G., A Protein Structure Initiative approach to expression, purification, and in situ delivery of human cytochrome b5 to membrane vesicles. *Protein Expr Purif*, 2008. 58(2): 229-41.
32. Bitto, E., Bingman, C.A., Bittova, L., Frederick, R.O., Fox, B.G. and Phillips, G.N., Jr., X-ray structure of *Danio rerio* secretagogin: A hexa-EF-hand calcium sensor. *Proteins Struct Funct Bioinf*, 2009. 76(2): 477-83.
33. Oppenheimer, M., Poulin, M.B., Lowary, T.L., Helm, R.F. and Sobrado, P., Characterization of recombinant UDP-galactopyranose mutase from *Aspergillus fumigatus*. *Arch Biochem Biophys*, 2010. 502(1): 31-8.
34. Wishart, D.S. and Sykes, B.D., The ^{13}C chemical-shift index: A simple method for the identification of protein secondary structure using ^{13}C chemical-shift data. *J Biomol NMR*, 1994. 4(2): 171-80.
35. Wishart, D.S., Bigam, C.G., Holm, A., Hodges, R.S. and Sykes, B.D., ^1H , ^{13}C and ^{15}N random coil NMR chemical shifts of the common amino acids. I. Investigations of nearest-neighbor effects. *J Biomol NMR*, 1995. 5(1): 67-81.
36. Yamazaki, T., Lee, W., Arrowsmith, C.H., Muhandiram, D.R. and Kay, L.E., A suite of triple resonance NMR experiments for the backbone assignment of ^{15}N , ^{13}C , ^2H labeled proteins with high sensitivity. *J Am Chem Soc*, 1994. 116(26): 11655-66.
37. Hendrickson, W.A., Horton, J.R. and LeMaster, D.M., Selenomethionyl proteins produced for analysis by multiwavelength anomalous diffraction (MAD): a vehicle for direct determination of three-dimensional structure. *EMBO J*, 1990. 9(5): 1665-72.
38. Hendrickson, W.A., Determination of macromolecular structures from anomalous diffraction of synchrotron radiation. *Science*, 1991. 254(5028): 51-8.
39. Fiaux, J., Bertelsen, E.B., Horwich, A.L. and Wuthrich, K., Uniform and residue-specific ^{15}N -labeling of proteins on a highly deuterated background. *J Biomol NMR*, 2004. 29(3): 289-97.
40. Leiting, B., Marsilio, F. and O'Connell, J.F., Predictable deuteration of recombinant proteins expressed in *Escherichia coli*. *Anal Biochem*, 1998. 265(2): 351-5.
41. Mac, T.T., Beyermann, M., Pires, J.R., Schmieder, P. and Oschkinat, H., High yield expression and purification of isotopically labelled human endothelin-1 for use in NMR studies. *Protein Expr Purif*, 2006. 48(2): 253-60.
42. Seo, E.S., Vargues, T., Clarke, D.J., Uhrin, D. and Campopiano, D.J., Preparation of isotopically labelled recombinant β -defensin for NMR studies. *Protein Expr Purif*, 2009. 65(2): 179-84.
43. Zhao, Q., Frederick, R., Seder, K., Thao, S., Sreenath, H., Peterson, F., Volkman, B.F., Markley, J.L. and Fox, B.G., Production in two-liter beverage bottles of proteins for NMR structure determination labeled with either ^{15}N - or ^{13}C - ^{15}N . *J Struct Funct Genomics*, 2004. 5(1-2): 87-93.
44. Ross, A., Kessler, W., Krumme, D., Menge, U., Wissing, J., van den Heuvel, J. and Flohe, L., Optimised fermentation strategy for $^{13}\text{C}/^{15}\text{N}$ recombinant protein labelling in *Escherichia coli* for NMR-structure analysis. *J Biotechnol*, 2004. 108(1): 31-9.

References

45. Studts, J.M. and Fox, B.G., Application of fed-batch fermentation to the preparation of isotopically labeled or selenomethionyl-labeled proteins. *Protein Expr Purif*, 1999. 16(1): 109-19.
46. Jansson, M., Li, Y.C., Jendeberg, L., Anderson, S., Montelione, B.T. and Nilsson, B., High-level production of uniformly ¹⁵N- and ¹³C-enriched fusion proteins in *Escherichia coli*. *J Biomol NMR*, 1996. 7(2): 131-41.
47. Zhang, J., Reddy, J., Buckland, B. and Greasham, R., Toward consistent and productive complex media for industrial fermentations: studies on yeast extract for a recombinant yeast fermentation process. *Biotechnol Bioeng*, 2003. 82(6): 640-52.
48. Majewski, R.A. and Domach, M.M., Simple constrained-optimization view of acetate overflow in *E. coli*. *Biotechnol Bioeng*, 1990. 35(7): 732-8.
49. Holms, H., Flux analysis and control of the central metabolic pathways in *Escherichia coli*. *FEMS Microbiol Rev*, 1996. 19(2): 85-116.
50. Umbarger, H.E., Amino acid biosynthesis and its regulation. *Annu Rev Biochem*, 1978. 47: 532-606.
51. Shiloach, J. and Rinas, U., Glucose and acetate metabolism in *E. coli* - System level analysis and biotechnological applications in protein production processes, in *Systems Biology and Biotechnology of Escherichia coli*, S.Y. Lee, Editor. 2009, Springer: New York / Heidelberg. 377-400.
52. Boonstra, B., French, C.E., Wainwright, I. and Bruce, N.C., The *udhA* gene of *Escherichia coli* encodes a soluble pyridine nucleotide transhydrogenase. *J Bacteriol*, 1999. 181: 1030-1034.
53. Sauer, U., Canonaco, F., Heri, S., Perrenoud, A. and Fischer, E., The soluble and membrane-bound transhydrogenases UdhA and PntAB have divergent functions in NADPH metabolism of *Escherichia coli*. *J Biol Chem*, 2004. 279(8): 6613-9.
54. Georgellis, D., Kwon, O. and Lin, E.C., Quinones as the redox signal for the arc two-component system of bacteria. *Science*, 2001. 292(5525): 2314-6.
55. Nyström, T., Larsson, C. and Gustafsson, L., Bacterial defense against aging: role of the *Escherichia coli* ArcA regulator in gene expression, readjusted energy flux and survival during stasis. *EMBO J.*, 1996. 15(13): 3219-3228.
56. Malpica, R., Franco, B., Rodriguez, C., Kwon, O. and Georgellis, D., Identification of a quinone-sensitive redox switch in the ArcB sensor kinase. *Proc Natl Acad Sci U S A*, 2004. 101(36): 13318-23.
57. Green, J. and Paget, M.S., Bacterial redox sensors. *Nat Rev Microbiol*, 2004. 2(12): 954-66.
58. Park, S.J., Tseng, C.P. and Gunsalus, R.P., Regulation of succinate dehydrogenase (*sdhCDAB*) operon expression in *Escherichia coli* in response to carbon supply and anaerobiosis: role of ArcA and Fnr. *Mol Microbiol*, 1995. 15(3): 473-82.
59. Alexeeva, S., Hellingwerf, K.J. and Teixeira de Mattos, M.J., Requirement of ArcA for redox regulation in *Escherichia coli* under microaerobic but not anaerobic or aerobic conditions. *J Bacteriol*, 2003. 185(1): 204-9.
60. Vemuri, G.N., Altman, E., Sangurdekar, D.P., Khodursky, A.B. and Eiteman, M.A., Overflow metabolism in *Escherichia coli* during steady-state growth: transcriptional regulation and effect of the redox ratio. *Appl Environ Microbiol*, 2006. 72(5): 3653-61.

61. Beg, Q.K., Vazquez, A., Ernst, J., de Menezes, M.A., Bar-Joseph, Z., Barabasi, A.L. and Oltvai, Z.N., Intracellular crowding defines the mode and sequence of substrate uptake by *Escherichia coli* and constrains its metabolic activity. *Proc Natl Acad Sci U S A*, 2007. 104(31): 12663-8.
62. Navarro Llorens, J.M., Tormo, A. and Martinez-Garcia, E., Stationary phase in gram-negative bacteria. *FEMS Microbiol Rev*, 2010. 34(4): 476-95.
63. Kolter, R., Siegele, D.A. and Tormo, A., The stationary phase of the bacterial life cycle. *Annu Rev Microbiol*, 1993. 47: 855-874.
64. Reeve, C.A., Amy, P.S. and Matin, A., Role of protein synthesis in the survival of carbon-starved *Escherichia coli* K-12. *J Bacteriol*, 1984. 160(3): 1041-6.
65. Matin, A., The molecular basis of carbon-starvation-induced general resistance in *Escherichia coli*. *Mol Microbiol*, 1991. 5(1): 3-10.
66. Groat, R.G., Schultz, J.E., Zychlinsky, E., Bockman, A. and Matin, A., Starvation proteins in *Escherichia coli*: kinetics of synthesis and role in starvation survival. *J Bacteriol*, 1986. 168(2): 486-93.
67. Dukan, S. and Nystrom, T., Oxidative stress defense and deterioration of growth-arrested *Escherichia coli* cells. *J Biol Chem*, 1999. 274(37): 26027-32.
68. Jenkins, D.E., Schultz, J.E. and Matin, A., Starvation-induced cross protection against heat or H₂O₂ challenge in *Escherichia coli*. *J Bacteriol*, 1988. 170(9): 3910-4.
69. Nyström, T., Stationary-phase physiology. *Annu Rev Microbiol*, 2004. 58: 161-81.
70. Weichart, D., Querfurth, N., Dreger, M. and Hengge-Aronis, R., Global role for ClpP-containing proteases in stationary-phase adaptation of *Escherichia coli*. *J Bacteriol*, 2003. 185(1): 115-25.
71. Groat, R.G. and Matin, A., Synthesis of unique proteins at the onset of carbon starvation in *Escherichia coli*. *J Ind Microbiol Biotechnol*, 1986. 1(2): 69-73.
72. Groat, R.G., Schultz, J.E., Zychlinsky, E., Bockman, A. and Matin, A., Starvation proteins in *Escherichia coli*: kinetics of synthesis and role in starvation survival. *J Bacteriol*, 1986. 168: 486-493.
73. Schultz, J.E., Latter, G.I. and Matin, A., Differential regulation by cyclic AMP of starvation protein synthesis in *Escherichia coli*. *J Bacteriol*, 1988. 170(9): 3903-9.
74. Bhattacharya, S.K. and Dubey, A.K., Metabolic burden as reflected by maintenance coefficient of recombinant *Escherichia coli* overpressing target gene. *Biotechnol Lett*, 1995. 17: 1155-1160.
75. Bentley, W.E., Mirjalili, N., Anderson, D.C., Davis, R. and Kompala, D.S., Plasmid-encoded protein: the principal factor in the "metabolic burden" associated with recombinant bacteria. *Biotechnol Bioeng*, 1990. 35: 668-681.
76. Rozkov, A., Avignone-Rossa, C.A., Ertl, P.F., Jones, P., O'Kennedy, R.D., Smith, J.J., Dale, J.W. and Bushell, M.E., Characterization of the metabolic burden on *Escherichia coli* DH1 cells imposed by the presence of a plasmid containing a gene therapy sequence. *Biotechnol Bioeng*, 2004. 88(7): 909-15.
77. Hoffmann, F. and Rinas, U., On-line estimation of the metabolic burden resulting from the synthesis of plasmid-encoded and heat-shock proteins by monitoring respiratory energy generation. *Biotechnol Bioeng*, 2001. 76(4): 333-40.

References

78. Ow, D.S.W., Nissom, P.M., Philp, R., Oh, S.K.W. and Yap, M.G.S., Global transcriptional analysis of metabolic burden due to plasmid maintenance in *Escherichia coli* DH5 alpha during batch fermentation. *Enzyme Microb Technol*, 2006. 39(3): 391-398.
79. Hoffmann, F., Weber, J. and Rinas, U., Metabolic adaptation of *Escherichia coli* during temperature-induced recombinant protein production: 1. Readjustment of metabolic enzyme synthesis. *Biotechnol Bioeng*, 2002. 80(3): 313-9.
80. Weber, J., Hoffmann, F. and Rinas, U., Metabolic adaptation of *Escherichia coli* during temperature-induced recombinant protein production: 2. Redirection of metabolic fluxes. *Biotechnol Bioeng*, 2002. 80(3): 320-30.
81. Hoffmann, F., Posten, C. and Rinas, U., Kinetic model of *in vivo* folding and inclusion body formation in recombinant *Escherichia coli*. *Biotechnol Bioeng*, 2001. 72(3): 315-22.
82. Hoffmann, F., van den Heuvel, J., Zidek, N. and Rinas, U., Minimizing inclusion body formation during recombinant protein production in *Escherichia coli* at bench and pilot plant scale. *Enzyme Microb Technol* 2004. 34: 235-241.
83. Rinas, U., Hoffmann, F., Betiku, E., Estape, D. and Marten, S., Inclusion body anatomy and functioning of chaperone-mediated *in vivo* inclusion body disassembly during high-level recombinant protein production in *Escherichia coli*. *J Biotechnol*, 2007. 127(2): 244-57.
84. de Groot, N.S., Espargaro, A., Morell, M. and Ventura, S., Studies on bacterial inclusion bodies. *Future Microbiol*, 2008. 3(4): 423-35.
85. Wang, L., Maji, S.K., Sawaya, M.R., Eisenberg, D. and Riek, R., Bacterial inclusion bodies contain amyloid-like structure. *PLoS Biol*, 2008. 6(8): e195.
86. Villaverde, A. and Carrio, M.M., Protein aggregation in recombinant bacteria: biological role of inclusion bodies. *Biotechnol Lett*, 2003. 25(17): 1385-95.
87. Allen, S.P., Polazzi, J.O., Gierse, J.K. and Easton, A.M., Two novel heat shock genes encoding proteins produced in response to heterologous protein expression in *Escherichia coli*. *J Bacteriol*, 1992. 174(21): 6938-47.
88. Jürgen, B., Lin, H.Y., Riemschneider, S., Scharf, C., Neubauer, P., Schmid, R., Hecker, M. and Schweder, T., Monitoring of genes that respond to overproduction of an insoluble recombinant protein in *Escherichia coli* glucose-limited fed-batch fermentations. *Biotechnol Bioeng*, 2000. 70(2): 217-24.
89. Harcum, S.W. and Bentley, W.E., Response dynamics of 26-, 34-, 39-, 54-, and 80-kDa proteases in induced cultures of recombinant *Escherichia coli*. *Biotechnol Bioeng*, 1993. 42(6): 675-85.
90. Goff, S.A. and Goldberg, A.L., Production of abnormal proteins in *E. coli* stimulates transcription of lon and other heat shock genes. *Cell*, 1985. 41(2): 587-95.
91. Dürschmid, K., Reischer, H., Schmidt-Heck, W., Hrebicek, T., Guthke, R., Rizzi, A. and Bayer, K., Monitoring of transcriptome and proteome profiles to investigate the cellular response of *E. coli* towards recombinant protein expression under defined chemostat conditions. *J Biotechnol*, 2008. 135: 34-44.
92. Aldor, I.S., Krawitz, D.C., Forrest, W., Chen, C., Nishihara, J.C., Joly, J.C. and Champion, K.M., Proteomic profiling of recombinant *Escherichia coli* in high-cell-density fermentations for improved production of an antibody fragment biopharmaceutical. *Appl Environ Microbiol*, 2005. 71: 1717-1728.

93. Han, M.J., Jeong, K.J., Yoo, J.S. and Lee, S.Y., Engineering *Escherichia coli* for increased productivity of serine-rich proteins based on proteome profiling. *Appl Environ Microbiol*, 2003. 69: 5772-5781.
94. Dürschmid, K., Marzban, G., Dürschmid, E., Striedner, G., Clementschitsch, F., Cserjan-Puschmann, M. and Bayer, K., Monitoring of protein profiles for the optimization of recombinant fermentation processes using public domain databases. *Electrophoresis*, 2003. 24: 303-310.
95. Champion, K.M., Nishihara, J.C., Aldor, I.S., Moreno, G., Andersen, D., Stults, K.L. and Vanderlaan, M., Comparison of the *Escherichia coli* proteomes for recombinant human growth hormone producing and nonproducing fermentations. *Proteomics*, 2003. 3: 1365-1373.
96. Champion, K.M., Nishihara, J.C., Joly, J.C. and Arnott, D., Similarity of the *Escherichia coli* proteome upon completion of different biopharmaceutical fermentation processes. *Proteomics*, 2001. 1: 1133-1148.
97. Lopez-Campistrous, A., Semchuk, P., Burke, L., Palmer-Stone, T., Brokx, S.J., Broderick, G., Bottorff, D., Bolch, S., Weiner, J.H. and Ellison, M.J., Localization, annotation, and comparison of the *Escherichia coli* K-12 proteome under two states of growth. *Mol Cell Proteomics*, 2005. 4(8): 1205-9.
98. Gevaert, K., Van Damme, J., Goethals, M., Thomas, G.R., Hoorelbeke, B., Demol, H., Martens, L., Puype, M., Staes, A. and Vandekerckhove, J., Chromatographic isolation of methionine-containing peptides for gel-free proteome analysis: identification of more than 800 *Escherichia coli* proteins. *Mol Cell Proteomics*, 2002. 1(11): 896-903.
99. Corbin, R.W., Paliy, O., Yang, F., Shabanowitz, J., Platt, M., Lyons, C.E., Jr., Root, K., McAuliffe, J., Jordan, M.I., Kustu, S., Soupene, E. and Hunt, D.F., Toward a protein profile of *Escherichia coli*: comparison to its transcription profile. *Proc Natl Acad Sci U S A*, 2003. 100(16): 9232-7.
100. Maillet, I., Berndt, P., Malo, C., Rodriguez, S., Brunisholz, R.A., Pragai, Z., Arnold, S., Langen, H. and Wyss, M., From the genome sequence to the proteome and back: evaluation of *E. coli* genome annotation with a 2-D gel-based proteomics approach. *Proteomics*, 2007. 7(7): 1097-106.
101. O'Farrell, P.H., High resolution two-dimensional electrophoresis of proteins. *J.Biol.Chem.*, 1975. 250: 4007-4021.
102. Hillenkamp, F., Karas, M., Beavis, R.C. and Chait, B.T., Matrix-assisted laser desorption/ionization mass spectrometry of biopolymers. *Anal Chem*, 1991. 63(24): 1193A-1203A.
103. Blackstock, W.P. and Weir, M.P., Proteomics: quantitative and physical mapping of cellular proteins. *Trends Biotechnol*, 1999. 17(3): 121-7.
104. Frederick, R.O., Bergeman, L., Blommel, P.G., Bailey, L.J., McCoy, J.G., Song, J., Meske, L., Bingman, C.A., Ritters, M., Dillon, N.A., Kunert, J., Yoon, J.W., Lim, A., Cassidy, M., Bunge, J., Aceti, D.J., Primm, J.G., Markley, J.L., Phillips, G.N., Jr. and Fox, B.G., Small-scale, semi-automated purification of eukaryotic proteins for structure determination. *J Struct Funct Genomics*, 2007. 8(4): 153-66.
105. Bitto, E., Bingman, C.A., Bittova, L., Kondrashov, D.A., Bannen, R.M., Fox, B.G., Markley, J.L. and Phillips, G.N., Jr., Structure of human J-type co-chaperone HscB reveals a tetracysteine metal-binding domain. *J Biol Chem*, 2008. 283(44): 30184-92.

References

106. Zahn, R., von Schroetter, C. and Wuthrich, K., Human prion proteins expressed in *Escherichia coli* and purified by high-affinity column refolding. *FEBS Lett*, 1997. 417(3): 400-4.
107. Cronet, P., Petersen, J.F., Folmer, R., Blomberg, N., Sjoblom, K., Karlsson, U., Lindstedt, E.L. and Bamberg, K., Structure of the PPAR α and γ ligand binding domain in complex with AZ 242; ligand selectivity and agonist activation in the PPAR family. *Structure*, 2001. 9(8): 699-706.
108. Machner, M.P. and Isberg, R.R., Targeting of host Rab GTPase function by the intravacuolar pathogen *Legionella pneumophila*. *Dev Cell*, 2006. 11(1): 47-56.
109. Bublitz, M., Polle, L., Holland, C., Heinz, D.W., Nimtz, M. and Schubert, W.D., Structural basis for autoinhibition and activation of Auto, a virulence-associated peptidoglycan hydrolase of *Listeria monocytogenes*. *Mol Microbiol*, 2009. 71(6): 1509-22.
110. Li, Z., Kessler, W., van den Heuvel, J. and Rinas, U., Simple defined autoinduction medium for high-level recombinant protein production using T7-based *Escherichia coli* expression systems. *Appl Microbiol Biotechnol*, 2011. 91(4): 1203-13.
111. Letzelter, M., Sorg, I., Mota, L.J., Meyer, S., Stalder, J., Feldman, M., Kuhn, M., Callebaut, I. and Cornelis, G.R., The discovery of SycO highlights a new function for type III secretion effector chaperones. *EMBO J*, 2006. 25(13): 3223-33.
112. Korz, D.J., Rinas, U., Hellmuth, K., Sanders, E.A. and Deckwer, W.D., Simple fed-batch technique for high cell density cultivation of *Escherichia coli*. *J Biotechnol*, 1995. 39(1): 59-65.
113. Sambrook, J. and Russell, D., *Molecular Cloning: A Laboratory Manual* (Third Edition). 2001, Cold Spring Harbor Laboratory Press: New York. A 2.7.
114. Bollag, D.M., Rozycki, M.D. and Edelman, S.J., *Protein Methods*, Second edition. 1996, Wiley-Liss, Inc.: New York. 107-151.
115. Candiano, G., Bruschi, M., Musante, L., Santucci, L., Ghiggeri, G.M., Carnemolla, B., Orecchia, P., Zardi, L. and Righetti, P.G., Blue silver: A very sensitive colloidal Coomassie G-250 staining for proteome analysis. *Electrophoresis*, 2004. 25(9): 1327-33.
116. Ingraham, J.L., Maaloe, O. and Neidhardt, F.C., Composition, organization, and structure of the bacterial cell. In: *Growth of the bacterial cell*. 1983, Massachusetts: Sinauer Associates Inc: Sunderland. 1-48.
117. Albano, C.R., Randers-Eichhorn, L., Chang, Q., Bentley, W.R. and Rao, G., Quantitative measurement of green fluorescent protein expression. *Biotechnol Tech*, 1996. 10(12): 953-58.
118. Chalfie, M., Tu, Y., Euskirchen, G., Ward, W.W. and Prasher, D.C., Green fluorescent protein as a marker for gene expression. *Science*, 1994. 263(5148): 802-5.
119. Tsien, R.Y., The green fluorescent protein. *Annu Rev Biochem*, 1998. 67: 509-44.
120. Faessel, H.M., Lévassieur, L.M., Slocum, H.K. and Greco, W.R., Parabolic growth patterns in 96-well plate cell growth experiments. *In Vitro Cell Dev Biol Anim*, 1999. 35(5): 270-8.
121. Kayser, A., Weber, J., Hecht, V. and Rinas, U., Metabolic flux analysis of *Escherichia coli* in glucose-limited continuous culture. I. Growth-rate-dependent metabolic efficiency at steady state. *Microbiology*, 2005. 151(3): 693-706.

122. Schmidt, M., Viaplana, E., Hoffmann, F., Marten, S., Villaverde, A. and Rinas, U., Secretion-dependent proteolysis of heterologous protein by recombinant *Escherichia coli* is connected to an increased activity of the energy-generating dissimilatory pathway. *Biotechnol Bioeng*, 1999. 66(1): 61-7.
123. Paliy, O., Bloor, D., Brockwell, D., Gilbert, P. and Barber, J., Improved methods of cultivation and production of deuteriated proteins from *E. coli* strains grown on fully deuteriated minimal medium. *J Appl Microbiol*, 2003. 94(4): 580-6.
124. Romanuka, J., van den Bulke, H., Kaptein, R., Boelens, R. and Folkers, G.E., Novel strategies to overcome expression problems encountered with toxic proteins: application to the production of Lac repressor proteins for NMR studies. *Protein Expr Purif*, 2009. 67(2): 104-12.
125. Marley, J., Lu, M. and Bracken, C., A method for efficient isotopic labeling of recombinant proteins. *J Biomol NMR*, 2001. 20(1): 71-5.
126. Lu, X., Sun, J., Nimtz, M., Wissing, J., Zeng, A.P. and Rinas, U., The intra- and extracellular proteome of *Aspergillus niger* growing on defined medium with xylose or maltose as carbon substrate. *Microb Cell Fact*, 2010. 9: 23.
127. Wang, W., Sun, J., Nimtz, M., Deckwer, W.D. and Zeng, A.P., Protein identification from two-dimensional gel electrophoresis analysis of *Klebsiella pneumoniae* by combined use of mass spectrometry data and raw genome sequences. *Proteome Sci*, 2003. 1(1): 6.
128. Culebras, J.M. and Moore, F.D., Total body water and the exchangeable hydrogen. I. Theoretical calculation of nonaqueous exchangeable hydrogen in man. *Am J Physiol*, 1977. 232(1): R54-9.
129. Zhao, K.Q., Hartmett, J. and Slater, M.R., Selenomethionine protein labeling using the *Escherichia coli* strain KRX. *Promega Notes*, 2007. 96: 24-26.
130. Link, A.J., Robison, K. and Church, G.M., Comparing the predicted and observed properties of proteins encoded in the genome of *Escherichia coli* K-12. *Electrophoresis*, 1997. 18(8): 1259-313.
131. Baek, J.H., Han, M.J., Lee, S.Y. and Yoo, J.S., Transcriptome and proteome analyses of adaptive responses to methyl methanesulfonate in *Escherichia coli* K-12 and *ada* mutant strains. *BMC Microbiol*, 2009. 9: 186.
132. Peng, L. and Shimizu, K., Global metabolic regulation analysis for *Escherichia coli* K12 based on protein expression by 2-dimensional electrophoresis and enzyme activity measurement. *Appl Microbiol Biotechnol*, 2003. 61(2): 163-78.
133. Yoon, S.H., Han, M.J., Lee, S.Y., Jeong, K.J. and Yoo, J.S., Combined transcriptome and proteome analysis of *Escherichia coli* during high cell density culture. *Biotechnol Bioeng*, 2003. 81: 753-767.
134. Xia, X.X., Han, M.J., Lee, S.Y. and Yoo, J.S., Comparison of the extracellular proteomes of *Escherichia coli* B and K-12 strains during high cell density cultivation. *Proteomics*, 2008. 8: 2089-2103.
135. Shiloach, J., Kaufmann, J., Guillard, A.S. and Fass, R., Effect of glucose supply strategy on acetate accumulation, growth, and recombinant protein production by *Escherichia coli* BL21 (λ DE3) and *Escherichia coli* JM109. *Biotechnol Bioeng*, 1996. 49(4): 421-428.

References

136. Phue, J.N., Noronha, S.B., Hattacharyya, R., Wolfe, A.J. and Shiloach, J., Glucose metabolism at high density growth of *E. coli* B and *E. coli* K: differences in metabolic pathways are responsible for efficient glucose utilization in *E. coli* B as determined by microarrays and northern blot analyses. *Biotechnol Bioeng*, 2005. 90(7): 805-820.
137. Phue, J.N. and Shiloach, J., Transcription levels of key metabolic genes are the cause for different glucose utilization pathways in *E. coli* B (BL21) and *E. coli* K (JM109). *J Biotechnol*, 2004. 109: 21-30.
138. Lee, D.H., Kim, S.G., Park, Y.C., Nam, S.W., Lee, K.H. and Seo, J.H., Proteome analysis of recombinant *Escherichia coli* producing human glucagon-like peptide-1. *J Chromatogr B*, 2007. 849: 323-330.
139. Han, K.Y., Park, J.S., Seo, H.S., Ahn, K.Y. and Lee, J., Multiple stressor-induced proteome responses of *Escherichia coli* BL21(DE3). *J Proteome Res*, 2008. 7: 1891-1903.
140. Cheng, C.H. and Lee, W.C., Protein solubility and differential proteomic profiling of recombinant *Escherichia coli* overexpressing double-tagged fusion proteins. *Microb Cell Fact*, 2010. 9: 63.
141. Li, Z., Nimtz, M. and Rinas, U., Optimized procedure to generate heavy isotope and selenomethionine-labeled proteins for structure determination using *Escherichia coli*-based expression systems. *Appl Microbiol Biotechnol*, 2011. 92: 823-833.
142. Wessel, D. and Flugge, U.I., A method for the quantitative recovery of protein in dilute solution in the presence of detergents and lipids. *Anal Biochem*, 1984. 138(1): 141-3.
143. Keseler, I.M., Collado-Vides, J., Gama-Castro, S., Ingraham, J., Paley, S., Paulsen, I.T., Peralta-Gil, M. and Karp, P.D., EcoCyc: a comprehensive database resource for *Escherichia coli*. *Nucleic Acids Res*, 2005. 33(Database issue): D334-7.
144. Kanehisa, M. and Goto, S., KEGG: kyoto encyclopedia of genes and genomes. *Nucleic Acids Res*, 2000. 28(1): 27-30.
145. Gama-Castro, S., Salgado, H., Peralta-Gil, M., Santos-Zavaleta, A., Muniz-Rascado, L., Solano-Lira, H., Jimenez-Jacinto, V., Weiss, V., Garcia-Sotelo, J.S., Lopez-Fuentes, A., Porron-Sotelo, L., Alquicira-Hernandez, S., Medina-Rivera, A., Martinez-Flores, I., Alquicira-Hernandez, K., Martinez-Adame, R., Bonavides-Martinez, C., Miranda-Rios, J., Huerta, A.M., Mendoza-Vargas, A., Collado-Torres, L., Taboada, B., Vega-Alvarado, L., Olvera, M., Olvera, L., Grande, R., Morett, E. and Collado-Vides, J., RegulonDB version 7.0: transcriptional regulation of *Escherichia coli* K-12 integrated within genetic sensory response units (Sensor Units). *Nucleic Acids Res*, 2011. 39(Database issue): D98-105.
146. Shimada, T., Yamamoto, K. and Ishihama, A., Novel members of the Cra regulon involved in carbon metabolism in *Escherichia coli*. *J Bacteriol*, 2011. 193(3): 649-59.
147. Fic, E., Bonarek, P., Gorecki, A., Kedracka-Krok, S., Mikolajczak, J., Polit, A., Tworzydło, M., Dziedzicka-Wasylewska, M. and Wasylewski, Z., cAMP receptor protein from *Escherichia coli* as a model of signal transduction in proteins--a review. *J Mol Microbiol Biotechnol*, 2009. 17(1): 1-11.
148. Shimada, T., Fujita, N., Maeda, M. and Ishihama, A., Systematic search for the Cra-binding promoters using genomic SELEX system. *Genes Cells*, 2005. 10(9): 907-18.

149. Ishizuka, H., Hanamura, A., Inada, T. and Aiba, H., Mechanism of the down-regulation of cAMP receptor protein by glucose in *Escherichia coli*: role of autoregulation of the *crp* gene. *EMBO J*, 1994. 13(13): 3077-82.
150. Abdel-Hamid, A.M., Attwood, M.M. and Guest, J.R., Pyruvate oxidase contributes to the aerobic growth efficiency of *Escherichia coli*. *Microbiology*, 2001. 147: 1483-1498.
151. Brown, T.D., Jones-Mortimer, M.C. and Kornberg, H.L., The enzymic interconversion of acetate and acetyl-coenzyme A in *Escherichia coli*. *J Gen Microbiol*, 1977. 102(2): 327-36.
152. Kumari, S., Tishel, R., Eisenbach, M. and Wolfe, A.J., Cloning, characterization, and functional expression of *acs*, the gene which encodes acetyl coenzyme A synthetase in *Escherichia coli*. *J Bacteriol*, 1995. 177(10): 2878-86.
153. Leonardo, M.R., Cunningham, P.R. and Clark, D.P., Anaerobic regulation of the *adhE* gene, encoding the fermentative alcohol dehydrogenase of *Escherichia coli*. *J Bacteriol*, 1993. 175(3): 870-8.
154. Sawers, G. and Bock, A., Anaerobic regulation of pyruvate formate-lyase from *Escherichia coli* K-12. *J Bacteriol*, 1988. 170(11): 5330-6.
155. Mat-Jan, F., Alam, K.Y. and Clark, D.P., Mutants of *Escherichia coli* deficient in the fermentative lactate dehydrogenase. *J Bacteriol*, 1989. 171(1): 342-8.
156. Liu, X. and De Wulf, P., Probing the ArcA-P modulon of *Escherichia coli* by whole genome transcriptional analysis and sequence recognition profiling. *J Biol Chem*, 2004. 279(13): 12588-97.
157. Park, S.J., Chao, G. and Gunsalus, R.P., Aerobic regulation of the *sucABCD* genes of *Escherichia coli*, which encode alpha-ketoglutarate dehydrogenase and succinyl coenzyme A synthetase: roles of ArcA, Fnr, and the upstream *sdhCDAB* promoter. *J Bacteriol*, 1997. 179(13): 4138-42.
158. Cunningham, L., Gruer, M.J. and Guest, J.R., Transcriptional regulation of the aconitase genes (*acnA* and *acnB*) of *Escherichia coli*. *Microbiology*, 1997. 143: 3795-805.
159. Park, S.J. and Gunsalus, R.P., Oxygen, iron, carbon, and superoxide control of the fumarase *fumA* and *fumC* genes of *Escherichia coli*: role of the *arca*, *fnr*, and *soxR* gene products. *J Bacteriol*, 1995. 177(21): 6255-62.
160. Cunningham, L. and Guest, J.R., Transcription and transcript processing in the *sdhCDAB-sucABCD* operon of *Escherichia coli*. *Microbiology*, 1998. 144: 2113-23.
161. Wilde, R.J. and Guest, J.R., Transcript analysis of the citrate synthase and succinate dehydrogenase genes of *Escherichia coli* K12. *J Gen Microbiol*, 1986. 132(12): 3239-51.
162. Zhang, Z., Gosset, G., Barabote, R., Gonzalez, C.S., Cuevas, W.A. and Saier, M.H., Jr., Functional interactions between the carbon and iron utilization regulators, Crp and Fur, in *Escherichia coli*. *J Bacteriol*, 2005. 187(3): 980-90.
163. Zheng, D., Constantinidou, C., Hobman, J.L. and Minchin, S.D., Identification of the CRP regulon using *in vitro* and *in vivo* transcriptional profiling. *Nucleic Acids Res*, 2004. 32(19): 5874-93.

References

164. Vogel, R.F., Entian, K.D. and Mecke, D., Cloning and sequence of the *mdh* structural gene of *Escherichia coli* coding for malate dehydrogenase. Arch Microbiol, 1987. 149(1): 36-42.
165. Nobelmann, B. and Lengeler, J.W., Molecular analysis of the *gat* genes from *Escherichia coli* and of their roles in galactitol transport and metabolism. J Bacteriol, 1996. 178(23): 6790-5.
166. Salmon, K.A., Hung, S.P., Steffen, N.R., Krupp, R., Baldi, P., Hatfield, G.W. and Gunsalus, R.P., Global gene expression profiling in *Escherichia coli* K12: effects of oxygen availability and ArcA. J Biol Chem, 2005. 280(15): 15084-96.
167. Hollands, K., Busby, S.J. and Lloyd, G.S., New targets for the cyclic AMP receptor protein in the *Escherichia coli* K-12 genome. FEMS Microbiol Lett, 2007. 274(1): 89-94.
168. Shalel-Levanon, S., San, K.-Y. and Bennett, G.N., Effect of oxygen, and ArcA and FNR regulators on the expression of genes related to the electron transfer chain and the TCA cycle in *Escherichia coli*. Metabolic Engineering, 2005. 7(5-6): 364-374.
169. Kasimoglu, E., Park, S.J., Malek, J., Tseng, C.P. and Gunsalus, R.P., Transcriptional regulation of the proton-translocating ATPase (*atpIBEFHAGDC*) operon of *Escherichia coli*: control by cell growth rate. J Bacteriol, 1996. 178(19): 5563-7.
170. Schneider, D.A. and Gourse, R.L., Relationship between growth rate and ATP concentration in *Escherichia coli*: a bioassay for available cellular ATP. J Biol Chem, 2004. 279(9): 8262-8.
171. He, B., Shiau, A., Choi, K.Y., Zalkin, H. and Smith, J.M., Genes of the *Escherichia coli* *pur* regulon are negatively controlled by a repressor-operator interaction. J Bacteriol, 1990. 172(8): 4555-62.
172. Meng, L.M., Kilstrup, M. and Nygaard, P., Autoregulation of PurR repressor synthesis and involvement of *purR* in the regulation of *purB*, *purC*, *purL*, *purMN* and *guaBA* expression in *Escherichia coli*. Eur J Biochem, 1990. 187(2): 373-9.
173. Cho, B.K., Federowicz, S.A., Embree, M., Park, Y.S., Kim, D. and Palsson, B.O., The PurR regulon in *Escherichia coli* K-12 MG1655. Nucleic Acids Res, 2011. 39(15): 6456-64.
174. Zalkin, H. and Nygaard, P., Biosynthesis of purine nucleotides, in *Escherichia coli and Salmonella: cellular and molecular biology*, 2nd edn, F.C. Neidhardt, Editor. 1996, American Society for Microbiology Press: Washington, D.C. 561-579.
175. Miksch, G., Bettenworth, F., Friehs, K., Flaschel, E., Saalbach, A., Twellmann, T. and Nattkemper, T.W., Libraries of synthetic stationary-phase and stress promoters as a tool for fine-tuning of expression of recombinant proteins in *Escherichia coli*. J Biotechnol, 2005. 120(1): 25-37.
176. Boos, W. and Shuman, H., Maltose/maltodextrin system of *Escherichia coli*: transport, metabolism, and regulation. Microbiol Mol Biol Rev, 1998. 62(1): 204-29.
177. Boos, W., Ehmann, U., Forkl, H., Klein, W., Rimmele, M. and Postma, P., Trehalose transport and metabolism in *Escherichia coli*. J Bacteriol, 1990. 172(6): 3450-61.

178. You, S.Y., Cosloy, S. and Schulz, H., Evidence for the essential function of 2,4-dienoyl-coenzyme A reductase in the beta-oxidation of unsaturated fatty acids *in vivo*. Isolation and characterization of an *Escherichia coli* mutant with a defective 2,4-dienoyl-coenzyme A reductase. *J Biol Chem*, 1989. 264(28): 16489-95.
179. Nagao, Y., Nakada, T., Imoto, M., Shimamoto, T., Sakai, S., Tsuda, M. and Tsuchiya, T., Purification and analysis of the structure of alpha-galactosidase from *Escherichia coli*. *Biochem Biophys Res Commun*, 1988. 151(1): 236-41.
180. Bartsch, K., von Johnn-Marteville, A. and Schulz, A., Molecular analysis of two genes of the *Escherichia coli* *gab* cluster: nucleotide sequence of the glutamate:succinic semialdehyde transaminase gene (*gabT*) and characterization of the succinic semialdehyde dehydrogenase gene (*gabD*). *J Bacteriol*, 1990. 172(12): 7035-42.
181. Samsonova, N.N., Smirnov, S.V., Novikova, A.E. and Ptitsyn, L.R., Identification of *Escherichia coli* K12 YdcW protein as a gamma-aminobutyraldehyde dehydrogenase. *FEBS Lett*, 2005. 579(19): 4107-12.
182. Liu, J., Burns, D.M. and Beacham, I.R., Isolation and sequence analysis of the gene (*cpdB*) encoding periplasmic 2',3'-cyclic phosphodiesterase. *J Bacteriol*, 1986. 165(3): 1002-10.
183. Campbell, J.W., Morgan-Kiss, R.M. and Cronan, J.E., Jr., A new *Escherichia coli* metabolic competency: growth on fatty acids by a novel anaerobic beta-oxidation pathway. *Mol Microbiol*, 2003. 47(3): 793-805.
184. Ko, J., Kim, I., Yoo, S., Min, B., Kim, K. and Park, C., Conversion of methylglyoxal to acetol by *Escherichia coli* aldo-keto reductases. *J Bacteriol*, 2005. 187(16): 5782-9.
185. Vimr, E.R. and Troy, F.A., Identification of an inducible catabolic system for sialic acids (*nan*) in *Escherichia coli*. *J Bacteriol*, 1985. 164(2): 845-53.
186. Plumbridge, J., Regulation of PTS gene expression by the homologous transcriptional regulators, Mlc and NagC, in *Escherichia coli* (or how two similar repressors can behave differently). *J Mol Microbiol Biotechnol*, 2001. 3(3): 371-80.
187. Seitz, S., Lee, S.J., Penner, C., Boos, W. and Plumbridge, J., Analysis of the interaction between the global regulator Mlc and EIIB^{Glc} of the glucose-specific phosphotransferase system in *Escherichia coli*. *J Biol Chem*, 2003. 278(12): 10744-51.
188. Vidal-Ingigliardi, D. and Raibaud, O., Three adjacent binding sites for cAMP receptor protein are involved in the activation of the divergent *malEp-malKp* promoters. *Proc Natl Acad Sci U S A*, 1991. 88(1): 229-33.
189. Schlegel, A., Bohm, A., Lee, S.J., Peist, R., Decker, K. and Boos, W., Network regulation of the *Escherichia coli* maltose system. *J Mol Microbiol Biotechnol*, 2002. 4(3): 301-7.
190. Gibert, I. and Barbe, J., Cyclic AMP stimulates transcription of the structural gene of the outer-membrane protein OmpA of *Escherichia coli*. *FEMS Microbiol Lett*, 1990. 56(3): 307-11.
191. Williams, M.D., Ouyang, T.X. and Flickinger, M.C., Starvation-induced expression of SspA and SspB: the effects of a null mutation in *sspA* on *Escherichia coli* protein synthesis and survival during growth and prolonged starvation. *Mol Microbiol*, 1994. 11(6): 1029-43.

References

192. Hansen, A.M., Qiu, Y., Yeh, N., Blattner, F.R., Durfee, T. and Jin, D.J., SspA is required for acid resistance in stationary phase by downregulation of H-NS in *Escherichia coli*. *Mol Microbiol*, 2005. 56(3): 719-34.
193. Perederina, A., Svetlov, V., Vassilyeva, M.N., Tahirov, T.H., Yokoyama, S., Artsimovitch, I. and Vassilyev, D.G., Regulation through the secondary channel--structural framework for ppGpp-DksA synergism during transcription. *Cell*, 2004. 118(3): 297-309.
194. Magnusson, L.U., Farewell, A. and Nystrom, T., ppGpp: a global regulator in *Escherichia coli*. *Trends Microbiol*, 2005. 13(5): 236-42.
195. Caldon, C.E., Yoong, P. and March, P.E., Evolution of a molecular switch: universal bacterial GTPases regulate ribosome function. *Mol Microbiol*, 2001. 41(2): 289-97.
196. Hoffmann, A., Bukau, B. and Kramer, G., Structure and function of the molecular chaperone Trigger Factor. *Biochim Biophys Acta*, 2010. 1803(6): 650-61.
197. Martinez-Hackert, E. and Hendrickson, W.A., Promiscuous substrate recognition in folding and assembly activities of the trigger factor chaperone. *Cell*, 2009. 138(5): 923-34.
198. Todorova, R.T. and Saihara, Y., Specific binding of ribosome recycling factor (RRF) with the *Escherichia coli* ribosomes by BIACORE. *Mol Biol Rep*, 2003. 30(2): 113-9.
199. Maki, Y., Yoshida, H. and Wada, A., Two proteins, YfiA and YhbH, associated with resting ribosomes in stationary phase *Escherichia coli*. *Genes Cells*, 2000. 5(12): 965-74.
200. Ibba, M. and Soll, D., Aminoacyl-tRNA synthesis. *Annu Rev Biochem*, 2000. 69: 617-50.
201. Mayer, C. and RajBhandary, U.L., Conformational change of *Escherichia coli* initiator methionyl-tRNA^{Met} upon binding to methionyl-tRNA formyl transferase. *Nucleic Acids Res*, 2002. 30(13): 2844-50.
202. Ote, T., Hashimoto, M., Ikeuchi, Y., Su'etsugu, M., Suzuki, T., Katayama, T. and Kato, J., Involvement of the *Escherichia coli* folate-binding protein YgfZ in RNA modification and regulation of chromosomal replication initiation. *Mol Microbiol*, 2006. 59(1): 265-75.
203. Ryals, J., Little, R. and Bremer, H., Temperature dependence of RNA synthesis parameters in *Escherichia coli*. *J Bacteriol*, 1982. 151(2): 879-87.
204. Nilsson, G., Belasco, J.G., Cohen, S.N. and von Gabain, A., Growth-rate dependent regulation of mRNA stability in *Escherichia coli*. *Nature*, 1984. 312(5989): 75-7.
205. Stymest, K.H. and Klappa, P., The periplasmic peptidyl prolyl cis-trans isomerases PpiD and SurA have partially overlapping substrate specificities. *FEBS J*, 2008. 275(13): 3470-9.
206. Schmid, F.X., Mayr, L.M., Mucke, M. and Schonbrunner, E.R., Prolyl isomerases: role in protein folding. *Adv Protein Chem*, 1993. 44: 25-66.
207. Gottesman, M.E. and Hendrickson, W.A., Protein folding and unfolding by *Escherichia coli* chaperones and chaperonins. *Curr Opin Microbiol*, 2000. 3(2): 197-202.

208. Hoffmann, F. and Rinas, U., Roles of heat-shock chaperones in the production of recombinant proteins in *Escherichia coli*. *Adv Biochem Eng Biotechnol*, 2004. 89: 143-61.
209. Mogk, A., Deuerling, E., Vorderwulbecke, S., Vierling, E. and Bukau, B., Small heat shock proteins, ClpB and the DnaK system form a functional triade in reversing protein aggregation. *Mol Microbiol*, 2003. 50(2): 585-95.
210. Laskowska, E., Wawrzynow, A. and Taylor, A., IbpA and IbpB, the new heat-shock proteins, bind to endogenous *Escherichia coli* proteins aggregated intracellularly by heat shock. *Biochimie*, 1996. 78(2): 117-22.
211. Shiau, A.K., Harris, S.F., Southworth, D.R. and Agard, D.A., Structural Analysis of *E. coli* hsp90 reveals dramatic nucleotide-dependent conformational rearrangements. *Cell*, 2006. 127(2): 329-40.
212. Hoskins, J.R., Kim, S.Y. and Wickner, S., Substrate recognition by the ClpA chaperone component of ClpAP protease. *J Biol Chem*, 2000. 275(45): 35361-7.
213. Genevaux, P., Georgopoulos, C. and Kelley, W.L., The Hsp70 chaperone machines of *Escherichia coli*: a paradigm for the repartition of chaperone functions. *Mol Microbiol*, 2007. 66(4): 840-57.
214. Gottesman, S., Proteases and their targets in *Escherichia coli*. *Annu Rev Genet*, 1996. 30: 465-506.
215. Tomoyasu, T., Mogk, A., Langen, H., Goloubinoff, P. and Bukau, B., Genetic dissection of the roles of chaperones and proteases in protein folding and degradation in the *Escherichia coli* cytosol. *Mol Microbiol*, 2001. 40(2): 397-413.
216. Strauch, K.L. and Beckwith, J., An *Escherichia coli* mutation preventing degradation of abnormal periplasmic proteins. *Proc Natl Acad Sci U S A*, 1988. 85(5): 1576-80.
217. Mandelstam, J., Protein turnover and its function in the economy of the cell. *Ann N Y Acad Sci*, 1963. 102(3): 621-636.
218. Pine, M.J., Heterogeneity of protein turnover in *Escherichia coli*. *Biochim Biophys Acta*, 1965. 104(2): 439-456.
219. Matin, A., Auger, E.A., Blum, P.H. and Schultz, J.E., Genetic basis of starvation survival in nondifferentiating bacteria. *Annu Rev Microbiol*, 1989. 43: 293-316.
220. Imlay, J.A., How oxygen damages microbes: oxygen tolerance and obligate anaerobiosis. *Adv Microb Physiol*, 2002. 46: 111-53.
221. Imlay, J.A., Cellular defenses against superoxide and hydrogen peroxide. *Annu Rev Biochem*, 2008. 77: 755-76.
222. Seaver, L.C. and Imlay, J.A., Are respiratory enzymes the primary sources of intracellular hydrogen peroxide? *J Biol Chem*, 2004. 279(47): 48742-50.
223. Cha, M.K., Kim, W.C., Lim, C.J., Kim, K. and Kim, I.H., *Escherichia coli* periplasmic thiol peroxidase acts as lipid hydroperoxide peroxidase and the principal antioxidative function during anaerobic growth. *J Biol Chem*, 2004. 279(10): 8769-78.
224. Grass, G., Thakali, K., Klebba, P.E., Thieme, D., Muller, A., Wildner, G.F. and Rensing, C., Linkage between catechol siderophores and the multicopper oxidase CueO in *Escherichia coli*. *J Bacteriol*, 2004. 186(17): 5826-33.

References

225. Bou-Abdallah, F., Lewin, A.C., Le Brun, N.E., Moore, G.R. and Chasteen, N.D., Iron detoxification properties of *Escherichia coli* bacterioferritin. Attenuation of oxyradical chemistry. *J Biol Chem*, 2002. 277(40): 37064-9.
226. Patridge, E.V. and Ferry, J.G., WrbA from *Escherichia coli* and *Archaeoglobus fulgidus* is an NAD(P)H:quinone oxidoreductase. *J Bacteriol*, 2006. 188(10): 3498-506.
227. Meyer, R.R. and Laine, P.S., The single-stranded DNA-binding protein of *Escherichia coli*. *Microbiol Rev*, 1990. 54(4): 342-80.
228. Almiron, M., Link, A.J., Furlong, D. and Kolter, R., A novel DNA-binding protein with regulatory and protective roles in starved *Escherichia coli*. *Genes Dev*, 1992. 6(12B): 2646-54.
229. Ueguchi, C., Kakeda, M., Yamada, H. and Mizuno, T., An analogue of the DnaJ molecular chaperone in *Escherichia coli*. *Proc Natl Acad Sci U S A*, 1994. 91(3): 1054-8.
230. Nyström, T. and Neidhardt, F.C., Isolation and properties of a mutant of *Escherichia coli* with an insertional inactivation of the *uspA* gene, which encodes a universal stress protein. *J Bacteriol*, 1993. 175(13): 3949-56.
231. Nyström, T. and Neidhardt, F.C., Expression and role of the universal stress protein, UspA, of *Escherichia coli* during growth arrest. *Mol Microbiol* 1994. 11(3): 537-544.
232. Diez, A., Gustavsson, N. and Nystrom, T., The universal stress protein A of *Escherichia coli* is required for resistance to DNA damaging agents and is regulated by a RecA/FtsK-dependent regulatory pathway. *Mol Microbiol*, 2000. 36(6): 1494-503.
233. Hopkin, K.A., Papazian, M.A. and Steinman, H.M., Functional differences between manganese and iron superoxide dismutases in *Escherichia coli* K-12. *J Biol Chem*, 1992. 267(34): 24253-8.
234. Chang, Y.Y., Wang, A.Y. and Cronan, Jr., Expression of *Escherichia coli* pyruvate oxidase (PoxB) depends on the sigma factor encoded by the *rpoS* (*katF*) gene. *Mol.Microbiol.*, 1994. 11: 1019-1028.
235. Chang, Y.Y. and Cronan, J.E., Jr., Genetic and biochemical analyses of *Escherichia coli* strains having a mutation in the structural gene (*poxB*) for pyruvate oxidase. *J Bacteriol*, 1983. 154(2): 756-62.

5 Appendix

5.1 Detailed experimental procedures of *E. coli* proteome analysis

5.1.1 Protocol of 2D gel electrophoresis

The following protocol of 2D gel electrophoresis is based on the manufacturer's instruction (GE Healthcare, UK) with some modifications for this study.

5.1.1.1 Harvest *E. coli* culture

For each 2D gel, add 1 mL of culture broth corresponding to an OD600 (optical density at 600 nm) of 12 (or 0.1 mL of culture broth with OD600 of 120) to a 1.5 mL or 2 mL microcentrifuge tube (Eppendorf, Germany). Centrifuge at 13300 rpm for 1 min and discard supernatant completely. When the original OD600 value is low (i.e. less than 6), a step of concentration is necessary. After collecting the sample, do not wash the sample. Freeze cell pellet in liquid nitrogen and store at $-80\text{ }^{\circ}\text{C}$ as quickly as possible. All the manipulations are preformed on ice at $4\text{ }^{\circ}\text{C}$.

5.1.1.2 Cell pellet washing

Take out microcentrifuge tube containing cell pellet stored at $-80\text{ }^{\circ}\text{C}$. Add 1.4 mL ice cold sonication buffer [Tris 40 mM (pH=7.5), EDTA 0.5 mM] to resuspend the cell pellet. Centrifuge the suspension at $4\text{ }^{\circ}\text{C}$, 13300 rpm for 1 min and discard the supernatant. The pellet should be washed twice. After the third centrifugation, adjust OD600 of the suspension to 18 with ice cold sonication buffer before performing the BugBuster treatment. Transfer 350 μL of suspension with OD600 of 18 to a new 1.5 mL microcentrifuge tube and centrifuge at $4\text{ }^{\circ}\text{C}$, 13300 rpm for 1 min. After centrifugation, discard supernatant.

5.1.1.3 BugBuster treatment

Prepare BugBuster (Novagen, USA) working solution [0.8 μL Benzonase (250 U/ μL , Merck, Germany) and 0.5 μL rLysozyme stock solution (2 KU/ μL , Novagen, USA) are added to 2 mL BugBuster stock solution]. Add 350 μL BugBuster working solution to the cell pellet after washing. Vortex a few seconds to completely resuspend cell pellet and put the sample to a bench top Eppendorf Thermomixer shaking at $27\text{ }^{\circ}\text{C}$, 350 rpm for 20 min. At the same time, thaw the resolubilization buffer (urea 9 M, thiourea 2 M, CHAPS 4%, Tris 2 mg/mL, SDS 0.2%, bromophenol blue 0.002%) using the Thermomixer.

5.1.1.4 Chloroform/Methanol precipitation

Take out 100 μL BugBuster treated whole cell suspension to perform the Chloroform/Methanol precipitation according to Suppl. Table 5.1.1. Also generate a water control sample using 100 μL water instead of 100 μL BugBuster treated whole cell suspension: From this control use the upper layer after Chloroform/Methanol precipitation and final centrifugation to gently wash the surface of the real sample protein pellet.

Suppl. Table 5.1.1 Simple protocol of Chloroform/Methanol precipitation

Step	Procedure
1	Place 100 μL BugBuster treated whole cell suspension into a 1.5 mL microcentrifuge tube. Prepare water control, using 100 μL Milli-Q (Millipore, USA) water to substitute 100 μL cell suspension to perform steps 2 to 5.
2	Add 600 μL methanol and vortex for 10 seconds.
3	Add 150 μL chloroform and vortex for 10 seconds.
4	Add 450 μL Milli-Q water and vortex for 10 seconds.
5	Centrifugation at 17000 g and 25 $^{\circ}\text{C}$ for 7 min (13300 rpm).
6	After centrifugation, a white layer of protein can be seen in the lower part of the solution. Use pipette to remove the upper part of solution. Use the upper layer of water control after the final centrifugation to wash the surface of protein pellet of the real sample. Only gently shake the tube and do not vortex. After that, use pipette to remove the upper part of solution and carefully turn around the microcentrifuge tube to let the white layer of protein stick to the inner wall of microcentrifuge tube, then carefully remove the rest of the solution with pipette. Let the residual methanol and chloroform evaporate till there is not smell of methanol. This drying procedure should not take more than 10 min and one should not over-dry the protein pellet.

5.1.1.5 Resolubilization of protein pellet

After the Chloroform/Methanol precipitation, add 500 μL resolubilization buffer (urea 9 M, thiourea 2 M, CHAPS 4%, Tris 2 mg/mL, SDS 0.2%, bromophenol blue 0.002%), 7.5 μL IPG buffer and 7.5 μL 1 M DTT stock solution to resolubilize the protein pellets. To facilitate the resolubilization, put the sample to a bench top Eppendorf Thermomixer shaking at 26 $^{\circ}\text{C}$, 1000 rpm for 4 h. During this time, use ultrasonic bath to sonicate the sample for 10 min twice. At this point, make sure the water temperature of ultrasonic bath does not surpass 35 $^{\circ}\text{C}$. After 4 h, freeze the sample in liquid nitrogen and store at -80°C .

5.1.1.6 Beginning of isoelectric focusing (IEF)

For IEF loading, take out the sample at -80°C to a bench top Eppendorf Thermomixer shaking at 28 $^{\circ}\text{C}$, 1000 rpm for 1.5 h. Ensure that urea and thiourea are completely dissolved. Add another 7.5 μL 1 M DTT stock solution to the sample to make the final DTT concentration 30 mM. After 1.5 h, centrifuge the sample at 25 $^{\circ}\text{C}$, 13300 rpm for 25 min. Chose the centrifuge with temperature control. After the centrifugation, transfer 420

μL supernatant to a new microcentrifuge tube.

Carefully clean the Ettan IPGphor strip holder (GE Healthcare, UK) using 10% SDS solution with a toothbrush. Then, use Milli-Q (Millipore, USA) water to thoroughly rinse the strip holder to remove the SDS and other contaminants. After drying, two of IEF sample application pieces (GE Healthcare, UK) are placed in the lateral wells at both ends of the strip holder. Add 20 μL rehydration solution (urea 9 M, thiourea 2 M, CHAPS 4%, Tris 2 mg/mL) onto each of the IEF sample application pieces.

Take care of the number on the IPG strip and which sample will be loaded to this IPG strip. Do not write on the IPG strip. Load 360 μL sample into the center of a cleaned strip holder. Use forceps to open the IPG strip from the “+” end. Let the gel slide down and put the IPG strip in the IPG holder with loaded sample. Do not generate bubbles. Add 2.5 mL silicone oil on plastic backing of the IPG strip and cover the strip holder. Start the IEF according to the following procedure (Suppl. Table 5.1.2):

Suppl. Table 5.1.2 IEF program

Procedure	Program Step	Voltage (V)	Step duration (hr)	Voltage gradient type
Rehydration		0	36	Step-n-hold
	1	50	4	Step-n-hold
	2	50-100	4	Gradient
	3	100-300	3	Gradient
Isoelectric Focusing	4	300-1000	3	Gradient
	5	1000-3500	3	Gradient
	6	3500-5000	3	Gradient
	7	5000	3	Step-n-hold
	8	5000-8000	3	Gradient
End	9	8000	10	Step-n-hold

Temperature: 20 °C, Current limit for each strip: 30 μA (3-10 NL strip) or 35 μA (3-10 strip)

5.1.1.7 Preparation of SDS equilibration buffer

Add DTT and iodoacetamide to two conical tubes, respectively. Add appropriate volume of SDS equilibration buffer (50mM Tris-HCl pH 8.8, 6 M urea, 30% glycerol, 2% SDS) to each conical tube to obtain final concentrations of 1% (w/v) DTT and 5% (w/v) iodoacetamide, respectively. Gently shake to dissolve the DTT and iodoacetamide. At this step, avoid generating bubbles in the SDS equilibration buffer.

5.1.1.8 IPG strip equilibration

After IEF, carefully remove silicone oil with pipette and take out the IPG strips using forceps to a blotting paper to absorb the excess oil. Make sure that the plastic backing touches the blotting paper and the gel side is up in the air. After removing excess silicone oil, use forceps to transfer the IPG strip to a self made plexiglass tray. Each tray can

accommodate two IPG strips (make sure the gel sides are up in the air). Add 4.5 mL SDS equilibration buffer with 1% DTT to each tray. Carefully place the self made plexiglass tray containing IPG strips and SDS equilibration buffer to a rocking shaker for 15 min with gentle shaking. After 15 min, pour out the SDS equilibration buffer with DTT. Add 4.5 mL SDS equilibration buffer with 5 % iodoacetamide to each line. Place the plexiglass tray to the rocking shaker for 18 min with gentle shaking. After 18 min, pour out the SDS equilibration buffer with iodoacetamide to a waste container.

5.1.1.9 Transfer the IPG strips to the SDS-PAGE electrophoresis

During the IPG strip equilibration step, melt the agarose sealing solution (agarose 1 %, Tris 24 mM, glycine 0.2 M, bromophenol blue 0.002 % and SDS 0.1 %) in a microwave (Do not allow the solution to boil!!!).

Take out gradient SDS-PAGE slab gel cassette from 4 °C storage place and wash with purified water. Apply some SDS electrophoresis buffer to the loading space for the IPG strip to facilitate the transition procedure. After the IPG strip equilibration step, carefully transfer the IPG strip on the surface of the SDS-PAGE gel, using forceps to make sure that the plastic backing is against one of the glass plates, and the IPG gel do not touch the glass plates. Pour out the SDS electrophoresis buffer and put IPG strip in the center of acrylamide gel. Lift one side of the cassette. Carefully deliver agarose sealing solution at the higher side of the cassette. Let the agarose sealing solution flow to the lower side, and slowly move the pipette from the higher side to the lower side across the gel, deliver agarose sealing solution onto the IPG strip to seal it in place (carefully avoid bubbles). Wait 10~15 minutes to allow the agarose to solidify.

5.1.1.10 Placement of cassettes into the DALT tank

Use purified water to wash the surface of the cassette to remove excess (un)polymerized acrylamide. Dip the hinge side of the cassette into the tank buffer to lubricate it before inserting it into the flap seals. Use both hands to slide cassette firmly to the bottom. The cassette is correctly loaded in running orientation in the DALT tank (GE Healthcare, UK) with the IPG strip vertical along the left side (the cathode).

Adjust the buffer level after all cassettes are loaded in position. Close the lid and connect the power supply. Turn on the cooling circulating bath (10 °C) and connect it to the DALT tank. Set the power supply to 40 V constant voltage for the first 45 min and increase to 80 V constant voltage for another 45 min. After 45 min electrophoresis at 80 V, increase the voltage to 105 V for overnight run. Migration proceeds toward the anode (or right end of the chamber).

5.1.1.11 Ending second-dimension SDS-PAGE electrophoresis

After the bromophenol blue tracking dye runs to the right edge of the polymerized

acrylamide gel, carefully take out and open the cassette. Carefully transfer the gel to a plastic box. Add fixing solution to submerge the gels and put the box on a horizontal rocking shaker. After 45 min, remove the fixing solution, and add new fixing solution for another 45 min shaking. After 1.5 h, remove the fixing solution and add Colloidal Silver Coomassie G-250 staining solution and shake overnight. Use Milli-Q water to destain the Coomassie stained gels.

5.1.2 Protocol of MALDI identification

5.1.2.1 Trypsin digestion protocol for MALDI

1. Preparation
 - 1.1. Wash SDS-PAGE gel with Milli-Q water (shaking on horizontal shaker overnight is recommended).
 - 1.2. Cut gel spots and put them into 1.5 mL microcentrifuge tubes.
 - 1.3. Wash the gel spots 5 times with 1 mL Milli-Q water. For each washing step, shake for 5 min. At the last step of washing, use a small pipette tip to cut gel spot into small pieces (one gel spot one tip!!!).
 - 1.4. After washing, samples can be stored in water at 4 °C for 1 day (or use Eppendorf vacufuge concentrator to dry and store at 4 °C for several days).
 - 1.5. After storage at 4 °C, wash samples with 1 mL Milli-Q water.
 - 1.6. Withdraw water (be careful to not suck out any pieces of the gel).
 - 1.7. Dehydration
 - Add 200 µL acetonitrile (ACN)
 - withdraw ACN completely
2. Carbamidomethylation
 - 2.1. Add 50 µL DTT solution [20 mM DTT (3.1 mg/mL) in 0.1 M NH₄HCO₃] in each sample.
 - 2.2. Incubate samples for 30 min at 56 °C in an Eppendorf thermomixer (not shaking).
 - 2.3. Withdraw DTT solution completely from each sample (be careful to not suck out any pieces of the gel).
 - 2.4. Dehydrate (as step 1.7 above).
 - 2.5. Add 50 µL iodoacetamide solution [55 mM iodoacetamide (10.2 mg/mL) in 0.1 M NH₄HCO₃] to each sample.
 - 2.6. Incubate 30 min at room temperature in the dark.
 - 2.7. Withdraw iodoacetamide solution completely.
 - 2.8. Dehydrate (as step 1.7 above)

3. Buffering
 - 3.1. Wash each sample with 200 μL 0.1 M NH_4HCO_3 . Incubate samples for 15 min at room temperature. After 15 min, withdraw NH_4HCO_3 solution.
 - 3.2. Dehydrate (as step 1.7 above)
 - 3.3. Use Eppendorf vacufuge concentrator to dry samples (about 20 min).
4. Digestion
 - 4.1. Preparation of trypsin working solution

Add 100 μL suspension buffer (Promega, USA) to one vial of trypsin (Promega, USA). Incubate 30 min at room temperature. Then add 900 μL 0.1 M NH_4HCO_3 . After mixing, aliquot 50 μL into 0.5 mL microcentrifuge tube and store at -20°C . Before use, thaw and add 450 μL H_2O to make 500 μL trypsin working solution.
 - 4.2. Add about 30 μL trypsin working solution to each gel spot.
 - 4.3. Incubate all the samples overnight at 37°C .
 - 4.4. Extract peptide using Prespotted AnchorChip (PAC) target (refer to 5.1.2.2) or ZipTips (Millipore, USA) (refer to 5.1.2.3)

5.1.2.2 Sample preparation for MALDI using Prespotted AnchorChip target

5. Peptide-Extraction
 - 5.1. Add 30 μL acetonitrile (ACN) to the gel spots. Shake on an Eppendorf thermomixer for 15 min at 37°C and 800 rpm.
 - 5.2. After shaking for 15 min, transfer the supernatant of each sample into another 1.5 mL microcentrifuge tube*.
 - 5.3. Add 30 μL 5% formic acid solution to each gel spot. Shake on an Eppendorf thermomixer for 15 min at 37°C and 800 rpm.
 - 5.4. Add 30 μL ACN to each gel spot. Shake for 15 min at 37°C and 800 rpm.
 - 5.5. After 15 min combine the supernatant with supernatant in the tube* from step 5.2.
 - 5.6. Use Eppendorf vacufuge concentrator to dry samples (the sample combined with the supernatant from step 5.2 and 5.5) for about 1~2 hour.
 - 5.7. After drying, add 7~8 μL 32% methanol and 0.5% formic acid solution and put samples into ultrasonic bath for 10 min.
6. Loading to PAC target for MALDI mass spectrometry analysis
 - 6.1. Deposit 1 μL sample solution onto matrix spot.
 - 6.2. Allow three minutes incubation.
 - 6.3. Add 7 μL PAC target washing buffer (10mM $\text{NH}_4\text{H}_2\text{PO}_4$, 0.1% TFA), and remove the whole droplet after 3~5 second.

5.1.2.3 Sample preparation for MALDI using ZipTips (C18)

5. Peptide-Extraction
 - 5.1. Add 30 μL acetonitrile (ACN) to the gel spots. Shake on an Eppendorf thermomixer for 15 min at 37 $^{\circ}\text{C}$ and 800 rpm.
 - 5.2. After shaking for 15 min, transfer the supernatant of each sample into another 1.5 mL microcentrifuge tube*.
 - 5.3. Add 30 μL 5% formic acid solution to each gel spot. Shake on an Eppendorf thermomixer for 15 min at 37 $^{\circ}\text{C}$ and 800 rpm.
 - 5.4. Add 30 μL ACN to each gel spot. Shake for 15 min at 37 $^{\circ}\text{C}$ and 800 rpm.
 - 5.5. After 15 min combine the supernatant with supernatant in the tube* from step 5.2.
 - 5.6. Use Eppendorf vacufuge concentrator to dry samples (the sample combined with the supernatant from step 5.2 and 5.5) about 1~2 hour.
 - 5.7. After drying, add 20 μL ZipTips washing solution (2% methanol, 0.5% formic acid) and put samples into ultrasonic bath for 10 min.
6. Desalting with ZipTips (C18)
 - No air into ZipTips!
 - ZipTips washing solution: 2% methanol, 0.5% formic acid
 - ZipTips elution solution: 65% methanol, 0.5% formic acid
 - 6.1. Clean ZipTip 3 times with 10 μL ZipTips elution solution.
 - 6.2. Equilibrate ZipTip 3 times with 10 μL ZipTips washing solution.
 - 6.3. Pipette sample up and down for 10 to 15 times very slowly.
 - 6.4. Wash ZipTip 3 times with 10 μL ZipTips washing solution.
 - 6.5. Elution for MALDI

Add 5 μL ZipTips elution solution into a 0.5 mL microcentrifuge tube. Using the ZipTip containing sample from step 6.4, pipette 5 μL ZipTips elution solution up and down 3 times to elute sample from ZipTip.
7. Loading for MALDI mass spectrometry analysis

Mix 1 μL of sample from ZipTips elution solution (from step 6.5) with 1 μL saturated matrix solution (10 mg α -Cyano-4-hydroxycinnamic acid, 400 μL acetonitril and 600 μL 0.1% TFA). Transfer 2 μL of this mixture onto a MALDI sample target. The mass spectrometry analysis is performed after the sample target is complete dry.

5.1.3 Buffers and solutions for 2D gel electrophoresis and MALDI MS identification

Suppl. Table 5.1.3 Buffers and solutions for 2D gel electrophoresis and MALDI identification

Name	Chemical	Concentration	Preparation method
1 M DTT stock solution	DTT	1 M	Add 0.925 g DTT (MW: 154.25) into a 15 mL conical tube and add about 5 mL Milli-Q water to bring the final volume to 6 mL. After complete dissolution aliquot 75 μ L of this solution to several PCR tubes and store at -80°C .
1 M Tris stock solution	Tris	1 M	Add 0.242 g Tris (MW: 121.14) into a 2 mL microcentrifuge tube and add about 1.7 mL Milli-Q water to bring the final volume to 2 mL. After complete dissolution, store in 4°C refrigerator. This solution is only Tris base solution, the pH does not need to be adjusted.
1 % bromophenol blue stock solution	Bromophenol blue	1 %	Add 100 mg bromophenol blue and 60 mg Tris (MW: 121.14) to a 15 mL conical tube and add Milli-Q water to bring the final volume to 10 mL. After complete dissolution, aliquot 1.2 mL of this solution to several microcentrifuge tubes and store at 4°C .
	Tris	50 mM	
1.5 M Tris-HCl, pH 8.8 stock solution (4 \times resolving gel buffer solution)	Tris	1.5 M	Add 181.71 g Tris (MW: 121.14), 600 mL Milli-Q water to a graduated cylinder and dissolve the Tris base. Adjust the pH to 8.8 using HCl. Add Milli-Q water to bring the final volume to 1000 mL and check the pH of the final solution. Filter this solution through a 0.2 μm membrane to an autoclaved glass bottle.
Sonication buffer	Tris	40 mM	Add 4.85 g Tris (MW: 121.14), 0.19 g Titriplex III and 970 mL Milli-Q into a 1 L graduated cylinder. Dissolve the solution completely. Adjust the pH to 7.5 using HCl. Store at 4°C .
	Titriplex III	0.5 mM	
10 % SDS stock solution	SDS	10 %	Add 100 g SDS powder (Bio-Rad, MW: 288.38) into a 1 L graduated cylinder, and add Milli-Q water to bring the final volume to 1 L. Dissolve the solution completely. Filter this solution through a 0.2 μm membrane to an autoclaved 1 L glass bottle.

Name	Chemical	Concentration	Preparation method
Rehydration solution for 2D electrophoresis (This rehydration solution is only for wetting IEF sample application pieces in IPGphor strip holder)	Urea	9 M	Add 10.81 g urea (MW: 60.06), 3.05 g thiourea (MW: 76.12), 0.8 g CHAPS (MW: 614.89), 37 μ L 1 M Tris stock solution (only Tris base solution, pH not adjusted) into a 20 mL glass beaker and add about 10 mL Milli-Q water to bring the final volume to 20 mL. After complete dissolution, aliquot 0.4 mL of this solution to several 1.5 mL microcentrifuge tubes and store at -20°C .
	Thiourea	2 M	
	CHAPS	4 %	
	Tris	0.2 mg/mL	
Resolubilization buffer for 2D electrophoresis	Urea	9 M	Add 32.43 g urea (MW: 60.06), 9.14 g thiourea (MW: 76.12), 2.4 g CHAPS (MW: 614.89), 111 μ L 1 M Tris stock solution (only Tris base solution, pH not adjusted), 1.2 mL 10 % SDS stock solution and 120 μ L 1 % bromophenol blue stock solution into a 100 mL graduated cylinder and add about 30 mL Milli-Q water to bring the final volume to 60 mL. After complete dissolution, aliquot 1.7 mL of this solution to several 2 mL microcentrifuge tubes and store at -20°C .
	Thiourea	2 M	
	CHAPS	4 %	
	Tris	0.2 mg/mL	
	SDS	0.2 %	
	Bromophenol Blue	0.002 %	
SDS equilibration buffer for 2-D electrophoresis	Tris-HCl, pH 8.8	50 mM	Add 108.15 g urea (MW: 60.06), 60 mL 10 % SDS stock solution, 103.5 mL (126.3 g) glycerol (86% w/w, MW: 92.1), and 10 mL 1.5 M Tris-HCl, pH 8.8 stock solution (4 \times resolving gel buffer solution) into a 500 mL graduated cylinder. Bring the final volume to 300 mL with Milli-Q water. After complete dissolution, aliquot 13 mL of this solution to several 15 mL conical tubes and store at -20°C . This is a stock solution without DTT or iodoacetamide.
	Urea	6 M	
	Glycerol	30 %	
	SDS	2 %	
SDS electrophoresis buffer for agarose sealing solution (Without SDS)	Tris	24 mM	Add 2.9 g Tris (MW: 121.1), 15.01 g glycine (MW: 75.07), into a 1 L graduated cylinder. Add Milli-Q water to bring the final volume to 1 L. Filter this solution through a 0.2 μ m membrane to an autoclaved 1 L glass bottle and store at 4°C .
	Glycine	0.2 M	
Agarose sealing solution for 2-D electrophoresis	Agarose	1 %	Add 0.5 g agarose (Biozym LE GP agarose) to a 100 mL glass bottle. And add 50 mL SDS electrophoresis buffer of agarose sealing solution (without SDS) into this bottle. Add 100 μ L 1 % bromophenol blue stock solution and 500 μ L 10 % SDS stock solution. Heat in microwave oven on low power until the agarose is completely dissolved.
	Tris	24 mM	
	Glycine	0.2 M	
	Bromophenol blue	0.002 %	
	SDS	0.1 %	

Appendix

Name	Chemical	Concentration	Preparation method
Tank electrophoresis buffer for 2-D electrophoresis	Tris	24 mM	Add 58 g Tris (MW: 121.1), 300 g glycine (MW: 75.07), 200 mL 10 % SDS stock solution in the electrophoresis tank and add Milli-Q water to bring the final volume to 20 L. Use the circulating pump to dissolve the compounds. After complete dissolution, put the two barrier-combs back to their original position. This buffer can be used for 3 runs of SDS-PAGE electrophoresis.
	Glycine	0.2 M	
	SDS	0.1 %	
Fixing solution	Acetic acid	10 %	Add 600 mL ethanol (or 857 mL 70 % ethanol) to a 2 L graduated cylinder. Add Milli-Q water to bring the volume to 1.8 L. Finally add 200 mL acetic acid (MW: 60.05) and mix the solution.
	Ethanol	30 %	
Colloidal Silver Coomassie G-250 staining solution	H ₃ PO ₄	8.5 %	First add 250 mL Milli-Q water to a glass bottle and add 250 mL 85 % H ₃ PO ₄ (MW: 98.0) and mix. Secondly, add 250 g (NH ₄) ₂ SO ₄ (MW: 132.0) to a 500 mL graduated cylinder and add Milli-Q water to bring the final volume to 500 mL. Add a magnetic stirrer for mixing. Thirdly, add 2.5 g Coomassie Blue G250 to a 500 mL glass graduated cylinder and add Milli-Q water to bring the final volume of 500 mL. Add a magnetic stirrer for mixing. After the (NH ₄) ₂ SO ₄ and Coomassie Blue G-250 are dissolved, mix them with the H ₃ PO ₄ solution and add 500 mL Milli-Q water to bring the volume to 2 L. Mix at high stirrer speed overnight. Then, very slowly (important) add 500 mL methanol (MW: 32.04) to this solution. It is better to store this solution in a brown bottle.
	(NH ₄) ₂ SO ₄	10 %	
	Coomassie Blue G250	0.1 %	
	Methanol	20 %	
Displacing solution for casting gradient gels	Tris	0.375 M	Add 100 mL glycerol (MW: 92.1), 50 mL Milli-Q water, 50 mL 1.5 M Tris-HCl, pH 8.8 stock solution (4× resolving gel buffer solution) and 200 µL 1 % bromophenol blue stock solution to a glass bottle and mix them.
	Glycerol	43 %	
	Bromophenol Blue	0.001 %	
10% TEMED for casting gradient gels	TEMED	10%	Add 300 µL TEMED (MW: 116.21) and 2700 µL Milli-Q water to a 15 mL conical tube. Vortex for mixing. Store at -20 °C.
10% APS for casting gradient gels	Ammonium persulfate	10 %	Add 2 g ammonium persulfate (MW: 228.2) to a 50 mL conical tube. Add Milli-Q water to bring the final volume to 20 mL and vortex for mixing. Store at -80 °C.

Name	Chemical	Concentration	Preparation method
0.1% SDS solution for 2-D electrophoresis	SDS	0.1 %	Add 5 mL 10 % SDS stock solution to 500 mL graduate cylinder. Add Milli-Q water to bring the final volume to 500 mL.
Gel storage solution	Tris	0.375 M	Add 20 mL 10 % SDS stock solution and 500 mL 1.5 M Tris-HCl, pH 8.8 stock solution (4× resolving gel buffer solution) to a 2 L glass bottle. Add Milli-Q water to bring the final volume to 2 L. Store at 4 °C.
	SDS	0.1 %	
Gel drying solution	Glycerol	13 %	Add 400 mL ethanol (or 570 mL 70 % ethanol) and 150 mL glycerol (86% w/w, MW: 92.1) to a 1 L graduated cylinder. Add Milli-Q water to bring the volume to 1 L.
	Ethanol	40 %	
0.1 M NH ₄ HCO ₃ solution	NH ₄ HCO ₃	0.1 M	Add 3.95 g NH ₄ HCO ₃ (MW: 79.06) to 500 mL graduate cylinder, and add Milli-Q water to bring the final volume to 500 mL. Filter this solution through a 0.2 µm membrane to an autoclaved glass bottle. Store at 4 °C.
0.1 M NH ₄ HCO ₃ with DTT	DTT	3.1 mg/mL	Add 31 mg DTT (MW: 154.25) into a 15 mL conical tube and add 10 mL 1 M NH ₄ HCO ₃ solution to bring the final volume to 10 mL.
	NH ₄ HCO ₃	0.1 M	
0.1 M NH ₄ HCO ₃ with iodoacetamide	Iodoacetamide	10.2 mg/mL	Add 102 mg iodoacetamide (MW: 184.96) into a 15 mL conical tube and add 10 mL 1 M NH ₄ HCO ₃ solution to bring the final volume to 10 mL.
	NH ₄ HCO ₃	0.1 M	
Trypsin working solution	Trypsin	2 µg/mL	One vial of trypsin (sequencing grade modified trypsin, Promega) is combined with 100 µL trypsin resuspension buffer (Promega) and incubated 30 min at room temperature. Then add 900 µL 1 M NH ₄ HCO ₃ solution. After mixing, aliquot 50 µL into 0.5 mL microcentrifuge tubes and store at -80 °C. Before using, thaw and add 450 µL Milli-Q to make 500 mL trypsin working solution.
5 % formic acid	Formic acid	5 %	Add 25 mL formic acid (MW: 46.03) to a 500 mL graduate cylinder, and add Milli-Q water to bring the final volume to 500 mL. Store at 4 °C.

Appendix

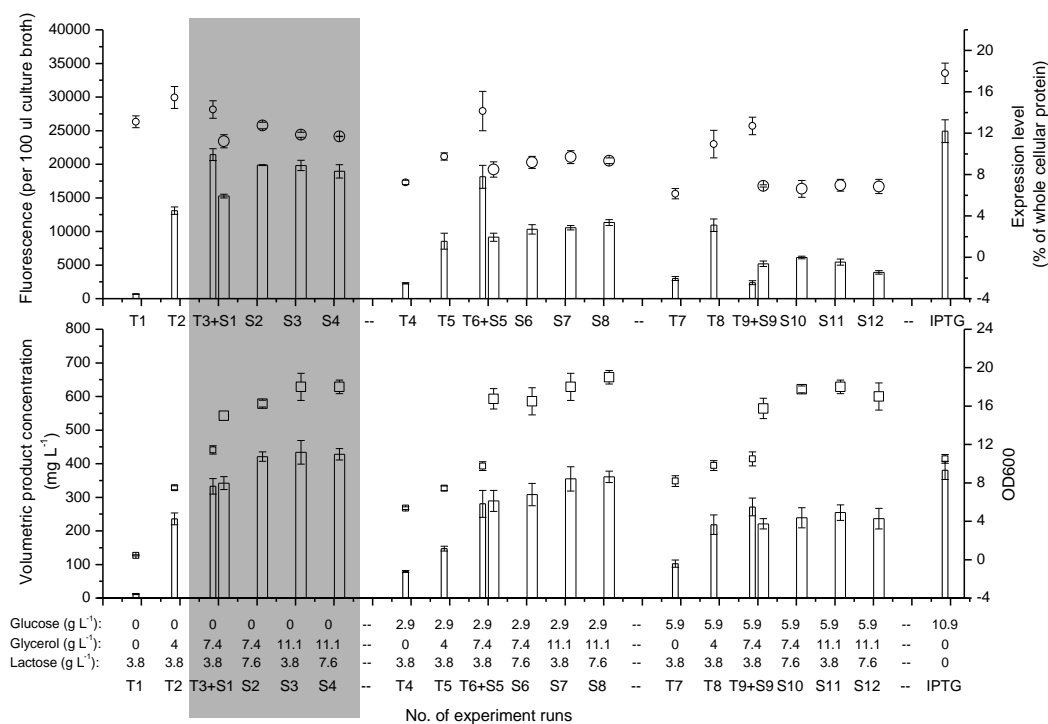
Name	Chemical	Concentration	Preparation method
32 % methanol and 0.5 % formic acid solution	Formic acid	0.5 %	Add 160 mL methanol (MW: 32.04) and 2.5 mL formic acid (MW: 46.03) to 500 mL graduate cylinder, and add Milli-Q water to bring the final volume to 500 mL. Store at 4 °C.
	Methanol	32 %	
PAC target washing buffer	TFA	0.1 %	Add 1 mL trifluoroacetic acid (TFA, MW: 114.02) to 1 L graduate cylinder, and add Milli-Q water to bring the final volume to 1 L.
	NH ₄ H ₂ PO ₄	10 mM	Add 23 mg NH ₄ H ₂ PO ₄ and 20 mL 0.1 % TFA solution to a glass bottle. Store at 4 °C.
ZipTips washing solution	Formic acid	0.5 %	Add 2 mL methanol (MW: 32.04) and 0.5 mL formic acid (MW: 46.03) to 100 mL graduate cylinder, and add Milli-Q water to bring the final volume to 100 mL. Store at 4 °C.
	Methanol	2 %	
ZipTips elution solution	Formic acid	0.5 %	Add 65 mL methanol (MW: 32.04) and 0.5 mL formic acid (MW: 46.03) to 100 mL graduate cylinder, and add Milli-Q water to bring the final volume to 100 mL. Store at 4 °C.
	Methanol	65 %	
Saturated matrix solution	TFA	0.06 %	Add 1 mL trifluoroacetic acid (TFA, MW: 114.02) to 1 L graduate cylinder, and add Milli-Q water to bring the final volume to 1 L to make 0.1 % TFA solution.
	Acetonitrile	40 %	Add 10 mg α -Cyano-4-hydroxycinnamic acid (MW: 189.17), 400 μ L acetonitrile (MW: 41.05) and 600 μ L 0.1 % TFA solution into a 1.5 mL microcentrifuge tube. Vortex for mixing. Store at 4 °C.
	α -Cyano-4-hydroxycinnamic acid	10 mg/mL	

Suppl. Table 5.1.4 Heavy solution and light solution for casting gradient gels

Stock solution	Light Solution		Heavy Solution	
	260 mL 10 small gels	1100 mL 23 big gels	260 mL 10 small gels	1100 mL 23 big gels
Acrylamide stock solution Rotiphorese Gel 30 (37,5:1)	84 mL	357 mL	127 mL	536 mL
1.5 M Tris-HCl, pH 8.8 stock solution	65 mL	275 mL	65.00 mL	275 mL
Milli-Q water	105 mL	444 mL	44 mL	184 mL
10 % SDS stock solution	2.6 mL	11 mL	2.6 mL	11 mL
86 % Glycerol	0	0	21 mL(16.91 g)	88 mL
Before addition of APS and TEMED to begin polymerization, bring above mixture to 4 °C for 3 h.				
10 % APS	2.60 mL	11 mL	1.30 mL	5.5 mL
10 % TEMED	0.44 mL	1.88 mL	100 μ L	0.42 mL

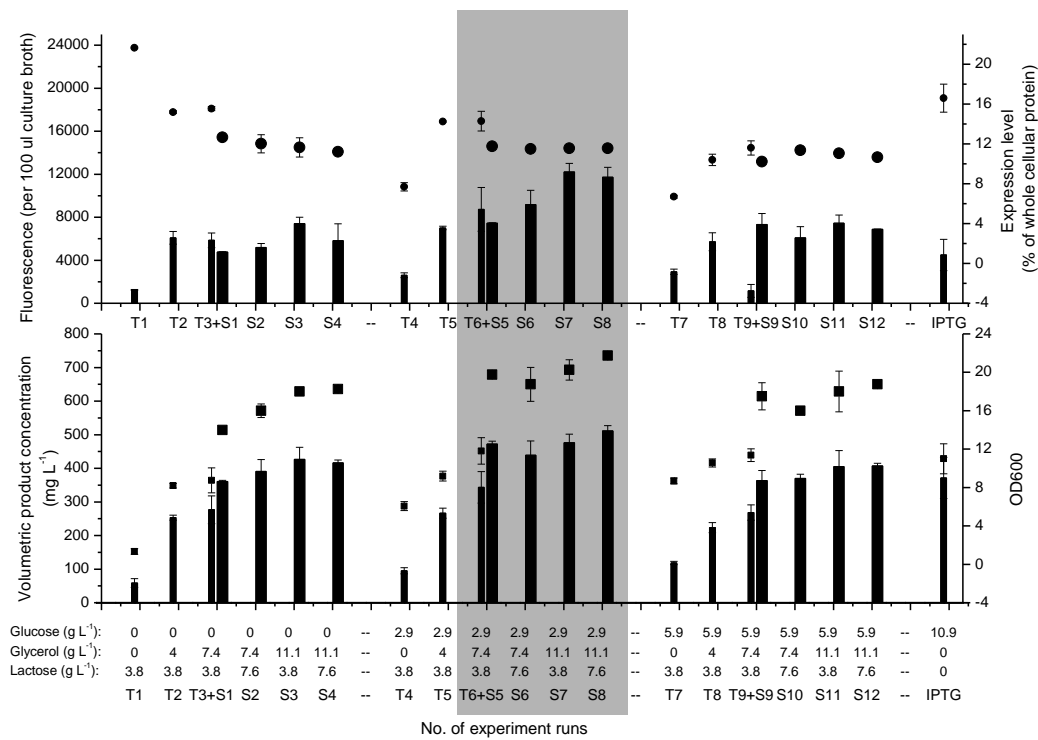
5.2 Supplementary material for Chapter 2 - Novel defined modular media to produce recombinant proteins

5.2.1 Supplementary figures



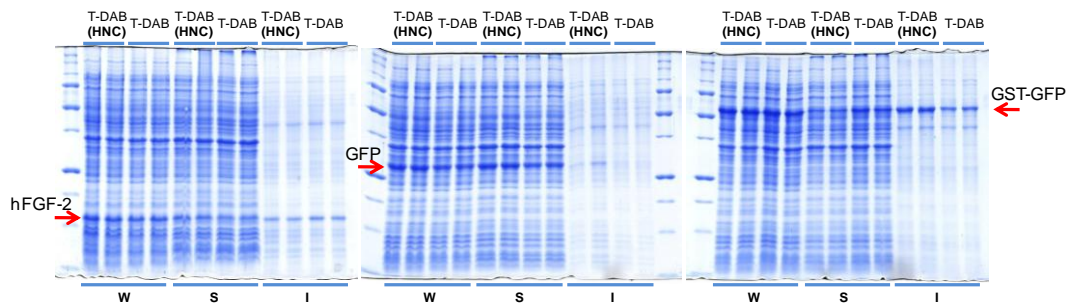
Suppl. Fig 5.2.1 Influence of carbon substrate composition on GFP production at 23 °C using autoinduction

Cells were grown in test tube (narrow column, small symbols) and shake flask cultures (broad column, big symbols). Upper panel: Expression level (○) and GFP fluorescence per 100 µl of GFP producing culture (□). Lower panel: Volumetric GFP concentration (□) and final cell density (□). The light gray shadow indicates the maximum product yield area. Test tube and shake flask run numbers and glucose, glycerol and lactose concentrations are indicated below (refer to Table 2.2.2).



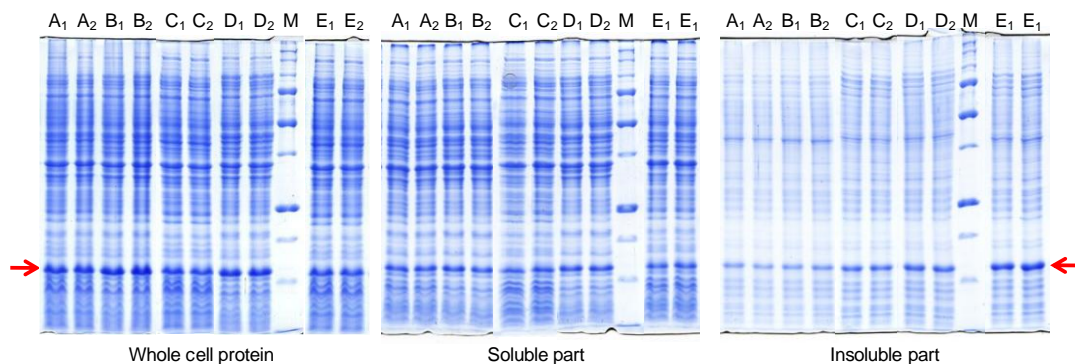
Suppl. Fig 5.2.2 Influence of carbon substrate composition on GST-GFP production at 23 °C using autoinduction.

Cells were grown in test tube (narrow column, small symbols) and shake flask (broad column, big symbols). Upper panel: Expression level (●) and GST-GFP fluorescence per 100 µl of GST-GFP producing culture (■). Lower panel: Volumetric GST-GFP concentration (■) and final cell density (■). The light gray shadow indicates the maximum product yield area. Test tube and shake flask run numbers and glucose, glycerol and lactose concentrations are indicated below (refer to Table 2.2.2).



Suppl. Fig 5.2.3 The influence of nitrogen content on protein production and partitioning of the recombinant protein into soluble and insoluble cell fractions at 23 °C using autoinduction.

Increasing the nitrogen content of S-DAB was accomplished by using ammonium hydroxide for pH adjustment instead of sodium hydroxide resulting in S-DAB (HNC). SDS-PAGE analysis of samples from duplicate experiments corresponding to whole cell protein, and soluble and insoluble fractions of cells producing (A) hFGF-2, (B) GFP and (C) GST-GFP, and. Arrows indicate the positions of the recombinant proteins. Below are indicated the cell fractions analyzed (W: whole cell protein. S: soluble part and I: insoluble part of whole cell protein) and above the medium employed.



Suppl. Fig 5.2.4 The influence of oxygen supply on hFGF-2 production and partitioning of the recombinant protein into soluble and insoluble cell fractions at 23 °C using S-DAB (HNC).

SDS-PAGE analysis of samples from duplicate experiments (X1 and X2) corresponding to whole cell protein, and soluble and insoluble cell fractions. Arrows indicate the position of hFGF-2. Below are indicated the cell fractions analyzed (W: whole cell protein. S: soluble part and I: insoluble part of whole cell protein) and above the experimental conditions employed (A): 10 ml in 100 ml shake flask at 140 rpm, (B): 25 ml in 100 ml shake flask at 140 rpm, (C): 10 ml in 100 ml shake flask at 80 rpm, (D): 50 ml in 100 ml shake flask at 140 rpm, and (E): 25 ml in 100 ml shake flask at 80 rpm.

5.2.2 Supplementary tables

Suppl. Table 5.2.1 (Part A) Media preparation (For 1 Liter)

Groups	No.	Name of media	S-DAB (HNC) [#]	S-DAB [#]	DNB [#]	
		General usage or of the medium	No labeled production with good oxygen supply	No labeled production with intermediate oxygen supply	Pre-cultures and IPTG induction	
		Inducer	Lactose	Lactose	IPTG	
		Volume of stock solution	mL	mL	mL	
A group	Magnesium	F1	50 X MgSO ₄ stock solution (H ₂ O)	20	20	20
		F2	50 X MgSO ₄ stock solution (D ₂ O)			
	Carbon source	A1	4 X 2.94-11.07-7.6 carbon source stock solution (H ₂ O)	250	250	
		A2	4 X 2.94-11.07-7.6 carbon source stock solution (D ₂ O)			
		A3	20 X Glucose stock solution (H ₂ O)			50
		A4	20 X Glucose stock solution (D ₂ O)			
		A5	¹³ C labeled Glucose stock solution (H ₂ O)			
		A6	¹³ C labeled Glucose stock solution (D ₂ O)			
Trace	G1	5000 X Na ₂ MoO ₄ .H ₂ O stock solution (H ₂ O)	0.2	0.2	0.2	
B group	elements	H1	2000 X trace element stock solution (H ₂ O)	0.5	0.5	0.5
	Nitrogen	B1	50 X (NH ₄) ₂ HPO ₄ stock solution (H ₂ O)	20	20	20
		B2	50 X NH ₄ Cl stock solution (H ₂ O)			
		B3	50 X ¹⁵ N labeled NH ₄ Cl stock solution (H ₂ O)			
		B4	50 X ¹⁵ N labeled NH ₄ Cl stock solution (D ₂ O)			
		B5	50 X NH ₄ Cl stock solution (D ₂ O)			
	Phosphate and other salts	C1	10 X KH ₂ PO ₄ (High concentration) stock solution (H ₂ O)			
		C2	10 X KH ₂ PO ₄ (High concentration) stock solution (D ₂ O)			
		C3	10 X KH ₂ PO ₄ (Low concentration) stock solution (H ₂ O)	100	100	100
		D1	50 X Citric acid stock solution (H ₂ O)	20	20	20
		D2	50 X Citric acid stock solution (D ₂ O)			
		E1	50 X Fe(III) citrate stock solution (H ₂ O)	20	20	20
	E2	50 X Fe(III) citrate stock solution (D ₂ O)				
	pH adjusting	I1	25 X NH ₄ OH stock solution (H ₂ O)	45~50		
		J1	50 X NaOH stock solution (H ₂ O)		13.5	13.5
		J2	50 X NaOH stock solution (D ₂ O)			
	Solvent	H1	Milli-Q water (H ₂ O)	520	556	756
H2		Deuterium oxide (D ₂ O)				

A group: Mix magnesium and carbon source solution, sterilize. After adding 5000 X Na₂MoO₄.H₂O stock solution, the solution (A group) can be kept for long term storage at room temperature. **B group:** Mix ammonium, phosphate and other salts and add solvent, adjust to pH 6.8, sterilize. After adding 2000 X trace element stock solution, the solution (B group) can be kept for long term storage at room temperature. #:autoclave (or sterilize by filtration); ##: sterilize by filtration.*: the labeling of ¹⁵N is optional. If ¹⁵N incorporation is not required, ¹⁵N-NH₄Cl in the medium can be replaced by normal NH₄Cl.

Suppl. Table 5.2.1 (Part B) Media preparation (For 1 Liter)

Groups		No.	Name of media	SL-DAB ^{##}	SL-DAB (in D ₂ O) ^{##}	rL-DNB ^{##}
			General usage or of the medium	¹⁵ N labeling	² H and ¹⁵ N* labeling	¹³ C and ¹⁵ N* labeling
			Inducer	Lactose	Lactose	IPTG
			Volume of stock solution	mL	mL	mL
A group	Magnesium	F1	50 X MgSO ₄ stock solution (H ₂ O)	20		20
		F2	50 X MgSO ₄ stock solution (D ₂ O)		20	
	Carbon source	A1	4 X 2.94-11.07-7.6 carbon source stock solution (H ₂ O)	250		
		A2	4 X 2.94-11.07-7.6 carbon source stock solution (D ₂ O)		250	
		A3	20 X Glucose stock solution (H ₂ O)			
		A4	20 X Glucose stock solution (D ₂ O)			
		A5	¹³ C labeled Glucose stock solution (H ₂ O)			50
		A6	¹³ C labeled Glucose stock solution (D ₂ O)			
Trace	G1	5000 X Na ₂ MoO ₄ .H ₂ O stock solution (H ₂ O)	0.2	0.2	0.2	
B group	elements	H1	2000 X trace element stock solution (H ₂ O)	0.5	0.5	0.5
	Nitrogen	B1	50 X (NH ₄) ₂ HPO ₄ stock solution (H ₂ O)			
		B2	50 X NH ₄ Cl stock solution (H ₂ O)			
		B3	50 X ¹⁵ N labeled NH ₄ Cl stock solution (H ₂ O)	20		16*
		B4	50 X ¹⁵ N labeled NH ₄ Cl stock solution (D ₂ O)		20*	
		B5	50 X NH ₄ Cl stock solution (D ₂ O)			
	Phosphate and other salts	C1	10 X KH ₂ PO ₄ (High concentration) stock solution (H ₂ O)	100		100
		C2	10 X KH ₂ PO ₄ (High concentration) stock solution (D ₂ O)		100	
		C3	10 X KH ₂ PO ₄ (Low concentration) stock solution (H ₂ O)			
		D1	50 X Citric acid stock solution (H ₂ O)	20		20
		D2	50 X Citric acid stock solution (D ₂ O)		20	
		E1	50 X Fe(III) citrate stock solution (H ₂ O)	20		20
		E2	50 X Fe(III) citrate stock solution (D ₂ O)		20	
	pH adjusting	I1	25 X NH ₄ OH stock solution (H ₂ O)			
		J1	50 X NaOH stock solution (H ₂ O)	20		20
		J2	50 X NaOH stock solution (D ₂ O)		20	
	Solvent	H1	Milli-Q water (H ₂ O)	550		754
H2		Deuterium oxide (D ₂ O)		550		

A group: Mix magnesium and carbon source solution, sterilize. After adding 5000 X Na₂MoO₄.H₂O stock solution, the solution (A group) can be kept for long term storage at room temperature. **B group:** Mix ammonium, phosphate and other salts and add solvent, adjust to pH 6.8, sterilize. After adding 2000 X trace element stock solution, the solution (B group) can be kept for long term storage at room temperature. #:autoclave (or sterilize by filtration); ##: sterilize by filtration.*: the labeling of ¹⁵N is optional. If ¹⁵N incorporation is not required, ¹⁵N-NH₄Cl in the medium can be replaced by normal NH₄Cl.

Suppl. Table 5.2.1 (Part C) Media preparation (For 1 Liter)

Groups		No.	Name of media	rL-DNB (in D ₂ O) ^{##}	L-DNB (in D ₂ O) ^{##}	L-DNB [#]
			General usage or of the medium	² H, ¹³ C and ¹⁵ N* labeling	Pre-culture for ¹⁵ N*, ¹³ C and ² H labeling	Pre-cultures and Se-Met labeling
			Inducer	IPTG	IPTG	IPTG
			Volume of stock solution	mL	mL	mL
A group	Magnesium	F1	50 X MgSO ₄ stock solution (H ₂ O)			20
		F2	50 X MgSO ₄ stock solution (D ₂ O)	20	20	
	Carbon source	A1	4 X 2.94-11.07-7.6 carbon source stock solution (H ₂ O)			
		A2	4 X 2.94-11.07-7.6 carbon source stock solution (D ₂ O)			
		A3	20 X Glucose stock solution (H ₂ O)			50
		A4	20 X Glucose stock solution (D ₂ O)		50	
		A5	¹³ C labeled Glucose stock solution (H ₂ O)			
		A6	¹³ C labeled Glucose stock solution (D ₂ O)	50		
	Trace	G1	5000 X Na ₂ MoO ₄ .H ₂ O stock solution (H ₂ O)	0.2	0.2	0.2
B group	elements	H1	2000 X trace element stock solution (H ₂ O)	0.5	0.5	0.5
	Nitrogen	B1	50 X (NH ₄) ₂ HPO ₄ stock solution (H ₂ O)			
		B2	50 X NH ₄ Cl stock solution (H ₂ O)			20
		B3	50 X ¹⁵ N labeled NH ₄ Cl stock solution (H ₂ O)			
		B4	50 X ¹⁵ N labeled NH ₄ Cl stock solution (D ₂ O)	16*	20*	
		B5	50 X NH ₄ Cl stock solution (D ₂ O)			
	Phosphate and other salts	C1	10 X KH ₂ PO ₄ (High concentration) stock solution (H ₂ O)			100
		C2	10 X KH ₂ PO ₄ (High concentration) stock solution (D ₂ O)	100	100	
		C3	10 X KH ₂ PO ₄ (Low concentration) stock solution (H ₂ O)			
		D1	50 X Citric acid stock solution (H ₂ O)			20
		D2	50 X Citric acid stock solution (D ₂ O)	20	20	
		E1	50 X Fe(III) citrate stock solution (H ₂ O)			20
		E2	50 X Fe(III) citrate stock solution (D ₂ O)	20	20	
	pH adjusting	I1	25 X NH ₄ OH stock solution (H ₂ O)			
		J1	50 X NaOH stock solution (H ₂ O)			20
		J2	50 X NaOH stock solution (D ₂ O)	20	20	
	Solvent	H1	Milli-Q water (H ₂ O)			750
H2		Deuterium oxide (D ₂ O)	754	750		

A group: Mix magnesium and carbon source solution, sterilize. After adding 5000 X Na₂MoO₄.H₂O stock solution, the solution (A group) can be kept for long term storage at room temperature. **B group:** Mix ammonium, phosphate and other salts and add solvent, adjust to pH 6.8, sterilize. After adding 2000 X trace element stock solution, the solution (B group) can be kept for long term storage at room temperature. #:autoclave (or sterilize by filtration); ##: sterilize by filtration.*: the labeling of ¹⁵N is optional. If ¹⁵N incorporation is not required, ¹⁵N-NH₄Cl in the medium can be replaced by normal NH₄Cl.

Suppl. Table 5.2.2 Stock solution preparation

No.	Name	Working concentration	Stock solution preparation	Sterilization method
F1	50 X MgSO ₄ stock solution (H ₂ O)	0.586 g L ⁻¹ MgSO ₄	Add 30 g MgSO ₄ ·7H ₂ O (MW: 246.47) to a 0.5 L graduated cylinder. Bring final volume to 0.5 L with water (Milli-Q or similar quality).	121 °C autoclave or filtration (0.2 µm)
F2	50 X MgSO ₄ stock solution (D ₂ O)		Add 3 g MgSO ₄ ·7H ₂ O (MW: 246.47) [or 1.47 g MgSO ₄ (MW: 120.37)] to a 50 mL graduated cylinder. Bring final volume to 50 mL with deuterium monoxide (D ₂ O).	Filtration (0.2 µm)
A1	4 X 2.94-11.07-7.6 carbon source stock solution (H ₂ O)	2.94 g L ⁻¹ glucose 11.07 g L ⁻¹ glycerol 7.6 g L ⁻¹ lactose	Add 12.92 g glucose·H ₂ O (MW: 198.17), 44.28 g glycerol (MW: 92.09) and 32 g lactose·H ₂ O (MW: 360.31) to a 1 L graduated cylinder. Bring final volume to 1 L with water (Milli-Q or similar quality).	121 °C autoclave or filtration (0.2 µm)
A2	4 X 2.94-11.07-7.6 carbon source stock solution (D ₂ O)		Add 1.292 g glucose·H ₂ O (MW: 198.17), 4.428 g glycerol (MW: 92.09) and 3.2 g lactose·H ₂ O (MW: 360.31) [or 1.176 g glucose (MW: 180.16), 4.428 g glycerol (MW: 92.09) and 3.04 g lactose (MW: 342.30)] to a 100 mL graduated cylinder. Bring final volume to 100 mL with deuterium monoxide (D ₂ O).	Filtration (0.2 µm)
A3	20 X Glucose stock solution (H ₂ O)	10.91 g L ⁻¹ glucose	Add 240 g glucose·H ₂ O (MW: 198.17) to a 1 L graduated cylinder. Bring final volume to 1 L with water (Milli-Q or similar quality).	121 °C autoclave or filtration (0.2 µm)
A4	20 X Glucose stock solution (D ₂ O)		Add 24 g glucose·H ₂ O (MW: 198.17) [or 21.82 g glucose (MW: 180.16)] to a 100 mL graduated cylinder. Bring final volume to 100 mL with deuterium monoxide (D ₂ O).	121 °C autoclave or filtration (0.2 µm)
A5	¹³ C labeled Glucose stock solution (H ₂ O)	6.55 g L ⁻¹ ¹³ C-glucose	Add 6.546 g ¹³ C-glucose to a 50 mL graduated cylinder. Bring final volume to 50 mL with water (Milli-Q or similar quality).	Filtration (0.2 µm)
A6	¹³ C labeled Glucose stock solution (D ₂ O)		Add 6.546 g ¹³ C-glucose to a 50 mL graduated cylinder. Bring final volume to 50 mL with deuterium monoxide (D ₂ O).	Filtration (0.2 µm)
G1	5000 X Na ₂ MoO ₄ ·H ₂ O stock solution (H ₂ O)	2.1 mg L ⁻¹ Na ₂ MoO ₄ ·2H ₂ O	Add 525 mg of Na ₂ MoO ₄ ·2H ₂ O (MW: 241.95) to a 50 mL graduated cylinder. Bring final volume to 50 mL with water (Milli-Q or similar quality).	Filtration (0.2 µm)
H1	2000 X trace element stock solution (H ₂ O)	2.5 mg L ⁻¹ CoCl ₂ ·6H ₂ O 15 mg L ⁻¹ MnCl ₂ ·4H ₂ O 1.5 mg L ⁻¹ CuCl ₂ ·2H ₂ O 3 mg L ⁻¹ H ₃ BO ₃ 33.8 mg L ⁻¹ Zn(CH ₃ COO) ₂ ·2H ₂ O 14.10 mg L ⁻¹ Titriplex III	Add 0.5 g of CoCl ₂ ·6H ₂ O (MW: 237.93), 3 g of MnCl ₂ ·4H ₂ O (MW: 197.9), 0.3 g of CuCl ₂ ·2H ₂ O (MW: 170.48), 0.6 g of H ₃ BO ₃ (MW: 61.83), 6.76 g of Zn(CH ₃ COO) ₂ ·2H ₂ O (MW: 219.49), 2.82 g of Titriplex III (MW: 372.24) to a 100 mL graduated cylinder. Bring final volume to 100 mL with Milli-Q water (or similar quality).	Filtration (0.2 µm)
B1	50 X (NH ₄) ₂ HPO ₄ stock solution (H ₂ O)	4 g L ⁻¹ (NH ₄) ₂ HPO ₄	Add 100 g (NH ₄) ₂ HPO ₄ (MW: 132.06) to a 0.5 L graduated cylinder. Bring final volume to 0.5 L with water (Milli-Q or similar quality).	121 °C autoclave or filtration (0.2 µm)

Appendix

No.	Name	Working concentration	Stock solution preparation	Sterilization method
B2	50 X NH ₄ Cl stock solution (H ₂ O)	3.24 g L ⁻¹ NH ₄ Cl	Add 81 g NH ₄ Cl (MW: 53.49) to a 0.5 L graduated cylinder. Bring final volume to 0.5 L with water (Milli-Q or similar quality).	121 °C autoclave or filtration (0.2 µm)
B3	50 X ¹⁵ N labeled NH ₄ Cl stock solution (H ₂ O)	3.24 g L ⁻¹ ¹⁵ N-NH ₄ Cl	Add 8.1 g ¹⁵ N-NH ₄ Cl to a 50 mL graduated cylinder. Bring final volume to 50 mL with water (Milli-Q or similar quality).	Filtration (0.2 µm)
B4	50 X ¹⁵ N labeled NH ₄ Cl stock solution (D ₂ O)		Add 8.1 g ¹⁵ N-NH ₄ Cl to a 50 mL graduated cylinder. Bring final volume to 50 mL with deuterium monoxide (D ₂ O).	Filtration (0.2 µm)
B5	50 X NH ₄ Cl stock solution (D ₂ O)	3.24 g L ⁻¹ NH ₄ Cl	Add 8.1 g NH ₄ Cl (MW: 53.49) to a 50 mL graduated cylinder. Bring final volume to 50 mL with deuterium monoxide (D ₂ O).	Filtration (0.2 µm)
C1	10 X KH ₂ PO ₄ (High concentration) stock solution (H ₂ O)	17.42 g L ⁻¹ KH ₂ PO ₄	Add 174.2 g KH ₂ PO ₄ (MW: 136.09) to a 1 L graduated cylinder. Bring final volume to 1 L with water (Milli-Q or similar quality).	121 °C autoclave or filtration (0.2 µm)
C2	10 X KH ₂ PO ₄ (High concentration) stock solution (D ₂ O)		Add 17.42 g KH ₂ PO ₄ (MW: 136.09) to a 100 mL graduated cylinder. Bring final volume to 100 mL with deuterium monoxide (D ₂ O).	Filtration (0.2 µm)
C3	10 X KH ₂ PO ₄ (Low concentration) stock solution (H ₂ O)	13.3 g L ⁻¹ KH ₂ PO ₄	Add 133 g KH ₂ PO ₄ (MW: 136.09) to a 1 L graduated cylinder. Bring final volume to 1 L with water (Milli-Q or similar quality).	121 °C autoclave or filtration (0.2 µm)
D1	50 X Citric acid stock solution (H ₂ O)	1.55 g L ⁻¹ Citric acid	Add 42.5 g Citric acid.H ₂ O (MW: 210.14) to a 0.5 L graduated cylinder. Bring final volume to 0.5 L with water (Milli-Q or similar quality)	121 °C autoclave or filtration (0.2 µm)
D2	50 X Citric acid stock solution (D ₂ O)		Add 4.25 g Citric acid.H ₂ O (MW: 210.14) [or 3.886 g Citric acid (MW: 192.12)] to a 50 mL graduated cylinder. Bring final volume to 50 mL with deuterium monoxide (D ₂ O).	Filtration (0.2 µm)
E1	50 X Fe(III) citrate stock solution (H ₂ O)	100.8 mg L ⁻¹ Fe(III) citrate	Add 2.52 g Fe(III) citrate (MW: 244.94) to a 0.5 L graduated cylinder. Bring final volume to 0.5 L with water (Milli-Q or similar quality).	121 °C autoclave or filtration (0.2 µm)
E2	50 X Fe(III) citrate stock solution (D ₂ O)		Add 0.252 g Fe(III) citrate (MW: 244.94) to a 50 mL graduated cylinder. Bring final volume to 50 mL with deuterium monoxide (D ₂ O).	Filtration (0.2 µm)
II	25 X NH ₄ OH stock solution (H ₂ O)	To bring final pH to 6.8	Add 50 mL 30~33 % Ammonium hydroxide to a 0.5 L graduated cylinder. Bring final volume to 0.5 L with water (Milli-Q or similar quality).	
J1	50 X NaOH stock solution (H ₂ O)		Add 100 g NaOH (MW: 40) to a 0.5 L graduated cylinder. Bring final volume to 0.5 L with water (Milli-Q or similar quality).	
J2	50 X NaOH stock solution (D ₂ O)		Add 10 g NaOH (MW: 40) to a 50 mL graduated cylinder. Bring final volume to 50 mL with deuterium monoxide (D ₂ O).	

5.3 Supplementary material for Chapter 3 - A comprehensive proteomic study of *Escherichia coli*

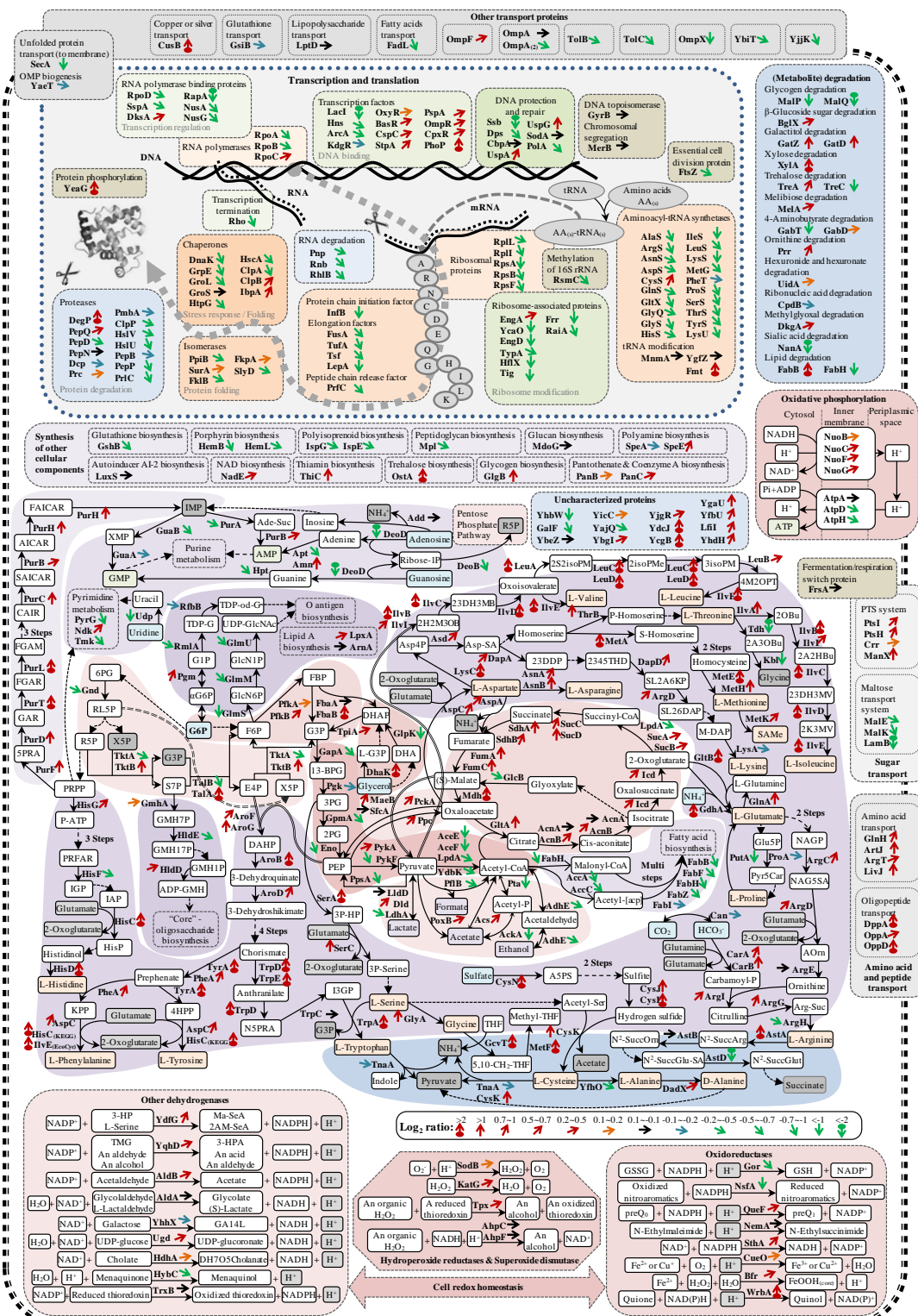
5.3.1 Supplementary figures

Abbreviation in Suppl. Figs 5.3.1 - 5.3.3 and 5.3.13 - 5.3.20

13-BPG	1,3-bisphospho-D-glycerate
2345THD	(<i>S</i>)-2,3,4,5-tetrahydrodipicolinate
23DDP	(<i>S</i>)-2,3-dihydrodipicolinate
23DH3MB	2,3-dihydroxy-3-methylbutanoate
23DH3MV	2,3-dihydroxy-3-methylvalerate
2A2HBu	2-aceto-2-hydroxy-butanoate
2A3OBu	2-amino-3-oxobutanoate
2AM-SeA	2-aminomalonnate-semialdehyde
2H2M3OB	(<i>S</i>)-2-hydroxy-2-methyl-3-oxobutanoate
2isoPMe	2-isopropylmaleate
2K3MV	2-keto-3-methyl-valerate
2OBu	2-oxobutanoate
2PG	2-phospho-D-glycerate
2S2isoPM	(2 <i>S</i>)-2-isopropylmalate
3-HP	3-hydroxypropionate
3-HPA	3-hydroxypropionaldehyde
3isoPM	(2 <i>R</i> ,3 <i>S</i>)-3-isopropylmalate
3PG	3-phospho-D-glycerate
3P-HP	3-phospho-hydroxypyruvate
3P-serine	3-phospho-L-serine
4HPP	4-hydroxyphenylpyruvate
4M2OPT	4-methyl-2-oxopentanoate
5,10-CH ₂ -THF	5,10-methylenetetrahydrofolate
5PRA	5-phospho-β-D-ribose-amine
6PG	6-phospho-D-gluconate
A5PS	adenosine 5'-phosphosulfate
Acetyl-P	acetylphosphate
Acetyl-Ser	<i>O</i> -acetyl-L-serine
Ade-Suc	adenylo-succinate
ADP-GMH	ADP-D-glycero-β-D-manno-heptose
AICAR	aminoimidazole carboxamide ribonucleotide
AOrn	<i>N</i> -acetyl-L-ornithine
Arg-Suc	L-arginino-succinate
Asp4P	L-aspartyl-4-phosphate

Asp-SA	L-aspartate-semialdehyde
CAIR	5-amino-1-(5-phospho-D-ribosyl)imidazole-4-carboxylate
Carbamoyl-P	carbamoyl-phosphate
DAHP	3-deoxy-D-arabino-heptulosonate-7-phosphate
DH7O5Cholanate	3 α ,12 α -dihydroxy-7-oxo-5 β -cholanate
DHA	dihydroxyacetone
DHAP	dihydroxyacetone phosphate
E4P	D-erythrose-4-phosphate
F6P	D-fructose-6-phosphate
FAICAR	phosphoribosyl-formamido-carboxamide
FBP	fructose-1,6-bisphosphate
FGAM	5-phosphoribosyl- <i>N</i> -formylglycineamidine
FGAR	5'-phosphoribosyl- <i>N</i> -formylglycineamide
G1P	α -D-glucose 1-phosphate
G3P	D-glyceraldehyde-3-phosphate
G6P	β -D-glucose-6-phosphate
GA14L	D-galactono-1,4-lactone
GAR	5-phospho-ribosyl-glycineamide
GlcN1P	D-glucosamine-1-phosphate
GlcN6P	D-glucosamine-6-phosphate
Glu5P	L-glutamate-5-phosphate
GMH17P	D-glycero- β -D-manno-heptose 1,7-bisphosphate
GMH1P	D-glycero- β -D-manno-heptose 1-phosphate
GMH7P	D-glycero-D-manno-heptose-7-phosphate
GSH	Glutathione
GSSG	Glutathione disulfide
HisP	L-histidinol-phosphate
I3GP	(1S,2R)-1-C-(indol-3-yl)glycerol 3-phosphate
IAP	imidazole acetol-phosphate
IGP	D-erythro-imidazole-glycerol-phosphate
IMP	inosine-5'-phosphate
KPP	keto-phenylpyruvate
L-G3P	<i>sn</i> -glycerol-3-phosphate
L-G3P	<i>sn</i> -glycerol-3-phosphate
Ma-SeA	malonate semialdehyde
M-DAP	<i>meso</i> -diaminopimelate
Methyl-THF	5-methyl-tetrahydrofolate
N ² -SuccArg	N ² -succinylarginine
N ² -SuccGlu-SA	N ² -succinylglutamic-semialdehyde
N ² -SuccGlu	N ² -succinylglutamate
N ² -SuccOrn	N ² -succinylornithine

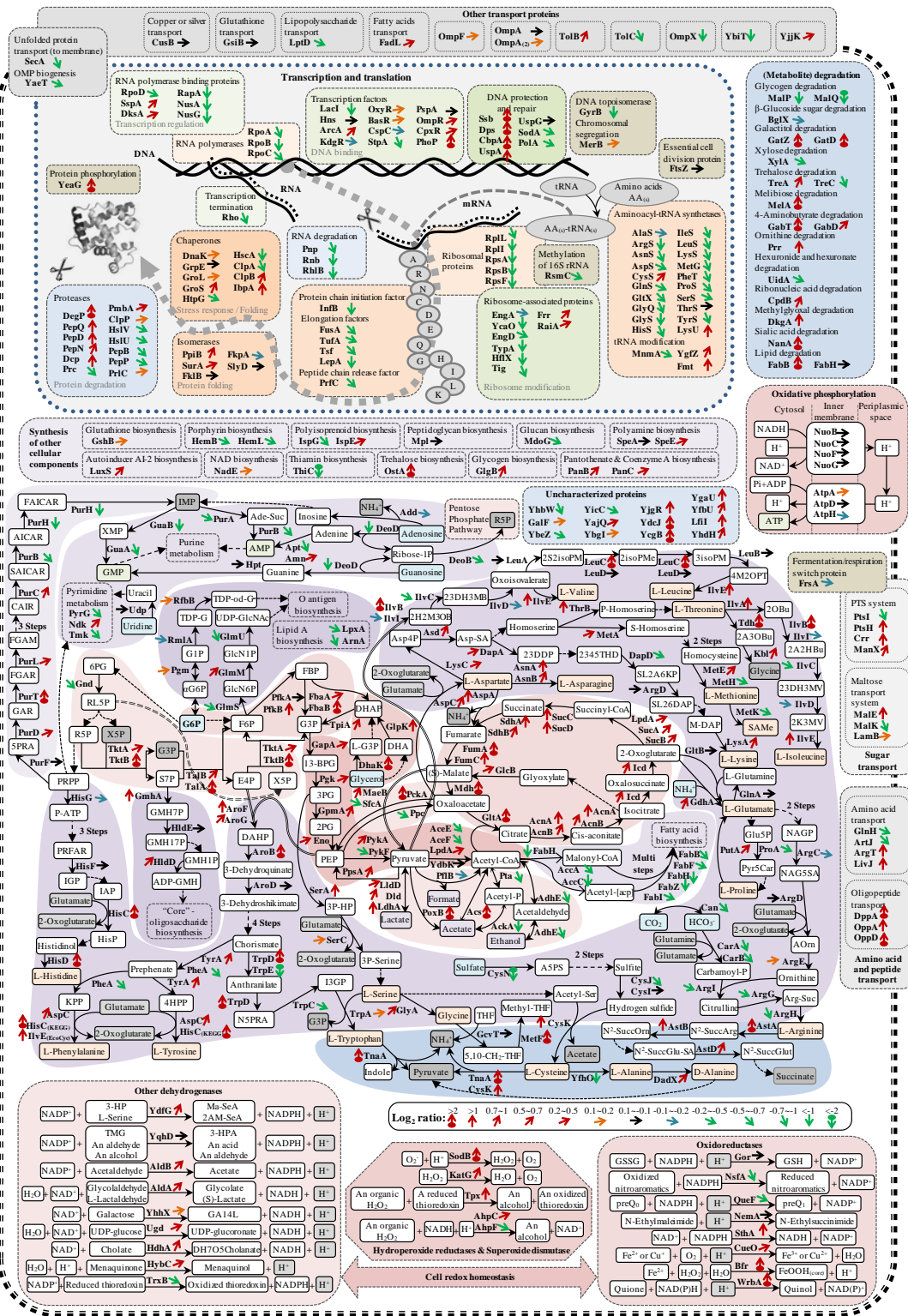
N5PRA	N-(5'-phosphoribosyl)-anthranilate
NAG5SA	<i>N</i> -acetyl-L-glutamate 5-semialdehyde
NAGP	<i>N</i> -acetylglutamyl-phosphate
Nitroaromatics	nitroaromatic compound
OC1D5P	1-(<i>o</i> -carboxyphenylamino)-1'-deoxyribose-5'-phosphate
P-ATP	phosphoribosyl-ATP
PEP	phosphoenolpyruvate
P-Homoserine	<i>O</i> -phospho- <i>L</i> -homoserine
preQ ₀	7-cyano-7-deazaguanine
preQ ₁	7-aminomethyl-7-deazaguanine
PRFAR	phosphoribulosylformimino-AICAR-P
PRPP	5-phospho- α -D-ribose 1-diphosphate
Pyr5Car	(<i>S</i>)-1-pyrroline-5-carboxylate
R5P	D-ribose-5-phosphate
Ribose-1P	α -D-ribose-1-phosphate
RL5P	D-ribulose-5-phosphate
S7P	D-sedoheptulose-7-phosphate
SAICAR	5'-phosphoribosyl-4-(<i>N</i> -succinocarboxamide)-5-
SAMe	<i>S</i> -adenosyl- <i>L</i> -methionine
S-Homoserine	<i>O</i> -succinyl- <i>L</i> -homoserine
SL26DAP	<i>N</i> -succinyl-L,L-2,6-diaminopimelate
SL2A6KP	<i>N</i> -succinyl-2-amino-6-ketopimelate
TDP-G	dTDP- α -D-glucose
TDP-od-G	dTDP-4-dehydro-6-deoxy-D-glucose
THF	tetrahydrofolate
TMG	1,3-propanediol
UDP-GlcNAc	UDP- α - <i>N</i> -acetyl-D-glucosamine
X5P	D-xylulose-5-phosphate
α G6P	α -D-glucose 6-phosphate



Suppl. Fig 5.3.1 Comparative proteome analysis of *E. coli*

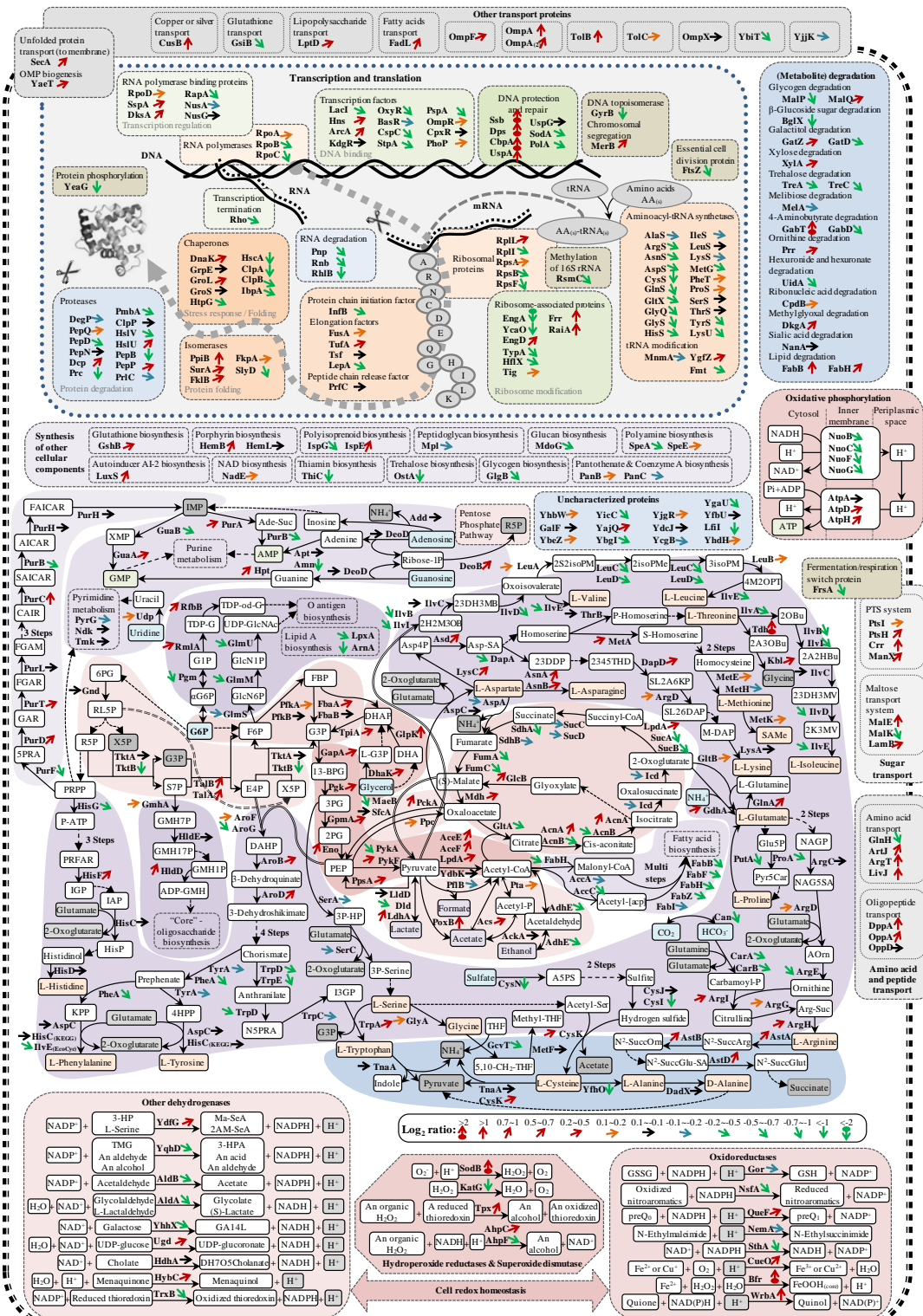
(exponential phase in defined medium versus exponential phase in complex medium)

Arrow indicates relative change of each protein (\log_2 ratio). Color code is shown in the figure. Number is given in Suppl. Table 5.3.1. Pathways are drawn according to EcoCyc database (<http://ecocyc.org/>) [confirmed by KEGG database (<http://www.genome.jp/kegg/>)].



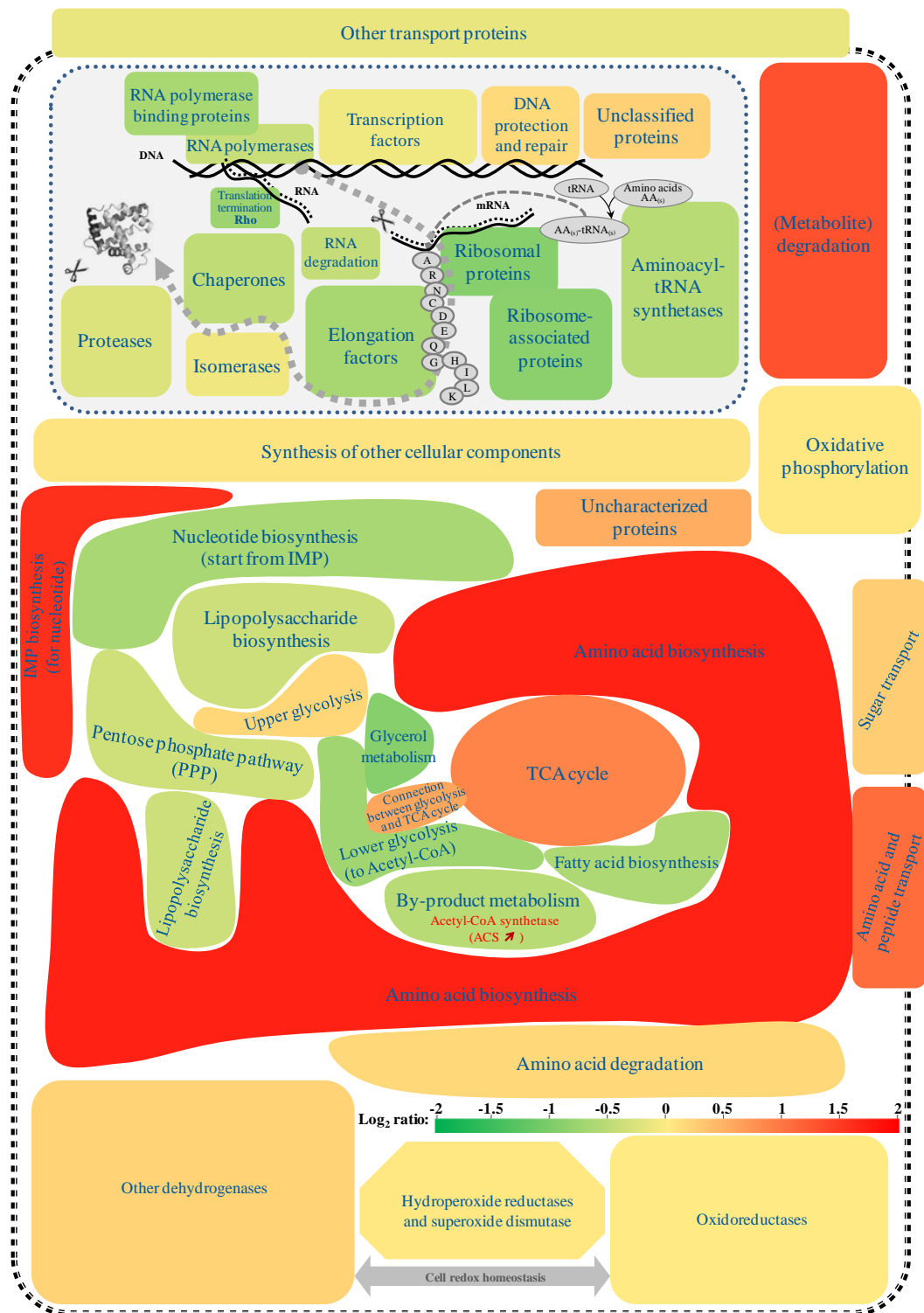
Suppl. Fig 5.3.2 Comparative proteome analysis of *E. coli* (stationary phase versus exponential phase in complex media)

Arrow indicates relative change of each protein (log₂ ratio). Color code is shown in the figure. Number is given in Suppl. Table 5.3.1. Pathways are drawn according to EcoCyc database (<http://ecocyc.org/>) [confirmed by KEGG database (<http://www.genome.jp/kegg/>)].



Suppl. Fig 5.3.3 Comparative proteome analysis of *E. coli* (stationary phase versus exponential phase in defined medium)

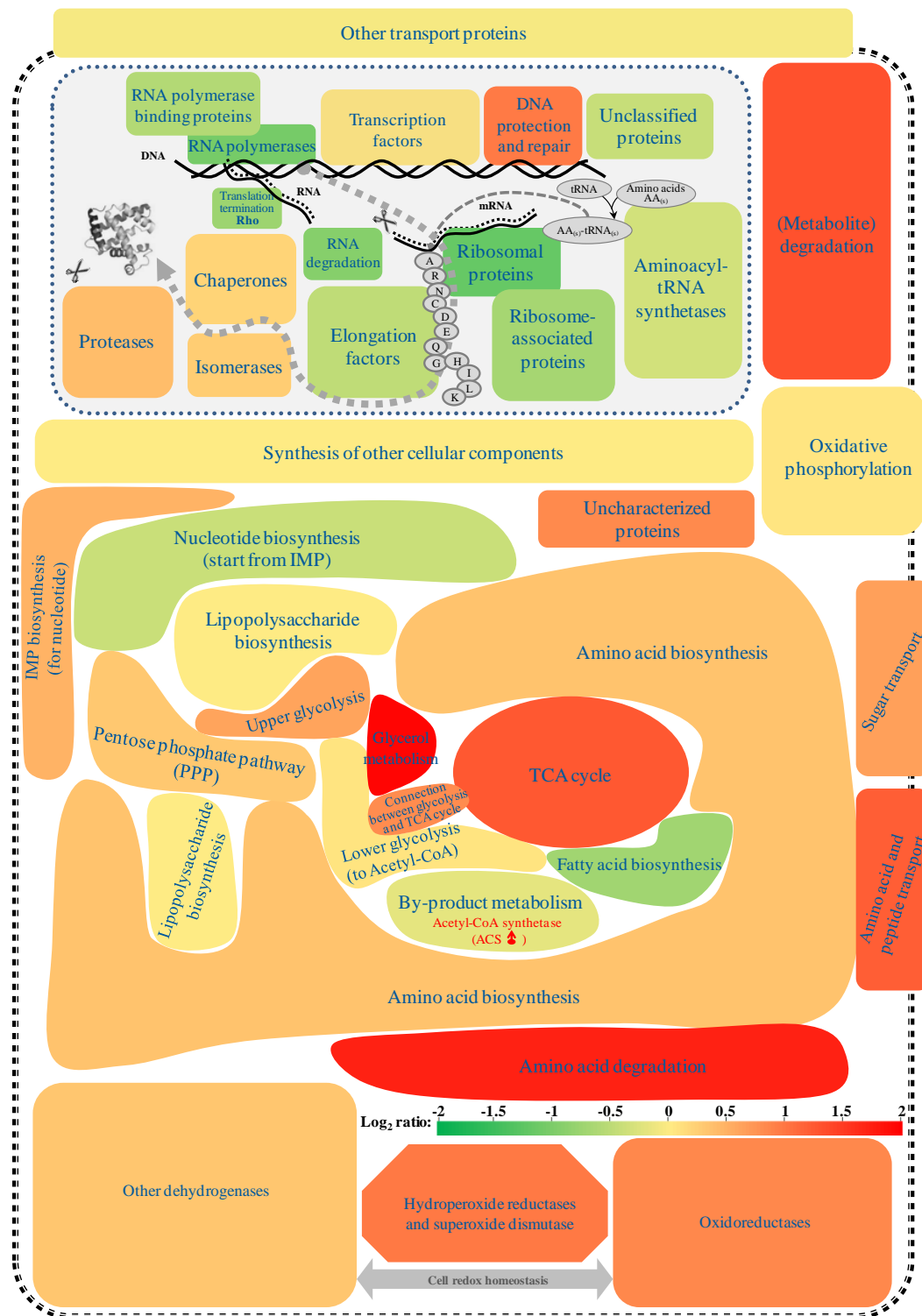
Arrow indicates relative change of each protein (\log_2 ratio). Color code is shown in the figure. Number is given in Suppl. Table 5.3.1. Pathways are drawn according to EcoCyc database (<http://ecocyc.org/>) [confirmed by KEGG database (<http://www.genome.jp/kegg/>)].



Suppl. Fig 5.3.4 Pathway comparison of *E. coli*

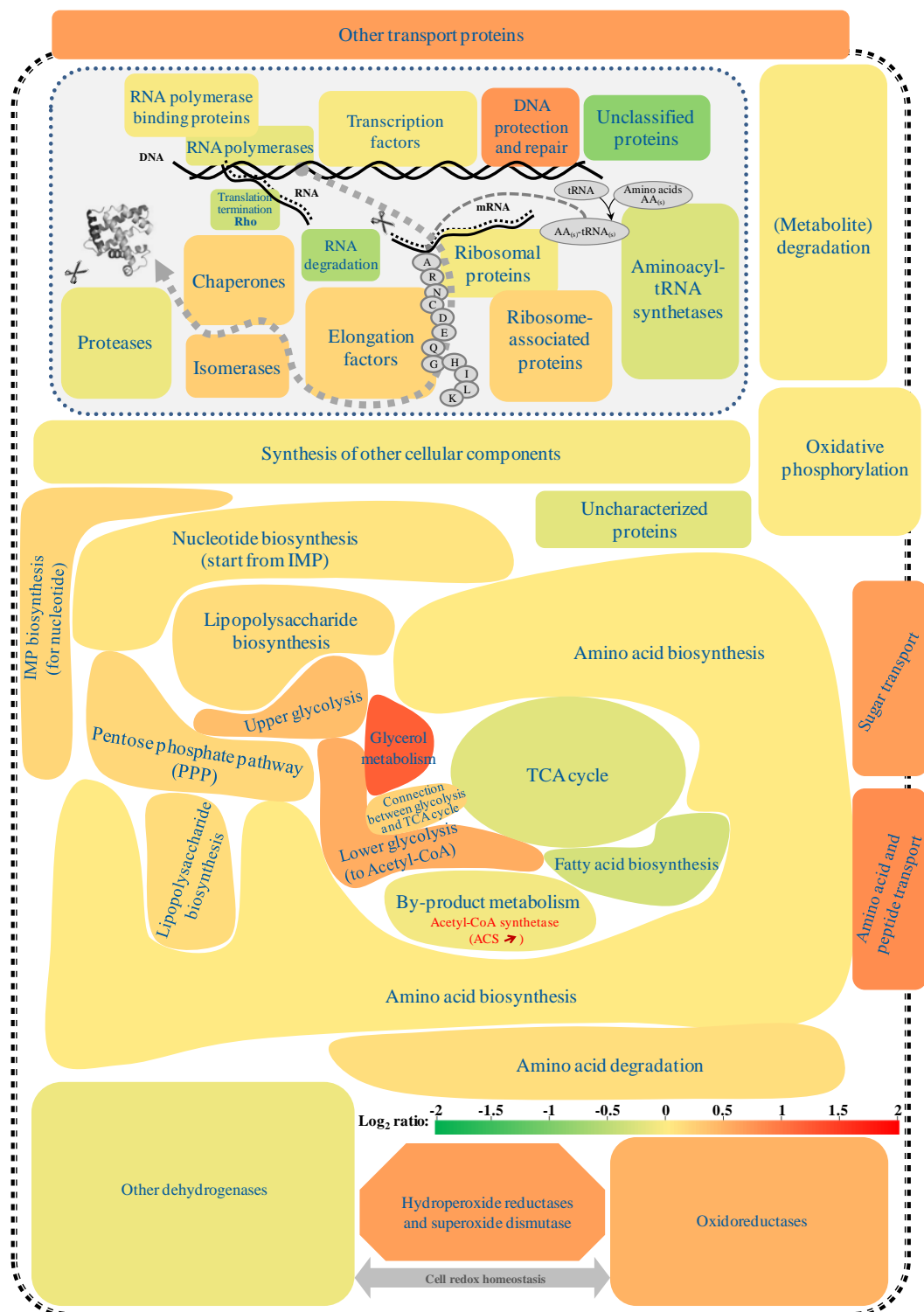
(exponential phase in defined medium versus exponential phase in complex medium)

Color indicates relative change of each pathway (\log_2 ratio). Color scale is shown in the figure. Number is given in Suppl. Table 5.3.2. Identified proteins are classified into each pathway according to EcoCyc database (<http://ecocyc.org/>) [confirmed by KEGG database (<http://www.genome.jp/kegg/>)].



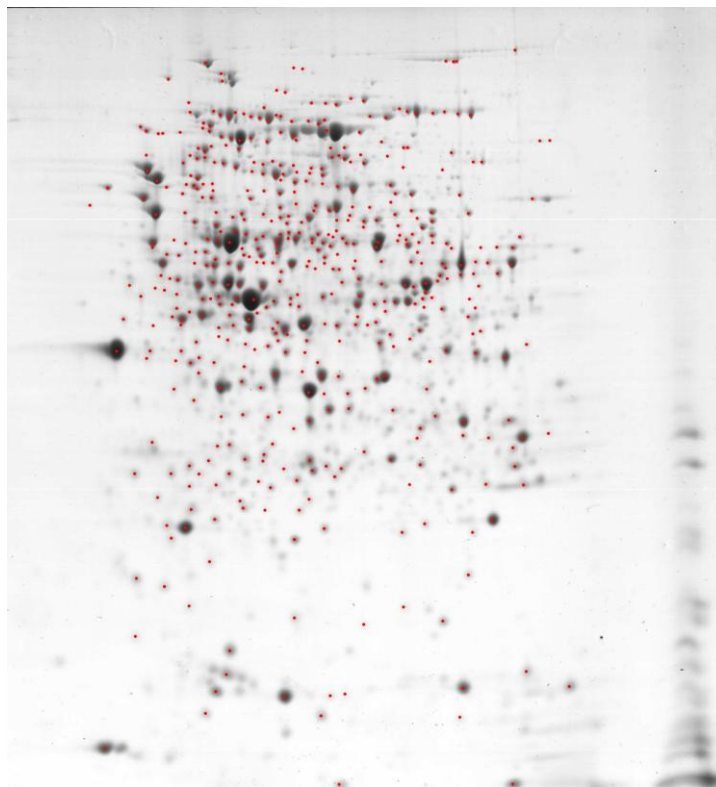
Suppl. Fig 5.3.5 Pathway comparison of *E. coli*
(stationary phase versus exponential phase in complex media)

Color indicates relative change of each pathway (\log_2 ratio). Color scale is shown in the figure. Number is given in Suppl. Table 5.3.2. Identified proteins are classified according to EcoCyc database (<http://ecocyc.org/>) database [confirmed by KEGG database (<http://www.genome.jp/kegg/>)].



Suppl. Fig 5.3.6 Pathway comparison of *E. coli*
(stationary phase versus exponential phase in defined medium)

Color indicates relative change of each pathway (log_2 ratio). Color scale is shown in the figure. Number is given in Suppl. Table 5.3.2. Identified proteins are classified according to EcoCyc database (<http://ecocyc.org/>) [confirmed by KEGG database (<http://www.genome.jp/kegg/>)].



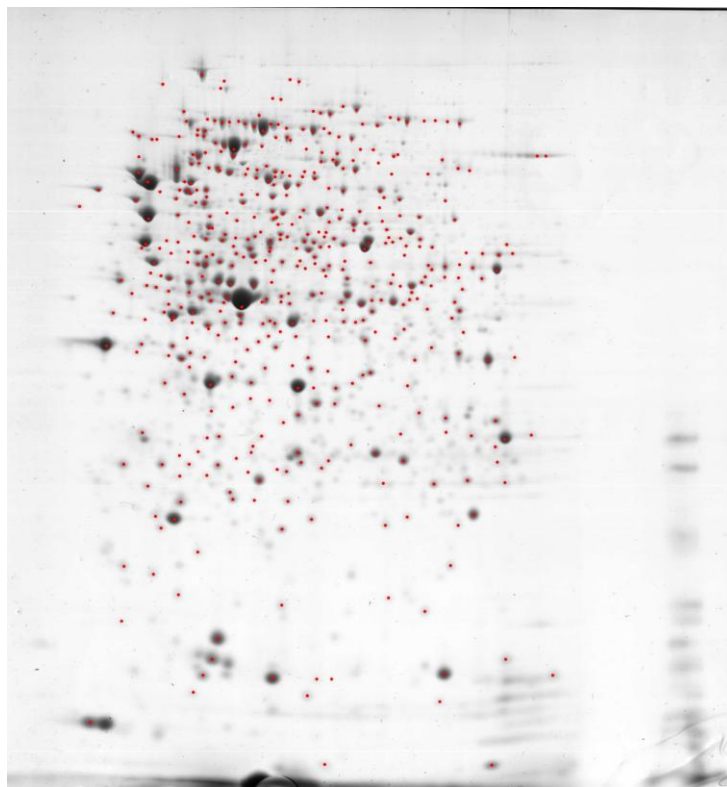
Suppl. Fig 5.3.7 2D gel of *E. coli* BL21 (DE3) growing in DNB medium at exponential phase

Identified proteins are marked as dots (red). Cultivation was carried out in shaker flask with baffles at 37 °C and 200 rpm.



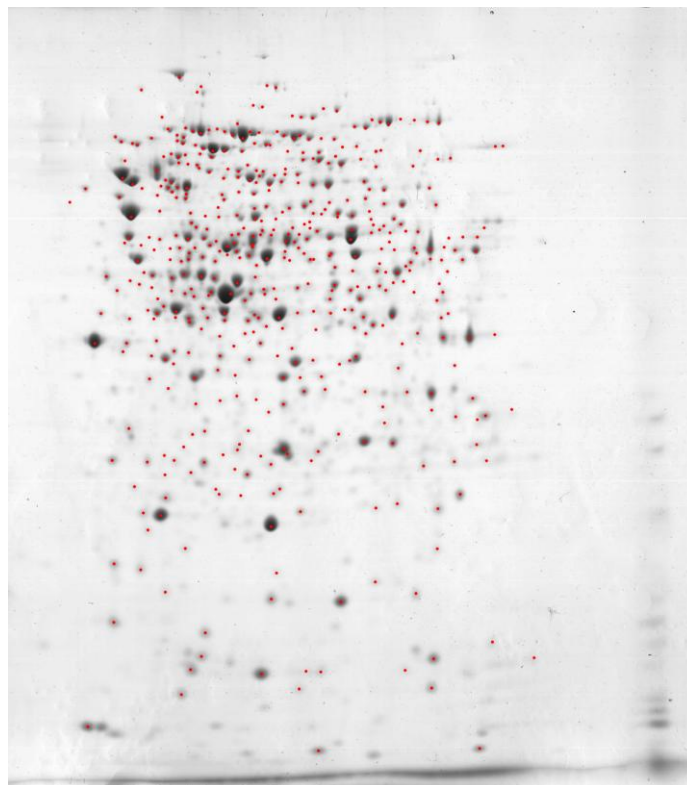
Suppl. Fig 5.3.8 2D gel of *E. coli* BL21 (DE3) growing in DNB medium at stationary phase

Identified proteins are marked as dots (red). Cultivation was carried out in shaker flask with baffles at 37 °C and 200 rpm.



Suppl. Fig 5.3.9 2D gel of *E. coli* BL21 (DE3) growing in TB medium at exponential phase

Identified proteins are marked as dots (red). Cultivation was carried out in shaker flask with baffles at 37 °C and 200 rpm.



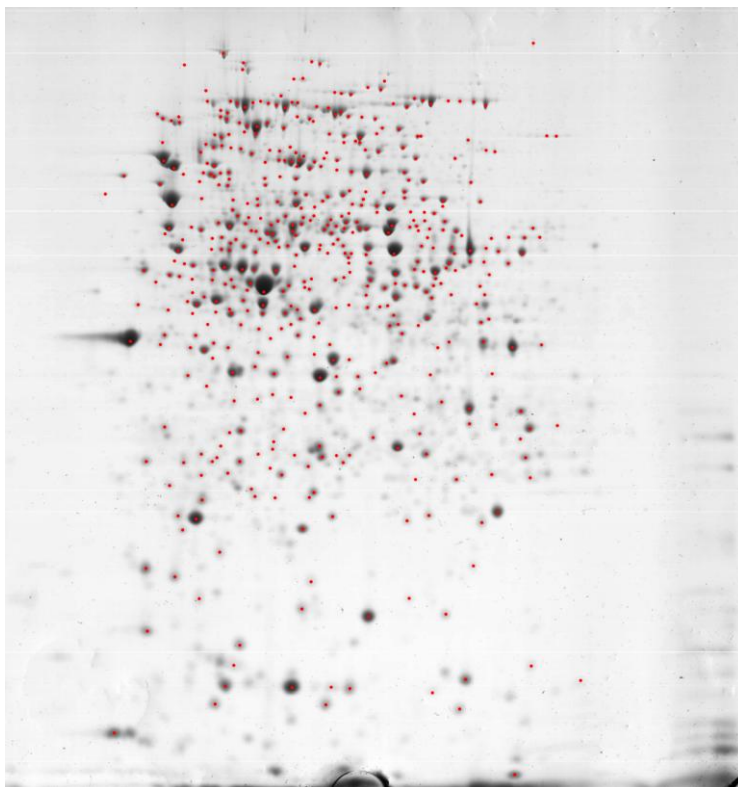
Suppl. Fig 5.3.10 2D gel of *E. coli* BL21 (DE3) growing in TB medium at stationary phase

Identified proteins are marked as dots (red). Cultivation was carried out in shaker flask with baffles at 37 °C and 200 rpm.



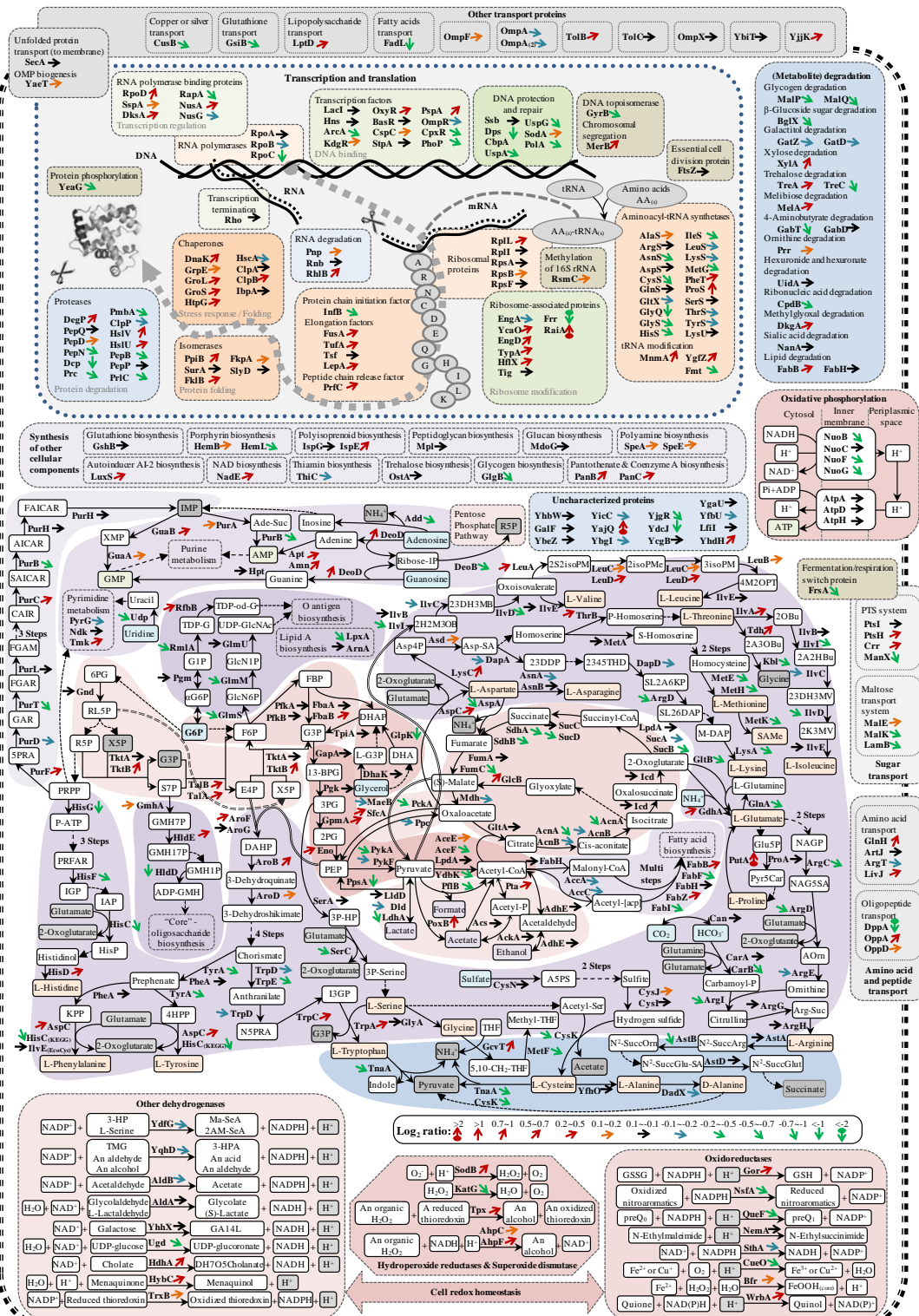
Suppl. Fig 5.3.11 2D gel of *E. coli* BL21 (DE3) growing in LB medium at exponential phase

Identified proteins are marked as dots (red). Cultivation was carried out in shaker flask with baffles at 37 °C and 200 rpm.



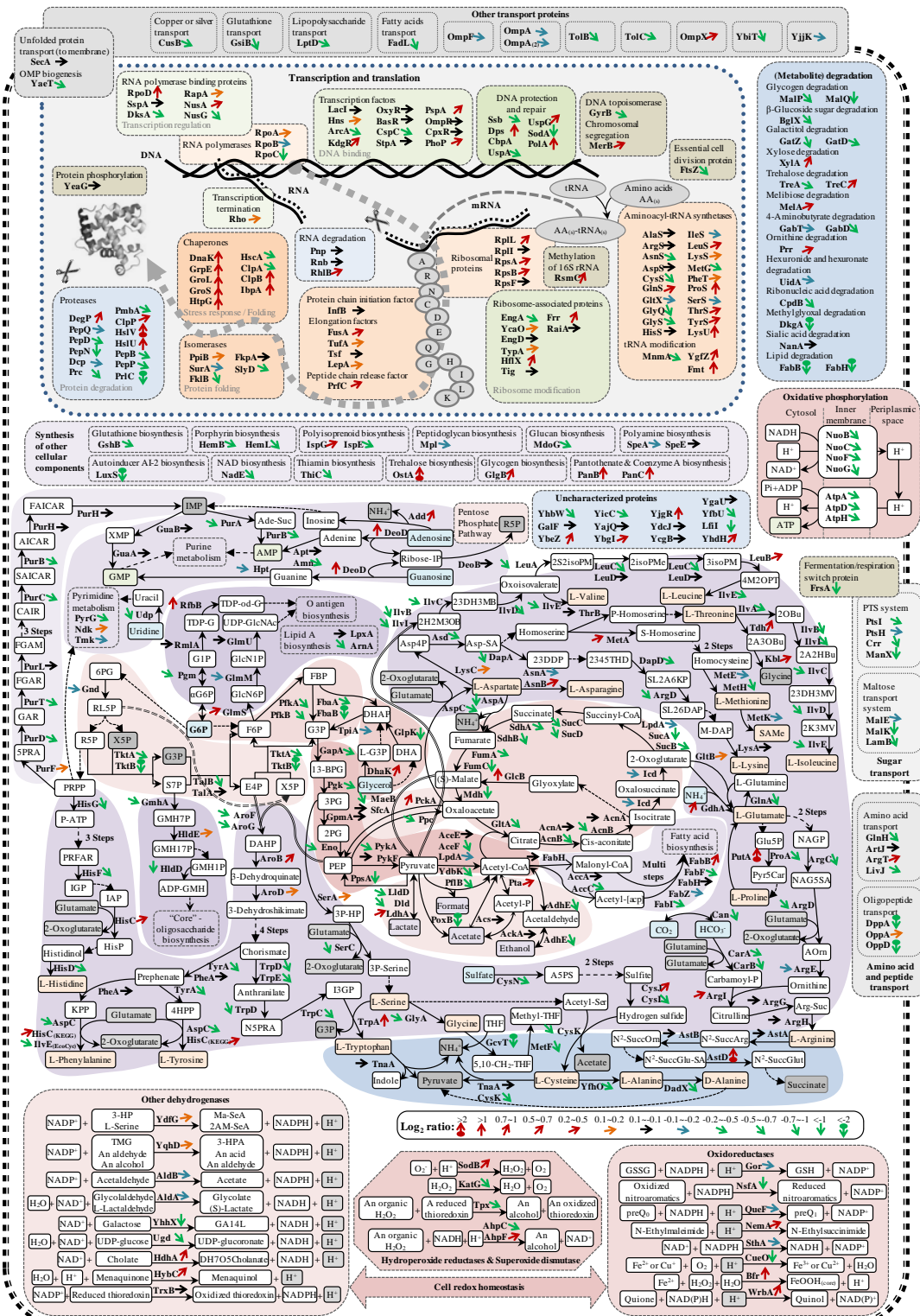
Suppl. Fig 5.3.12 2D gel of *E. coli* BL21 (DE3) growing in LB medium at stationary phase

Identified proteins are marked as dots (red). Cultivation was carried out in shaker flask with baffles at 37 °C and 200 rpm.



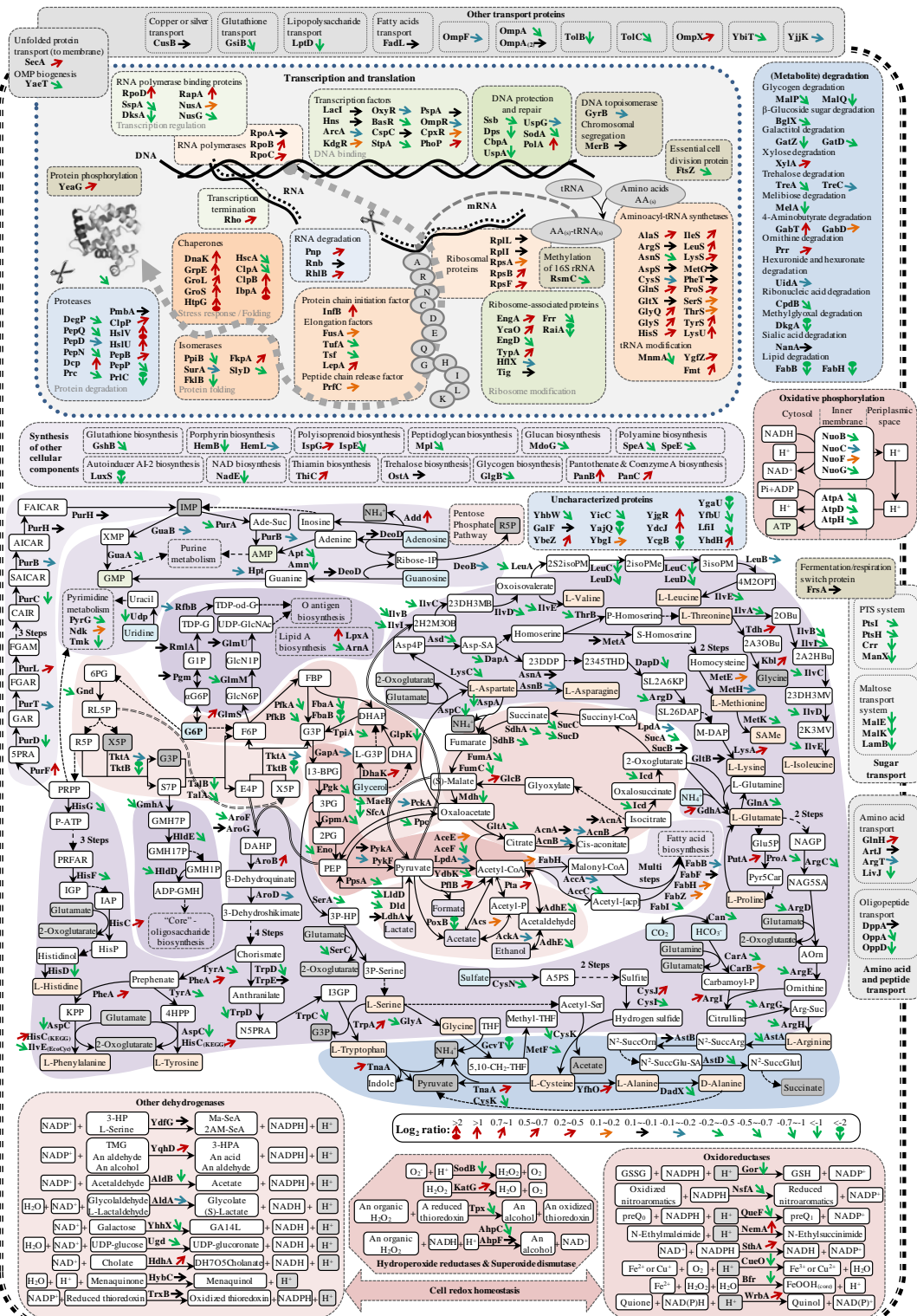
Suppl. Fig 5.3.13 Comparative proteome analysis of *E. coli* during hFGF-2 production (1h after IPTG induction versus exponential phase (before induction) in defined medium)

Arrow indicates relative change of each protein (log₂ ratio). Color code is shown in the figure. Number is given in Suppl. Table 5.3.5. Pathways are drawn according to EcoCyc database (<http://ecocyc.org/>) [confirmed by KEGG database (<http://www.genome.jp/kegg/>)].



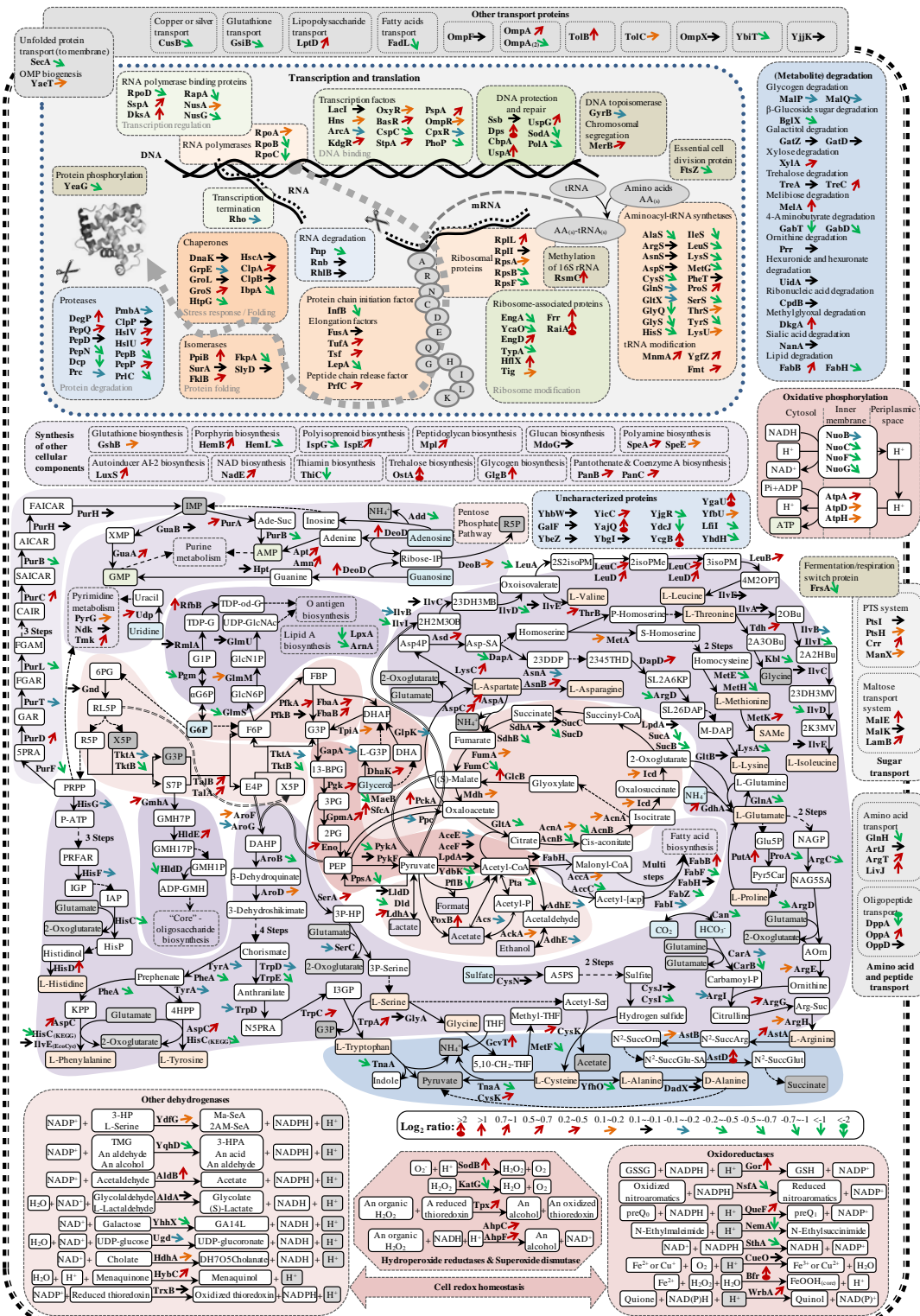
Suppl. Fig 5.3.14 Comparative proteome analysis of *E. coli* during hFGF-2 production (5h after IPTG induction versus exponential phase (before induction) in defined medium)

Arrow indicates relative change of each protein (log₂ ratio). Color code is shown in the figure. Number is given in Suppl. Table 5.3.5. Pathways are drawn according to EcoCyc database (<http://ecocyc.org/>) [confirmed by KEGG database (<http://www.genome.jp/kegg/>)].



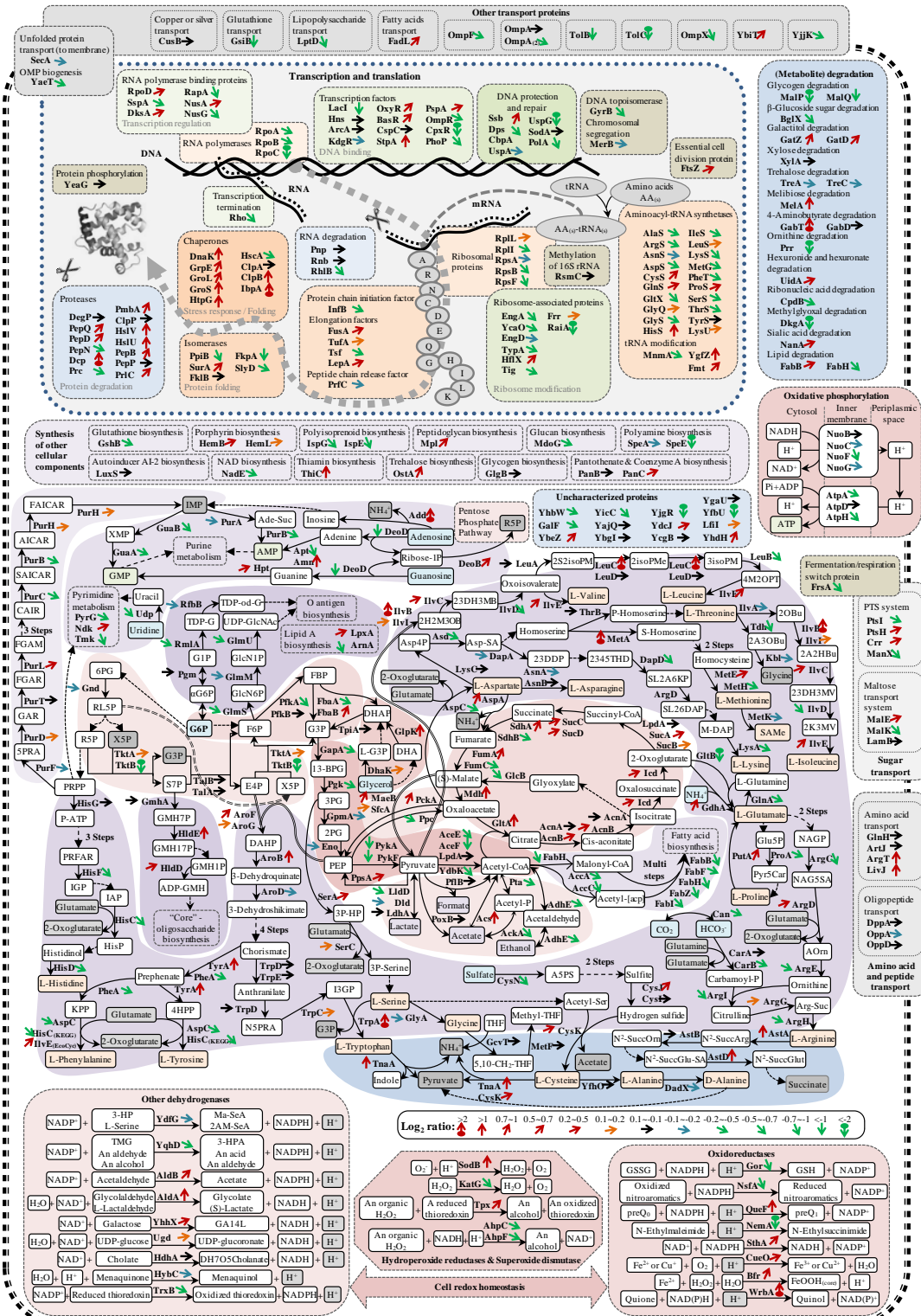
Suppl. Fig 5.3.15 Comparative proteome analysis of *E. coli* during hFGF-2 production (5h after IPTG induction versus stationary phase (without induction) in defined medium)

Arrow indicates relative change of each protein (log₂ ratio). Color code is shown in the figure. Number is given in Suppl. Table 5.3.5. Pathways are drawn according to EcoCyc database (<http://ecocyc.org/>) [confirmed by KEGG database (<http://www.genome.jp/kegg/>)].



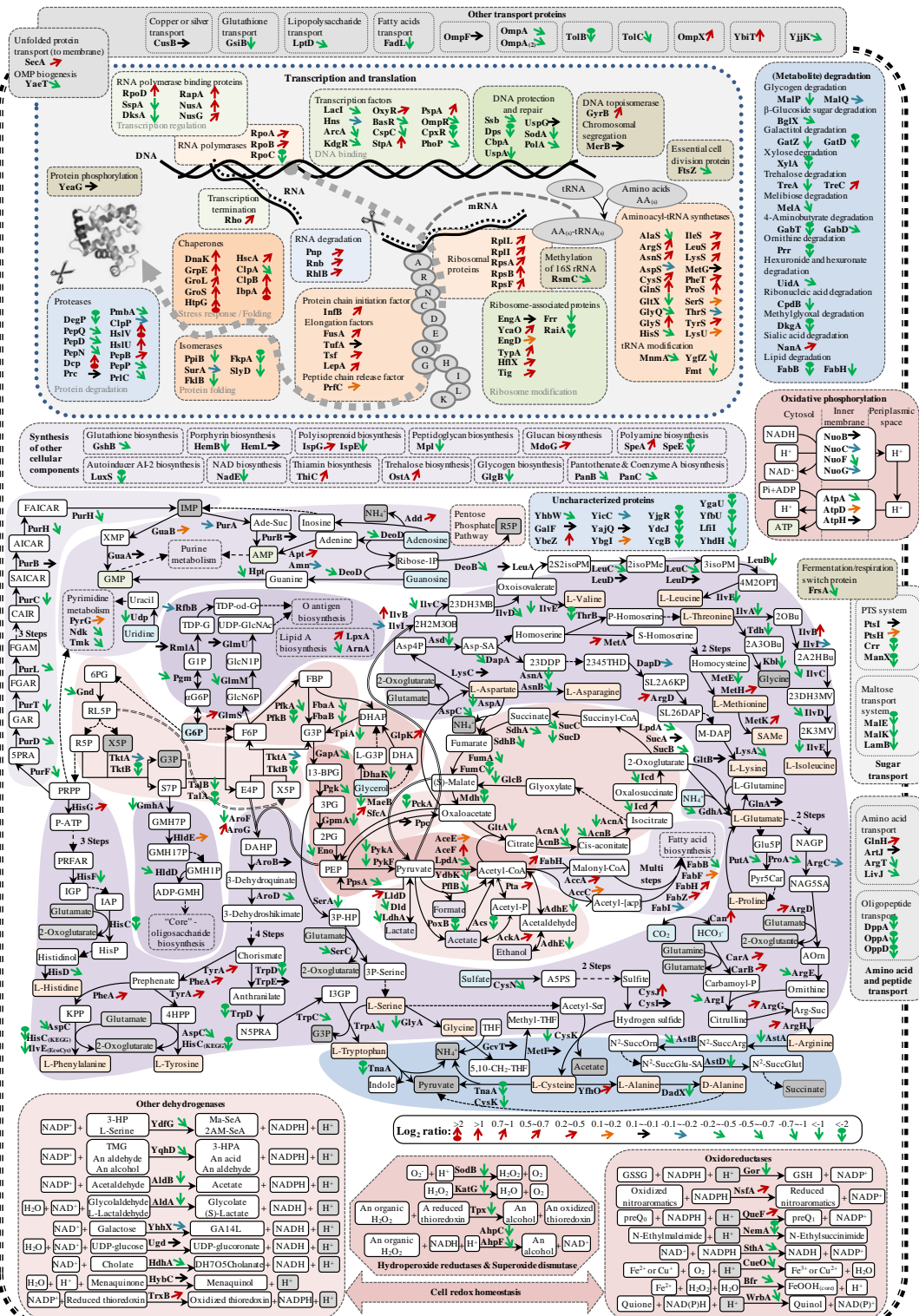
Suppl. Fig 5.3.16 Comparative proteome analysis of *E. coli* during hFGF-2 production (stationary phase versus exponential phase in defined medium without protein production)

Arrow indicates relative change of each protein (log₂ ratio). Color code is shown in the figure. Number is given in Suppl. Table 5.3.5. Pathways are drawn according to EcoCyc database (<http://ecocyc.org/>) [confirmed by KEGG database (<http://www.genome.jp/kegg/>)].



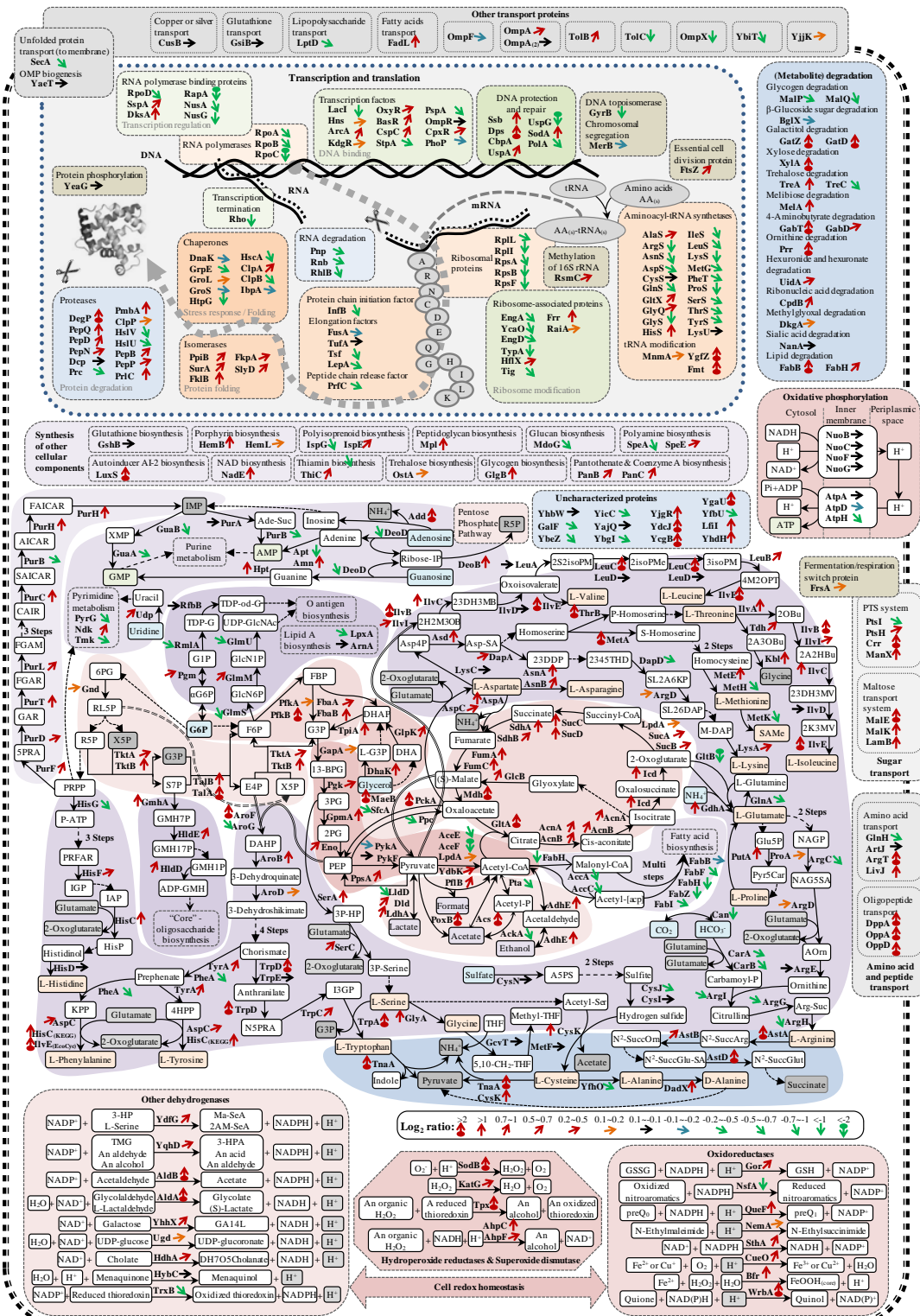
Suppl. Fig 5.3.18 Comparative proteome analysis of *E. coli* during hFGF-2 production (3.5h after IPTG induction versus exponential phase (before induction) in complex medium)

Arrow indicates relative change of each protein (\log_2 ratio). Color code is shown in the figure. Number is given in Suppl. Table 5.3.5. Pathways are drawn according to EcoCyc database (<http://ecocyc.org/>) [confirmed by KEGG database (<http://www.genome.jp/kegg/>)].



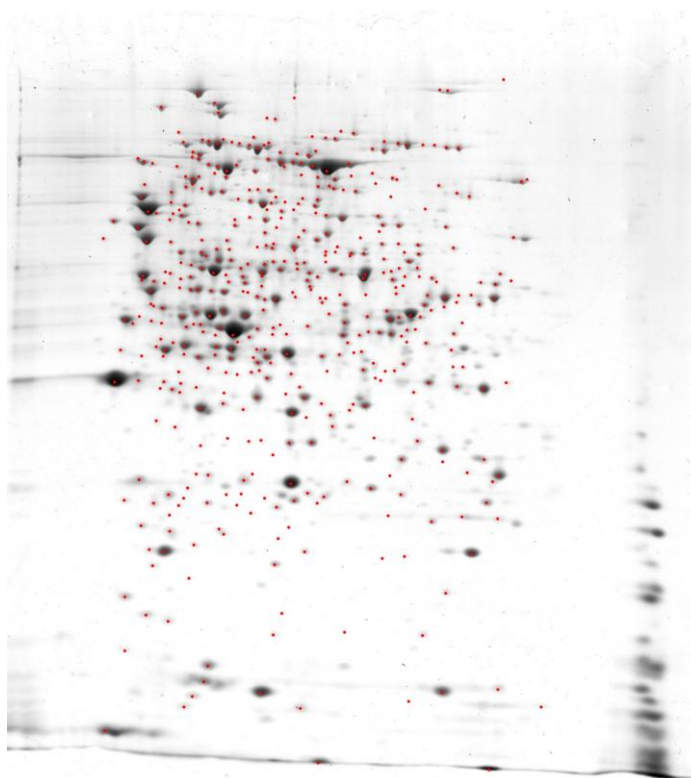
Suppl. Fig 5.3.19 Comparative proteome analysis of *E. coli* during hFGF-2 production (3.5h after IPTG induction versus stationary phase (without induction) in complex medium)

Arrow indicates relative change of each protein (log₂ ratio). Color code is shown in the figure. Number is given in Suppl. Table 5.3.5. Pathways are drawn according to EcoCyc database (<http://ecocyc.org/>) [confirmed by KEGG database (<http://www.genome.jp/kegg/>)].



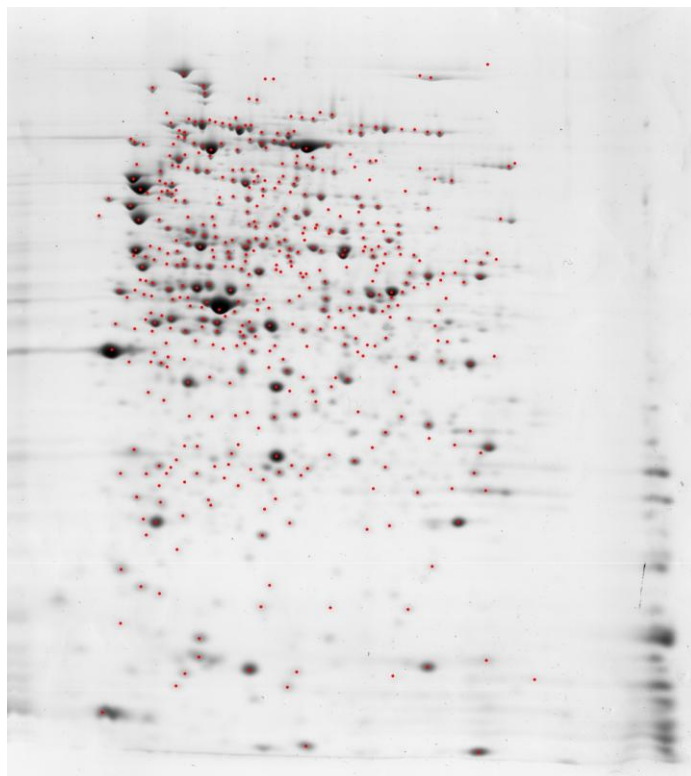
Suppl. Fig 5.3.20 Comparative proteome analysis of *E. coli* during hFGF-2 production (stationary phase versus exponential phase in complex medium without protein production)

Arrow indicates relative change of each protein (log₂ ratio). Color code is shown in the figure. Number is given in Suppl. Table 5.3.5. Pathways are drawn according to EcoCyc database (<http://ecocyc.org/>) [confirmed by KEGG database (<http://www.genome.jp/kegg/>)].



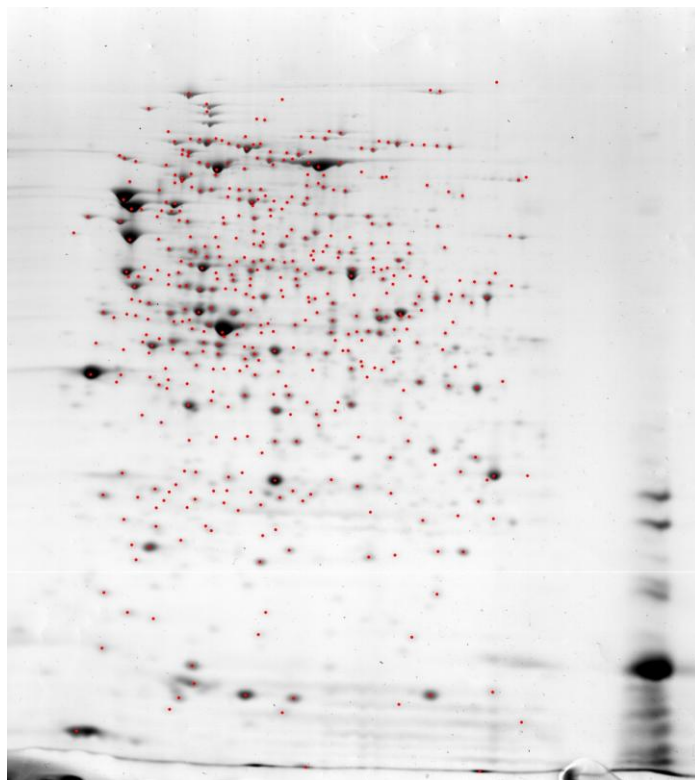
Suppl. Fig 5.3.21 2D gel of *E. coli* BL21 (DE3) harbouring plasmid pET-29c-hFGF-2 growing in DNB medium at exponential phase (before IPTG induction)

Identified proteins are marked as dots (red). Cultivation was carried out in shaker flask with baffles at 30 °C and 180 rpm



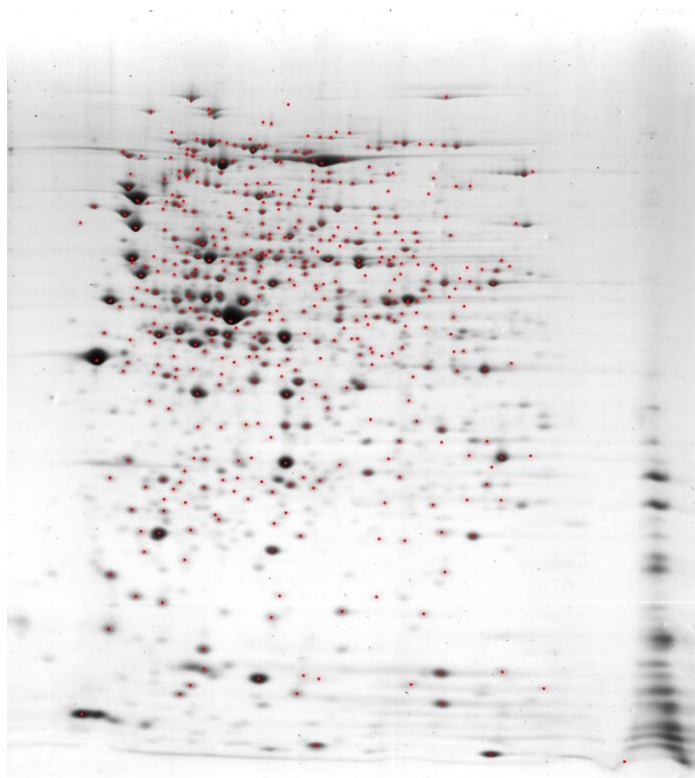
Suppl. Fig 5.3.22 2D gel of *E. coli* BL21 (DE3) harbouring plasmid pET-29c-hFGF-2 growing in DNB medium 1 h after induction with 0.25 mM IPTG

Identified proteins are marked as dots (red). Cultivation was carried out in shaker flask with baffles at 30 °C and 180 rpm



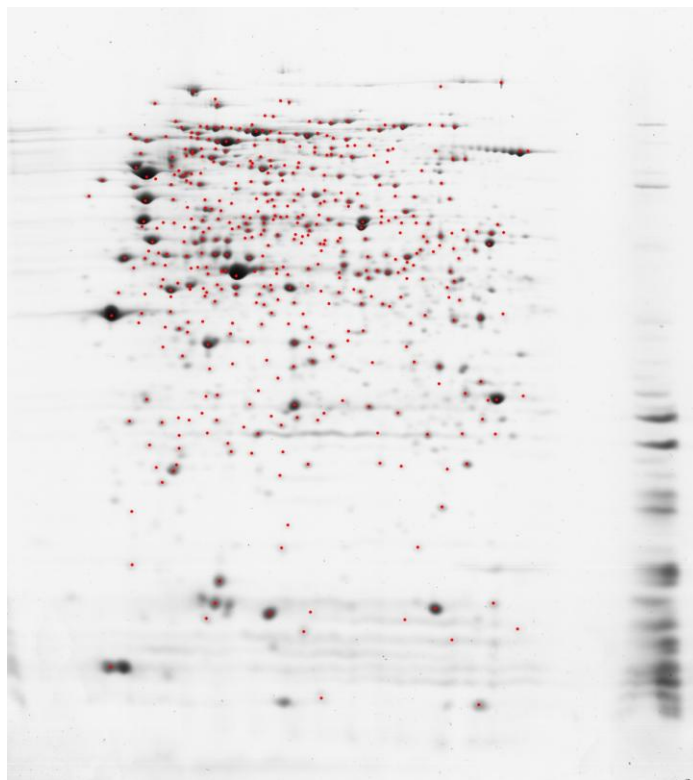
Suppl. Fig 5.3.23 2D gel of *E. coli* BL21 (DE3) harbouring plasmid pET-29c-hFGF-2 growing in DNB medium 5 h after induction with 0.25 mM IPTG

Identified proteins are marked as dots (red). Cultivation was carried out in shaker flask with baffles at 30 °C and 180 rpm



Suppl. Fig 5.3.24 2D gel of *E. coli* BL21 (DE3) harbouring plasmid pET-29c-hFGF-2 growing in DNB medium at stationary phase (without IPTG induction)

Identified proteins are marked as dots (red). Cultivation was carried out in shaker flask with baffles at 30 °C and 180 rpm



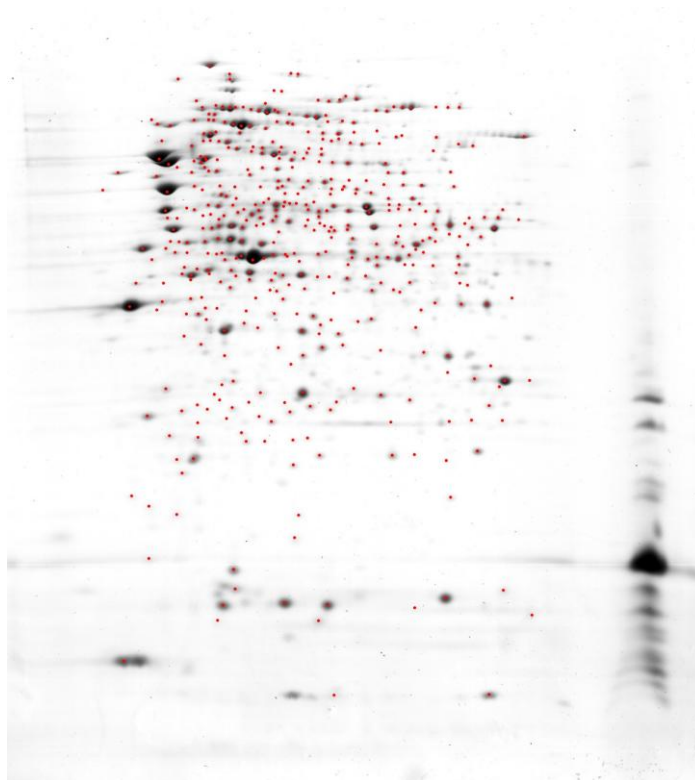
Suppl. Fig 5.3.25 2D gel of *E. coli* BL21 (DE3) harbouring plasmid pET-29c-hFGF-2 growing in LB medium at exponential phase (before IPTG induction)

Identified proteins are marked as dots (red). Cultivation was carried out in shaker flask with baffles at 30 °C and 180 rpm



Suppl. Fig 5.3.26 2D gel of *E. coli* BL21 (DE3) harbouring plasmid pET-29c-hFGF-2 growing in LB medium 1 h after induction with 0.25 mM IPTG

Identified proteins are marked as dots (red). Cultivation was carried out in shaker flask with baffles at 30 °C and 180 rpm



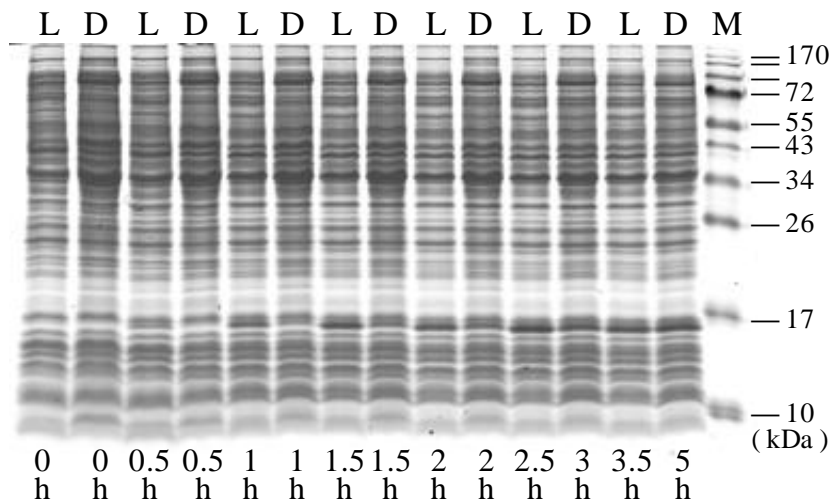
Suppl. Fig 5.3.27 2D gel of *E. coli* BL21 (DE3) harbouring plasmid pET-29c-hFGF-2 growing in LB medium 3.5 h after induction with 0.25 mM IPTG

Identified proteins are marked as dots (red). Cultivation was carried out in shaker flask with baffles at 30 °C and 180 rpm



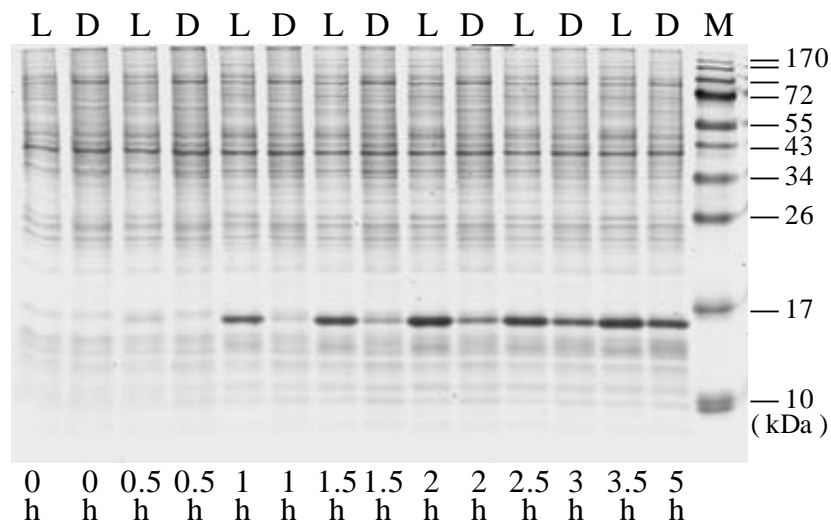
Suppl. Fig 5.3.28 2D gel of *E. coli* BL21 (DE3) harbouring plasmid pET-29c-hFGF-2 growing in LB medium at stationary phase (without IPTG induction)

Identified proteins are marked as dots (red). Cultivation was carried out in shaker flask with baffles at 30 °C and 180 rpm



Suppl. Fig 5.3.29 SDS-PAGE of soluble hFGF-2 production in LB and DNB medium

The time after induction is indicated below of the figure. The media are indicated above (L: LB medium, D: DNB medium, M: marker)



Suppl. Fig 5.3.30 SDS-PAGE of insoluble hFGF-2 production in LB and DNB medium

The time after induction is indicated below of the figure. The media are indicated above (L: LB medium, D: DNB medium, M: marker)

5.3.2 Supplementary tables

Suppl. Table 5.3.1 Proteome data of *E. coli* BL21 (DE3) growing in different media

Whole Cell Protein Mass (WCPM) - %: Each spot's intensity was normalized by the whole spots intensity on each 2D gel. The corresponding average from two duplicated gels was used indicating each spot's protein portion (%) of whole cell protein mass (WCPM). The total "WCPM %" of all spots representing the same protein was used for indicating the abundance of the corresponding protein.

For each protein's WCPM (%), number with two digits after the decimal point is given. But for a better comparison of low abundance proteins (WCPM <0.05 %), three digits after the decimal point are given.

Log₂(defined/complex) at exp. phase: Average of Log₂[DNB (medium)/TB (medium)] and Log₂[DNB (medium)/LB (medium)] at exponential phase

Log₂(stationary phase/exp. phase) in complex medium: Average of Log₂(stationary phase/exponential phase) in TB and LB media

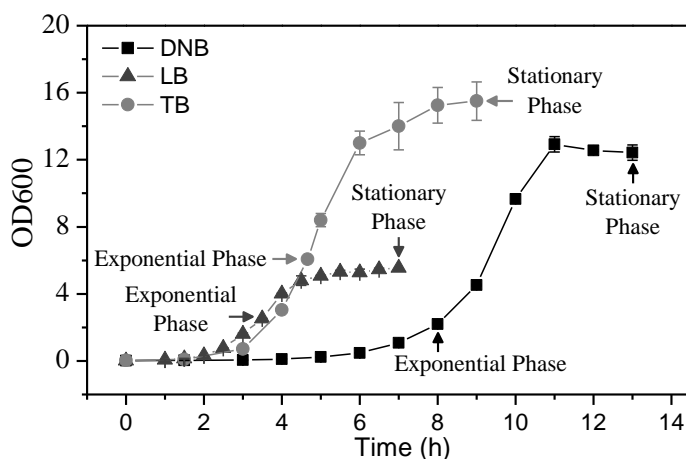
Log₂(stationary phase/exp. phase) in defined medium: Average of Log₂(stationary phase/exponential phase) in DNB medium

If WCPM (%) of a protein is zero, an artificial Log₂ ratio: ">5" or "<-5" was given, indicating the corresponding Log₂ ratio is larger than 5 or smaller than -5.

DNB medium: 10.91 g L⁻¹ glucose, 4 g L⁻¹ (NH₄)₂HPO₄, 13.3 g L⁻¹ KH₂PO₄, 1.554 g L⁻¹ Citric acid, 0.586 g L⁻¹ MgSO₄, 0.1008 g L⁻¹ Fe(III) citrate, 2.1 mg L⁻¹ Na₂MoO₄·2H₂O, 2.5 mg L⁻¹ CoCl₂·6H₂O, 15 mg L⁻¹ MnCl₂·4H₂O, 1.5 mg L⁻¹ CuCl₂·2H₂O, 3 mg L⁻¹ H₃BO₃, 33.8 mg L⁻¹ Zn(CH₃COOH)₂·2H₂O, 14.10 mg L⁻¹ Titriplex III. $\mu_{\max} = 0.8 \text{ h}^{-1}$

TB medium: 12 g L⁻¹ tryptone, 24 g L⁻¹ yeast extract, 5 g L⁻¹ glycerol, 2.31 g L⁻¹ KH₂PO₄, 12.54 g L⁻¹ K₂HPO₄. $\mu_{\max} = 1.4 \text{ h}^{-1}$

LB medium: 10 g L⁻¹ tryptone, 5 g L⁻¹ yeast extract, 5 g L⁻¹ NaCl. $\mu_{\max} = 1.6 \text{ h}^{-1}$



Suppl. Table 5.3.1 Proteome data of *E. coli* BL21 (DE3) growing in different media

Name ¹	Protein name ¹	Uniprot ID ¹	Molecular mass ² (Da)	Calculated pI value ²	Mascot score ²	Expect ²	Mascot seq. cover. ²	Defind medium		Complex medium				Log ₂ (DNB /TB)	Log ₂ (DNB /LB)	Log ₂ (defined/ complex)	Log ₂ (stationary phase /exp. phase)				
								exp. phase	stationary phase	exp. phase	stationary phase	exp. phase	stationary phase				in TB medium	in LB medium	in complex media	in defined medium	
								Whole Cell Protein Mass (WCPM) - %						At exp. phase							
Central carbon metabolism (24 proteins): Upper and lower glycolysis, glycerol metabolism and pentose phosphate pathway.								Total WCPM:	6.64	9.15	9.73	14.22	9.67	9.24	-0.6	-0.5	-0.5	0.5	-0.1	0.2	0.5
Sub-group: Upper glycolysis (5 proteins)								Total WCPM:	1.35	1.76	1.21	2.16	1.18	1.51	0.2	0.2	0.2	0.8	0.4	0.6	0.4
PfkA	6-Phosphofructokinase	P0A797	35162	5.47	105	2.7E-06	41%	0.13	0.15	0.11	0.11	0.12	0.11	0.2	0.1	0.2	0.0	-0.1	-0.1	0.2	
PfkB	6-Phosphofructokinase isozyme 2	P06999	32664	5.25	145	7.2E-11	83%	0.038	0.037	0.025	0.05	0.025	0.06	0.6	0.6	0.6	1.0	1.3	1.1	0.0	
FbaA	Fructose-bisphosphate aldolase class 2	P0AB71	39351	5.52	80	2.3E-04	25%	0.90	1.22	0.88	1.52	0.80	0.86	0.0	0.2	0.1	0.8	0.1	0.4	0.4	
FbaB	Fructose-bisphosphate aldolase class 1	P0A991	38313	6.25	59	2.8E-02	29%	0.031	0.030	0.00	0.06	0.00	0.12	>5	>5	>5	>5	>5	>5	0.0	
TpiA	Triosephosphate isomerase	C2DNX7	26392	5.41	95	2.5E-05	44%	0.25	0.32	0.19	0.42	0.23	0.36	0.4	0.1	0.3	1.1	0.6	0.9	0.4	
Sub-group: Lower glycolysis (to Acetyl-CoA) (11 proteins)								Total WCPM:	4.20	6.06	7.08	9.44	7.01	5.73	-0.8	-0.7	-0.7	0.4	-0.3	0.1	0.5
GapA	Glyceraldehyde-3-phosphate dehydrogenase A	P0A9B2	35681	6.61	58	3.8E-02	22%	0.66	0.91	0.89	1.30	0.98	1.26	-0.4	-0.6	-0.5	0.5	0.4	0.5	0.5	
Pgk	Phosphoglycerate kinase	P0A799	41264	5.08	231	6.6E-19	66%	0.71	0.98	0.75	1.08	0.77	0.75	-0.1	-0.1	-0.1	0.5	0.0	0.2	0.5	
GpmA	Phosphoglyceromutase	P62709	28539	5.85	64	3.6E-02	37%	0.25	0.34	0.42	0.73	0.31	0.52	-0.7	-0.3	-0.5	0.8	0.7	0.8	0.4	
Eno	Enolase	C6EJ93	45683	5.32	166	2.1E-12	47%	0.35	0.70	0.52	0.91	0.67	0.51	-0.6	-0.9	-0.8	0.8	-0.4	0.2	1.0	
PykA	Pyruvate kinase	Q1RAT0	57338	6.78	135	2.7E-09	32%	0.11	0.08	0.09	0.14	0.08	0.10	0.3	0.5	0.4	0.6	0.3	0.5	-0.5	
PykF	Pyruvate kinase I	P0AD61	50675	5.77	89	1.1E-04	32%	0.19	0.24	0.35	0.29	0.31	0.22	-0.9	-0.7	-0.8	-0.3	-0.5	-0.4	0.3	
PpsA	Phosphoenolpyruvate synthase	Q8FH33	87798	4.93	126	2.1E-08	19%	0.06	0.08	0.07	0.15	0.14	0.22	-0.2	-1.2	-0.7	1.1	0.7	0.9	0.4	
YdbK	Pyruvate flavodoxin/ferredoxin oxidoreductase domain protein	A7ZZU0	129871	5.51	76	2.0E-03	14%	0.042	0.041	0.044	0.043	0.05	0.06	-0.1	-0.3	-0.2	0.0	0.3	0.1	0.0	

A-47

Suppl. Table 5.3.1 Proteome data of *E. coli* BL21 (DE3) growing in different media

Name ¹	Protein name ¹	Uniprot ID ¹	Molecular mass ² (Da)	Calculated pI value ²	Mascot score ²	Expect ²	Mascot seq. cover. ²	Defind medium		Complex medium				Log ₂ (DNB /TB)	Log ₂ (DNB /LB)	Log ₂ (defined/complex)	Log ₂ (stationary phase /exp. phase)				
								DNB medium		TB medium		LB medium					in TB medium	in LB medium	in complex media	in defined medium	
								exp. phase	stationary phase	exp. phase	stationary phase	exp. phase	stationary phase	At exp. phase							
								Whole Cell Protein Mass (WCPM) - %													
AceE	Pyruvate dehydrogenase (acetyl-transferring), homodimeric type	B3XKK6	99978	5.46	179	1.1E-13	28%	0.77	1.32	2.01	2.25	2.13	0.81	-1.4	-1.5	-1.4	0.2	-1.4	-0.6	0.8	
AceF	Pyruvate dehydrogenase, dihydrolipoyltransacetylase component E2	P06959	66112	5.09	156	2.1E-11	32%	0.32	0.52	0.94	0.86	0.63	0.31	-1.6	-1.0	-1.3	-0.1	-1.0	-0.6	0.7	
LpdA	Dihydrolipoamide dehydrogenase	P0A9P2	50942	5.79	85	2.9E-04	25%	0.74	0.86	1.01	1.68	0.93	0.97	-0.4	-0.3	-0.4	0.7	0.1	0.4	0.2	
Sub-group: Glycerol metabolism (2 proteins)								Total WCPM:	0.09	0.20	0.16	1.06	0.17	0.37	-0.8	-0.9	-0.9	2.7	1.1	1.9	1.1
GlpK	Glycerol kinase	C5A093	56480	5.36	129	2.9E-09	28%	0.07	0.17	0.14	1.00	0.17	0.33	-1.0	-1.3	-1.1	2.8	1.0	1.9	1.3	
Dhak	Dihydroxyacetone kinase subunit DhaK	A7ZZD5	38620	4.82	104	3.4E-06	44%	0.019	0.026	0.015	0.06	0.00	0.044	0.3	>5	>2.7	2.0	>5	>3.6	0.5	
Sub-group: Pentose phosphate pathway (PPP) (6 proteins)								Total WCPM:	1.00	1.14	1.29	1.56	1.31	1.63	-0.4	-0.4	-0.4	0.3	0.3	0.3	0.2
Gnd	6-Phosphogluconate dehydrogenase	Q8FG44	51547	5.06	208	1.3E-16	56%	0.25	0.25	0.29	0.24	0.35	0.20	-0.2	-0.5	-0.3	-0.3	-0.8	-0.5	0.0	
TktA	Transketolase	P27302	72465	5.43	104	3.3E-06	22%	0.46	0.46	0.62	0.65	0.57	0.74	-0.4	-0.3	-0.4	0.1	0.4	0.2	0.0	
TktB	Transketolase 2	P33570	73225	5.86	190	2.3E-15	27%	0.033	0.015	0.017	0.043	0.010	0.12	1.0	1.7	1.3	1.3	3.6	2.5	-1.1	
TalB	Chain A, Structure Of Transaldolase B	P0A870	35237	5.1	147	1.7E-10	59%	0.18	0.30	0.27	0.48	0.32	0.40	-0.6	-0.8	-0.7	0.8	0.3	0.6	0.7	
TalA	Transaldolase A	P0A867	35865	5.89	211	1.8E-17	62%	0.017	0.030	0.00	0.049	0.00	0.10	>5	>5	>5	>5	>5	>5	0.8	
Eda	KHG/KDPG aldolase	P0A955	22441	5.57	108	3.6E-07	49%	0.06	0.08	0.09	0.10	0.06	0.07	-0.6	0.0	-0.3	0.2	0.2	0.2	0.4	
By-product metabolism (9 proteins)								Total WCPM:	1.48	1.40	1.77	1.59	2.69	2.27	-0.3	-0.9	-0.6	-0.2	-0.2	-0.2	-0.1
Acs	Acetyl-coenzyme A synthetase	Q8FAY8	72321	5.5	100	9.5E-06	23%	0.09	0.11	0.07	0.13	0.06	0.59	0.4	0.6	0.5	0.9	3.3	2.1	0.3	
PoxB	Pyruvate dehydrogenase [ubiquinone]	Q47520	62542	5.86	160	2.3E-12	44%	0.018	0.047	0.018	0.06	0.013	0.11	0.0	0.5	0.2	1.7	3.1	2.4	1.4	

Suppl. Table 5.3.1 Proteome data of *E. coli* BL21 (DE3) growing in different media

Name ¹	Protein name ¹	Uniprot ID ¹	Molecular mass ² (Da)	Calculated pI value ²	Mascot score ²	Expect ²	Mascot seq. cover. ²	Defind medium		Complex medium				Log ₂ (DNB /TB)	Log ₂ (DNB /LB)	Log ₂ (defined/complex)	Log ₂ (stationary phase /exp. phase)				
								DNB medium		TB medium		LB medium					in TB medium	in LB medium	in complex media	in defined medium	
								exp. phase	stationary phase	exp. phase	stationary phase	exp. phase	stationary phase	At exp. phase							
								Whole Cell Protein Mass (WCPM) - %													
Pta	Phosphate acetyltransferase	P0A9M8	77466	5.28	159	1.1E-11	37%	0.13	0.15	0.35	0.21	0.31	0.14	-1.4	-1.3	-1.3	-0.7	-1.1	-0.9	0.2	
AckA	Acetate kinase	P0A6A3	43605	5.85	64	1.0E-02	18%	0.11	0.11	0.37	0.13	0.32	0.18	-1.8	-1.5	-1.6	-1.5	-0.8	-1.2	0.0	
AdhE	Bifunctional acetaldehyde-CoA/alcohol dehydrogenase	P0A9Q8	96580	6.32	192	5.3E-15	26%	0.48	0.36	0.29	0.33	1.15	0.36	0.7	-1.3	-0.3	0.2	-1.7	-0.7	-0.4	
PflB	Formate acetyltransferase 1	P09373	85588	5.69	91	1.7E-05	20%	0.52	0.48	0.56	0.46	0.70	0.66	-0.1	-0.4	-0.3	-0.3	-0.1	-0.2	-0.1	
LldD	L-Lactate dehydrogenase	A7ZTF9	42902	6.33	107	1.1E-05	22%	0.06	0.06	0.06	0.06	0.06	0.09	0.0	0.0	0.0	0.0	0.6	0.3	0.0	
Dld	D-Lactate dehydrogenase	Q8FFW1	66546	6.39	106	2.1E-06	15%	0.043	0.031	0.024	0.06	0.035	0.042	0.8	0.3	0.6	1.3	0.3	0.8	-0.5	
LdhA	D-Lactate dehydrogenase	P52643	36854	5.29	115	7.2E-08	33%	0.029	0.05	0.031	0.15	0.043	0.10	-0.1	-0.6	-0.3	2.3	1.2	1.7	0.8	
TCA cycle (14 proteins)								Total WCPM:	6.94	5.89	3.45	8.55	4.16	9.49	1.0	0.7	0.9	1.3	1.2	1.2	-0.2
GlhA	Citrate synthase	P0ABH7	48383	6.21	142	5.3E-10	36%	1.20	0.99	0.32	1.12	0.32	1.53	1.9	1.9	1.9	1.8	2.3	2.0	-0.3	
AcnA	Aconitate hydratase 1	P25516	97985	5.59	219	1.1E-17	35%	0.17	0.33	0.17	0.52	0.19	0.62	0.0	-0.2	-0.1	1.6	1.7	1.7	1.0	
AcnB	Aconitate hydratase 2	B1LGR9	91078	5.22	213	4.2E-17	46%	0.82	0.65	0.49	1.09	0.67	1.15	0.7	0.3	0.5	1.2	0.8	1.0	-0.3	
Icd	Isocitrate dehydrogenase	Q7WV51	43029	5.18	197	1.7E-15	55%	1.00	0.94	0.69	1.14	0.64	1.43	0.5	0.6	0.6	0.7	1.2	0.9	-0.1	
SucA	2-Oxoglutarate dehydrogenase E1 component	P0AFG5	105566	6.04	99	1.0E-05	14%	0.57	0.30	0.31	0.73	0.59	0.62	0.9	0.0	0.4	1.2	0.1	0.7	-0.9	
SucB	Dihydrolipoamide succinyltransferase	A7ZXY7	44014	5.58	127	1.7E-08	38%	0.64	0.40	0.42	0.90	0.60	0.71	0.6	0.1	0.4	1.1	0.2	0.7	-0.7	
SucC	Succinyl-CoA synthetase subunit beta	P0A838	41652	5.37	256	2.1E-21	55%	0.56	0.52	0.28	0.79	0.29	0.70	1.0	0.9	1.0	1.5	1.3	1.4	-0.1	
SucD	Succinyl-CoA ligase [ADP-forming] subunit alpha	P0AGE9	29913	6.31	152	5.3E-11	60%	0.47	0.42	0.17	0.61	0.25	0.61	1.5	0.9	1.2	1.8	1.3	1.6	-0.2	
SdhA	Succinate dehydrogenase flavoprotein subunit	P0AC43	65008	5.85	108	1.3E-06	27%	0.60	0.37	0.24	0.62	0.26	0.63	1.3	1.2	1.3	1.4	1.3	1.3	-0.7	

A-49

Suppl. Table 5.3.1 Proteome data of *E. coli* BL21 (DE3) growing in different media

Name ¹	Protein name ¹	Uniprot ID ¹	Molecular mass ² (Da)	Calculated pI value ²	Mascot score ²	Expect ²	Mascot seq. cover. ²	Defind medium		Complex medium				Log ₂ (DNB /TB)	Log ₂ (DNB /LB)	Log ₂ (defined/complex)	Log ₂ (stationary phase /exp. phase)				
								DNB medium		TB medium		LB medium					in TB medium	in LB medium	in complex media	in defined medium	
								exp. phase	stationary phase	exp. phase	stationary phase	exp. phase	stationary phase	At exp. phase							
								Whole Cell Protein Mass (WCPM) - %													
SdhB	Succinate dehydrogenase and fumarate reductase iron-sulfur protein	Q8X9A8	27335	6.81	102	5.3E-06	34%	0.15	0.13	0.07	0.16	0.10	0.18	1.1	0.6	0.8	1.2	0.8	1.0	-0.2	
FumA	Fumarate hydratase (fumarase A), aerobic Class I	P0AC33	60774	6.11	116	2.1E-07	26%	0.06	0.038	0.028	0.08	0.021	0.12	1.1	1.5	1.3	1.5	2.5	2.0	-0.7	
FumC	Fumarate hydratase (fumarase C), aerobic Class II	P05042	50856	6.12	127	1.7E-08	29%	0.14	0.10	0.05	0.13	0.06	0.26	1.5	1.2	1.4	1.4	2.1	1.7	-0.5	
Mdh	Malate dehydrogenase	P61891	32488	5.61	79	1.0E-03	50%	0.51	0.63	0.13	0.62	0.10	0.76	2.0	2.4	2.2	2.3	2.9	2.6	0.3	
GlcB	Malate synthase G	P37330	80780	5.79	222	1.4E-18	37%	0.05	0.07	0.08	0.043	0.07	0.17	-0.7	-0.5	-0.6	-0.9	1.3	0.2	0.5	
Connection between glycolysis and TCA cycle (4 proteins)								Total WCPM:	0.74	0.86	0.56	0.89	0.43	0.82	0.4	0.8	0.6	0.7	0.9	0.8	0.2
Ppc	Phosphoenolpyruvate carboxylase	Q8FB98	99470	5.52	93	3.9E-05	21%	0.43	0.50	0.29	0.22	0.28	0.21	0.6	0.6	0.6	-0.4	-0.4	-0.4	0.2	
PckA	Phosphoenolpyruvate carboxykinase	P22259	59891	5.46	133	4.2E-09	33%	0.15	0.25	0.14	0.54	0.07	0.45	0.1	1.1	0.6	1.9	2.7	2.3	0.7	
MaeB	Malate dehydrogenase (Oxaloacetate-decarboxylating) (NADP(+))	A8A2V3	82908	5.34	185	2.7E-14	46%	0.12	0.07	0.08	0.09	0.045	0.13	0.6	1.4	1.0	0.2	1.5	0.9	-0.8	
SfcA	NAD-dependent malic enzyme	A7ZLS1	63481	5.19	88	3.2E-05	24%	0.042	0.041	0.05	0.040	0.030	0.029	-0.3	0.5	0.1	-0.3	0.0	-0.2	0.0	
Oxidative phosphorylation (7 proteins)								Total WCPM:	2.54	2.50	2.25	2.72	2.74	2.41	0.2	-0.1	0.0	0.3	-0.2	0.0	0.0
AtpA	F0F1 ATP synthase subunit alpha	P0ABB2	55416	5.8	128	1.3E-08	33%	1.19	1.23	1.02	1.33	1.21	1.09	0.2	0.0	0.1	0.4	-0.2	0.1	0.0	
AtpD	F0F1 ATP synthase subunit beta	P0ABB6	50351	4.9	113	4.2E-07	48%	0.47	0.62	0.61	0.67	0.66	0.57	-0.4	-0.5	-0.4	0.1	-0.2	0.0	0.4	
AtpH	F0F1 ATP synthase subunit delta	P0ABA5	19434	4.94	81	6.8E-04	41%	0.06	0.10	0.07	0.06	0.08	0.06	-0.2	-0.4	-0.3	-0.2	-0.4	-0.3	0.7	
NuoF	NADH dehydrogenase I subunit F	Q8XCX1	49802	6.44	117	1.7E-07	33%	0.18	0.11	0.12	0.14	0.18	0.16	0.6	0.0	0.3	0.2	-0.2	0.0	-0.7	
NuoG	NADH dehydrogenase subunit G	A8A2F2	101129	5.83	200	8.4E-16	35%	0.33	0.23	0.20	0.27	0.32	0.26	0.7	0.0	0.4	0.4	-0.3	0.1	-0.5	

Suppl. Table 5.3.1 Proteome data of *E. coli* BL21 (DE3) growing in different media

Name ¹	Protein name ¹	Uniprot ID ¹	Molecular mass ² (Da)	Calculated pI value ²	Mascot score ²	Expect ²	Mascot seq. cover. ²	Defind medium		Complex medium				Log ₂ (DNB /TB)	Log ₂ (DNB /LB)	Log ₂ (defined/complex)	Log ₂ (stationary phase /exp. phase)			
								DNB medium		TB medium		LB medium					in TB medium	in LB medium	in complex media	in defined medium
								exp. phase	stationary phase	exp. phase	stationary phase	exp. phase	stationary phase	At exp. phase						
NuoC	Bifunctional NADH:ubiquinone oxidoreductase subunit C/D	Q0TFG0	68451	5.98	64	3.1E-02	16%	0.21	0.13	0.15	0.16	0.18	0.18	0.5	0.2	0.4	0.1	0.0	0.0	-0.7
NuoB	NADH-quinone oxidoreductase subunit B	C4ZUD0	25325	5.58	74	8.7E-04	36%	0.10	0.08	0.08	0.09	0.11	0.09	0.3	-0.1	0.1	0.2	-0.3	-0.1	-0.3
Amino acid biosynthesis and metabolism (68 proteins): Amino acid biosynthesis and amino acid degradation							Total WCPM:	18.08	18.27	5.95	8.60	6.09	10.03	1.6	1.6	1.6	0.5	0.7	0.6	0.0
Sub-group: Amino acid biosynthesis (57 proteins)							Total WCPM:	17.80	17.29	5.25	6.39	5.17	6.82	1.7	1.7	1.7	0.3	0.4	0.3	0.0
AroD	3-Dehydroquinate dehydratase	A8A0N9	27459	5.3	68	3.8E-03	44%	0.08	0.12	0.043	0.05	0.047	0.044	0.9	0.8	0.8	0.2	-0.1	0.1	0.6
AroB	3-Dehydroquinate synthase	C4ZUP4	39141	5.72	91	1.7E-05	37%	0.024	0.028	0.021	0.027	0.00	0.028	0.2	>5	>2.56	0.4	>5	>2.7	0.2
AroF	Phospho-2-dehydro-3-deoxyheptonate aldolase	Q3YYP3	39079	5.42	131	6.7E-09	35%	0.13	0.14	0.08	0.18	0.09	0.25	0.7	0.5	0.6	1.2	1.5	1.3	0.1
AroG	Phospho-2-dehydro-3-deoxyheptonate aldolase, Phe-sensitive	P0AB91	38385	6.14	131	1.8E-09	53%	0.26	0.17	0.08	0.11	0.09	0.14	1.7	1.5	1.6	0.5	0.6	0.5	-0.6
TrpD	Anthranilate synthase, component II	B3HP12	57176	6.26	157	1.7E-11	37%	0.13	0.10	0.002	0.002	0.002	0.038	6.0	6.0	6.0	0.0	4.2	2.1	-0.4
TrpE	Component I of anthranilate synthase	P00895	58142	5.32	138	1.3E-09	30%	0.22	0.13	0.045	0.00	0.06	0.022	2.3	1.9	2.1	<-5	-1.4	<-3.2	-0.8
TrpC	Anthranilate isomerase	C5W377	49774	5.43	191	6.7E-15	56%	0.11	0.10	0.11	0.11	0.11	0.07	0.0	0.0	0.0	0.0	-0.7	-0.3	-0.1
TrpA	Tryptophan synthase alpha chain	B7L492	28905	5.31	107	4.6E-07	38%	0.12	0.16	0.026	0.026	0.027	0.031	2.2	2.2	2.2	0.0	0.2	0.1	0.4
PheA	P-protein	P0A9J8	43312	6.21	154	9.1E-12	40%	0.08	0.05	0.037	0.028	0.046	0.028	1.1	0.8	1.0	-0.4	-0.7	-0.6	-0.7
TyrA	T-protein	P07023	42187	5.68	165	7.2E-13	47%	0.11	0.10	0.028	0.046	0.028	0.06	2.0	2.0	2.0	0.7	1.1	0.9	-0.1
AspC	Aspartate aminotransferase, PLP-dependent	P00509	43831	5.54	151	6.7E-11	46%	0.23	0.24	0.12	0.24	0.11	0.19	0.9	1.1	1.0	1.0	0.8	0.9	0.1
SerA	D-3-Phosphoglycerate dehydrogenase	P0A9T2	44376	5.92	100	8.3E-06	32%	0.81	0.75	0.16	0.20	0.19	0.59	2.3	2.1	2.2	0.3	1.6	1.0	-0.1
SerC	Phosphoserine aminotransferase	Q8FJB7	39974	5.36	169	1.1E-10	41%	0.46	0.43	0.18	0.16	0.17	0.22	1.4	1.4	1.4	-0.2	0.4	0.1	-0.1

A-51

Suppl. Table 5.3.1 Proteome data of *E. coli* BL21 (DE3) growing in different media

Name ¹	Protein name ¹	Uniprot ID ¹	Molecular mass ² (Da)	Calculated pI value ²	Mascot score ²	Expect ²	Mascot seq. cover. ²	Defind medium		Complex medium		Log ₂ (DNB /TB)	Log ₂ (DNB /LB)	Log ₂ (defined/complex)	Log ₂ (stationary phase /exp. phase)					
								DNB medium		TB medium					LB medium		in TB medium	in LB medium	in complex media	in defined medium
								Whole Cell Protein Mass (WCPM) - %						At exp. phase						
								exp. phase	stationary phase	exp. phase	stationary phase	exp. phase	stationary phase							
GdhA	Glutamate dehydrogenase, NADP-specific	P00370	48778	5.98	179	1.1E-13	52%	0.13	0.17	0.020	0.041	0.029	0.048	2.7	2.2	2.4	1.0	0.7	0.9	0.4
GlnA	Glutamine synthetase	P0A9C7	52099	5.26	70	2.1E-03	15%	0.57	0.86	0.25	0.24	0.20	0.23	1.2	1.5	1.3	-0.1	0.2	0.1	0.6
GltB	Glutamate synthase subunit alpha	A8A527	164335	6.15	111	6.7E-07	15%	0.09	0.10	0.002	0.002	0.002	0.002	5.5	5.5	5.5	0.0	0.0	0.0	0.2
HisG	ATP phosphoribosyltransferase	Q8X8T4	33615	5.59	104	9.1E-07	38%	0.14	0.11	0.11	0.08	0.08	0.09	0.3	0.8	0.6	-0.5	0.2	-0.1	-0.3
HisF	Imidazole glycerol phosphate synthase subunit hisF	C4ZSB4	28722	5.03	80	2.5E-04	38%	0.09	0.13	0.14	0.12	0.09	0.10	-0.6	0.0	-0.3	-0.2	0.2	0.0	0.5
HisC	Histidinol-phosphate aminotransferase	B7NQG9	39907	5	144	9.1E-11	51%	0.08	0.09	0.036	0.047	0.00	0.033	1.2	>5	>3.1	0.4	>5	>2.7	0.2
HisD	Histidinol dehydrogenase	A1ACN2	46939	5.13	125	2.7E-08	34%	0.038	0.040	0.029	0.026	0.00	0.014	0.4	>5	>2.7	-0.2	>5	>2.4	0.1
GlyA	Serine hydroxymethyltransferase	P0A825	45459	6.03	138	1.3E-09	42%	0.74	0.80	0.32	0.53	0.36	0.55	1.2	1.0	1.1	0.7	0.6	0.7	0.1
CysK	Cysteine synthase A	P0ABK5	34525	5.83	176	5.7E-14	60%	0.63	0.84	0.24	0.56	0.12	0.37	1.4	2.4	1.9	1.2	1.6	1.4	0.4
CysN	Sulfate adenylyltransferase, subunit 1	P23845	52640	4.98	120	8.4E-08	22%	0.10	0.042	0.022	0.00	0.019	0.00	2.2	2.4	2.3	<-5	<-5	<-5	-1.3
CysJ	Sulfite reductase subunit alpha	A8A3P5	66415	4.92	161	6.6E-12	33%	0.07	0.07	0.014	0.017	0.032	0.012	2.3	1.1	1.7	0.3	-1.4	-0.6	0.0
CysI	Sulfite reductase subunit beta	Q8X7U2	64262	7.27	79	9.9E-04	21%	0.07	0.030	0.00	0.00	0.00	0.00	>5	>5	>5	0.0	0.0	0.0	-1.2
LysC	Aspartokinase III	P08660	48787	5.03	237	1.7E-19	62%	0.05	0.08	0.015	0.022	0.00	0.00	1.7	>5	>3.4	0.6	0.0	0.3	0.7
Asd	Maltose-binding periplasmic protein	P0A9R0	43360	5.53	155	5.9E-12	42%	0.36	0.57	0.33	0.45	0.16	0.36	0.1	1.2	0.6	0.4	1.2	0.8	0.7
DapA	Dihydrodipicolinate synthase	A7ZPS4	31549	5.98	119	2.9E-08	42%	0.14	0.10	0.08	0.10	0.10	0.14	0.8	0.5	0.6	0.3	0.5	0.4	-0.5
DapD	2,3,4,5-Tetrahydropyridine-2-carboxylate N-succinyltransferase	P0A9D8	30045	5.56	169	1.0E-12	63%	0.30	0.34	0.20	0.16	0.16	0.15	0.6	0.9	0.7	-0.3	-0.1	-0.2	0.2
LysA	Diaminopimelate decarboxylase	P00861	46377	5.63	106	1.3E-05	45%	0.11	0.11	0.12	0.29	0.12	0.16	-0.1	-0.1	-0.1	1.3	0.4	0.8	0.0

Suppl. Table 5.3.1 Proteome data of *E. coli* BL21 (DE3) growing in different media

Name ¹	Protein name ¹	Uniprot ID ¹	Molecular mass ² (Da)	Calculated pI value ²	Mascot score ²	Expect ²	Mascot seq. cover. ²	Defind medium		Complex medium				Log ₂ (DNB /TB)	Log ₂ (DNB /LB)	Log ₂ (defined/ complex)	Log ₂ (stationary phase /exp. phase)			
								DNB medium		TB medium		LB medium					in TB medium	in LB medium	in complex media	in defined medium
								exp. phase	stationary phase	exp. phase	stationary phase	exp. phase	stationary phase	At exp. phase						
ThrB	Homoserine kinase	A7ZH92	34101	5.44	90	2.3E-05	34%	0.07	0.07	0.032	0.07	0.016	0.05	1.1	2.1	1.6	1.1	1.6	1.4	0.0
MetA	Homoserine O-succinyltransferase	C5A0V0	35819	5.06	106	5.7E-07	35%	0.05	0.07	0.024	0.00	0.00	0.048	1.1	>5	>3.1	<-5	>5	-	0.5
Meth	Methionine synthase	B3XC96	136639	4.97	291	6.7E-25	38%	0.07	0.06	0.027	0.030	0.028	0.014	1.4	1.3	1.3	0.2	-1.0	-0.4	-0.2
MetE	5-Methyltetrahydropteroylglutamate-homocysteine S-methyltransferase	B3XGD6	85074	5.61	107	1.7E-06	31%	3.38	3.65	0.08	0.22	0.12	0.10	5.4	4.8	5.1	1.5	-0.3	0.6	0.1
IlvA	Threonine dehydratase biosynthetic	P04968	56559	5.57	213	2.7E-16	48%	0.26	0.19	0.08	0.13	0.05	0.16	1.7	2.4	2.0	0.7	1.7	1.2	-0.5
IlvB	Acetolactate synthase I, large subunit	P08142	60915	5.3	85	2.4E-04	24%	0.10	0.049	0.00	0.044	0.010	0.05	>5	3.3	>4.1	>5	2.3	>3.7	-1.0
IlvC	Ketol-acid reductoisomerase, NAD(P)-binding	P05793	54376	5.2	233	4.2E-19	54%	2.69	2.79	0.17	0.19	0.14	0.08	4.0	4.3	4.1	0.2	-0.8	-0.3	0.1
IlvD	Dihydroxyacid dehydratase	P05791	66174	5.59	235	2.6E-19	41%	0.55	0.35	0.09	0.07	0.06	0.06	2.6	3.2	2.9	-0.4	0.0	-0.2	-0.7
IlvE	Chain A, Branched-Chain Amino Acid Aminotransferase	P0AB80	34112	5.54	108	1.3E-06	44%	0.51	0.40	0.06	0.14	0.044	0.20	3.1	3.5	3.3	1.2	2.2	1.7	-0.4
IlvI	Acetolactate synthase isozyme 3 large subunit	P00893	63286	5.88	81	4.3E-03	25%	0.06	0.042	0.043	0.027	0.044	0.06	0.5	0.4	0.5	-0.7	0.4	-0.1	-0.5
LeuA	2-Isopropylmalate synthase	P09151	57604	5.47	98	1.4E-05	22%	0.08	0.09	0.00	0.00	0.00	0.00	>5	>5	>5	0.0	0.0	0.0	0.2
LeuB	3-Isopropylmalate dehydrogenase	P30125	39834	5.14	72	5.6E-03	27%	0.14	0.16	0.16	0.13	0.09	0.11	-0.2	0.6	0.2	-0.3	0.3	0.0	0.2
LeuC	Isopropylmalate isomerase large subunit	A7ZW23	50377	5.9	162	5.3E-12	42%	0.19	0.13	0.00	0.00	0.00	0.020	>5	>5	>5	0.0	>5	>2.5	-0.5
LeuD	3-Isopropylmalate isomerase subunit	P30126	22587	5.16	128	1.3E-08	56%	0.08	0.05	0.00	0.00	0.00	0.00	>5	>5	>5	0.0	0.0	0.0	-0.7
AsnA	Aspartate--ammonia ligase	B1LL71	36770	5.55	89	1.1E-04	33%	0.06	0.11	0.023	0.07	0.041	0.14	1.4	0.5	1.0	1.6	1.8	1.7	0.9
AsnB	Asparagine synthase	B3ISY7	63075	5.55	84	3.4E-04	27%	0.09	0.12	0.036	0.05	0.042	0.08	1.3	1.1	1.2	0.5	0.9	0.7	0.4
CarA	Carbamoyl phosphate synthase small subunit	B7NHD6	41677	5.91	107	1.7E-06	39%	0.21	0.15	0.08	0.041	0.16	0.10	1.4	0.4	0.9	-1.0	-0.7	-0.8	-0.5

A-53

Suppl. Table 5.3.1 Proteome data of *E. coli* BL21 (DE3) growing in different media

Name ¹	Protein name ¹	Uniprot ID ¹	Molecular mass ² (Da)	Calculated pI value ²	Mascot score ²	Expect ²	Mascot seq. cover. ²	Defind medium		Complex medium				Log ₂ (DNB /TB)	Log ₂ (DNB /LB)	Log ₂ (defined/complex)	Log ₂ (stationary phase /exp. phase)				
								DNB medium		TB medium		LB medium					in TB medium	in LB medium	in complex media	in defined medium	
								exp. phase	stationary phase	exp. phase	stationary phase	exp. phase	stationary phase	At exp. phase							
								Whole Cell Protein Mass (WCPM) - %													
CarB	Carbamoyl phosphate synthase large subunit	B7MNN9	118633	5.22	103	4.2E-06	14%	0.47	0.35	0.15	0.12	0.32	0.18	1.6	0.6	1.1	-0.3	-0.8	-0.6	-0.4	
ArgC	N-Acetyl-gamma-glutamyl-phosphate reductase	B1LNR8	36328	5.58	105	2.7E-06	33%	0.08	0.08	0.040	0.035	0.05	0.046	1.0	0.7	0.8	-0.2	-0.1	-0.2	0.0	
ArgD	Acetylmithine/succinyldiaminopimelate aminotransferase	P18335	44081	5.79	141	6.6E-10	60%	0.29	0.32	0.18	0.19	0.18	0.17	0.7	0.7	0.7	0.1	-0.1	0.0	0.1	
ArgE	Acetylmithine deacetylase	C5A0C3	42777	5.54	99	3.0E-06	37%	0.06	0.041	0.07	0.05	0.047	0.08	-0.2	0.4	0.1	-0.5	0.8	0.1	-0.5	
ArgI	Ornithine carbamoyltransferase chain I	P04391	37112	5.46	93	1.2E-05	35%	0.05	0.07	0.033	0.022	0.039	0.040	0.6	0.4	0.5	-0.6	0.0	-0.3	0.5	
ArgG	Argininosuccinate synthase	B1XGY3	50038	5.23	143	2.6E-09	35%	0.26	0.29	0.12	0.09	0.17	0.13	1.1	0.6	0.9	-0.4	-0.4	-0.4	0.2	
ArgH	Argininosuccinate lyase	P11447	50686	5.11	128	1.3E-08	38%	0.13	0.17	0.15	0.11	0.20	0.10	-0.2	-0.6	-0.4	-0.4	-1.0	-0.7	0.4	
AspA	Aspartate ammonia-lyase	P0AC38	52950	5.19	135	7.2E-10	29%	0.35	0.33	0.24	0.52	0.28	0.54	0.5	0.3	0.4	1.1	0.9	1.0	-0.1	
ProA	Gamma-glutamyl phosphate reductase	B3XF57	45031	5.42	205	2.7E-16	52%	0.049	0.037	0.06	0.040	0.05	0.046	-0.3	0.0	-0.2	-0.6	-0.1	-0.4	-0.4	
IscS (Yfh)	Cysteine desulfurase	C4ZXA5	45232	5.94	127	4.6E-09	57%	0.38	0.12	0.44	0.14	0.55	0.25	-0.2	-0.5	-0.4	-1.7	-1.1	-1.4	-1.7	
Sub-group: Amino acid degradation (11 proteins)								Total WCPM:	0.90	0.98	0.70	2.21	0.92	3.20	0.4	0.0	0.2	1.7	1.8	1.7	0.1
DadX	Alanine racemase, catabolic	P29012	39048	6.56	60	2.6E-02	31%	0.042	0.044	0.029	0.038	0.031	0.05	0.5	0.4	0.5	0.4	0.7	0.5	0.1	
TnaA	Tryptophanase	B1LL35	53107	5.88	97	4.8E-06	20%	0.11	0.11	0.10	1.11	0.15	1.92	0.1	-0.4	-0.2	3.5	3.7	3.6	0.0	
MetF	5,10-Methylenetetrahydrofolate reductase	P0AEZ1	33253	6	169	1.0E-12	69%	0.11	0.11	0.00	0.041	0.00	0.031	>5	>5	>5	>5	>5	>5	0.0	
MetK	Chain A, S-Adenosylmethionine Synthetase	P0A817	42022	5.1	155	2.6E-11	61%	0.35	0.37	0.24	0.23	0.25	0.17	0.5	0.5	0.5	-0.1	-0.6	-0.3	0.1	
GcvT	Glycine cleavage system T protein	B2ND95	40251	5.36	88	1.3E-04	34%	0.10	0.08	0.00	0.00	0.00	0.00	>5	>5	>5	0.0	0.0	0.0	-0.3	
AstA	Arginine N-succinyltransferase	C4ZZA3	38831	6.02	172	1.4E-13	58%	0.024	0.038	0.00	0.00	0.00	0.10	>5	>5	>5	0.0	>5	>2.5	0.7	

Suppl. Table 5.3.1 Proteome data of *E. coli* BL21 (DE3) growing in different media

Name ¹	Protein name ¹	Uniprot ID ¹	Molecular mass ² (Da)	Calculated pI value ²	Mascot score ²	Expect ²	Mascot seq. cover. ²	Defind medium		Complex medium				Log ₂ (DNB /TB)	Log ₂ (DNB /LB)	Log ₂ (defined/complex)	Log ₂ (stationary phase /exp. phase)				
								DNB medium		TB medium		LB medium					in TB medium	in LB medium	in complex media	in defined medium	
								exp. phase	stationary phase	exp. phase	stationary phase	exp. phase	stationary phase	At exp. phase							
								Whole Cell Protein Mass (WCPM) - %													
AstB	N-Succinylarginine dihydrolase	C4ZZA1	49439	5.74	116	5.7E-08	41%	0.027	0.040	0.026	0.037	0.026	0.09	0.1	0.1	0.1	0.5	1.8	1.2	0.6	
AstD	N-Succinylglutamate 5-semialdehyde dehydrogenase	C4ZZA2	53278	5.69	85	6.8E-05	29%	0.010	0.017	0.038	0.040	0.044	0.12	-1.9	-2.1	-2.0	0.1	1.4	0.8	0.8	
Tdh	L-threonine 3-dehydrogenase	C4ZXK8	37557	5.94	126	5.7E-09	56%	0.00	0.033	0.00	0.18	0.11	0.16	0.0	<-5	<-2.5	>5	0.5	>2.8	>5	
Kbl	2-Amino-3-ketobutyrate coenzyme A ligase	A8A682	43360	5.74	132	5.3E-09	45%	0.11	0.13	0.20	0.42	0.25	0.46	-0.9	-1.2	-1.0	1.1	0.9	1.0	0.2	
PutA	Bifunctional protein putA	P09546	144467	5.69	148	3.6E-11	13%	0.020	0.011	0.07	0.11	0.06	0.10	-1.8	-1.6	-1.7	0.7	0.7	0.7	-0.9	
IMP biosynthesis (for nucleotide) (7 proteins)								Total WCPM:	1.19	1.36	0.41	0.51	0.39	0.61	1.5	1.6	1.6	0.3	0.6	0.5	0.2
PurF	Amidophosphoribosyltransferase	P0AG16	56852	5.33	82	4.7E-04	22%	0.06	0.031	0.025	0.024	0.014	0.016	1.3	2.1	1.7	-0.1	0.2	0.1	-1.0	
PurD	Phosphoribosylamine--glycine ligase	A7ZUM2	46326	4.89	80	8.9E-04	36%	0.15	0.24	0.07	0.11	0.06	0.07	1.1	1.3	1.2	0.7	0.2	0.4	0.7	
PurT	Phosphoribosylglycinamide formyltransferase 2	C4ZZK6	42692	5.48	178	3.6E-14	46%	0.09	0.11	0.05	0.22	0.00	0.20	0.8	>5	>3	2.1	>5	>3.6	0.3	
PurL	Phosphoribosylformyl-glycineamide synthetase	B3Y153	142036	5.23	149	1.0E-10	24%	0.34	0.36	0.022	0.015	0.06	0.11	3.9	2.5	3.2	-0.6	0.9	0.2	0.1	
PurC	Phosphoribosylaminoimidazole-succinocarboxamide synthase	A7ZPS1	27149	5.07	136	5.7E-10	51%	0.09	0.20	0.023	0.034	0.034	0.07	2.0	1.4	1.7	0.6	1.0	0.8	1.2	
PurB	Adenylosuccinate lyase	Q8X737	51652	5.68	173	4.2E-13	45%	0.16	0.12	0.11	0.08	0.14	0.08	0.5	0.2	0.4	-0.5	-0.8	-0.6	-0.4	
PurH	Bifunctional purine biosynthesis protein PurH	Q1R5X1	57747	5.53	81	6.4E-04	19%	0.30	0.30	0.11	0.026	0.08	0.06	1.4	1.9	1.7	-2.1	-0.4	-1.2	0.0	
Nucleotide biosynthesis (start from IMP) (13 proteins)								Total WCPM:	1.66	1.74	2.83	2.05	2.46	1.91	-0.8	-0.6	-0.7	-0.5	-0.4	-0.4	0.1
PurA	Adenylosuccinate synthetase	A7ZV47	47543	5.31	227	3.7E-19	65%	0.33	0.39	0.43	0.38	0.46	0.29	-0.4	-0.5	-0.4	-0.2	-0.7	-0.4	0.2	
GuaA	GMP synthetase (glutamine aminotransferase)	P04079	59041	5.24	178	1.3E-13	41%	0.15	0.19	0.19	0.10	0.16	0.08	-0.3	-0.1	-0.2	-0.9	-1.0	-1.0	0.3	

A-55

Suppl. Table 5.3.1 Proteome data of *E. coli* BL21 (DE3) growing in different media

Name ¹	Protein name ¹	Uniprot ID ¹	Molecular mass ² (Da)	Calculated pI value ²	Mascot score ²	Expect ²	Mascot seq. cover. ²	Defind medium		Complex medium				Log ₂ (DNB /TB)	Log ₂ (DNB /LB)	Log ₂ (defined/complex)	Log ₂ (stationary phase /exp. phase)				
								DNB medium		TB medium		LB medium					in TB medium	in LB medium	in complex media	in defined medium	
								exp. phase	stationary phase	exp. phase	stationary phase	exp. phase	stationary phase	At exp. phase							
Whole Cell Protein Mass (WCPM) - %																					
GuaB	Inositol-5-monophosphate dehydrogenase	P0ADG8	52275	6.02	94	3.7E-05	35%	0.17	0.13	0.25	0.12	0.25	0.08	-0.6	-0.6	-0.6	-1.1	-1.6	-1.4	-0.4	
Add	Adenosine deaminase	C4ZY85	36603	5.36	72	1.6E-03	40%	0.038	0.039	0.045	0.030	0.031	0.035	-0.2	0.3	0.0	-0.6	0.2	-0.2	0.0	
DeoB	Phosphopentomutase	C4ZT65	44684	5.11	158	3.6E-12	44%	0.05	0.08	0.13	0.10	0.07	0.06	-1.4	-0.5	-0.9	-0.4	-0.2	-0.3	0.7	
DeoD	Chain A, Purine Nucleoside Phosphorylase	P0ABP8	26030	5.42	130	8.3E-09	62%	0.06	0.07	0.36	0.19	0.31	0.15	-2.6	-2.4	-2.5	-0.9	-1.0	-1.0	0.2	
Hpt	Hypoxanthine phosphoribosyltransferase	B1LGS6	20315	5.09	76	2.0E-03	56%	0.14	0.20	0.23	0.23	0.21	0.24	-0.7	-0.6	-0.7	0.0	0.2	0.1	0.5	
Apt	Adenine phosphoribosyltransferase	P69503	19847	5.26	71	6.5E-03	52%	0.09	0.09	0.12	0.07	0.14	0.08	-0.4	-0.6	-0.5	-0.8	-0.8	-0.8	0.0	
Udp	Uridine phosphorylase	Q8X8L3	27304	5.71	81	6.8E-04	54%	0.10	0.11	0.32	0.32	0.21	0.21	-1.7	-1.1	-1.4	0.0	0.0	0.0	0.1	
PyrG	CTP synthase	A7ZQM3	60792	5.63	74	1.0E-03	15%	0.24	0.21	0.50	0.33	0.43	0.32	-1.1	-0.8	-1.0	-0.6	-0.4	-0.5	-0.2	
Tmk	Thymidylate kinase	A7ZKK1	23768	5.33	65	7.6E-03	48%	0.05	0.05	0.11	0.047	0.06	0.07	-1.1	-0.3	-0.7	-1.2	0.2	-0.5	0.0	
Ndk	Nucleoside diphosphate kinase	C4ZX93	15511	5.54	120	2.3E-08	62%	0.14	0.14	0.11	0.08	0.08	0.24	0.3	0.8	0.6	-0.5	1.6	0.6	0.0	
Amn	AMP nucleosidase	P0AE13	54246	5.9	104	3.4E-06	35%	0.10	0.043	0.034	0.05	0.049	0.05	1.6	1.0	1.3	0.6	0.0	0.3	-1.2	
Fatty acid biosynthesis (7 proteins)								Total WCPM:	1.21	0.96	1.72	1.14	2.05	1.12	-0.5	-0.8	-0.6	-0.6	-0.9	-0.7	-0.3
AccA	Acetyl-coenzyme A carboxylase carboxyl transferase subunit alpha	A7ZHS5	35333	5.76	212	1.4E-17	57%	0.08	0.07	0.12	0.08	0.17	0.09	-0.6	-1.1	-0.8	-0.6	-0.9	-0.8	-0.2	
AccC	Acetyl-CoA carboxylase, biotin carboxylase subunit	P24182	49745	6.65	210	8.5E-17	43%	0.14	0.09	0.23	0.09	0.22	0.10	-0.7	-0.7	-0.7	-1.4	-1.1	-1.2	-0.6	
FabH	3-Oxoacyl-[acyl-carrier-protein] synthase 3	P0A6R0	33779	5.08	63	1.0E-02	19%	0.039	0.031	0.08	0.035	0.07	0.036	-1.0	-0.8	-0.9	-1.2	-1.0	-1.1	-0.3	
FabB	3-Oxoacyl-[acyl-carrier-protein] synthase I	P0A953	42928	5.35	259	1.1E-21	64%	0.21	0.14	0.32	0.25	0.45	0.25	-0.6	-1.1	-0.9	-0.4	-0.8	-0.6	-0.6	
FabF	3-Oxoacyl-(acyl carrier protein) synthase II	P0AAI7	43247	5.71	222	5.3E-18	71%	0.29	0.25	0.47	0.35	0.46	0.31	-0.7	-0.7	-0.7	-0.4	-0.6	-0.5	-0.2	

Suppl. Table 5.3.1 Proteome data of *E. coli* BL21 (DE3) growing in different media

Name ¹	Protein name ¹	Uniprot ID ¹	Molecular mass ² (Da)	Calculated pI value ²	Mascot score ²	Expect ²	Mascot seq. cover. ²	Defind medium		Complex medium				Log ₂ (DNB /TB)	Log ₂ (DNB /LB)	Log ₂ (defined/complex)	Log ₂ (stationary phase /exp. phase)							
								DNB medium		TB medium		LB medium					in TB medium	in LB medium	in complex media	in defined medium				
								exp. phase	stationary phase	exp. phase	stationary phase	exp. phase	stationary phase	At exp. phase										
FabI	Enoyl-[acyl-carrier-protein] reductase [NADH] FabI	P0AEK4	28074	5.58	117	4.6E-08	51%	0.30	0.27	0.35	0.25	0.34	0.26	-0.2	-0.2	-0.2	-0.5	-0.4	-0.4	-0.2				
FabZ	(3R)-Hydroxymyristoyl-[acyl-carrier-protein] dehydratase	A7ZHS0	17136	6.84	71	4.5E-02	25%	0.15	0.11	0.15	0.08	0.34	0.07	0.0	-1.2	-0.6	-0.9	-2.3	-1.6	-0.4				
Lipopolysaccharide biosynthesis (10 proteins)								Total WCPM:				0.81	0.88	1.22	1.24	0.93	0.91	-0.6	-0.2	-0.4	0.0	0.0	0.0	0.1
GmhA	Phosphoheptose isomerase	C2DM95	21686	5.97	142	5.3E-10	63%	0.048	0.05	0.045	0.09	0.042	0.08	0.1	0.2	0.1	1.0	0.9	1.0	0.1				
HldE	Bifunctional protein hldE	Q8FDH5	51232	5.29	122	5.3E-08	31%	0.045	0.048	0.06	0.06	0.06	0.06	-0.4	-0.4	-0.4	0.0	0.0	0.0	0.1				
HldD	ADP-L-glycero-D-manno-heptose-6-epimerase	C4ZXL1	34985	4.8	83	1.2E-04	41%	0.15	0.25	0.17	0.21	0.09	0.16	-0.2	0.7	0.3	0.3	0.8	0.6	0.7				
LpxA	Acyl-[acyl-carrier-protein]-UDP-N-acetylglucosamine O-acyltransferase	C4ZRS3	28348	6.63	58	3.8E-02	32%	0.07	0.06	0.05	0.047	0.06	0.034	0.5	0.2	0.4	-0.1	-0.8	-0.5	-0.2				
ArnA	Bifunctional polymyxin resistance protein ArnA	P77398	74869	6.39	185	2.7E-14	39%	0.06	0.028	0.05	0.05	0.08	0.030	0.3	-0.4	-0.1	0.0	-1.4	-0.7	-1.1				
GlmS	Glucosamine--fructose-6-phosphate aminotransferase [isomerizing]	P17169	67081	5.56	220	2.3E-18	38%	0.20	0.18	0.50	0.44	0.34	0.26	-1.3	-0.8	-1.0	-0.2	-0.4	-0.3	-0.2				
GlmM	Phosphoglucosamine mutase	P31120	47799	5.71	140	8.5E-10	36%	0.046	0.037	0.07	0.11	0.06	0.09	-0.6	-0.4	-0.5	0.7	0.6	0.6	-0.3				
GlmU	Bifunctional protein GlmU	P0ACC8	49384	6.2	116	2.1E-07	30%	0.05	0.040	0.07	0.048	0.07	0.031	-0.5	-0.5	-0.5	-0.5	-1.2	-0.9	-0.3				
RmlA	Glucose-1-phosphate thymidyltransferase	P55253	32703	5.27	114	9.1E-08	48%	0.049	0.06	0.08	0.05	0.046	0.06	-0.7	0.1	-0.3	-0.7	0.4	-0.1	0.3				
RfbB	dTDP-glucose 4,6-dehydratase	P55293	40787	5.09	122	1.4E-08	44%	0.09	0.13	0.12	0.13	0.08	0.10	-0.4	0.2	-0.1	0.1	0.3	0.2	0.5				
Synthesis of other cellular components (16 proteins)								Total WCPM:				0.98	0.96	1.06	0.99	0.87	0.93	-0.1	0.2	0.0	-0.1	0.1	0.0	0.0
HemB	Delta-aminolevulinic acid dehydratase	B2NAC8	35962	5.25	95	2.4E-05	31%	0.07	0.13	0.12	0.13	0.13	0.07	-0.8	-0.9	-0.8	0.1	-0.9	-0.4	0.9				
HemL	Glutamate-1-semialdehyde 2,1-aminomutase	C4ZRP7	45907	4.73	127	4.6E-09	36%	0.05	0.05	0.07	0.06	0.05	0.041	-0.5	0.0	-0.2	-0.2	-0.3	-0.3	0.0				

A-57

Suppl. Table 5.3.1 Proteome data of *E. coli* BL21 (DE3) growing in different media

Name ¹	Protein name ¹	Uniprot ID ¹	Molecular mass ² (Da)	Calculated pI value ²	Mascot score ²	Expect ²	Mascot seq. cover. ²	Defind medium		Complex medium				Log ₂ (DNB /TB)	Log ₂ (DNB /LB)	Log ₂ (defined/complex)	Log ₂ (stationary phase /exp. phase)				
								DNB medium		TB medium		LB medium					in TB medium	in LB medium	in complex media	in defined medium	
								exp. phase	stationary phase	exp. phase	stationary phase	exp. phase	stationary phase	At exp. phase							
IspG	4-Hydroxy-3-methylbut-2-en-1-yl diphosphate synthase	A7ZPV8	40943	5.87	146	5.7E-11	44%	0.08	0.06	0.11	0.09	0.11	0.06	-0.5	-0.5	-0.5	-0.3	-0.9	-0.6	-0.4	
IspE	4-Diphosphocytidyl-2-C-methyl-D-erythritol kinase	Q8FI04	31182	5.13	69	2.9E-03	33%	0.05	0.09	0.09	0.08	0.05	0.08	-0.8	0.0	-0.4	-0.2	0.7	0.3	0.8	
Mpl	UDP-N-acetylmuramate:L-alanyl-gamma-D-glutamyl-meso-diaminopimelate ligase	P37773	50298	5.53	64	8.3E-03	28%	0.034	0.030	0.047	0.05	0.039	0.041	-0.5	-0.2	-0.3	0.1	0.1	0.1	-0.2	
GshB	Glutathione synthetase	P04425	35766	5.11	154	9.1E-12	47%	0.05	0.06	0.09	0.11	0.07	0.07	-0.8	-0.5	-0.7	0.3	0.0	0.1	0.3	
MdoG	Glucan biosynthesis protein, periplasmic	P33136	57876	6.7	89	1.0E-04	22%	0.09	0.07	0.09	0.07	0.09	0.07	0.0	0.0	0.0	-0.4	-0.4	-0.4	-0.4	
SpeA	Biosynthetic arginine decarboxylase	P21170	74308	4.83	76	5.5E-04	16%	0.08	0.06	0.11	0.08	0.07	0.09	-0.5	0.2	-0.1	-0.5	0.4	0.0	-0.4	
SpeE	Spermidine synthase	B1XC96	32643	5.33	87	4.3E-05	38%	0.06	0.07	0.043	0.040	0.034	0.06	0.5	0.8	0.7	-0.1	0.8	0.4	0.2	
LuxS	S-ribosylhomocysteine lyase	C4ZYT7	19575	5.18	77	4.4E-04	54%	0.046	0.08	0.05	0.06	0.041	0.09	-0.1	0.2	0.0	0.3	1.1	0.7	0.8	
NadE	NH(3)-dependent NAD(+) synthetase	B1XGK1	30789	5.41	63	1.0E-02	39%	0.06	0.06	0.06	0.06	0.036	0.048	0.0	0.7	0.4	0.0	0.4	0.2	0.0	
PanB	3-Methyl-2-oxobutanoate hydroxymethyltransferase	A7ZHM4	28389	5.16	63	1.1E-02	26%	0.034	0.037	0.034	0.037	0.030	0.06	0.0	0.2	0.1	0.1	1.0	0.6	0.1	
PanC	Pantothenate synthetase	C4ZRM6	31692	5.91	109	2.9E-07	42%	0.06	0.06	0.048	0.07	0.049	0.06	0.3	0.3	0.3	0.5	0.3	0.4	0.0	
ThiC	Phosphomethylpyrimidine synthase	B7NRS7	71320	5.66	66	6.3E-03	11%	0.14	0.06	0.07	0.014	0.049	0.014	1.0	1.5	1.3	-2.3	-1.8	-2.1	-1.2	
GlgB	1,4-Alpha-glucan branching enzyme	P07762	84398	5.91	71	7.0E-03	19%	0.041	0.029	0.012	0.017	0.019	0.044	1.8	1.1	1.4	0.5	1.2	0.9	-0.5	
OtsA	Alpha, alpha-trehalose-phosphate synthase [UDP-forming]	B1X658	53749	6.37	91	1.7E-05	35%	0.039	0.015	0.016	0.020	0.00	0.034	1.3	>5	>3.1	0.3	>5	>2.6	-1.4	
(Metabolite) degradation (19 proteins)								Total WCPM:	1.48	1.44	1.32	3.97	1.27	2.61	0.2	0.2	0.2	1.6	1.0	1.3	0.0
MalP	Maltodextrin phosphorylase	P00490	90865	6.94	118	3.6E-08	20%	0.06	0.030	0.17	0.08	0.14	0.046	-1.5	-1.2	-1.4	-1.1	-1.6	-1.3	-1.0	
MalQ	4-Alpha-glucanotransferase	P15977	79080	6.14	123	1.1E-08	28%	0.019	0.025	0.17	0.07	0.15	0.020	-3.2	-3.0	-3.1	-1.3	-2.9	-2.1	0.4	

Suppl. Table 5.3.1 Proteome data of *E. coli* BL21 (DE3) growing in different media

Name ¹	Protein name ¹	Uniprot ID ¹	Molecular mass ² (Da)	Calculated pI value ²	Mascot score ²	Expect ²	Mascot seq. cover. ²	Defind medium		Complex medium				Log ₂ (DNB /TB)	Log ₂ (DNB /LB)	Log ₂ (defined/ complex)	Log ₂ (stationary phase /exp. phase)			
								DNB medium		TB medium		LB medium					in TB medium	in LB medium	in complex media	in defined medium
								exp. phase	stationary phase	exp. phase	stationary phase	exp. phase	stationary phase	At exp. phase						
Pgm	Phosphoglucomutase	P36938	58610	5.43	75	7.8E-04	19%	0.20	0.11	0.11	0.14	0.10	0.10	0.9	1.0	0.9	0.3	0.0	0.2	-0.9
BglX	Periplasmic beta-glucosidase precursor	Q8CVX0	83562	5.85	113	4.2E-07	27%	0.08	0.035	0.07	0.08	0.06	0.049	0.2	0.4	0.3	0.2	-0.3	0.0	-1.2
GatZ	D-Tagatose-1,6-bisphosphate aldolase subunit gatZ	B3X944	47440	5.52	74	3.8E-03	33%	0.39	0.52	0.16	1.80	0.21	0.76	1.3	0.9	1.1	3.5	1.9	2.7	0.4
GatD	Galactitol-1-phosphate 5-dehydrogenase	P0A9S3	37822	5.94	61	2.0E-02	17%	0.21	0.17	0.08	0.65	0.08	0.40	1.4	1.4	1.4	3.0	2.3	2.7	-0.3
XylA	Xylose isomerase	C4ZXF6	49939	5.75	63	1.2E-02	24%	0.025	0.030	0.038	0.00	0.00	0.024	-0.6	>5	-	<-5	>5	-	0.3
TreA	Periplasmic trehalase	C4ZTN8	63825	5.6	213	1.1E-17	46%	0.06	0.046	0.035	0.038	0.025	0.08	0.8	1.3	1.0	0.1	1.7	0.9	-0.4
TreC	Trehalose-6-phosphate hydrolase	P28904	64082	5.51	122	1.4E-08	25%	0.06	0.036	0.15	0.09	0.17	0.08	-1.3	-1.5	-1.4	-0.7	-1.1	-0.9	-0.7
MelA	Alpha-galactosidase	P06720	51309	5.52	109	2.9E-07	23%	0.07	0.07	0.05	0.62	0.06	0.16	0.5	0.2	0.4	3.6	1.4	2.5	0.0
GabT	4-Aminobutyrate aminotransferase GabT	P22256	46202	5.78	227	4.6E-19	67%	0.00	0.06	0.013	0.028	0.00	0.15	<-5	0.0	<-2.5	1.1	>5	>3.1	>5
GabD	Succinate-semialdehyde dehydrogenase [NADP+] GabD	P25526	52030	5.44	125	7.2E-09	28%	0.10	0.06	0.09	0.11	0.09	0.17	0.2	0.2	0.2	0.3	0.9	0.6	-0.7
Prr	Gamma-aminobutyraldehyde dehydrogenase	C4ZVI3	51197	5.65	80	2.1E-04	41%	0.06	0.07	0.036	0.041	0.025	0.18	0.7	1.3	1.0	0.2	2.8	1.5	0.2
UidA	Beta-glucuronidase	P05804	68917	5.24	80	2.3E-04	21%	0.05	0.035	0.046	0.040	0.043	0.036	0.1	0.2	0.2	-0.2	-0.3	-0.2	-0.5
CpdB	2',3'-Cyclic-nucleotide 2'-phosphodiesterase/3'-nucleotidase	P08331	70902	5.45	114	9.1E-08	34%	0.024	0.026	0.028	0.05	0.024	0.044	-0.2	0.0	-0.1	0.8	0.9	0.9	0.1
DkgA	2,5-Diketo-D-gluconic acid reductase A	Q46857	31147	6	151	1.8E-11	53%	0.043	0.07	0.042	0.07	0.027	0.11	0.0	0.7	0.4	0.7	2.0	1.4	0.7
NanA	N-Acetylneuraminate lyase	C4ZSW3	32801	5.61	119	2.9E-08	36%	0.00	0.00	0.00	0.025	0.043	0.045	0.0	<-5	<-2.5	>5	0.1	>2.5	0.0
FadB	Multifunctional fatty acid oxidation complex subunit alpha	Q0TAL0	79829	6.01	136	2.1E-09	26%	0.016	0.034	0.011	0.022	0.00	0.13	0.5	>5	>2.8	1.0	>5	>3	1.1
FadH	2,4-Dienoyl-CoA reductase [NADPH]	P42593	73203	6.11	89	3.2E-05	9%	0.010	0.014	0.020	0.018	0.026	0.028	-1.0	-1.4	-1.2	-0.2	0.1	0.0	0.5

A-59

Suppl. Table 5.3.1 Proteome data of *E. coli* BL21 (DE3) growing in different media

Name ¹	Protein name ¹	Uniprot ID ¹	Molecular mass ² (Da)	Calculated pI value ²	Mascot score ²	Expect ²	Mascot seq. cover. ²	Defind medium		Complex medium				Log ₂ (DNB /TB)	Log ₂ (DNB /LB)	Log ₂ (defined/complex)	Log ₂ (stationary phase /exp. phase)			
								DNB medium		TB medium		LB medium					in TB medium	in LB medium	in complex media	in defined medium
								exp. phase	stationary phase	exp. phase	stationary phase	exp. phase	stationary phase	At exp. phase						
Sugar transport (7 proteins)							Total WCPM:	1.02	1.60	0.92	1.30	0.81	1.38	0.1	0.3	0.2	0.5	0.8	0.6	0.6
PtsI	Phosphoenolpyruvate-protein phosphotransferase	Q8XBL3	63722	4.78	109	1.0E-06	28%	0.40	0.44	0.30	0.17	0.25	0.17	0.4	0.7	0.5	-0.8	-0.6	-0.7	0.1
PtsH	Phosphocarrier protein HPr	P0AA06	9114	5.65	123	4.2E-08	90%	0.19	0.29	0.07	0.23	0.15	0.19	1.4	0.3	0.9	1.7	0.3	1.0	0.6
Crr	Glucose-specific enzyme IIA component of PTS	P69783	18240	4.73	104	3.6E-04	74%	0.11	0.32	0.09	0.16	0.10	0.29	0.3	0.1	0.2	0.8	1.5	1.2	1.5
ManX	PTS system mannose-specific EIIBAB component	P69797	35026	5.74	143	1.1E-10	42%	0.21	0.30	0.10	0.15	0.09	0.16	1.1	1.2	1.1	0.6	0.8	0.7	0.5
MalE	Maltose-binding periplasmic protein	P0AEX9	43360	5.53	65	6.9E-03	16%	0.032	0.18	0.08	0.43	0.022	0.25	-1.3	0.5	-0.4	2.4	3.5	3.0	2.5
MalK	Maltose/maltodextrin import ATP-binding protein MalK	P68188	41136	6.23	88	8.0E-04	33%	0.036	0.022	0.08	0.031	0.045	0.037	-1.2	-0.3	-0.7	-1.4	-0.3	-0.8	-0.7
LamB	Chain A, Maltoporin Maltose Complex	P02943	47469	4.72	97	1.7E-05	35%	0.043	0.05	0.20	0.13	0.15	0.28	-2.2	-1.8	-2.0	-0.6	0.9	0.1	0.2
Amino acid and peptide transport (7 proteins)							Total WCPM:	0.72	1.26	0.43	0.58	0.28	1.12	0.7	1.4	1.1	0.4	2.0	1.2	0.8
GlnH	Glutamine ABC transporter periplasmic protein	P0AEQ5	27173	8.44	75	2.8E-03	48%	0.20	0.12	0.09	0.08	0.12	0.07	1.2	0.7	0.9	-0.2	-0.8	-0.5	-0.7
ArtJ	Arginine transporter subunit	P30860	26927	6.84	90	8.1E-05	38%	0.030	0.05	0.11	0.027	0.00	0.044	-1.9	>5	-	-2.0	>5	-	0.7
ArgT	Lysine-arginine-ornithine-binding periplasmic protein	P09551	28088	5.62	94	8.5E-06	51%	0.045	0.13	0.047	0.07	0.031	0.10	-0.1	0.5	0.2	0.6	1.7	1.1	1.5
LivJ	Leucine/isoleucine/valine transporter subunit	P0AD96	39223	5.54	131	6.6E-09	55%	0.11	0.34	0.028	0.09	0.027	0.11	2.0	2.0	2.0	1.7	2.0	1.9	1.6
DppA	Chain A, Dipeptide Binding Protein Complex With Glycyl-L-Leucine	P23847	57599	5.75	116	2.1E-07	42%	0.13	0.28	0.00	0.00	0.00	0.29	>5	>5	>5	0.0	>5	>2.5	1.1
OppA	Periplasmic oligopeptide-binding protein	P23843	60975	6.05	138	3.0E-10	51%	0.16	0.29	0.15	0.31	0.10	0.47	0.1	0.7	0.4	1.0	2.2	1.6	0.9
OppD	Oligopeptide transport ATP-binding protein OppD	P76027	37506	5.78	67	4.2E-03	41%	0.048	0.048	0.00	0.00	0.00	0.032	>5	>5	>5	0.0	>5	>2.5	0.0

Suppl. Table 5.3.1 Proteome data of *E. coli* BL21 (DE3) growing in different media

Name ¹	Protein name ¹	Uniprot ID ¹	Molecular mass ² (Da)	Calculated pI value ²	Mascot score ²	Expect ²	Mascot seq. cover. ²	Defined medium		Complex medium				Log ₂ (DNB /TB)	Log ₂ (DNB /LB)	Log ₂ (defined/complex)	Log ₂ (stationary phase /exp. phase)			
								DNB medium		TB medium		LB medium					in TB medium	in LB medium	in complex media	in defined medium
								exp. phase	stationary phase	exp. phase	stationary phase	exp. phase	stationary phase	Whole Cell Protein Mass (WCPM) - %			At exp. phase			
Other transport proteins (14 proteins)							Total WCPM:	4.51	7.10	4.81	4.54	5.42	5.19	-0.1	-0.3	-0.2	-0.1	-0.1	-0.1	0.7
CusB	Copper/silver efflux system, membrane fusion protein	P77239	44277	5.93	253	4.2E-21	62%	0.032	0.10	0.00	0.00	0.00	0.00	>5	>5	>5	0.0	0.0	0.0	1.6
GsiB	Glutathione ABC transporter, periplasmic glutathione-binding protein GsiB	B3IL13	56479	8.23	80	7.7E-04	22%	0.038	0.027	0.046	0.036	0.037	0.045	-0.3	0.0	-0.1	-0.4	0.3	0.0	-0.5
LptD	Exported protein required for envelope biosynthesis and integrity	P31554	89843	4.94	158	1.3E-11	27%	0.06	0.07	0.06	0.047	0.07	0.05	0.0	-0.2	-0.1	-0.4	-0.5	-0.4	0.2
FadL	Long-chain fatty acid transport protein	Q8XCN6	48509	5.19	84	7.1E-05	34%	0.019	0.032	0.042	0.021	0.033	0.11	-1.1	-0.8	-1.0	-1.0	1.7	0.4	0.8
OmpF	Outer membrane porin 1a (Ia;b;F)	P02931	39309	4.76	197	1.7E-15	69%	2.17	2.68	1.30	1.66	2.49	2.35	0.7	-0.2	0.3	0.4	-0.1	0.1	0.3
OmpA	Outer membrane protein A	P0A911	37292	5.99	133	9.4E-10	45%	1.00	2.37	1.13	1.02	0.85	1.05	-0.2	0.2	0.0	-0.1	0.3	0.1	1.2
OmpA (2)	Outer membrane protein A	ZP_03085789 ^(NCBI_3)	28830	5.98	114	9.2E-07	49%	0.51	1.01	0.77	0.89	0.67	0.76	-0.6	-0.4	-0.5	0.2	0.2	0.2	1.0
TolB	Translocation protein TolB	A7ZJC2	41502	6.22	100	8.5E-06	31%	0.05	0.14	0.07	0.07	0.06	0.19	-0.5	-0.3	-0.4	0.0	1.7	0.8	1.5
TolC	Outer membrane protein TolC	B3I0L1	53784	5.46	72	5.3E-03	20%	0.10	0.10	0.15	0.09	0.13	0.07	-0.6	-0.4	-0.5	-0.7	-0.9	-0.8	0.0
OmpX	Outer membrane protein X	P0A919	18648	6.56	110	8.3E-07	68%	0.25	0.26	0.69	0.29	0.57	0.19	-1.5	-1.2	-1.3	-1.3	-1.6	-1.4	0.1
YbiT	Putative ATP-binding component of a transport system	P0A9U5	59877	4.99	123	4.2E-08	31%	0.05	0.033	0.09	0.030	0.044	0.026	-0.8	0.2	-0.3	-1.6	-0.8	-1.2	-0.6
YjjK	Uncharacterized ABC transporter ATP-binding protein YjjK	P0A9W3	62518	5.43	118	3.6E-08	34%	0.07	0.07	0.14	0.14	0.12	0.17	-1.0	-0.8	-0.9	0.0	0.5	0.3	0.0
SecA	Preprotein translocase subunit, ATPase	P10408	102187	5.43	196	2.1E-15	36%	0.06	0.09	0.21	0.17	0.23	0.08	-1.8	-1.9	-1.9	-0.3	-1.5	-0.9	0.6
YaeT	Outer membrane protein assembly factor yaeT	A7ZHR7	90611	4.93	161	1.5E-12	26%	0.10	0.12	0.11	0.08	0.12	0.10	-0.1	-0.3	-0.2	-0.5	-0.3	-0.4	0.3
RNA polymerases (3 proteins)							Total WCPM:	1.16	1.02	1.47	0.76	1.65	0.73	-0.3	-0.5	-0.4	-1.0	-1.2	-1.1	-0.2
RpoA	DNA-directed RNA polymerase subunit alpha	P0A7Z6	36717	4.98	247	1.7E-20	69%	0.48	0.52	0.72	0.39	0.74	0.34	-0.6	-0.6	-0.6	-0.9	-1.1	-1.0	0.1

A-61

Suppl. Table 5.3.1 Proteome data of *E. coli* BL21 (DE3) growing in different media

Name ¹	Protein name ¹	Uniprot ID ¹	Molecular mass ² (Da)	Calculated pI value ²	Mascot score ²	Expect ²	Mascot seq. cover. ²	Defind medium		Complex medium				Log ₂ (DNB /TB)	Log ₂ (DNB /LB)	Log ₂ (defined/complex)	Log ₂ (stationary phase /exp. phase)				
								DNB medium		TB medium		LB medium					in TB medium	in LB medium	in complex media	in defined medium	
								exp. phase	stationary phase	exp. phase	stationary phase	exp. phase	stationary phase	At exp. phase							
								Whole Cell Protein Mass (WCPM) - %													
RpoB	DNA-directed RNA polymerase subunit beta	P0A8V4	150935	5.15	117	1.7E-07	18%	0.58	0.44	0.68	0.31	0.82	0.33	-0.2	-0.5	-0.4	-1.1	-1.3	-1.2	-0.4	
RpoC	DNA-directed RNA polymerase subunit beta'	P0A8T8	155918	6.67	74	3.4E-03	15%	0.10	0.06	0.07	0.06	0.09	0.06	0.5	0.2	0.3	-0.2	-0.6	-0.4	-0.7	
RNA polymerase binding proteins (7 proteins)								Total WCPM:	0.90	0.84	1.35	0.97	1.49	0.91	-0.6	-0.7	-0.7	-0.5	-0.7	-0.6	-0.1
RapA	RNA polymerase-associated protein rapA	A7ZHF0	110057	5.04	65	6.9E-03	12%	0.018	0.012	0.08	0.021	0.07	0.017	-2.2	-2.0	-2.1	-1.9	-2.0	-2.0	-0.6	
NusA	Transcription elongation protein nusA	P0AFF8	55008	4.53	77	4.8E-04	20%	0.12	0.10	0.18	0.08	0.20	0.09	-0.6	-0.7	-0.7	-1.2	-1.2	-1.2	-0.3	
NusG	Transcription antitermination protein NusG	P0AFG1	20518	6.34	92	5.4E-05	64%	0.07	0.07	0.09	0.045	0.13	0.06	-0.4	-0.9	-0.6	-1.0	-1.1	-1.1	0.0	
Rho	Transcription termination factor Rho	P0AG32	47032	6.75	166	5.7E-13	33%	0.45	0.34	0.70	0.48	0.84	0.42	-0.6	-0.9	-0.8	-0.5	-1.0	-0.8	-0.4	
RpoD	RNA polymerase sigma-subunit	Q59371	69157	4.87	97	1.6E-05	31%	0.06	0.07	0.10	0.06	0.07	0.07	-0.7	-0.2	-0.5	-0.7	0.0	-0.4	0.2	
SspA	Stringent starvation protein A	P0ACA3	24346	5.22	128	3.6E-09	58%	0.10	0.13	0.14	0.21	0.12	0.17	-0.5	-0.3	-0.4	0.6	0.5	0.5	0.4	
DksA	DnaK transcriptional regulator DksA	P0ABS3	17745	5.06	72	6.0E-03	64%	0.08	0.12	0.06	0.07	0.06	0.08	0.4	0.4	0.4	0.2	0.4	0.3	0.6	
Transcription factors (12 proteins)								Total WCPM:	1.73	1.66	1.75	1.51	2.01	2.12	0.0	-0.2	-0.1	-0.2	0.1	-0.1	-0.1
LacI	Lactose operon repressor	P03023	38737	6.39	58	4.1E-02	28%	0.043	0.035	0.16	0.07	0.18	0.037	-1.9	-2.1	-2.0	-1.2	-2.3	-1.7	-0.3	
Hns	Global DNA-binding transcriptional dual regulator H-NS	P0ACG0	15587	5.43	92	5.9E-05	62%	0.67	0.79	0.76	0.76	1.07	1.06	-0.2	-0.7	-0.4	0.0	0.0	0.0	0.2	
ArcA	Aerobic respiration control protein ArcA	P0A9Q1	27389	5.21	156	5.7E-12	46%	0.07	0.10	0.08	0.07	0.09	0.21	-0.2	-0.4	-0.3	-0.2	1.2	0.5	0.5	
KdgR	Transcriptional regulator kdgR	P76268	30067	5.43	164	9.1E-13	74%	0.033	0.035	0.035	0.027	0.038	0.040	-0.1	-0.2	-0.1	-0.4	0.1	-0.2	0.1	
OxyR	Hydrogen peroxide-inducible genes activator	P0ACQ4	34596	5.96	95	7.1E-06	34%	0.08	0.06	0.06	0.08	0.08	0.07	0.4	0.0	0.2	0.4	-0.2	0.1	-0.4	

Suppl. Table 5.3.1 Proteome data of *E. coli* BL21 (DE3) growing in different media

Name ¹	Protein name ¹	Uniprot ID ¹	Molecular mass ² (Da)	Calculated pI value ²	Mascot score ²	Expect ²	Mascot seq. cover. ²	Defind medium		Complex medium			Log ₂ (DNB /TB)	Log ₂ (DNB /LB)	Log ₂ (defined/complex)	Log ₂ (stationary phase /exp. phase)					
								DNB medium		TB medium		LB medium				in TB medium	in LB medium	in complex media	in defined medium		
								exp. phase	stationary phase	exp. phase	stationary phase	exp. phase	stationary phase	Whole Cell Protein Mass (WCPM) - %			At exp. phase				
BasR	Transcriptional regulatory protein BasR	P30843	25072	5.66	70	2.1E-03	31%	0.07	0.06	0.06	0.049	0.046	0.07	0.2	0.6	0.4	-0.3	0.6	0.2	-0.2	
CspC	CspC	Q1PG46	7497	8.09	56	2.2E-01	60%	0.36	0.22	0.30	0.19	0.27	0.36	0.3	0.4	0.3	-0.7	0.4	-0.1	-0.7	
StpA	DNA binding protein, nucleoid-associated	P0ACG2	15338	7.93	50	8.1E-01	33%	0.19	0.15	0.13	0.07	0.12	0.07	0.5	0.7	0.6	-0.9	-0.8	-0.8	-0.3	
PspA	Phage shock protein A	P0AFM6	25477	5.39	76	6.3E-04	57%	0.033	0.021	0.026	0.029	0.025	0.022	0.3	0.4	0.4	0.2	-0.2	0.0	-0.7	
OmpR	Transcriptional regulatory protein ompR	P0AA16	27393	6.04	132	1.4E-09	52%	0.08	0.08	0.07	0.06	0.05	0.11	0.2	0.7	0.4	-0.2	1.1	0.5	0.0	
CpxR	Transcriptional regulatory protein CpxR	P0AE88	26296	5.39	71	1.9E-03	38%	0.06	0.06	0.046	0.06	0.039	0.047	0.4	0.6	0.5	0.4	0.3	0.3	0.0	
PhoP	Transcriptional regulatory protein phoP	P23836	25519	5.1	123	1.1E-08	51%	0.041	0.047	0.026	0.049	0.00	0.028	0.7	>5	>2.8	0.9	>5	>2.9	0.2	
Ribosomal proteins (5 proteins)								Total WCPM:	2.82	2.67	5.10	2.45	5.73	2.25	-0.9	-1.0	-0.9	-1.1	-1.3	-1.2	-0.1
RplL	50S ribosomal protein L7/L12	P0A7K2	12069	4.6	70	7.8E-03	44%	0.67	0.77	0.74	0.46	1.09	0.55	-0.1	-0.7	-0.4	-0.7	-1.0	-0.8	0.2	
RplI	50S ribosomal protein L9	P0A7R3	15759	6.17	197	1.7E-15	81%	0.47	0.38	0.78	0.34	0.77	0.36	-0.7	-0.7	-0.7	-1.2	-1.1	-1.1	-0.3	
RpsA	30S ribosomal protein S1	P0AG69	61235	4.89	189	1.0E-14	35%	0.81	0.93	1.98	0.94	2.10	0.78	-1.3	-1.4	-1.3	-1.1	-1.4	-1.3	0.2	
RpsB	30S ribosomal protein S2	A7ZHQ9	26798	6.62	137	3.7E-10	74%	0.59	0.43	1.06	0.48	1.24	0.44	-0.8	-1.1	-1.0	-1.1	-1.5	-1.3	-0.5	
RpsF	30S ribosomal protein S6	A7ZV71	15177	5.26	61	1.7E-02	39%	0.28	0.16	0.54	0.23	0.53	0.12	-0.9	-0.9	-0.9	-1.2	-2.1	-1.7	-0.8	
Ribosome-associated proteins (8 proteins)								Total WCPM:	0.85	0.95	1.58	1.02	1.60	0.98	-0.9	-0.9	-0.9	-0.6	-0.7	-0.7	0.2
EngA	Predicted GTP-binding protein	P0A6P5	55058	5.6	150	8.4E-11	32%	0.042	0.010	0.039	0.028	0.028	0.031	0.1	0.6	0.3	-0.5	0.1	-0.2	-2.1	
YcaO	UPF0142 protein ycaO	P75838	66009	4.38	75	7.8E-04	13%	0.019	0.009	0.032	0.023	0.049	0.015	-0.8	-1.4	-1.1	-0.5	-1.7	-1.1	-1.1	

A-63

Suppl. Table 5.3.1 Proteome data of *E. coli* BL21 (DE3) growing in different media

Name ¹	Protein name ¹	Uniprot ID ¹	Molecular mass ² (Da)	Calculated pI value ²	Mascot score ²	Expect ²	Mascot seq. cover. ²	Defind medium		Complex medium				Log ₂ (DNB /TB)	Log ₂ (DNB /LB)	Log ₂ (defined/ complex)	Log ₂ (stationary phase /exp. phase)				
								DNB medium		TB medium		LB medium					in TB medium	in LB medium	in complex media	in defined medium	
								exp. phase	stationary phase	exp. phase	stationary phase	exp. phase	stationary phase	At exp. phase							
EngD (YchF)	GTP-dependent nucleic acid-binding protein EngD	P0ABU3	39984	4.87	211	6.7E-17	60%	0.029	0.042	0.06	0.037	0.07	0.06	-1.0	-1.3	-1.2	-0.7	-0.2	-0.5	0.5	
TypA	GTP-binding protein typA/BipA	P32132	67542	5.16	71	4.1E-02	22%	0.19	0.12	0.25	0.11	0.26	0.13	-0.4	-0.5	-0.4	-1.2	-1.0	-1.1	-0.7	
HflX	GTP-binding protein hflX	P25519	48468	5.68	88	8.6E-04	21%	0.030	0.021	0.11	0.024	0.08	0.036	-1.9	-1.4	-1.6	-2.2	-1.2	-1.7	-0.5	
Tig	Trigger factor	Q1RFA0	47836	4.83	205	2.6E-16	46%	0.42	0.45	0.93	0.45	0.81	0.47	-1.1	-0.9	-1.0	-1.0	-0.8	-0.9	0.1	
Frr	Ribosome recycling factor	A1A7L6	19269	6.43	66	2.3E-02	40%	0.038	0.09	0.06	0.15	0.12	0.10	-0.7	-1.7	-1.2	1.3	-0.3	0.5	1.2	
RaiA	Ribosome-associated inhibitor A	P0AD51	12777	6.2	62	1.4E-02	46%	0.08	0.21	0.10	0.20	0.18	0.14	-0.3	-1.2	-0.7	1.0	-0.4	0.3	1.4	
Aminoacyl-tRNA synthetases (23 proteins)								Total WCPM:	3.40	2.79	5.14	4.63	4.89	3.27	-0.6	-0.5	-0.6	-0.2	-0.6	-0.4	-0.3
AlaS	Alanyl-tRNA synthetase	B1XCM5	96315	5.53	99	2.8E-06	16%	0.30	0.28	0.46	0.49	0.56	0.41	-0.6	-0.9	-0.8	0.1	-0.4	-0.2	-0.1	
ArgS	Arginyl-tRNA synthetase	Q8XCH2	64851	5.31	131	6.7E-09	26%	0.07	0.05	0.13	0.06	0.13	0.05	-0.9	-0.9	-0.9	-1.1	-1.4	-1.2	-0.5	
AsnS	Asparaginyl tRNA synthetase	P0A8M0	52766	5.17	182	5.3E-14	40%	0.25	0.18	0.29	0.19	0.30	0.17	-0.2	-0.3	-0.2	-0.6	-0.8	-0.7	-0.5	
AspS	Aspartyl-tRNA synthetase	P21889	66157	5.47	141	6.7E-10	29%	0.19	0.16	0.25	0.18	0.22	0.16	-0.4	-0.2	-0.3	-0.5	-0.5	-0.5	-0.2	
CysS	Cysteiny-tRNA synthetase	Q8FK44	52436	5.33	76	2.0E-03	28%	0.22	0.10	0.13	0.22	0.11	0.16	0.8	1.0	0.9	0.8	0.5	0.6	-1.1	
GlnS	Glutaminy-tRNA synthetase	Q8X9H8	64040	5.88	109	1.1E-06	31%	0.14	0.08	0.17	0.12	0.17	0.15	-0.3	-0.3	-0.3	-0.5	-0.2	-0.3	-0.8	
GltX	Glutamyl-tRNA synthetase	P04805	54181	5.59	151	6.7E-11	29%	0.14	0.10	0.26	0.17	0.23	0.16	-0.9	-0.7	-0.8	-0.6	-0.5	-0.6	-0.5	
GlyQ	Glycyl-tRNA synthetase alpha subunit	A7ZTA6	34979	4.94	106	5.7E-07	45%	0.09	0.06	0.13	0.07	0.10	0.06	-0.5	-0.2	-0.3	-0.9	-0.7	-0.8	-0.6	
GlyS	Glycyl-tRNA synthetase beta subunit	P00961	76936	5.29	181	1.8E-14	28%	0.20	0.10	0.36	0.16	0.34	0.16	-0.8	-0.8	-0.8	-1.2	-1.1	-1.1	-1.0	
HisS	Histidyl-tRNA synthetase	P60908	47285	5.65	148	1.3E-10	44%	0.08	0.06	0.11	0.06	0.11	0.05	-0.5	-0.5	-0.5	-0.9	-1.1	-1.0	-0.4	

Suppl. Table 5.3.1 Proteome data of *E. coli* BL21 (DE3) growing in different media

Name ¹	Protein name ¹	Uniprot ID ¹	Molecular mass ² (Da)	Calculated pI value ²	Mascot score ²	Expect ²	Mascot seq. cover. ²	Defind medium		Complex medium				Log ₂ (DNB /TB)	Log ₂ (DNB /LB)	Log ₂ (defined/complex)	Log ₂ (stationary phase /exp. phase)				
								DNB medium		TB medium		LB medium					in TB medium	in LB medium	in complex media	in defined medium	
								exp. phase	stationary phase	exp. phase	stationary phase	exp. phase	stationary phase	At exp. phase							
IleS	Isoleucyl-tRNA synthetase	P00956	105042	5.7	169	1.1E-12	33%	0.16	0.14	0.32	0.22	0.33	0.16	-1.0	-1.0	-1.0	-0.5	-1.0	-0.8	-0.2	
LeuS	Leucyl-tRNA synthetase	B3I479	97801	5.11	132	5.3E-09	26%	0.19	0.21	0.35	0.17	0.27	0.16	-0.9	-0.5	-0.7	-1.0	-0.8	-0.9	0.1	
LysS	Lysyl-tRNA synthetase	Q8XD57	57614	5.11	159	1.1E-11	42%	0.13	0.11	0.25	0.16	0.26	0.13	-0.9	-1.0	-1.0	-0.6	-1.0	-0.8	-0.2	
MetG	Methionyl-tRNA synthetase	A8A1X8	76675	5.56	64	3.7E-02	14%	0.11	0.09	0.18	0.11	0.19	0.09	-0.7	-0.8	-0.7	-0.7	-1.1	-0.9	-0.3	
PheT	Phenylalanyl-tRNA synthetase subunit beta	Q8XE32	88119	5.12	181	6.6E-14	31%	0.19	0.21	0.20	0.13	0.23	0.11	-0.1	-0.3	-0.2	-0.6	-1.1	-0.8	0.1	
ProS	Prolyl-tRNA synthetase	A7ZHT6	63622	5.08	139	1.0E-09	36%	0.20	0.21	0.35	0.26	0.31	0.19	-0.8	-0.6	-0.7	-0.4	-0.7	-0.6	0.1	
SerS	Seryl-tRNA synthetase	P0A8L3	48669	5.34	119	1.1E-07	33%	0.13	0.14	0.23	0.22	0.23	0.16	-0.8	-0.8	-0.8	-0.1	-0.5	-0.3	0.1	
ThrS	Threonyl-tRNA synthetase	Q8XE27	74722	5.8	52	5.8E-01	17%	0.15	0.15	0.27	0.34	0.27	0.21	-0.8	-0.8	-0.8	0.3	-0.4	0.0	0.0	
TyrS	Tyrosyl-tRNA synthetase	P0AGK0	48382	5.49	125	2.7E-08	40%	0.17	0.12	0.28	0.16	0.23	0.13	-0.7	-0.4	-0.6	-0.8	-0.8	-0.8	-0.5	
LysU	Lysyl-tRNA synthetase, heat inducible	P0A8N5	57847	5.1	166	5.7E-13	40%	0.13	0.09	0.29	1.00	0.21	0.24	-1.2	-0.7	-0.9	1.8	0.2	1.0	-0.5	
MnmA	tRNA-Specific 2-thiouridylase mnmA	A7ZKS3	41333	4.94	69	2.9E-03	33%	0.049	0.044	0.05	0.036	0.042	0.031	0.0	0.2	0.1	-0.5	-0.4	-0.5	-0.2	
YgfZ	tRNA-modifying protein ygfZ	C5A0H0	36185	5.17	211	1.8E-17	54%	0.044	0.06	0.06	0.08	0.036	0.08	-0.4	0.3	-0.1	0.4	1.2	0.8	0.4	
Fmt	Methionyl-tRNA formyltransferase	P23882	34318	5.56	65	7.8E-03	22%	0.07	0.05	0.017	0.026	0.016	0.048	2.0	2.1	2.1	0.6	1.6	1.1	-0.5	
Elongation factors (6 proteins)								Total WCPM:	5.66	6.45	8.93	7.12	9.21	5.77	-0.7	-0.7	-0.7	-0.3	-0.7	-0.5	0.2
InfB	Initiation factor IF2-gamma	P0A705	78978	5.65	79	1.1E-03	26%	0.13	0.11	0.28	0.13	0.29	0.14	-1.1	-1.2	-1.1	-1.1	-1.1	-1.1	-0.2	
FusA	Elongation factor G	A7ZSL5	77704	5.24	102	1.4E-06	23%	1.39	1.55	2.03	1.66	2.14	1.22	-0.5	-0.6	-0.6	-0.3	-0.8	-0.6	0.2	
TufA	Elongation factor Tu 1	A7ZSL4	43427	5.3	109	2.9E-07	28%	3.32	3.99	5.30	4.58	5.54	3.58	-0.7	-0.7	-0.7	-0.2	-0.6	-0.4	0.3	

A-65

Suppl. Table 5.3.1 Proteome data of *E. coli* BL21 (DE3) growing in different media

Name ¹	Protein name ¹	Uniprot ID ¹	Molecular mass ² (Da)	Calculated pI value ²	Mascot score ²	Expect ²	Mascot seq. cover. ²	Defind medium		Complex medium				Log ₂ (DNB /TB)	Log ₂ (DNB /LB)	Log ₂ (defined/complex)	Log ₂ (stationary phase /exp. phase)				
								DNB medium		TB medium		LB medium					in TB medium	in LB medium	in complex media	in defined medium	
								exp. phase	stationary phase	exp. phase	stationary phase	exp. phase	stationary phase	At exp. phase							
								Whole Cell Protein Mass (WCPM) - %													
Tsf	Chain B, Elongation Factor Complex Ef-TuEF-Ts	P0A6P1	30387	5.22	245	2.6E-20	73%	0.75	0.74	1.18	0.67	1.12	0.76	-0.7	-0.6	-0.6	-0.8	-0.6	-0.7	0.0	
LepA	GTP-binding protein LepA	P60787	67099	5.4	193	4.2E-15	40%	0.032	0.026	0.07	0.045	0.07	0.024	-1.1	-1.1	-1.1	-0.6	-1.5	-1.1	-0.3	
PrfC	Peptide chain release factor 3	Q1R270	59632	5.66	75	2.9E-03	20%	0.036	0.035	0.07	0.038	0.045	0.041	-1.0	-0.3	-0.6	-0.9	-0.1	-0.5	0.0	
RNA degradation (3 proteins)								Total WCPM:	0.51	0.34	0.75	0.34	0.66	0.38	-0.6	-0.4	-0.5	-1.1	-0.8	-1.0	-0.6
Pnp	Polyribonucleotide nucleotidyltransferase	B11QV7	77093	5.09	100	2.6E-06	15%	0.38	0.26	0.53	0.27	0.48	0.28	-0.5	-0.3	-0.4	-1.0	-0.8	-0.9	-0.5	
Rnb	Exoribonuclease II	B3XC13	72829	5.44	136	2.1E-09	30%	0.09	0.06	0.17	0.06	0.12	0.07	-0.9	-0.4	-0.7	-1.5	-0.8	-1.1	-0.6	
RhlB	ATP-dependent RNA helicase	P0A8J8	47325	7.29	104	3.4E-06	29%	0.035	0.015	0.045	0.013	0.06	0.031	-0.4	-0.8	-0.6	-1.8	-1.0	-1.4	-1.2	
Isomerases (5 proteins)								Total WCPM:	0.51	0.62	0.64	0.66	0.49	0.69	-0.3	0.1	-0.1	0.0	0.5	0.3	0.3
PpiB	Peptidyl-prolyl cis-trans isomerase B (rotamase B)	Q8XCU0	18270	5.52	62	5.5E-02	38%	0.08	0.17	0.09	0.24	0.12	0.18	-0.2	-0.6	-0.4	1.4	0.6	1.0	1.1	
SurA	Peptidyl-prolyl cis-trans isomerase SurA	P0ABZ8	47254	6.48	135	2.7E-09	28%	0.08	0.11	0.11	0.10	0.05	0.11	-0.5	0.7	0.1	-0.1	1.1	0.5	0.5	
FklB	FKBP-type 22 kDa peptidyl-prolyl cis-trans isomerase	P0A9L3	22203	4.85	146	4.7E-11	37%	0.047	0.06	0.07	0.06	0.048	0.06	-0.6	0.0	-0.3	-0.2	0.3	0.0	0.4	
FkpA	FKBP-type peptidyl-prolyl cis-trans isomerase	P65765	28894	8.39	94	3.3E-05	44%	0.21	0.23	0.24	0.15	0.16	0.21	-0.2	0.4	0.1	-0.7	0.4	-0.1	0.1	
SlyD	FKBP-type peptidyl-prolyl cis-trans isomerase slyD	P0A9L1	21182	4.86	100	2.6E-06	31%	0.09	0.05	0.13	0.11	0.11	0.13	-0.5	-0.3	-0.4	-0.2	0.2	0.0	-0.8	
Chaperones (9 proteins)								Total WCPM:	2.67	3.05	3.79	4.52	3.89	4.01	-0.5	-0.5	-0.5	0.3	0.0	0.1	0.2
DnaK	Molecular chaperone DnaK	P0A6Z0	69130	4.83	192	5.3E-15	39%	0.65	0.84	1.12	1.27	1.06	1.15	-0.8	-0.7	-0.7	0.2	0.1	0.1	0.4	
GrpE	Heat shock protein GrpE	A7ZQ54	21727	4.68	54	3.3E-01	32%	0.09	0.10	0.15	0.17	0.17	0.14	-0.7	-0.9	-0.8	0.2	-0.3	0.0	0.2	

Suppl. Table 5.3.1 Proteome data of *E. coli* BL21 (DE3) growing in different media

Name ¹	Protein name ¹	Uniprot ID ¹	Molecular mass ² (Da)	Calculated pI value ²	Mascot score ²	Expect ²	Mascot seq. cover. ²	Defind medium		Complex medium				Log ₂ (DNB /TB)	Log ₂ (DNB /LB)	Log ₂ (defined/complex)	Log ₂ (stationary phase /exp. phase)			
								DNB medium		TB medium		LB medium					in TB medium	in LB medium	in complex media	in defined medium
								exp. phase	stationary phase	exp. phase	stationary phase	exp. phase	stationary phase	At exp. phase						
GroL	60 kDa chaperonin (GroEL protein)	P0A6F5	55224	4.84	219	1.0E-17	52%	1.05	1.37	1.55	1.90	1.75	1.66	-0.6	-0.7	-0.6	0.3	-0.1	0.1	0.4
GroS	Co-chaperonin GroES	P0A6G1	10381	5.15	100	8.3E-06	64%	0.29	0.29	0.31	0.43	0.24	0.48	-0.1	0.3	0.1	0.5	1.0	0.7	0.0
HtpG	Heat shock protein 90	P0A6Z5	71378	5.09	262	5.3E-22	50%	0.26	0.22	0.41	0.31	0.35	0.26	-0.7	-0.4	-0.5	-0.4	-0.4	-0.4	-0.2
HscA	Fe-S protein assembly chaperone HscA	B3XD15	65726	5.02	85	2.9E-04	21%	0.043	0.018	0.07	0.026	0.05	0.023	-0.7	-0.2	-0.5	-1.4	-1.1	-1.3	-1.3
ClpA	ATP-dependent Clp protease ATP-binding subunit	P0ABI1	84326	5.91	87	1.6E-04	21%	0.046	0.019	0.06	0.037	0.09	0.05	-0.4	-1.0	-0.7	-0.7	-0.8	-0.8	-1.3
ClpB	Protein disaggregation chaperone	P63285	95697	5.37	160	8.3E-12	27%	0.12	0.09	0.08	0.19	0.08	0.10	0.6	0.6	0.6	1.2	0.3	0.8	-0.4
IbpA	Small heat shock protein ibpA	A7ZTP1	15764	5.57	168	8.4E-12	70%	0.12	0.10	0.039	0.19	0.10	0.15	1.6	0.3	0.9	2.3	0.6	1.4	-0.3
Proteases (13 proteins)							Total WCPM:	1.15	1.05	1.50	1.93	1.30	1.73	-0.4	-0.2	-0.3	0.4	0.4	0.4	-0.1
DegP	Serine endoprotease	P0C0V1	49438	8.65	119	1.1E-07	31%	0.028	0.024	0.00	0.020	0.00	0.040	>5	>5	>5	>5	>5	>5	-0.2
PepQ	Proline dipeptidase	Q8FBI1	50328	5.6	132	5.3E-09	36%	0.12	0.13	0.11	0.23	0.08	0.19	0.1	0.6	0.4	1.1	1.2	1.2	0.1
PepD	Aminoacyl-histidine dipeptidase	P15288	53110	5.2	78	8.0E-03	27%	0.18	0.14	0.26	0.62	0.18	0.39	-0.5	0.0	-0.3	1.3	1.1	1.2	-0.4
PepN	Aminopeptidase N	B7UN18	99343	5.09	131	6.7E-09	22%	0.12	0.12	0.12	0.17	0.11	0.22	0.0	0.1	0.1	0.5	1.0	0.8	0.0
Dcp	Dipeptidyl carboxypeptidase II	Q8XB30	77516	5.35	189	1.1E-14	33%	0.031	0.044	0.05	0.09	0.024	0.11	-0.7	0.4	-0.2	0.8	2.2	1.5	0.5
Prc	Carboxy-terminal protease	Q321Y5	76514	6.38	105	2.7E-06	28%	0.048	0.024	0.040	0.022	0.046	0.036	0.3	0.1	0.2	-0.9	-0.4	-0.6	-1.0
PmbA	Protein pmbA	P0AFK0	48625	5.4	124	9.1E-09	35%	0.046	0.035	0.05	0.06	0.048	0.05	-0.1	-0.1	-0.1	0.3	0.1	0.2	-0.4
ClpP	ATP-dependent Clp protease proteolytic subunit	P0A6G9	23286	5.52	63	4.6E-02	30%	0.09	0.09	0.10	0.11	0.12	0.12	-0.2	-0.4	-0.3	0.1	0.0	0.1	0.0
HslV	ATP-dependent protease peptidase subunit	P0A7C0	19138	5.96	79	1.0E-03	46%	0.06	0.044	0.07	0.047	0.08	0.08	-0.2	-0.4	-0.3	-0.6	0.0	-0.3	-0.4

A-67

Suppl. Table 5.3.1 Proteome data of *E. coli* BL21 (DE3) growing in different media

Name ¹	Protein name ¹	Uniprot ID ¹	Molecular mass ² (Da)	Calculated pI value ²	Mascot score ²	Expect ²	Mascot seq. cover. ²	Defind medium		Complex medium				Log ₂ (DNB /TB)	Log ₂ (DNB /LB)	Log ₂ (defined/ complex)	Log ₂ (stationary phase /exp. phase)			
								DNB medium		TB medium		LB medium					in TB medium	in LB medium	in complex media	in defined medium
								exp. phase	stationary phase	exp. phase	stationary phase	exp. phase	stationary phase	At exp. phase						
								Whole Cell Protein Mass (WCPM) - %												
HslU	ATP-dependent protease ATP-binding subunit	P0A6H6	49677	5.24	166	2.3E-10	48%	0.11	0.16	0.18	0.14	0.18	0.14	-0.7	-0.7	-0.7	-0.4	-0.4	-0.4	0.5
PepB	Peptidase B	B7UGW9	46483	5.49	69	2.6E-03	29%	0.18	0.07	0.22	0.16	0.18	0.12	-0.3	0.0	-0.1	-0.5	-0.6	-0.5	-1.4
PepP	Proline aminopeptidase P II	A7ZR18	50000	5.2	69	1.1E-02	27%	0.08	0.11	0.16	0.14	0.16	0.11	-1.0	-1.0	-1.0	-0.2	-0.5	-0.4	0.5
PrIC	Oligopeptidase A	P27298	77461	5.15	209	2.9E-17	41%	0.06	0.06	0.14	0.12	0.09	0.12	-1.2	-0.6	-0.9	-0.2	0.4	0.1	0.0
Other dehydrogenases (9 proteins)							Total WCPM:	0.87	0.79	0.76	0.89	0.76	1.00	0.2	0.2	0.2	0.2	0.4	0.3	-0.1
YdfG	3-Hydroxy acid dehydrogenase	Q8X505	27360	5.65	86	2.1E-04	40%	0.10	0.11	0.06	0.11	0.045	0.08	0.7	1.2	0.9	0.9	0.8	0.9	0.1
YqhD	Alcohol dehydrogenase, NAD(P)-dependent	Q46856	42128	5.72	83	4.5E-04	32%	0.19	0.16	0.19	0.19	0.15	0.16	0.0	0.3	0.2	0.0	0.1	0.0	-0.2
AldB	Aldehyde dehydrogenase B	P37685	56670	5.44	62	1.3E-02	17%	0.07	0.05	0.041	0.045	0.06	0.13	0.8	0.2	0.5	0.1	1.1	0.6	-0.5
AldA	Lactaldehyde dehydrogenase	B3XAH7	52362	5.02	132	5.3E-09	32%	0.07	0.05	0.07	0.06	0.08	0.18	0.0	-0.2	-0.1	-0.2	1.2	0.5	-0.5
YhhX	Predicted oxidoreductase with NAD(P)-binding Rossmann-fold domain	P46853	38912	6.07	131	6.7E-09	32%	0.033	0.025	0.029	0.035	0.043	0.042	0.2	-0.4	-0.1	0.3	0.0	0.1	-0.4
Ugd	UDP-Glucose 6-dehydrogenase	P76373	43744	6.06	76	1.5E-02	33%	0.17	0.20	0.11	0.18	0.15	0.16	0.6	0.2	0.4	0.7	0.1	0.4	0.2
HdhA	7-Alpha-hydroxysteroid dehydrogenase	P0AET8	26990	5.22	67	4.3E-03	36%	0.045	0.044	0.036	0.07	0.045	0.07	0.3	0.0	0.2	1.0	0.6	0.8	0.0
HybC	Hydrogenase-2 large chain	P0ACE0	62908	5.84	60	2.3E-02	25%	0.05	0.06	0.06	0.08	0.07	0.09	-0.3	-0.5	-0.4	0.4	0.4	0.4	0.3
TrxB	Thioredoxin reductase	P0A9P4	34829	5.3	128	3.6E-09	48%	0.14	0.09	0.16	0.12	0.12	0.09	-0.2	0.2	0.0	-0.4	-0.4	-0.4	-0.6
Oxidoreductases (8 proteins)							Total WCPM:	0.49	0.68	0.47	0.82	0.49	0.91	0.1	0.0	0.0	0.8	0.9	0.8	0.5
Gor	Glutathione reductase	P06715	49084	5.64	78	8.4E-03	29%	0.06	0.049	0.08	0.09	0.07	0.07	-0.4	-0.2	-0.3	0.2	0.0	0.1	-0.3

Suppl. Table 5.3.1 Proteome data of *E. coli* BL21 (DE3) growing in different media

Name ¹	Protein name ¹	Uniprot ID ¹	Molecular mass ² (Da)	Calculated pI value ²	Mascot score ²	Expect ²	Mascot seq. cover. ²	Defind medium		Complex medium				Log ₂ (DNB /TB)	Log ₂ (DNB /LB)	Log ₂ (defined/complex)	Log ₂ (stationary phase /exp. phase)				
								DNB medium		TB medium		LB medium					in TB medium	in LB medium	in complex media	in defined medium	
								exp. phase	stationary phase	exp. phase	stationary phase	exp. phase	stationary phase	At exp. phase							
								Whole Cell Protein Mass (WCPM) - %													
NfsA	Oxygen-insensitive NADPH nitroreductase	P17117	27069	6.45	117	4.6E-08	40%	0.07	0.049	0.15	0.09	0.14	0.08	-1.1	-1.0	-1.0	-0.7	-0.8	-0.8	-0.5	
QueF	NADPH-dependent 7-cyano-7-deazaguanine reductase	C4ZZU9	32909	5.73	131	1.8E-09	39%	0.06	0.08	0.06	0.036	0.035	0.043	0.0	0.8	0.4	-0.7	0.3	-0.2	0.4	
NemA	N-Ethylmaleimide reductase	P77258	39492	5.8	90	2.2E-05	38%	0.046	0.040	0.05	0.048	0.035	0.043	-0.1	0.4	0.1	-0.1	0.3	0.1	-0.2	
SthA	Soluble pyridine nucleotide transhydrogenase	A7ZUI2	51984	6.08	109	6.6E-06	22%	0.11	0.06	0.06	0.12	0.10	0.21	0.9	0.1	0.5	1.0	1.1	1.0	-0.9	
CueO	Blue copper oxidase CueO	P36649	53557	6.07	63	4.4E-02	18%	0.040	0.06	0.036	0.06	0.037	0.043	0.2	0.1	0.1	0.7	0.2	0.5	0.6	
Bfr	Bacterioferritin, iron storage and detoxification protein	P0ABD3	18483	4.69	156	2.1E-11	60%	0.06	0.25	0.032	0.29	0.07	0.22	0.9	-0.2	0.3	3.2	1.7	2.4	2.1	
WrbA	Flavoprotein wrbA	C4ZQD2	20832	5.59	85	7.6E-05	53%	0.047	0.09	0.00	0.09	0.00	0.20	>5	>5	>5	>5	>5	>5	0.9	
Hydroperoxide reductases and superoxide dismutase (5 proteins)								Total WCPM:	1.38	2.16	1.50	3.48	1.22	2.04	-0.1	0.2	0.0	1.2	0.7	1.0	0.6
AhpF	Alkyl hydroperoxide reductase subunit F	B3XD66	56496	5.47	101	6.7E-06	28%	0.10	0.08	0.12	0.10	0.09	0.07	-0.3	0.2	-0.1	-0.3	-0.4	-0.3	-0.3	
AhpC	Alkyl hydroperoxide reductase subunit C	P0AE08	20862	5.03	108	3.6E-07	70%	0.85	1.19	0.97	1.40	0.84	1.12	-0.2	0.0	-0.1	0.5	0.4	0.5	0.5	
Tpx	Thiol peroxidase	P0A864	17995	4.75	103	1.1E-06	48%	0.08	0.15	0.06	0.15	0.05	0.16	0.4	0.7	0.5	1.3	1.7	1.5	0.9	
SodB	Superoxide dismutase [Fe]	P0AGD5	21310	5.58	125	2.6E-08	87%	0.13	0.63	0.11	1.52	0.11	0.30	0.2	0.2	0.2	3.8	1.4	2.6	2.3	
KatG	Catalase/hydroperoxidase HPI(I)	P13029	80031	5.14	76	2.1E-03	18%	0.22	0.11	0.24	0.31	0.13	0.39	-0.1	0.8	0.3	0.4	1.6	1.0	-1.0	
DNA protection and repair (7 proteins)								Total WCPM:	0.83	1.37	0.72	1.23	0.76	1.74	0.2	0.1	0.2	0.8	1.2	1.0	0.7
Ssb	Single-stranded DNA-binding protein	P0AGE0	18963	5.44	132	1.4E-09	41%	0.00	0.033	0.00	0.041	0.06	0.08	0.0	<-5	<-2.5	>5	0.4	>2.6	>5	
Dps	DNA starvation/stationary phase protection protein Dps	P0ABT3	18684	5.72	142	5.3E-10	66%	0.028	0.47	0.034	0.59	0.05	0.74	-0.3	-0.8	-0.6	4.1	3.9	4.0	4.1	

A-69

Suppl. Table 5.3.1 Proteome data of *E. coli* BL21 (DE3) growing in different media

Name ¹	Protein name ¹	Uniprot ID ¹	Molecular mass ² (Da)	Calculated pI value ²	Mascot score ²	Expect ²	Mascot seq. cover. ²	Defind medium		Complex medium		Log ₂ (DNB /TB)	Log ₂ (DNB /LB)	Log ₂ (defined/complex)	Log ₂ (stationary phase /exp. phase)					
								DNB medium		TB medium					LB medium		in TB medium	in LB medium	in complex media	in defined medium
								Whole Cell Protein Mass (WCPM) - %						At exp. phase						
								exp. phase	stationary phase	exp. phase	stationary phase	exp. phase	stationary phase							
CbpA	Curved DNA-binding protein	C4ZQC8	34434	6.33	82	1.4E-04	24%	0.00	0.019	0.00	0.029	0.00	0.034	0.0	0.0	0.0	>5	>5	>5	>5
UspA	Universal stress protein A	P0AED2	16113	5.11	110	8.3E-07	79%	0.11	0.25	0.07	0.17	0.06	0.20	0.7	0.9	0.8	1.3	1.7	1.5	1.2
UspG	Universal stress protein G	P39177	15925	6.03	101	1.8E-06	52%	0.11	0.11	0.07	0.044	0.030	0.05	0.7	1.9	1.3	-0.7	0.7	0.0	0.0
SodA	Chain A, Manganese Superoxide Dismutase	P00448	22952	6.44	64	3.6E-02	44%	0.54	0.45	0.49	0.30	0.49	0.59	0.1	0.1	0.1	-0.7	0.3	-0.2	-0.3
PolA	DNA polymerase I	P00582	103168	5.4	119	2.4E-08	25%	0.043	0.034	0.06	0.06	0.07	0.045	-0.5	-0.7	-0.6	0.0	-0.6	-0.3	-0.3
Unclassified proteins (7 proteins)						Total WCPM:		0.55	0.30	0.43	0.33	0.51	0.36	0.4	0.1	0.2	-0.4	-0.5	-0.4	-0.9
GyrB	DNA gyrase subunit B	P0AES6	90153	5.68	135	2.7E-09	24%	0.14	0.043	0.13	0.06	0.14	0.06	0.1	0.0	0.1	-1.1	-1.2	-1.2	-1.7
MreB	Regulator of ftsI, penicillin binding protein 3, septation function	Q8X9C9	37140	5.19	101	6.7E-06	34%	0.047	0.07	0.042	0.05	0.06	0.06	0.2	-0.4	-0.1	0.3	0.0	0.1	0.6
FtsZ	Cell division protein FtsZ	P0A9A8	40299	4.65	138	1.3E-09	39%	0.043	0.025	0.06	0.06	0.05	0.047	-0.5	-0.2	-0.3	0.0	-0.1	0.0	-0.8
RsmC	Ribosomal RNA small subunit methyltransferase C	B1XF10	37829	6	156	5.7E-12	51%	0.025	0.016	0.030	0.025	0.041	0.028	-0.3	-0.7	-0.5	-0.3	-0.6	-0.4	-0.6
Can	Carbonic anhydrase	P61517	25366	6.16	89	9.8E-05	35%	0.15	0.09	0.13	0.10	0.18	0.09	0.2	-0.3	0.0	-0.4	-1.0	-0.7	-0.7
FrsA	Fermentation/respiration switch protein	Q8FKM5	47336	6.47	75	2.5E-03	24%	0.032	0.018	0.034	0.033	0.035	0.028	-0.1	-0.1	-0.1	0.0	-0.3	-0.2	-0.8
YeaG	Uncharacterized protein yeaG	P0ACY3	74776	5.63	66	5.2E-03	10%	0.11	0.041	0.00	0.00	0.00	0.047	>5	>5	>5	0.0	>5	>2.5	-1.4
Uncharacterized proteins (13 proteins)						Total WCPM:		0.82	0.71	0.57	0.92	0.59	1.12	0.5	0.5	0.5	0.7	0.9	0.8	-0.2
YhbW	Uncharacterized protein yhbW	P0ADV5	37163	5.99	89	2.9E-05	33%	0.023	0.026	0.06	0.026	0.06	0.037	-1.4	-1.4	-1.4	-1.2	-0.7	-1.0	0.2
GalF	UTP-glucose-1-phosphate uridylyltransferase	P0AAB6	32979	5.73	61	1.9E-02	26%	0.019	0.019	0.032	0.044	0.032	0.028	-0.8	-0.8	-0.8	0.5	-0.2	0.1	0.0

Suppl. Table 5.3.1 Proteome data of *E. coli* BL21 (DE3) growing in different media

Name ¹	Protein name ¹	Uniprot ID ¹	Molecular mass ² (Da)	Calculated pI value ²	Mascot score ²	Expect ²	Mascot seq. cover. ²	Defind medium		Complex medium				Log ₂ (DNB /TB)	Log ₂ (DNB /LB)	Log ₂ (defined/ complex)	Log ₂ (stationary phase /exp. phase)			
								DNB medium		TB medium		LB medium					in TB medium	in LB medium	in complex media	in defined medium
								exp. phase	stationary phase	exp. phase	stationary phase	exp. phase	stationary phase	At exp. phase						
YbeZ	Putative ATP-binding protein in pho regulon	Q0T6R9	39129	5.71	84	3.8E-04	41%	0.08	0.09	0.08	0.05	0.08	0.07	0.0	0.0	0.0	-0.7	-0.2	-0.4	0.2
YicC	UPF0701 protein yicC	P23839	33211	5.1	86	6.2E-05	43%	0.05	0.038	0.06	0.039	0.041	0.032	-0.3	0.3	0.0	-0.6	-0.4	-0.5	-0.4
YajQ	UPF0234 protein yajQ	C4ZT13	18333	5.96	178	3.6E-14	64%	0.033	0.041	0.039	0.08	0.05	0.048	-0.2	-0.6	-0.4	1.0	-0.1	0.5	0.3
YbgI	UPF0135 protein ybgI	P0AFP6	26990	5.07	89	2.7E-05	46%	0.05	0.044	0.042	0.033	0.037	0.05	0.3	0.4	0.3	-0.3	0.4	0.0	-0.2
YjgR	Uncharacterized protein yjgR	P39342	54355	5.91	84	9.3E-05	28%	0.015	0.017	0.012	0.021	0.013	0.030	0.3	0.2	0.3	0.8	1.2	1.0	0.2
YdcJ	Uncharacterized protein ydcJ	P76097	51353	5.35	58	3.6E-02	34%	0.06	0.06	0.00	0.07	0.035	0.07	>5	0.8	>2.9	>5	1.0	>3	0.0
YcgB	Uncharacterized protein ycgB	P29013	61117	5.66	69	2.7E-03	15%	0.032	0.029	0.014	0.024	0.00	0.08	1.2	>5	>3.1	0.8	>5	>2.9	-0.1
YgaU	Uncharacterized protein ygaU	P0ADE6	16053	5.71	70	2.1E-03	36%	0.11	0.07	0.026	0.09	0.06	0.28	2.1	0.9	1.5	1.8	2.2	2.0	-0.7
YfbU	Hypothetical protein	P0A8W8	19638	6.06	111	6.6E-07	50%	0.12	0.12	0.06	0.12	0.07	0.09	1.0	0.8	0.9	1.0	0.4	0.7	0.0
LfiI	Lateral flagellar export/assembly protein LfiI	B1LHP6	48085	6.53	77	1.6E-03	32%	0.15	0.07	0.08	0.25	0.08	0.23	0.9	0.9	0.9	1.6	1.5	1.6	-1.1
YhdH	Putative quinone oxidoreductase YhdH	P26646	34873	5.63	111	1.8E-07	33%	0.08	0.09	0.06	0.07	0.030	0.07	0.4	1.4	0.9	0.2	1.2	0.7	0.2

¹ Name, protein name and Uniprot ID are according to Uniprot database (<http://www.uniprot.org/>). Functional classifications are mostly according to EcoCyc database (<http://ecocyc.org/>). The classifications are confirmed by KEGG database (<http://www.genome.jp/kegg/>).

² Molecular mass, calculated pI, Mascot score, expect and sequence coverage are from MASCOT search program (Matrix Science, UK, <http://www.matrixscience.com/>), based on the annotated *E. coli* genome [Uniprot (<http://www.uniprot.org/>) serving as database].

³ A truncated outer membrane protein A is identified in the NCBI database (<http://www.ncbi.nlm.nih.gov/>).

Suppl. Table 5.3.2 Summary of proteome data of *E. coli* BL21 (DE3) growing in different media

Cat. Nr.	Nr.	Name	Defined medium		Complex medium			Log ₂ (DNB /TB)	Log ₂ (DNB /LB)	Log ₂ (defined/complex)	Log ₂ (stationary phase/exponential phase)				
			DNB medium		TB medium		LB medium				in TB medium	in LB medium	in complex media	in defined medium	
			exp. phase	stationary phase	exp. phase	stationary phase	exp. phase								stationary phase
			Whole Cell Protein Mass (WCPM) - %						At exp. phase						
I		Carbohydrate metabolism (51 proteins) Sum 1 ~ 4	15.80	17.30	15.51	25.26	16.94	21.83	0.0	-0.1	0.0	0.7	0.4	0.5	0.1
	1	Central carbon metabolism (24 proteins) Sum 1.1 ~ 1.4	6.64	9.15	9.73	14.22	9.67	9.24	-0.6	-0.5	-0.5	0.5	-0.1	0.2	0.5
	1.1	Sub-group: Upper glycolysis (5 proteins)	1.35	1.76	1.21	2.16	1.18	1.51	0.2	0.2	0.2	0.8	0.4	0.6	0.4
	1.2	Sub-group: Lower glycolysis (to Acetyl-CoA) (11 proteins)	4.20	6.06	7.08	9.44	7.01	5.73	-0.8	-0.7	-0.7	0.4	-0.3	0.1	0.5
	1.3	Sub-group: Glycerol metabolism (2 proteins)	0.09	0.20	0.16	1.06	0.17	0.37	-0.8	-0.9	-0.9	2.8	1.1	2.0	1.1
	1.4	Sub-group: Pentose phosphate pathway (PPP) (6 proteins)	1.00	1.14	1.29	1.56	1.31	1.63	-0.4	-0.4	-0.4	0.3	0.3	0.3	0.2
	2	By-product metabolism (9 proteins)	1.48	1.40	1.77	1.59	2.69	2.27	-0.3	-0.9	-0.6	-0.2	-0.2	-0.2	-0.1
	3	TCA cycle (14 proteins)	6.94	5.89	3.45	8.55	4.16	9.49	1.0	0.7	0.9	1.3	1.2	1.3	-0.2
	4	Connection between glycolysis and TCA cycle (4 proteins)	0.74	0.86	0.56	0.89	0.43	0.82	0.4	0.8	0.6	0.7	0.9	0.8	0.2
II	5	Oxidative phosphorylation (7 proteins)	2.54	2.50	2.25	2.72	2.74	2.41	0.2	-0.1	0.0	0.3	-0.2	0.0	0.0
III		Biomass blocks biosynthesis (121 proteins): Sum 9 ~ 14	23.93	24.18	13.19	14.51	12.79	15.49	0.9	0.9	0.9	0.1	0.3	0.2	0.0
	6	Amino acid biosynthesis and metabolism (68 proteins). Sum 6.1 ~ 6.2	18.08	18.27	5.95	8.60	6.09	10.03	1.6	1.6	1.6	0.5	0.7	0.6	0.0
	6.1	Sub-group: Amino acid biosynthesis (57 proteins)	17.18	17.29	5.25	6.39	5.17	6.82	1.7	1.7	1.7	0.3	0.4	0.3	0.0
	6.2	Sub-group: Amino acid degradation (11 proteins)	0.90	0.98	0.70	2.21	0.92	3.20	0.4	0.0	0.2	1.6	1.8	1.7	0.1
	7.1	IMP biosynthesis (for nucleotide) (7 proteins)	1.19	1.36	0.41	0.51	0.39	0.61	1.5	1.6	1.6	0.3	0.6	0.5	0.2
	7.2	Nucleotide biosynthesis (start from IMP) (13 proteins)	1.66	1.74	2.83	2.05	2.46	1.91	-0.8	-0.6	-0.7	-0.5	-0.4	-0.4	0.1
	8	Fatty acid biosynthesis (7 proteins)	1.21	0.96	1.72	1.14	2.05	1.12	-0.5	-0.8	-0.6	-0.6	-0.9	-0.7	-0.3
	9	Lipopolysaccharide biosynthesis (10 proteins)	0.81	0.88	1.22	1.24	0.93	0.91	-0.6	-0.2	-0.4	0.0	0.0	0.0	0.1
	10	Synthesis of other cellular components (16 proteins)	0.98	0.96	1.06	0.99	0.87	0.93	-0.1	0.2	0.0	-0.1	0.1	0.0	0.0
IV	11	(Metabolite) degradation (19 proteins)	1.48	1.44	1.32	3.97	1.27	2.61	0.2	0.2	0.2	1.6	1.0	1.3	0.0
V		Transportation (28 proteins): Sum 28 ~ 30	6.25	9.96	6.15	6.42	6.51	7.68	0.0	-0.1	0.0	0.1	0.2	0.2	0.7
	12	Sugar transport (7 proteins)	1.02	1.60	0.92	1.30	0.81	1.38	0.2	0.3	0.2	0.5	0.8	0.6	0.6
	13	Amino acid and peptide transport (7 proteins)	0.72	1.26	0.43	0.58	0.28	1.12	0.8	1.4	1.1	0.4	2.0	1.2	0.8

Suppl. Table 5.3.2 Summary of proteome data of *E. coli* BL21 (DE3) growing in different media

Cat. Nr.	Nr.	Name	Defined medium		Complex medium		Log ₂ (DNB /TB)	Log ₂ (DNB /LB)	Log ₂ (defined/ complex)	Log ₂ (stationary phase/exponential phase)					
			DNB medium		TB medium					LB medium		in TB medium	in LB medium	in complex media	in defined medium
			exp. phase	stationary phase	exp. phase	stationary phase				exp. phase	stationary phase				
			Whole Cell Protein Mass (WCPM) - %						At exp. phase						
	14	Other transport proteins (14 proteins)	4.51	7.10	4.81	4.54	5.42	5.19	-0.1	-0.3	-0.2	-0.1	-0.1	-0.1	0.7
VI		Transcription and translation (66 proteins): Sum 16 ~ 23	17.02	16.72	26.07	18.81	27.23	16.41	-0.6	-0.7	-0.6	-0.5	-0.7	-0.6	0.0
	15	RNA polymerases (3 proteins)	1.16	1.02	1.47	0.76	1.65	0.73	-0.3	-0.5	-0.4	-1.0	-1.2	-1.1	-0.2
	16	RNA polymerase binding proteins (7 proteins)	0.90	0.84	1.35	0.97	1.49	0.91	-0.6	-0.7	-0.7	-0.5	-0.7	-0.6	-0.1
	17	Transcription factors (12 proteins)	1.73	1.66	1.75	1.51	2.01	2.12	0.0	-0.2	-0.1	-0.2	0.1	-0.1	-0.1
	18	Ribosomal proteins (5 proteins)	2.82	2.67	5.10	2.45	5.73	2.25	-0.9	-1.0	-0.9	-1.1	-1.3	-1.2	-0.1
	19	Ribosome-associated proteins (8 proteins)	0.85	0.95	1.58	1.02	1.60	0.98	-0.9	-0.9	-0.9	-0.6	-0.7	-0.7	0.2
	20	Aminoacyl-tRNA synthetases (23 proteins)	3.40	2.79	5.14	4.63	4.89	3.27	-0.6	-0.5	-0.6	-0.1	-0.6	-0.4	-0.3
	21	Elongation factors (6 proteins)	5.66	6.45	8.93	7.12	9.21	5.77	-0.7	-0.7	-0.7	-0.3	-0.7	-0.5	0.2
	22	RNA degradation (3 proteins)	0.51	0.34	0.75	0.34	0.66	0.38	-0.6	-0.4	-0.5	-1.1	-0.8	-1.0	-0.6
VII		Protein folding and degradation (28 proteins): Sum 24 ~ 26	4.33	4.72	5.93	7.11	5.68	6.43	-0.5	-0.4	-0.4	0.3	0.2	0.2	0.1
	23	Isomerases (5 proteins)	0.51	0.62	0.64	0.66	0.49	0.69	-0.3	0.1	-0.1	0.0	0.5	0.3	0.3
	24	Chaperones (9 proteins)	2.67	3.05	3.79	4.52	3.89	4.01	-0.5	-0.5	-0.5	0.3	0.0	0.2	0.2
	25	Proteases (13 proteins)	1.15	1.05	1.50	1.93	1.30	1.73	-0.4	-0.2	-0.3	0.4	0.4	0.4	-0.1
VIII		Cell redox balance (22 proteins): Sum 6 ~ 8	2.74	3.63	2.72	5.19	2.47	3.95	0.0	0.2	0.1	0.9	0.7	0.8	0.4
	26.1	Other dehydrogenases (9 proteins)	0.87	0.79	0.76	0.89	0.76	1.00	0.2	0.2	0.2	0.2	0.4	0.3	-0.1
	26.2	Oxidoreductases (8 proteins)	0.49	0.68	0.47	0.82	0.49	0.91	0.1	0.0	0.0	0.8	0.9	0.9	0.5
	26.3	Hydroperoxide reductases and superoxide dismutase (5 proteins)	1.38	2.16	1.50	3.48	1.22	2.04	-0.1	0.2	0.0	1.2	0.7	1.0	0.6
IX	27	DNA protection and repair (7 proteins)	0.83	1.37	0.72	1.23	0.76	1.74	0.2	0.1	0.2	0.8	1.2	1.0	0.7
X	28	Unclassified proteins (7 proteins)	0.55	0.30	0.43	0.33	0.51	0.36	0.4	0.1	0.2	-0.4	-0.5	-0.4	-0.9
XI	29	Uncharacterized proteins (13 proteins)	0.82	0.71	0.57	0.92	0.59	1.12	0.5	0.5	0.5	0.7	0.9	0.8	-0.2

A-73

Suppl. Table 5.3.3 Sigma and transcription factors of the glycolysis and TCA cycle genes

Pathway	Genes	Identified in this study?	Promoter ¹	Sigma factor ^{1,2}	Transcription factor ^{1,3}	Function ¹	Binding sites ^{1,3}	Binding sequence ^{1,3}
Upper glycolysis	<i>pgi</i>	No	<i>pgip</i>	sigmaS , sigmaD	SoxS	activator	1	cattacgctaACGGCACTAAAACCATCACAtttctgtg
	<i>pfkA</i>	Yes	<i>pfkAp2</i>	sigmaS , sigmaD	Cra (FruR)	repressor	1	attggcctgACCTGAATCAATTCAGCAggaagtgatt
			<i>pfkAp1</i>	sigmaS , sigmaD				
	<i>pfkB</i>	Yes	<i>pfkBp2</i>	sigmaS				
			<i>pfkBp1</i>	sigmaS				
	<i>fbaA</i>	Yes	<i>epdp</i>	sigmaS , sigmaD	CRP-cAMP Cra (FruR)	activator repressor	1 1	aagaagacatTTATCTGACTCACATCACACTTtatcccctt acatttaatcGACTGAAACGCTTCAGCTaggataagcg
			<i>pgkp13</i>	sigmaD				
			<i>pgkp2</i>					
	<i>fbaB</i>	Yes	<i>fbaBp</i>	sigmaS	Cra (FruR)	repressor	1	cagcgtttcTGTTGGCTCGATTCATCAgaaaaatgt
	<i>tpiA</i>	Yes	<i>tpiAp2</i>	sigmaS , sigmaD	Cra (FruR)	repressor	1	agatagcgccAGCTTAATCGGTTCAACAgcgaagtca
		<i>tpiAp1</i>						
Lower glycolysis	<i>gapA</i>	Yes	<i>gapAp3</i>	sigmaD	CRP-cAMP	activator	1	gctgcacctaAATCGTGATGAAAATCACATTTtatcgtaat
			<i>gapAp1</i>	sigmaS , sigmaD	Cra (FruR)	repressor		
			<i>gapAp2</i>	sigmaS				
			<i>gapAp4</i>	sigmaD				
	<i>pgk</i>	Yes	<i>epdp</i>	sigmaS , sigmaD	CRP-cAMP Cra (FruR)	activator repressor	1 1	aagaagacatTTATCTGACTCACATCACACTTtatcccctt acatttaatcGACTGAAACGCTTCAGCTaggataagcg
			<i>pgkp13</i>	sigmaD				
			<i>pgkp2</i>					
	<i>gpmA</i>	Yes	<i>gpmAp</i>	sigmaS , sigmaD	Fur	repressor	2	atcatcttttAATGATAATAATTCTCATTatattgccgc caaatcatctTTAATGATAATAATTCTCattatattgc
	<i>gpmM</i>	No	<i>pmAp2</i>	sigmaS , sigmaD				
			<i>gpmMp</i>	sigmaS	Cra (FruR)	repressor	1	cttcagaggcTATTTTATCGATTTCAGCTgtagtaaaat
		<i>gpmMp2</i>						
<i>eno</i>	Yes	<i>enop123</i>		Cra (FruR)	repressor			
		<i>enop47</i>	sigmaS , sigmaD					
		<i>enop6</i>						
		<i>pyrGp</i>						
		<i>pyrGp2</i>						
		<i>pyrGp1</i>						
<i>pykA</i>	Yes	<i>pykAp12</i>	sigmaS , sigmaD					

Suppl. Table 5.3.3 Sigma and transcription factors of the glycolysis and TCA cycle genes

Pathway	Genes	Identified in this study?	Promoter ¹	Sigma factor ^{1,2}	Transcription factor ^{1,3}	Function ¹	Binding sites ^{1,3}	Binding sequence ^{1,3}	
Lower glycolysis	<i>pykF</i>	Yes	<i>pykFp</i> <i>pykFp12</i> <i>pykFp3</i>	sigmaD sigmaS , sigmaD	Cra (FruR)	repressor	1	gccaaatgacTCTTGAATGGTTTCAGCActtggactg	
		Yes	<i>ppsP</i>	sigmaD	Cra (FruR)	repressor	1	tgaaaaaacGGTGAATCGTTCAAGCaaatatattt	
		Yes	<i>pdhRp</i>	sigmaS , sigmaD	CRP-cAMP	activator	6	atgtgcacagTTTCATGATTTCAATCAAAAACctgatggaca caagttgtaAAATGTGCACAGTTTCATGATTtcaatcaaaa taaagtctacATTTGTGCATAGTTACAACCTTgaaacgttat tacatcaagAAGTTTGAATTGTTACAAAAAGactccgtca cttgaacgTTATATATGTCAAGTTGTTAAAtgtgcacag atatatgcaAGTTGTTAAAATGTGCACAGTTtcatgatttc caaaattggtAAGTGAATCGGTTCAATTcggatttita cacagacatgAAATTGGTAAGACCAATtgacttcggc gcacagttcATGATTTCAATCAAaacctgatg	
	<i>lpdA</i>	Yes	<i>pdhRp</i>	sigmaS , sigmaD	Phospho-AcrA FNR NsrR-nitric oxide	CRP-cAMP	repressor	1	aattatccagAAGATGTTGTAaatcaagcgc
							repressor	1	atgtgcacagTTTCATGATTTCAATCAAAAACctgatggaca
							repressor	1	caagttgtaAAATGTGCACAGTTTCATGATTtcaatcaaaa
							repressor	1	taaagtctacATTTGTGCATAGTTACAACCTTgaaacgttat
							repressor	1	tacatcaagAAGTTTGAATTGTTACAAAAAGactccgtca
							repressor	1	cttgaacgTTATATATGTCAAGTTGTTAAAtgtgcacag
							repressor	1	atatatgcaAGTTGTTAAAATGTGCACAGTTtcatgatttc
<i>lpdAp</i>	sigmaD	Phospho-AcrA	sigmaD	Phospho-AcrA	CRP-cAMP	repressor	1	caaaattggtAAGTGAATCGGTTCAATTcggatttita	
						repressor	1	cacagacatgAAATTGGTAAGACCAATtgacttcggc	
						dual	1	gcacagttcATGATTTCAATCAAaacctgatg	
						repressor	2	tttaaaattGTTAACAATTTTGTAAaataccgac	
						repressor ?	1	cgtttgttGTTAAAAATTGTTAACaattttaa	
<i>lpdAp</i>	sigmaD	Phospho-AcrA	sigmaD	Phospho-AcrA	CRP-cAMP	dual	1	ggttttaaaAATTGTTAACAATTTTGTAAAAataccgacgga	
						repressor	1	gcccgttgttGTTAAAAATTGTTAacaatttgt	
						dual	1		

Suppl. Table 5.3.3 Sigma and transcription factors of the glycolysis and TCA cycle genes

Pathway	Genes	Identified in this study?	Promoter ¹	Sigma factor ^{1,2}	Transcription factor ^{1,3}	Function ¹	Binding sites ^{1,3}	Binding sequence ^{1,3}				
TCA cycle	<i>gltA</i>	Yes	<i>gltAp1</i>	sigmaD	Phospho-AcrA	repressor	1	gtaatgttgTAACAACCTTTGTTGAatgattgtca taaagtgtgtTATCGTGACCTGGATCACTGTTcaggataaaa aatgattgtcAAATTAGATGATTaaaaattaa				
					CRP-cAMP	activator	1					
					IHF	activator	1					
	<i>acnA</i>	Yes	<i>gltAp2</i> <i>acnAp2</i>	sigmaD	Phospho-AcrA	repressor	1	aattgggttGTTATCAAATCGTTAcgcatggtt ctctttatcAATTTGGGTTGTTATCAAATCGttacgcatg ttatcaattTGGGTTGTTATCAAatcgttacgc				
					CRP-cAMP	activator	1					
					FNR	repressor	1					
					Cra (FruR)	activator	1					
					MarA	activator	1					
					Rob	activator	1					
	SoxS	activator	1									
	<i>acnB</i>	Yes	<i>acnAp1</i> <i>acnBp</i>	sigmaS, sigmaD sigmaD	Phospho-AcrA	repressor	7	gaggcgtagTTTAAATTTGACTAatctgggat cttgggattcGTTGAGAAAGGTGATtaccatg ggattcgttgAGAAAGGTGATTATCaccatgcaa ccatgcgaafTAACGAAGTTTTTACggaggaaac ttaccatGCGAATTAACGAAGTtttacggag gattcacccaCTTTTTTATGTTGCTttttgtaa actttttatGTTGCTTTTTTGTAaAcagattaac actttttatGTTGCTTTTTTGTAaAcagattaac aagaggcgtAGTTTAAATTTTGACTaatctggg tctagaccatCCTTAACGATTCAGCacttttta ttgtaacaGATTAACACCTCGTCaaaatcctgc				
					CRP-cAMP	activator	1					
Fis					repressor	3						
Cra (FruR)					repressor							
<i>icd</i>					Yes	<i>acnBp2</i> <i>icdAp1</i>	sigmaD		Phospho-AcrA	repressor	2	ggtagtattGACAAGCCAATTACAatcattaac attgacaagcCAATTACAAATCATTaacaanaaat gaactgtgcAGCTGAATCGCTTAACCTgggattct tgtaacaacTTTGTTGAATGATTGtcaaatgata tgttacataaGTTAATCTTAGGTGAaataccgact acaagacctGTTAATCTGGACCTAcagaccatcc atgtaggtaATTGTAATGATTTTgtgaacacct ggtaattgtAATGATTTTGTGAACagcctatact taaagtgtgtTATCGTGACCTGGATCACTGTTcaggataaaa
									CRP-cAMP	activator	1	
<i>sucABCD</i>	Yes	<i>icdAp2</i> <i>sdhCp</i>	sigmaD	Phospho-AcrA	repressor	5	aaatgattgtTATCGTGACCTGGATCACTGTTcaggataaaa					
				CRP-cAMP	repressor							

Suppl. Table 5.3.3 Sigma and transcription factors of the glycolysis and TCA cycle genes

Pathway	Genes	Identified in this study?	Promoter ¹	Sigma factor ^{1,2}	Transcription factor ^{1,3}	Function ¹	Binding sites ^{1,3}	Binding sequence ^{1,3}	
TCA cycle			<i>sucAp</i>	sigmaS	Fur Phospho-AcrA FNR IHF	activator repressor repressor repressor	1	ctatatgtagGTTAATTGTAATGATTTTgtgaacagcct	
		<i>sdhAB</i> <i>sdhCD</i>	Yes No	<i>sdhCp</i>	sigmaD CRP-cAMP FNR	repressor repressor repressor activator	5 1 1	ttgtaacaacTTTGTGAATGATTGtcaaattaga tgttacataaGTTAATCTTAGGTGAaataccgact acaaagacctGTTAATCTGGACCTAcagaccatcc atgtaggtaATTGTAATGATTTTgtgaacagcct ggtaattgtAATGATTTTGTGAACagcctatact taaatgtgtTATCGTGACCTGGATCACTGTTcaggataaaa	
		<i>fumA</i>	Yes	<i>sdhDp2</i> <i>fumAp</i>	sigmaD sigmaD	Phospho-AcrA CRP-cAMP CRP-cAMP	repressor activator activator	1 1 1	ctatatgtagGTTAATTGTAATGATTTTgtgaacagcct tgggcagcttCTTCGTCAAATTTATCATGTGGgcatcctta
		<i>fumB</i>	No	<i>fumBp</i>	sigmaD	FNR Phospho-AcrA FNR	repressor activator activator	1 3	ttcctgttcaAAGTATTATGCGCAGCACAGCCactctccatt gcacgatacgCTCACACCAATCAAcccggcaga gcacgcaaagTGCATTTATAAGAAcccgtacatc gcaaagtcaTTTATAAGAACCCGtacatcgcg
				<i>dcuBp</i>		Fis Fur CRP-cAMP FNR NarL-Phosphorylated	repressor activator activator activator repressor	1 1 1 1 6	tcgttaccggCTTTAGCAAATACCTCACAGTGaatattggct cagtcagttCTGTTTTGTATGAActgtttcag tggatagtaaATAACATgtgtgaacc tatcagtattATGATAAgttgatagt agtaaataacATGTGTGaacctcgcg aacctcgcgATAATCCtatttaaat tcacgttctgTTTTGTAtgaactgtt cttagcaaaTACCTCAcagtgaat ggtgacataaTAGTTAATTAACTTTTGtagcgttt ttttagcGTTTTGAAATTA AAAACaccgttcacc
		<i>fumC</i>	Yes	<i>fumCp</i>		Phospho-AcrA FNR Fur	repressor repressor repressor	2	

A-77

Suppl. Table 5.3.3 Sigma and transcription factors of the glycolysis and TCA cycle genes

Pathway	Genes	Identified in this study?	Promoter ¹	Sigma factor ^{1,2}	Transcription factor ^{1,3}	Function ¹	Binding sites ^{1,3}	Binding sequence ^{1,3}	
TCA cycle					MarA	activator	1	ttcacacagcGGGTGCATTGTGTGAGTTGTAtctgctggaa	
					Rob	activator			
					SoxR	activator			
					SoxS	activator	1	ataacaaatgTTTGGTCTTTCGTGCCATgtaaaaaaac	
		<i>mdh</i>	Yes	<i>mdhp1</i>	sigmaD	Phospho-AcrA	repressor	1	ctaaactcctTATTATATTGATAAAActaatgatg
						CRP-cAMP	activator	1	ccacatcctcaAGAATGTGTAGTCACGCAAGTTtagcgtttat
						DpiA-P ^{asp}	activator		
						FlhDC	repressor		
				<i>mdhp2</i>		DpiA-P ^{asp}	activator		
		<i>glcB</i>	Yes	<i>glcDp</i>	sigmaD	Phospho-AcrA	repressor	2	tcttggttaaCTCAATGTAAATTGatgtaacata taactcaatgTTAAATTGATGTAACataatcactt
						GlcC-Glycolate	activator	1	cagaaaaattGGTCCTACCTGTGCACgaggtccgg
				<i>glcBp</i>		IHF	activator	1	ggttaactcaATGTAAATTGATgtaacataat

¹ The information in Suppl. Table 5.3.3 is from RegulonDB Version 7.0 [1] (<http://regulondb.ccg.unam.mx>).

² Sigma factor σ^S (sigmaS) is marked as bold letter.

³ When a predicted binding site exists, three major transcription factors [Cra (FruR), CRP-cAMP and Phospho-AcrA] are marked as bold letter.

[1] Gama-Castro, S., et al., RegulonDB version 7.0: transcriptional regulation of *Escherichia coli* K-12 integrated within genetic sensory response units (Gensor Units). Nucleic Acids Res, 2011. 39(Database issue): p. D98-105.

Suppl. Table 5.3.4 Amino acid feedback inhibition

Protein(s)	Involved pathways [1]	Inhibitor	References
HisG	Histidine biosynthesis	Histidine	[2]
SerA	Superpathway of serine and glycine biosynthesis	Serine	[3]
AroF	Superpathway of phenylalanine, tyrosine, and tryptophan biosynthesis	Tyrosine	[4]
TrpDE	Tryptophan biosynthesis	Tryptophan	[5]
PheA	Phenylalanine and tyrosine biosynthesis	Phenylalanine	[6]
CysE	Cysteine biosynthesis	Cysteine	[7]
ProB	Proline biosynthesis	Proline	[8]
ArgA	Arginine biosynthesis	Arginine	[9]
AsnA	Asparagine biosynthesis	Asparagine	[10]
LysC	Superpathway of lysine, threonine and methionine biosynthesis	Lysine	[11]
ThrAB	Threonine and methionine biosynthesis	Threonine	[12]
MetA	Methionine biosynthesis	Methionine	[13]
DapA	Lysine biosynthesis	Lysine	[14]
IlvBHIN	Superpathway of leucine, valine, and isoleucine biosynthesis	Leucine	[15-17]
IlvA	Superpathway of leucine, valine, and isoleucine biosynthesis	Leucine	[18]
leuA	Superpathway of leucine, valine, and isoleucine biosynthesis	Leucine	[16]

References:

1. Keseler, I.M., Collado-Vides, J., Gama-Castro, S., Ingraham, J., Paley, S., Paulsen, I.T., Peralta-Gil, M. and Karp, P.D., EcoCyc: a comprehensive database resource for *Escherichia coli*. Nucleic Acids Res, 2005. 33(Database issue): D334-7.
2. Tebar, A.R. and Ballesteros, A.O., Kinetic properties of ATP phosphoribosyltransferase of *Escherichia coli*. Mol Cell Biochem, 1976. 11(3): 131-6.
3. Grant, G.A., Schuller, D.J. and Banaszak, L.J., A model for the regulation of D-3-phosphoglycerate dehydrogenase, a Vmax-type allosteric enzyme. Protein Sci, 1996. 5(1): 34-41.
4. Shultz, J., Hermodson, M.A., Garner, C.C. and Herrmann, K.M., The nucleotide sequence of the *aroF* gene of *Escherichia coli* and the amino acid sequence of the encoded protein, the tyrosine-sensitive 3-deoxy-D-arabino-heptulosonate 7-phosphate synthase. J Biol Chem, 1984. 259(15): 9655-61.
5. Pabst, M.J., Kuhn, J.C. and Somerville, R.L., Feedback regulation in the anthranilate aggregate from wild type and mutant strains of *Escherichia coli*. J Biol Chem, 1973. 248(3): 901-14.
6. Dopheide, T.A., Crewther, P. and Davidson, B.E., Chorismate mutase-prephenate dehydratase from *Escherichia coli* K-12. II. Kinetic properties. J Biol Chem, 1972. 247(14): 4447-52.
7. Hindson, V.J., Serine acetyltransferase of *Escherichia coli*: substrate specificity and feedback control by cysteine. Biochem J, 2003. 375(Pt 3): 745-52.
8. Perez-Arellano, I., Rubio, V. and Cervera, J., Dissection of *Escherichia coli* glutamate 5-kinase: functional impact of the deletion of the PUA domain. FEBS Lett, 2005. 579(30): 6903-8.
9. Marvil, D.K. and Leisinger, T., N-acetylglutamate synthase of *Escherichia coli*: purification, characterization, and molecular properties. J Biol Chem, 1977. 252(10): 3295-303.
10. Cedar, H. and Schwartz, J.H., The asparagine synthetase of *Escherichia coli*. II. Studies on mechanism. J Biol Chem, 1969. 244(15): 4122-7.
11. Kotaka, M., Ren, J., Lockyer, M., Hawkins, A.R. and Stammers, D.K., Structures of R- and T-state *Escherichia coli* aspartokinase III. Mechanisms of the allosteric transition and inhibition

- by lysine. *J Biol Chem*, 2006. 281(42): 31544-52.
12. Chassagnole, C., Rais, B., Quentin, E., Fell, D.A. and Mazat, J.P., An integrated study of threonine-pathway enzyme kinetics in *Escherichia coli*. *Biochem J*, 2001. 356(Pt 2): 415-23.
 13. Born, T.L. and Blanchard, J.S., Enzyme-catalyzed acylation of homoserine: mechanistic characterization of the *Escherichia coli* metA-encoded homoserine transsuccinylase. *Biochemistry*, 1999. 38(43): 14416-23.
 14. Shedlarski, J.G. and Gilvarg, C., The pyruvate-aspartic semialdehyde condensing enzyme of *Escherichia coli*. *J Biol Chem*, 1970. 245(6): 1362-73.
 15. Barak, Z., Calvo, J.M. and Schloss, J.V., Acetolactate synthase isozyme III from *Escherichia coli*. *Methods Enzymol*, 1988. 166: 455-8.
 16. Stieglitz, B.I. and Calvo, J.M., Distribution of the isopropylmalate pathway to leucine among diverse bacteria. *J Bacteriol*, 1974. 118(3): 935-41.
 17. Gollop, N., Tavori, H. and Barak, Z., Acetohydroxy acid synthase is a target for leucine containing peptide toxicity in *Escherichia coli*. *J Bacteriol*, 1982. 149(1): 387-90.
 18. Vonder Haar, R.A. and Umbarger, H.E., Isoleucine and valine metabolism in *Escherichia coli*. XIX. Inhibition of isoleucine biosynthesis by glycyl-leucine. *J Bacteriol*, 1972. 112(1): 142-7.

Suppl. Table 5.3.5 Proteome data of *E. coli* BL21 (DE3) during hFGF-2 production in defined and complex media

Whole Cell Protein Mass (WCPM) - %: Each spot's intensity was normalized by the whole spots intensity on each 2D gel. The corresponding average from two duplicated gels was used indicating each spot's protein portion (%) of whole cell protein mass (WCPM). The total "WCPM %" of all spots representing the same protein was used for indicating the abundance of the corresponding protein.

For each protein's WCPM (%), number with two digits after the decimal point is given. But for a better comparison of the low abundance protein (WCPM <0.05 %), three digits after the decimal point are given.

Log₂(1h after IPTG/exp. before IPTG): Log₂(1h after IPTG induction/exponential phase before IPTG induction)

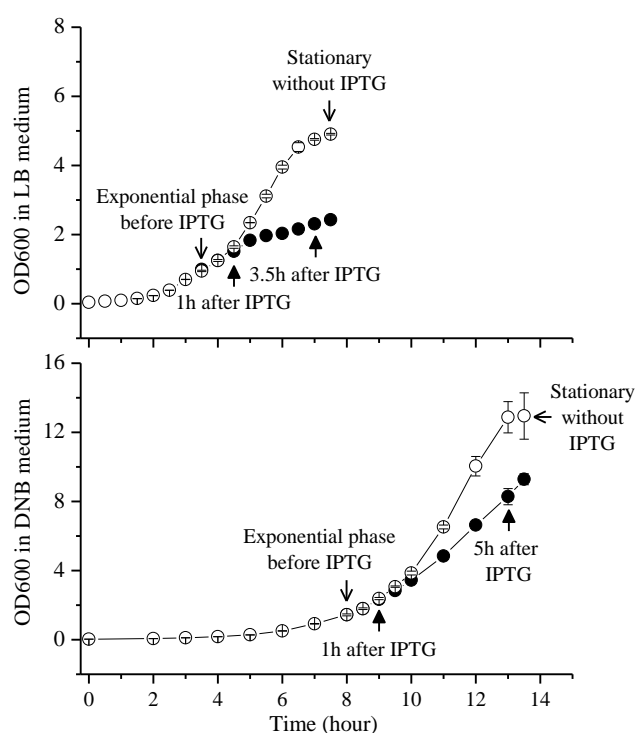
Log₂(5h or 3.5h after IPTG/exp. before IPTG): Log₂(5h or 3.5 after IPTG induction/exponential phase before IPTG induction)

Log₂(5h or 3.5h after IPTG/stationary without IPTG): Log₂(5h or 3.5h after IPTG induction/stationary phase without IPTG induction)

Log₂(stationary without IPTG/exp. before IPTG): Log₂(stationary phase without IPTG induction/exponential phase before IPTG induction)

Log₂(DNB medium/LB Medium) exp. before IPTG: Log₂(exponential phase before IPTG induction in DNB medium/exponential phase before IPTG induction in LB medium)

If WCPM (%) of a protein is zero, an artificial Log₂ ratio: ">5" or "<-5" was given, indicating the corresponding Log₂ ratio is larger than 5 or smaller than -5, respectively.



Suppl. Table 5.3.5 Proteome data of hFGF-2 production in *E. coli* BL21 (DE3) using defined and complex media

Name ¹	Protein name ¹	Defind (DNB) medium				Complex (LB) medium				Log ₂ (Ratio in Defind (DNB) medium)				Log ₂ (Ratio in Complex (LB) medium)				Log ₂ (DNB
		exp. phase before IPTG	1h after IPTG	5h after IPTG	stationary phase without IPTG	exp. phase before IPTG	1h after IPTG	3.5h after IPTG	stationary phase without IPTG	(1h after IPTG/ exp. before IPTG)	(5h after IPTG/ exp. before IPTG)	(5h after IPTG/ stationary without IPTG)	(stationary without IPTG/ exp. before IPTG)	(1h after IPTG/ exp. before IPTG)	(3.5h after IPTG/ exp. before IPTG)	(3.5h after IPTG/ stationary without IPTG)	(stationary without IPTG/ exp. before IPTG)	medium/ LB medium) exp.before IPTG
		Whole Cell Protein Mass (WCPM) - %																
Central carbon metabolism (24 proteins): Upper and lower glycolysis, glycerol metabolism and pentose phosphate pathway.		6.59	6.61	5.29	7.01	7.36	7.70	6.14	8.26	0.0	-0.3	-0.4	0.1	0.1	-0.3	-0.4	0.2	-0.2
Sub-group: Upper glycolysis (5 proteins)		1.26	1.28	0.93	1.50	0.91	0.98	0.75	1.35	0.0	-0.4	-0.7	0.3	0.1	-0.3	-0.8	0.6	0.5
PfkA	6-Phosphofructokinase	0.12	0.12	0.08	0.14	0.09	0.08	0.06	0.10	0.0	-0.6	-0.8	0.2	-0.2	-0.6	-0.7	0.2	0.4
PfkB	6-Phosphofructokinase isozyme 2	0.038	0.039	0.024	0.039	0.00	0.00	0.00	0.044	0.0	-0.7	-0.7	0.0	0.0	0.0	<-5	>5	>5
FbaA	Fructose-bisphosphate aldolase class 2	0.86	0.87	0.62	1.03	0.67	0.77	0.51	0.85	0.0	-0.5	-0.7	0.3	0.2	-0.4	-0.7	0.3	0.4
FbaB	Fructose-bisphosphate aldolase class 1	0.019	0.024	0.00	0.030	0.018	0.00	0.033	0.07	0.3	<-5	<-5	0.7	<-5	0.9	-1.1	2.0	0.1
TpiA	Triosephosphate isomerase	0.23	0.23	0.21	0.26	0.14	0.12	0.14	0.29	0.0	-0.1	-0.3	0.2	-0.2	0.0	-1.1	1.1	0.7
Sub-group: Lower glycolysis (to Acetyl-CoA) (11 proteins)		4.21	4.24	3.49	4.28	5.18	5.05	3.95	5.05	0.0	-0.3	-0.3	0.0	0.0	-0.4	-0.4	0.0	-0.3
GapA	Glyceraldehyde-3-phosphate dehydrogenase A	0.64	0.63	0.53	0.58	0.64	0.56	0.48	0.72	0.0	-0.3	-0.1	-0.1	-0.2	-0.4	-0.6	0.2	0.0
Pgk	Phosphoglycerate kinase	0.58	0.60	0.47	0.73	0.55	0.58	0.45	0.69	0.0	-0.3	-0.6	0.3	0.1	-0.3	-0.6	0.3	0.1
GpmA	Phosphoglyceromutase	0.18	0.21	0.17	0.26	0.18	0.25	0.16	0.37	0.2	-0.1	-0.6	0.5	0.5	-0.2	-1.2	1.0	0.0
Eno	Enolase	0.49	0.59	0.40	0.61	0.37	0.48	0.34	0.56	0.3	-0.3	-0.6	0.3	0.4	-0.1	-0.7	0.6	0.4
PykA	Pyruvate kinase	0.06	0.05	0.049	0.047	0.09	0.027	0.033	0.08	-0.3	-0.3	0.1	-0.4	-1.7	-1.4	-1.3	-0.2	-0.6
PykF	Pyruvate kinase I	0.18	0.16	0.17	0.19	0.25	0.17	0.12	0.24	-0.2	-0.1	-0.2	0.1	-0.6	-1.1	-1.0	-0.1	-0.5
PpsA	Phosphoenolpyruvate synthase	0.12	0.06	0.05	0.07	0.24	0.33	0.30	0.41	-1.0	-1.3	-0.5	-0.8	0.5	0.3	-0.5	0.8	-1.0
YdbK	Pyruvate flavodoxin/ferredoxin oxidoreductase domain protein	0.07	0.06	0.043	0.050	0.05	0.043	0.033	0.06	-0.2	-0.7	-0.2	-0.5	-0.2	-0.6	-0.9	0.3	0.5

Suppl. Table 5.3.5 Proteome data of hFGF-2 production in *E. coli* BL21 (DE3) using defined and complex media

Name ¹	Protein name ¹	Defind (DNB) medium				Complex (LB) medium				Log ₂ (Ratio in Defind (DNB) medium)				Log ₂ (Ratio in Complex (LB) medium)				Log ₂ (DNB medium/ LB medium)	
		exp. phase before IPTG	1h after IPTG induction	5h after IPTG induction	stationary phase without IPTG	exp. phase before IPTG	1h after IPTG induction	3.5h after IPTG induction	stationary phase without IPTG	(1h after IPTG/ exp. before IPTG)	(5h after IPTG/ exp. before IPTG)	(5h after IPTG/ stationary without exp. before IPTG)	(stationary without exp. before IPTG)	(1h after IPTG/ exp. before IPTG)	(3.5h after IPTG/ exp. before IPTG)	(3.5h after IPTG/ stationary without exp. before IPTG)	(stationary without exp. before IPTG)		
		Whole Cell Protein Mass (WCPM) - %																	
AceE	Pyruvate dehydrogenase (acetyl-transferring), homodimeric type	0.87	0.96	0.82	0.76	1.51	1.35	1.02	0.92	0.1	-0.1	0.1	-0.2	-0.2	-0.6	0.1	-0.7	-0.8	
AceF	Pyruvate dehydrogenase, dihydrolipoyltransacetylase component E2	0.35	0.28	0.21	0.36	0.47	0.38	0.23	0.08	-0.3	-0.7	-0.8	0.0	-0.3	-1.0	1.5	-2.6	-0.4	
LpdA	Dihydrolipoamide dehydrogenase	0.64	0.63	0.57	0.62	0.83	0.89	0.80	0.93	0.0	-0.2	-0.1	0.0	0.1	-0.1	-0.2	0.2	-0.4	
Sub-group: Glycerol metabolism (2 proteins)		0.13	0.06	0.08	0.14	0.15	0.47	0.32	0.29	-1.1	-0.7	-0.8	0.1	1.6	1.1	0.1	1.0	-0.2	
GlpK	Glycerol kinase	0.10	0.032	0.026	0.09	0.12	0.43	0.29	0.20	-1.6	-1.9	-1.8	-0.2	1.8	1.3	0.5	0.7	-0.3	
Dhak	Dihydroxyacetone kinase subunit DhaK	0.030	0.030	0.05	0.042	0.027	0.036	0.031	0.09	0.0	0.7	0.3	0.5	0.4	0.2	-1.5	1.7	0.2	
Sub-group: Pentose phosphate pathway (PPP) (6 proteins)		0.99	1.03	0.79	1.09	1.12	1.21	1.13	1.57	0.1	-0.3	-0.5	0.1	0.1	0.0	-0.5	0.5	-0.2	
Gnd	6-Phosphogluconate dehydrogenase	0.30	0.30	0.27	0.32	0.39	0.42	0.36	0.42	0.0	-0.2	-0.2	0.1	0.1	-0.1	-0.2	0.1	-0.4	
TktA	Transketolase	0.46	0.45	0.38	0.42	0.53	0.57	0.58	0.65	0.0	-0.3	-0.1	-0.1	0.1	0.1	-0.2	0.3	-0.2	
TktB	Transketolase 2	0.017	0.028	0.00	0.011	0.013	0.00	0.00	0.05	0.7	<-5	<-5	-0.6	<-5	<-5	<-5	1.9	0.4	
TalB	Chain A, Structure Of Transaldolase B	0.13	0.15	0.07	0.21	0.15	0.18	0.16	0.37	0.2	-0.9	-1.6	0.7	0.3	0.1	-1.2	1.3	-0.2	
TalA	Transaldolase A	0.048	0.06	0.045	0.07	0.00	0.00	0.00	0.06	0.3	-0.1	-0.6	0.5	0.0	0.0	<-5	>5	>5	
Eda	KHG/KDPG aldolase	0.032	0.039	0.031	0.06	0.029	0.035	0.029	0.041	0.3	0.0	-1.0	0.9	0.3	0.0	-0.5	0.5	0.1	
By-product metabolism (9 proteins)		1.20	1.12	0.89	0.95	1.06	1.13	0.96	2.12	-0.1	-0.4	-0.1	-0.3	0.1	-0.1	-1.1	1.0	0.2	
Acs	Acetyl-coenzyme A synthetase	0.10	0.10	0.10	0.09	0.05	0.10	0.13	0.71	0.0	0.0	0.2	-0.2	1.0	1.4	-2.4	3.8	1.0	
PoxB	Pyruvate dehydrogenase [ubiquinone]	0.012	0.037	0.00	0.025	0.00	0.00	0.00	0.047	1.6	<-5	<-5	1.1	0.0	0.0	<-5	>5	>5	

A-83

Suppl. Table 5.3.5 Proteome data of hFGF-2 production in *E. coli* BL21 (DE3) using defined and complex media

Name ¹	Protein name ¹	Defind (DNB) medium				Complex (LB) medium				Log ₂ (Ratio in Defind (DNB) medium)				Log ₂ (Ratio in Complex (LB) medium)				Log ₂ (DNB
		exp. phase before	1h after IPTG	5h after IPTG	stationary phase without	exp. phase before	1h after IPTG	3.5h after IPTG	stationary phase without	(1h after IPTG/ exp. before	(5h after IPTG/ exp. before	(5h after IPTG/ stationary without	(stationary IPTG/ exp. before	(1h after IPTG/ exp. before	(3.5h after IPTG/ exp. before	(3.5h after IPTG/ stationary without	(stationary IPTG/ exp. before	medium/ LB medium)
		IPTG	induction	induction	IPTG	IPTG	induction	induction	IPTG	IPTG)	IPTG)	IPTG)	IPTG)	IPTG)	IPTG)	IPTG)	IPTG)	IPTG)
		Whole Cell Protein Mass (WCPM) - %																
Pta	Phosphate acetyltransferase	0.13	0.16	0.15	0.11	0.17	0.30	0.14	0.12	0.3	0.2	0.4	-0.2	0.8	-0.3	0.2	-0.5	-0.4
AckA	Acetate kinase	0.08	0.08	0.08	0.09	0.21	0.17	0.14	0.11	0.0	0.0	-0.2	0.2	-0.3	-0.6	0.3	-0.9	-1.4
AdhE	Bifunctional acetaldehyde-CoA/alcohol dehydrogenase	0.33	0.31	0.18	0.29	0.21	0.09	0.15	0.46	-0.1	-0.9	-0.7	-0.2	-1.2	-0.5	-1.6	1.1	0.7
PflB	Formate acetyltransferase 1	0.41	0.32	0.26	0.20	0.32	0.38	0.32	0.55	-0.4	-0.7	0.4	-1.0	0.2	0.0	-0.8	0.8	0.4
LldD	L-Lactate dehydrogenase	0.05	0.05	0.039	0.05	0.049	0.029	0.042	0.031	0.0	-0.4	-0.4	0.0	-0.8	-0.2	0.4	-0.7	0.0
Dld	D-Lactate dehydrogenase	0.047	0.044	0.031	0.039	0.031	0.016	0.029	0.05	-0.1	-0.6	-0.3	-0.3	-1.0	-0.1	-0.8	0.7	0.6
LdhA	D-Lactate dehydrogenase	0.032	0.018	0.043	0.042	0.017	0.036	0.017	0.033	-0.8	0.4	0.0	0.4	1.1	0.0	-1.0	1.0	0.9
	TCA cycle (14 proteins)	5.50	4.84	3.74	4.70	3.61	4.78	4.84	8.42	-0.2	-0.6	-0.3	-0.2	0.4	0.4	-0.8	1.2	0.6
GltA	Citrate synthase	0.69	0.65	0.43	0.55	0.29	0.37	0.61	1.36	-0.1	-0.7	-0.4	-0.3	0.4	1.1	-1.2	2.2	1.3
AcnA	Aconitate hydratase 1	0.15	0.10	0.16	0.17	0.21	0.26	0.20	0.41	-0.6	0.1	-0.1	0.2	0.3	-0.1	-1.0	1.0	-0.5
AcnB	Aconitate hydratase 2	0.86	0.76	0.55	0.59	0.61	0.93	0.85	1.21	-0.2	-0.6	-0.1	-0.5	0.6	0.5	-0.5	1.0	0.5
Icd	Isocitrate dehydrogenase	0.94	0.93	0.82	1.02	0.59	0.79	0.79	1.35	0.0	-0.2	-0.3	0.1	0.4	0.4	-0.8	1.2	0.7
SucA	2-Oxoglutarate dehydrogenase E1 component	0.47	0.41	0.22	0.27	0.45	0.37	0.54	0.56	-0.2	-1.1	-0.3	-0.8	-0.3	0.3	-0.1	0.3	0.1
SucB	Dihydrolypoamide succinyltransferase	0.48	0.37	0.37	0.38	0.43	0.57	0.46	0.54	-0.4	-0.4	0.0	-0.3	0.4	0.1	-0.2	0.3	0.2
SucC	Succinyl-CoA synthetase subunit beta	0.44	0.43	0.30	0.44	0.28	0.44	0.39	0.59	0.0	-0.6	-0.6	0.0	0.7	0.5	-0.6	1.1	0.7
SucD	Succinyl-CoA ligase [ADP-forming] subunit alpha	0.39	0.30	0.22	0.27	0.28	0.29	0.33	0.66	-0.4	-0.8	-0.3	-0.5	0.1	0.2	-1.0	1.2	0.5
SdhA	Succinate dehydrogenase flavoprotein subunit	0.40	0.33	0.31	0.39	0.18	0.36	0.33	0.46	-0.3	-0.4	-0.3	0.0	1.0	0.9	-0.5	1.4	1.2

Suppl. Table 5.3.5 Proteome data of hFGF-2 production in *E. coli* BL21 (DE3) using defined and complex media

Name ¹	Protein name ¹	Defind (DNB) medium				Complex (LB) medium				Log ₂ (Ratio in Defind (DNB) medium)				Log ₂ (Ratio in Complex (LB) medium)				Log ₂ (DNB medium/ LB medium)
		exp. phase before IPTG	1h after IPTG induction	5h after IPTG induction	stationary phase without IPTG	exp. phase before IPTG	1h after IPTG induction	3.5h after IPTG induction	stationary phase without IPTG	(1h after IPTG) exp. before	(5h after IPTG) exp. before	(5h after IPTG) stationary without	(stationary without IPTG) exp. before	(1h after IPTG) exp. before	(3.5h after IPTG) exp. before	(3.5h after IPTG) stationary without	(stationary without IPTG) exp. before	exp.before
		Whole Cell Protein Mass (WCPM) - %																
SdhB	Succinate dehydrogenase and fumarate reductase iron-sulfur protein	0.16	0.12	0.09	0.11	0.07	0.06	0.06	0.11	-0.4	-0.8	-0.3	-0.5	-0.2	-0.2	-0.9	0.7	1.2
FumA	Fumarate hydratase (fumarase A), aerobic Class I	0.029	0.030	0.021	0.032	0.025	0.035	0.044	0.08	0.0	-0.5	-0.6	0.1	0.5	0.8	-0.9	1.7	0.2
FumC	Fumarate hydratase (fumarase C), aerobic Class II	0.16	0.11	0.06	0.10	0.08	0.08	0.06	0.27	-0.5	-1.4	-0.7	-0.7	0.0	-0.4	-2.2	1.8	1.0
Mdh	Malate dehydrogenase	0.32	0.28	0.14	0.35	0.07	0.18	0.15	0.74	-0.2	-1.2	-1.3	0.1	1.4	1.1	-2.3	3.4	2.2
GlcB	Malate synthase G	0.015	0.022	0.041	0.034	0.039	0.05	0.024	0.07	0.6	1.5	0.3	1.2	0.4	-0.7	-1.5	0.8	-1.4
Connection between glycolysis and TCA cycle (4 proteins)		0.67	0.61	0.60	0.72	0.36	0.43	0.40	0.83	-0.1	-0.2	-0.3	0.1	0.3	0.2	-1.1	1.2	0.9
Ppc	Phosphoenolpyruvate carboxylase	0.46	0.42	0.36	0.42	0.24	0.23	0.20	0.20	-0.1	-0.4	-0.2	-0.1	-0.1	-0.3	0.0	-0.3	0.9
PckA	Phosphoenolpyruvate carboxykinase	0.09	0.07	0.16	0.18	0.046	0.08	0.08	0.43	-0.4	0.8	-0.2	1.0	0.8	0.8	-2.4	3.2	1.0
MaeB	Malate dehydrogenase (Oxaloacetate-decarboxylating) (NADP(+))	0.09	0.08	0.048	0.06	0.040	0.08	0.07	0.17	-0.2	-0.9	-0.3	-0.6	1.0	0.8	-1.3	2.1	1.2
SfcA	NAD-dependent malic enzyme	0.034	0.041	0.033	0.07	0.033	0.035	0.037	0.026	0.3	0.0	-1.1	1.0	0.1	0.2	0.5	-0.3	0.0
Oxidative phosphorylation (7 proteins)		2.44	2.31	1.89	2.65	2.53	2.61	2.22	2.39	-0.1	-0.4	-0.5	0.1	0.0	-0.2	-0.1	-0.1	-0.1
AtpA	F0F1 ATP synthase subunit alpha	1.13	1.12	0.91	1.38	1.06	1.19	0.90	1.06	0.0	-0.3	-0.6	0.3	0.2	-0.2	-0.2	0.0	0.1
AtpD	F0F1 ATP synthase subunit beta	0.59	0.60	0.48	0.67	0.80	0.94	0.78	0.70	0.0	-0.3	-0.5	0.2	0.2	0.0	0.2	-0.2	-0.4
AtpH	F0F1 ATP synthase subunit delta	0.07	0.07	0.06	0.08	0.09	0.09	0.06	0.06	0.0	-0.2	-0.4	0.2	0.0	-0.6	0.0	-0.6	-0.4
NuoF	NADH dehydrogenase I subunit F	0.14	0.11	0.12	0.11	0.14	0.08	0.08	0.14	-0.3	-0.2	0.1	-0.3	-0.8	-0.8	-0.8	0.0	0.0
NuoG	NADH dehydrogenase subunit G	0.24	0.16	0.13	0.17	0.21	0.12	0.19	0.21	-0.6	-0.9	-0.4	-0.5	-0.8	-0.1	-0.1	0.0	0.2

Suppl. Table 5.3.5 Proteome data of hFGF-2 production in *E. coli* BL21 (DE3) using defined and complex media

Name ¹	Protein name ¹	Defind (DNB) medium				Complex (LB) medium				Log ₂ (Ratio in Defind (DNB) medium)				Log ₂ (Ratio in Complex (LB) medium)				Log ₂ (DNB
		exp. phase before	1h after IPTG	5h after IPTG	stationary phase without IPTG	exp. phase before	1h after IPTG	3.5h after IPTG	stationary phase without IPTG	(1h after IPTG/ exp. before	(5h after IPTG/ exp. before	(5h after IPTG/ stationary without exp. before	(stationary without IPTG/ exp. before	(1h after IPTG/ exp. before	(3.5h after IPTG/ exp. before	(3.5h after IPTG/ stationary without exp. before	(stationary without IPTG/ exp. before	medium/ LB medium)
		IPTG	induction	induction	IPTG	IPTG	induction	induction	IPTG	IPTG)	IPTG)	IPTG)	IPTG)	IPTG)	IPTG)	IPTG)	IPTG)	IPTG)
		Whole Cell Protein Mass (WCPM) - %																
NuoC	Bifunctional NADH:ubiquinone oxidoreductase subunit C/D	0.18	0.18	0.13	0.14	0.16	0.12	0.14	0.15	0.0	-0.5	-0.1	-0.4	-0.4	-0.2	-0.1	-0.1	0.2
NuoB	NADH-quinone oxidoreductase subunit B	0.10	0.07	0.07	0.09	0.07	0.07	0.07	0.07	-0.5	-0.5	-0.4	-0.2	0.0	0.0	0.0	0.0	0.5
Amino acid biosynthesis and metabolism (68 proteins): Amino acid biosynthesis and amino acid degradation		13.15	12.08	10.89	12.82	5.21	5.62	5.67	10.65	-0.1	-0.3	-0.2	0.0	0.1	0.1	-0.9	1.0	1.3
Sub-group: Amino acid biosynthesis (57 proteins)		12.37	11.37	10.17	11.93	4.42	4.60	4.43	6.91	-0.1	-0.3	-0.2	-0.1	0.1	0.0	-0.6	0.6	1.5
AroD	3-Dehydroquinase dehydratase	0.14	0.15	0.15	0.16	0.10	0.14	0.09	0.11	0.1	0.1	-0.1	0.2	0.5	-0.2	-0.3	0.1	0.5
AroB	3-Dehydroquinase synthase	0.024	0.036	0.034	0.019	0.014	0.00	0.029	0.030	0.6	0.5	0.8	-0.3	<-5	1.1	0.0	1.1	0.8
AroF	Phospho-2-dehydro-3-deoxyheptonate aldolase	0.16	0.19	0.13	0.18	0.07	0.09	0.10	0.38	0.2	-0.3	-0.5	0.2	0.4	0.5	-1.9	2.4	1.2
AroG	Phospho-2-dehydro-3-deoxyheptonate aldolase, Phe-sensitive	0.21	0.22	0.18	0.19	0.07	0.06	0.08	0.048	0.1	-0.2	-0.1	-0.1	-0.2	0.2	0.7	-0.5	1.6
TrpD	Anthranilate synthase, component II	0.09	0.08	0.047	0.08	0.00	0.00	0.00	0.022	-0.2	-0.9	-0.8	-0.2	0.0	0.0	<-5	>5	>5
TrpE	Component I of anthranilate synthase	0.16	0.12	0.10	0.10	0.00	0.00	0.00	0.00	-0.4	-0.7	0.0	-0.7	0.0	0.0	0.0	0.0	>5
TrpC	Anthranilate isomerase	0.10	0.13	0.07	0.12	0.09	0.12	0.10	0.13	0.4	-0.5	-0.8	0.3	0.4	0.2	-0.4	0.5	0.2
TrpA	Tryptophan synthase alpha chain	0.030	0.035	0.07	0.046	0.00	0.00	0.017	0.031	0.2	1.2	0.6	0.6	0.0	>5	-0.9	>5	>5
PheA	P-protein	0.06	0.06	0.06	0.05	0.042	0.027	0.033	0.027	0.0	0.0	0.3	-0.3	-0.6	-0.3	0.3	-0.6	0.5
TyrA	T-protein	0.12	0.10	0.08	0.11	0.020	0.039	0.043	0.036	-0.3	-0.6	-0.5	-0.1	1.0	1.1	0.3	0.8	2.6
AspC	Aspartate aminotransferase, PLP-dependent	0.19	0.22	0.15	0.30	0.14	0.14	0.12	0.19	0.2	-0.3	-1.0	0.7	0.0	-0.2	-0.7	0.4	0.4
SerA	D-3-Phosphoglycerate dehydrogenase	0.58	0.59	0.54	0.69	0.23	0.22	0.27	0.64	0.0	-0.1	-0.4	0.3	-0.1	0.2	-1.2	1.5	1.3

Suppl. Table 5.3.5 Proteome data of hFGF-2 production in *E. coli* BL21 (DE3) using defined and complex media

Name ¹	Protein name ¹	Defind (DNB) medium				Complex (LB) medium				Log ₂ (Ratio in Defind (DNB) medium)				Log ₂ (Ratio in Complex (LB) medium)				Log ₂ (DNB
		exp. phase before IPTG	1h after IPTG induction	5h after IPTG induction	stationary phase without IPTG	exp. phase before IPTG	1h after IPTG induction	3.5h after IPTG induction	stationary phase without IPTG	(1h after IPTG/ exp. before IPTG)	(5h after IPTG/ exp. before IPTG)	(5h after IPTG/ stationary without IPTG)	(stationary without IPTG/ exp. before IPTG)	(1h after IPTG/ exp. before IPTG)	(3.5h after IPTG/ exp. before IPTG)	(3.5h after IPTG/ stationary without IPTG)	(stationary without IPTG/ exp. before IPTG)	medium/ LB medium) exp.before IPTG
		Whole Cell Protein Mass (WCPM) - %																
SerC	Phosphoserine aminotransferase	0.31	0.23	0.18	0.27	0.10	0.14	0.11	0.15	-0.4	-0.8	-0.6	-0.2	0.5	0.1	-0.4	0.6	1.6
GdhA	Glutamate dehydrogenase, NADP-specific	0.09	0.12	0.17	0.14	0.030	0.045	0.05	0.06	0.4	0.9	0.3	0.6	0.6	0.7	-0.3	1.0	1.6
GlnA	Glutamine synthetase	0.41	0.35	0.25	0.31	0.19	0.13	0.15	0.16	-0.2	-0.7	-0.3	-0.4	-0.5	-0.3	-0.1	-0.2	1.1
GltB	Glutamate synthase subunit alpha	0.15	0.12	0.17	0.16	0.037	0.00	0.00	0.00	-0.3	0.2	0.1	0.1	<-5	<-5	0.0	<-5	2.0
HisG	ATP phosphoribosyltransferase	0.10	0.05	0.06	0.09	0.07	0.06	0.07	0.06	-1.0	-0.7	-0.6	-0.2	-0.2	0.0	0.2	-0.2	0.5
HisF	Imidazole glycerol phosphate synthase subunit hisF	0.09	0.07	0.06	0.08	0.08	0.09	0.05	0.10	-0.4	-0.6	-0.4	-0.2	0.2	-0.7	-1.0	0.3	0.2
HisC	Histidinol-phosphate aminotransferase	0.06	0.035	0.07	0.05	0.038	0.048	0.025	0.11	-0.8	0.2	0.5	-0.3	0.3	-0.6	-2.1	1.5	0.7
HisD	Histidinol dehydrogenase	0.022	0.031	0.016	0.046	0.030	0.019	0.024	0.032	0.5	-0.5	-1.5	1.1	-0.7	-0.3	-0.4	0.1	-0.4
GlyA	Serine hydroxymethyltransferase	0.71	0.68	0.59	0.75	0.32	0.31	0.28	0.67	-0.1	-0.3	-0.3	0.1	0.0	-0.2	-1.3	1.1	1.1
CysK	Cysteine synthase A	0.41	0.35	0.28	0.49	0.11	0.10	0.13	0.40	-0.2	-0.6	-0.8	0.3	-0.1	0.2	-1.6	1.9	1.9
CysN	Sulfate adenyltransferase, subunit 1	0.12	0.12	0.09	0.12	0.020	0.035	0.013	0.019	0.0	-0.4	-0.4	0.0	0.8	-0.6	-0.5	-0.1	2.6
CysJ	Sulfite reductase subunit alpha	0.07	0.08	0.10	0.07	0.024	0.05	0.041	0.020	0.2	0.5	0.5	0.0	1.1	0.8	1.0	-0.3	1.5
CysI	Sulfite reductase subunit beta	0.05	0.049	0.031	0.037	0.00	0.00	0.00	0.00	0.0	-0.7	-0.3	-0.4	0.0	0.0	0.0	0.0	>5
LysC	Aspartokinase III	0.034	0.06	0.039	0.06	0.00	0.00	0.00	0.00	0.8	0.2	-0.6	0.8	0.0	0.0	0.0	0.0	>5
Asd	Maltose-binding periplasmic protein	0.25	0.27	0.21	0.29	0.13	0.13	0.11	0.26	0.1	-0.3	-0.5	0.2	0.0	-0.2	-1.2	1.0	0.9
DapA	Dihydrodipicolinate synthase	0.10	0.09	0.06	0.08	0.08	0.08	0.07	0.10	-0.2	-0.7	-0.4	-0.3	0.0	-0.2	-0.5	0.3	0.3
DapD	2,3,4,5-Tetrahydropyridine-2-carboxylate N-succinyltransferase	0.18	0.16	0.13	0.25	0.13	0.13	0.09	0.10	-0.2	-0.5	-0.9	0.5	0.0	-0.5	-0.2	-0.4	0.5

A-87

Suppl. Table 5.3.5 Proteome data of hFGF-2 production in *E. coli* BL21 (DE3) using defined and complex media

Name ¹	Protein name ¹	Defind (DNB) medium				Complex (LB) medium				Log ₂ (Ratio in Defind (DNB) medium)				Log ₂ (Ratio in Complex (LB) medium)				Log ₂ (DNB
		exp. phase before	1h after IPTG	5h after IPTG	stationary phase without IPTG	exp. phase before	1h after IPTG	3.5h after IPTG	stationary phase without IPTG	(1h after IPTG/ exp. before	(5h after IPTG/ exp. before	(5h after IPTG/ stationary without exp. before	(stationary IPTG/ exp. before	(1h after IPTG/ exp. before	(3.5h after IPTG/ exp. before	(3.5h after IPTG/ stationary without exp. before	(stationary IPTG/ exp. before	medium/ LB medium) exp.before
		IPTG	induction	induction	IPTG	IPTG	induction	induction	IPTG	IPTG)	IPTG)	IPTG)	IPTG)	IPTG)	IPTG)	IPTG)	IPTG)	IPTG)
		Whole Cell Protein Mass (WCPM) - %																
LysA	Diaminopimelate decarboxylase	0.06	0.05	0.06	0.05	0.10	0.09	0.08	0.13	-0.3	0.0	0.3	-0.3	-0.2	-0.3	-0.7	0.4	-0.7
ThrB	Homoserine kinase	0.039	0.045	0.039	0.05	0.00	0.00	0.00	0.037	0.2	0.0	-0.4	0.4	0.0	0.0	<-5	>5	>5
MetA	Homoserine O-succinyltransferase	0.036	0.034	0.042	0.040	0.00	0.00	0.035	0.025	-0.1	0.2	0.1	0.2	0.0	>5	0.5	>5	>5
MetH	Methionine synthase	0.12	0.09	0.07	0.08	0.06	0.06	0.05	0.038	-0.4	-0.8	-0.2	-0.6	0.0	-0.3	0.4	-0.7	1.0
MetE	5-Methyltetrahydropteroyltriglutamate-homocysteine S-methyltransferase	3.00	2.58	2.71	2.38	0.09	0.07	0.12	0.24	-0.2	-0.1	0.2	-0.3	-0.4	0.4	-1.0	1.4	5.1
IlvA	Threonine dehydratase biosynthetic	0.15	0.18	0.13	0.16	0.08	0.09	0.07	0.16	0.3	-0.2	-0.3	0.1	0.2	-0.2	-1.2	1.0	0.9
IlvB	Acetolactate synthase I, large subunit	0.05	0.05	0.030	0.045	0.00	0.00	0.05	0.018	0.0	-0.7	-0.6	-0.2	0.0	>5	1.5	>5	>5
IlvC	Ketol-acid reductoisomerase, NAD(P)-binding	1.01	0.91	0.78	1.06	0.06	0.07	0.07	0.13	-0.2	-0.4	-0.4	0.1	0.2	0.2	-0.9	1.1	4.1
IlvD	Dihydroxyacid dehydratase	0.31	0.26	0.20	0.25	0.07	0.06	0.048	0.07	-0.3	-0.6	-0.3	-0.3	-0.2	-0.5	-0.5	0.0	2.1
IlvE	Chain A, Branched-Chain Amino Acid Aminotransferase	0.33	0.33	0.24	0.33	0.048	0.07	0.07	0.23	0.0	-0.5	-0.5	0.0	0.5	0.5	-1.7	2.3	2.8
IlvI	Acetolactate synthase isozyme 3 large subunit	0.06	0.048	0.040	0.049	0.020	0.012	0.023	0.026	-0.3	-0.6	-0.3	-0.3	-0.7	0.2	-0.2	0.4	1.6
LeuA	2-Isopropylmalate synthase	0.18	0.21	0.12	0.15	0.00	0.07	0.00	0.00	0.2	-0.6	-0.3	-0.3	>5	0.0	0.0	0.0	>5
LeuB	3-Isopropylmalate dehydrogenase	0.10	0.11	0.12	0.13	0.07	0.13	0.048	0.10	0.1	0.3	-0.1	0.4	0.9	-0.5	-1.1	0.5	0.5
LeuC	Isopropylmalate isomerase large subunit	0.12	0.13	0.08	0.16	0.00	0.00	0.015	0.018	0.1	-0.6	-1.0	0.4	0.0	>5	-0.3	>5	>5
LeuD	3-Isopropylmalate isomerase subunit	0.06	0.08	0.06	0.10	0.00	0.00	0.00	0.00	0.4	0.0	-0.7	0.7	0.0	0.0	0.0	0.0	>5
AsnA	Aspartate--ammonia ligase	0.09	0.08	0.08	0.08	0.036	0.020	0.032	0.11	-0.2	-0.2	0.0	-0.2	-0.8	-0.2	-1.8	1.6	1.3
AsnB	Asparagine synthase	0.10	0.10	0.13	0.12	0.045	0.023	0.048	0.08	0.0	0.4	0.1	0.3	-1.0	0.1	-0.7	0.8	1.2

Suppl. Table 5.3.5 Proteome data of hFGF-2 production in *E. coli* BL21 (DE3) using defined and complex media

Name ¹	Protein name ¹	Defind (DNB) medium				Complex (LB) medium				Log ₂ (Ratio in Defind (DNB) medium)				Log ₂ (Ratio in Complex (LB) medium)				Log ₂ (DNB
		exp. phase before IPTG	1h after IPTG induction	5h after IPTG induction	stationary phase without IPTG	exp. phase before IPTG	1h after IPTG induction	3.5h after IPTG induction	stationary phase without IPTG	(1h after IPTG/ exp. before IPTG)	(5h after IPTG/ exp. before IPTG)	(5h after IPTG/ stationary without IPTG)	(stationary without IPTG/ exp. before IPTG)	(1h after IPTG/ exp. before IPTG)	(3.5h after IPTG/ exp. before IPTG)	(3.5h after IPTG/ stationary without IPTG)	(stationary without IPTG/ exp. before IPTG)	medium/ LB medium) exp.before
		Whole Cell Protein Mass (WCPM) - %																
CarA	Carbamoyl phosphate synthase small subunit	0.15	0.15	0.11	0.14	0.15	0.14	0.15	0.13	0.0	-0.4	-0.3	-0.1	-0.1	0.0	0.2	-0.2	0.0
CarB	Carbamoyl phosphate synthase large subunit	0.38	0.26	0.22	0.20	0.42	0.27	0.33	0.28	-0.5	-0.8	0.1	-0.9	-0.6	-0.3	0.2	-0.6	-0.1
ArgC	N-Acetyl-gamma-glutamyl-phosphate reductase	0.06	0.043	0.034	0.05	0.07	0.06	0.042	0.047	-0.5	-0.8	-0.6	-0.3	-0.2	-0.7	-0.2	-0.6	-0.2
ArgD	Acetylornithine/succinyldiaminopimelate aminotransferase	0.25	0.18	0.16	0.19	0.09	0.14	0.12	0.10	-0.5	-0.6	-0.2	-0.4	0.6	0.4	0.3	0.2	1.5
ArgE	Acetylornithine deacetylase	0.043	0.039	0.040	0.047	0.045	0.046	0.035	0.048	-0.1	-0.1	-0.2	0.1	0.0	-0.4	-0.5	0.1	-0.1
ArgI	Ornithine carbamoyltransferase chain I	0.041	0.031	0.05	0.037	0.06	0.06	0.038	0.049	-0.4	0.3	0.4	-0.1	0.0	-0.7	-0.4	-0.3	-0.5
ArgG	Argininosuccinate synthase	0.20	0.21	0.19	0.25	0.22	0.23	0.25	0.18	0.1	-0.1	-0.4	0.3	0.1	0.2	0.5	-0.3	-0.1
ArgH	Argininosuccinate lyase	0.16	0.17	0.15	0.18	0.25	0.27	0.21	0.15	0.1	-0.1	-0.3	0.2	0.1	-0.3	0.5	-0.7	-0.6
AspA	Aspartate ammonia-lyase	0.12	0.08	0.06	0.17	0.14	0.30	0.24	0.50	-0.6	-1.0	-1.5	0.5	1.1	0.8	-1.1	1.8	-0.2
ProA	Gamma-glutamyl phosphate reductase	0.06	0.06	0.037	0.05	0.039	0.039	0.032	0.043	0.0	-0.7	-0.4	-0.3	0.0	-0.3	-0.4	0.1	0.6
IscS (Yfh)	Cysteine desulfurase	0.07	0.07	0.06	0.05	0.10	0.09	0.10	0.08	0.0	-0.2	0.3	-0.5	-0.2	0.0	0.3	-0.3	-0.5
Sub-group: Amino acid degradation (11 proteins)		0.78	0.71	0.72	0.89	0.79	1.02	1.24	3.74	-0.1	-0.1	-0.3	0.2	0.4	0.7	-1.6	2.2	0.0
DadX	Alanine racemase, catabolic	0.038	0.035	0.026	0.037	0.039	0.028	0.036	0.08	-0.1	-0.5	-0.5	0.0	-0.5	-0.1	-1.2	1.0	0.0
TnaA	Tryptophanase	0.06	0.05	0.06	0.05	0.16	0.34	0.57	2.59	-0.3	0.0	0.3	-0.3	1.1	1.8	-2.2	4.0	-1.4
MetF	5,10-Methylenetetrahydrofolate reductase	0.17	0.13	0.09	0.11	0.00	0.00	0.00	0.00	-0.4	-0.9	-0.3	-0.6	0.0	0.0	0.0	0.0	>5
MetK	Chain A, S-Adenosylmethionine Synthetase	0.27	0.21	0.24	0.32	0.19	0.18	0.17	0.11	-0.4	-0.2	-0.4	0.2	-0.1	-0.2	0.6	-0.8	0.5
GcvT	Glycine cleavage system T protein	0.036	0.07	0.00	0.09	0.00	0.00	0.00	0.00	1.0	<-5	<-5	1.3	0.0	0.0	0.0	0.0	>5

A-89

Suppl. Table 5.3.5 Proteome data of hFGF-2 production in *E. coli* BL21 (DE3) using defined and complex media

Name ¹	Protein name ¹	Defind (DNB) medium				Complex (LB) medium				Log ₂ (Ratio in Defind (DNB) medium)				Log ₂ (Ratio in Complex (LB) medium)				Log ₂ (DNB
		exp. phase before	1h after IPTG	5h after IPTG	stationary phase without IPTG	exp. phase before	1h after IPTG	3.5h after IPTG	stationary phase without IPTG	(1h after IPTG/ exp. before	(5h after IPTG/ exp. before	(5h after IPTG/ stationary without exp. before	(stationary IPTG/ exp. before	(1h after IPTG/ exp. before	(3.5h after IPTG/ exp. before	(3.5h after IPTG/ stationary without exp. before	(stationary IPTG/ exp. before	medium/ LB medium)
		IPTG	induction	induction	IPTG	IPTG	induction	induction	IPTG	IPTG	IPTG	IPTG	IPTG	IPTG	IPTG	IPTG	IPTG	IPTG
		Whole Cell Protein Mass (WCPM) - %																
AstA	Arginine N-succinyltransferase	0.030	0.031	0.031	0.045	0.015	0.00	0.032	0.10	0.0	0.0	-0.5	0.6	<-5	1.1	-1.6	2.7	1.0
AstB	N-Succinylarginine dihydrolase	0.033	0.017	0.035	0.036	0.026	0.038	0.027	0.040	-1.0	0.1	0.0	0.1	0.5	0.1	-0.6	0.6	0.3
AstD	N-Succinylglutamate 5-semialdehyde dehydrogenase	0.00	0.00	0.031	0.05	0.022	0.08	0.06	0.15	0.0	>5	-0.7	>5	1.9	1.4	-1.3	2.8	<-5
Tdh	L-threonine 3-dehydrogenase	0.021	0.031	0.037	0.029	0.08	0.05	0.048	0.12	0.6	0.8	0.4	0.5	-0.7	-0.7	-1.3	0.6	-1.9
Kbl	2-Amino-3-ketobutyrate coenzyme A ligase	0.11	0.09	0.14	0.09	0.18	0.17	0.16	0.37	-0.3	0.3	0.6	-0.3	-0.1	-0.2	-1.2	1.0	-0.7
PutA	Bifunctional protein putA	0.007	0.035	0.033	0.026	0.08	0.13	0.14	0.18	2.3	2.2	0.3	1.9	0.7	0.8	-0.4	1.2	-3.5
	IMP biosynthesis (for nucleotide) (7 proteins)	1.27	1.23	1.17	1.39	0.59	0.59	0.60	1.00	0.0	-0.1	-0.2	0.1	0.0	0.0	-0.7	0.8	1.1
PurF	Amidophosphoribosyltransferase	0.07	0.09	0.08	0.039	0.019	0.029	0.017	0.033	0.4	0.2	1.0	-0.8	0.6	-0.2	-1.0	0.8	1.9
PurD	Phosphoribosylamine--glycine ligase	0.23	0.21	0.18	0.39	0.14	0.21	0.15	0.18	-0.1	-0.4	-1.1	0.8	0.6	0.1	-0.3	0.4	0.7
PurT	Phosphoribosylglycinamide formyltransferase 2	0.09	0.06	0.07	0.08	0.05	0.047	0.05	0.19	-0.6	-0.4	-0.2	-0.2	-0.1	0.0	-1.9	1.9	0.8
PurL	Phosphoribosylformyl-glycineamide synthetase	0.36	0.36	0.36	0.28	0.13	0.08	0.15	0.19	0.0	0.0	0.4	-0.4	-0.7	0.2	-0.3	0.5	1.5
PurC	Phosphoribosylaminoimidazole-succinocarboxamide synthase	0.12	0.14	0.10	0.22	0.036	0.05	0.029	0.10	0.2	-0.3	-1.1	0.9	0.5	-0.3	-1.8	1.5	1.7
PurB	Adenylosuccinate lyase	0.14	0.11	0.11	0.12	0.11	0.09	0.09	0.09	-0.3	-0.3	-0.1	-0.2	-0.3	-0.3	0.0	-0.3	0.3
PurH	Bifunctional purine biosynthesis protein PurH	0.26	0.25	0.26	0.27	0.10	0.08	0.11	0.21	-0.1	0.0	-0.1	0.1	-0.3	0.1	-0.9	1.1	1.4
	Nucleotide biosynthesis (start from IMP) (13 proteins)	1.53	1.64	1.48	1.87	1.90	1.83	1.59	1.88	0.1	0.0	-0.3	0.3	-0.1	-0.3	-0.2	0.0	-0.3
PurA	Adenylosuccinate synthetase	0.41	0.45	0.35	0.48	0.42	0.46	0.38	0.43	0.1	-0.2	-0.5	0.2	0.1	-0.1	-0.2	0.0	0.0

Suppl. Table 5.3.5 Proteome data of hFGF-2 production in *E. coli* BL21 (DE3) using defined and complex media

Name ¹	Protein name ¹	Defind (DNB) medium				Complex (LB) medium				Log ₂ (Ratio in Defind (DNB) medium)				Log ₂ (Ratio in Complex (LB) medium)				Log ₂ (DNB
		exp. phase before IPTG	1h after IPTG induction	5h after IPTG induction	stationary phase without IPTG	exp. phase before IPTG	1h after IPTG induction	3.5h after IPTG induction	stationary phase without IPTG	(1h after IPTG/ exp. before IPTG)	(5h after IPTG/ exp. before IPTG)	(5h after IPTG/ stationary without IPTG)	(stationary without IPTG/ exp. before IPTG)	(1h after IPTG/ exp. before IPTG)	(3.5h after IPTG/ exp. before IPTG)	(3.5h after IPTG/ stationary without IPTG)	(stationary without IPTG/ exp. before IPTG)	medium/ LB medium)
		Whole Cell Protein Mass (WCPM) - %																exp.before
GuaA	GMP synthetase (glutamine aminotransferase)	0.14	0.15	0.14	0.20	0.14	0.15	0.12	0.12	0.1	0.0	-0.5	0.5	0.1	-0.2	0.0	-0.2	0.0
GuaB	Inositol-5-monophosphate dehydrogenase	0.16	0.19	0.15	0.17	0.22	0.15	0.14	0.13	0.2	-0.1	-0.2	0.1	-0.6	-0.7	0.1	-0.8	-0.5
Add	Adenosine deaminase	0.037	0.028	0.07	0.031	0.00	0.00	0.031	0.026	-0.4	0.9	1.2	-0.3	0.0	>5	0.3	>5	>5
DeoB	Phosphopentomutase	0.042	0.030	0.041	0.045	0.046	0.07	0.07	0.10	-0.5	0.0	-0.1	0.1	0.6	0.6	-0.5	1.1	-0.1
DeoD	Chain A, Purine Nucleoside Phosphorylase	0.048	0.09	0.10	0.10	0.21	0.15	0.10	0.12	0.9	1.1	0.0	1.1	-0.5	-1.1	-0.3	-0.8	-2.1
Hpt	Hypoxanthine phosphoribosyltransferase	0.15	0.16	0.14	0.16	0.07	0.09	0.09	0.16	0.1	-0.1	-0.2	0.1	0.4	0.4	-0.8	1.2	1.1
Apt	Adenine phosphoribosyltransferase	0.06	0.07	0.06	0.09	0.10	0.07	0.06	0.049	0.2	0.0	-0.6	0.6	-0.5	-0.7	0.3	-1.0	-0.7
Udp	Uridine phosphorylase	0.07	0.06	0.042	0.09	0.11	0.12	0.07	0.16	-0.2	-0.7	-1.1	0.4	0.1	-0.7	-1.2	0.5	-0.7
PyrG	CTP synthase	0.19	0.17	0.16	0.21	0.37	0.36	0.28	0.25	-0.2	-0.2	-0.4	0.1	0.0	-0.4	0.2	-0.6	-1.0
Tmk	Thymidylate kinase	0.046	0.06	0.040	0.08	0.07	0.06	0.042	0.06	0.4	-0.2	-1.0	0.8	-0.2	-0.7	-0.5	-0.2	-0.6
Ndk	Nucleoside diphosphate kinase	0.15	0.15	0.17	0.15	0.11	0.15	0.13	0.21	0.0	0.2	0.2	0.0	0.4	0.2	-0.7	0.9	0.4
Amn	AMP nucleosidase	0.031	0.05	0.024	0.06	0.034	0.00	0.07	0.08	0.7	-0.4	-1.3	1.0	<-5	1.0	-0.2	1.2	-0.1
Fatty acid biosynthesis (7 proteins)		1.13	1.09	1.10	1.17	1.62	1.31	1.08	1.12	-0.1	0.0	-0.1	0.1	-0.3	-0.6	-0.1	-0.5	-0.5
AccA	Acetyl-coenzyme A carboxylase carboxyl transferase subunit alpha	0.09	0.08	0.09	0.10	0.14	0.11	0.11	0.08	-0.2	0.0	-0.2	0.2	-0.3	-0.3	0.5	-0.8	-0.6
AccC	Acetyl-CoA carboxylase, biotin carboxylase subunit	0.14	0.13	0.10	0.12	0.25	0.13	0.15	0.14	-0.1	-0.5	-0.3	-0.2	-0.9	-0.7	0.1	-0.8	-0.8
FabH	3-Oxoacyl-[acyl-carrier-protein] synthase 3	0.045	0.045	0.047	0.043	0.07	0.07	0.041	0.029	0.0	0.1	0.1	-0.1	0.0	-0.8	0.5	-1.3	-0.6

A-91

Appendix

Suppl. Table 5.3.5 Proteome data of hFGF-2 production in *E. coli* BL21 (DE3) using defined and complex media

Name ¹	Protein name ¹	Defind (DNB) medium				Complex (LB) medium				Log ₂ (Ratio in Defind (DNB) medium)				Log ₂ (Ratio in Complex (LB) medium)				Log ₂ (DNB
		exp. phase before	1h after IPTG	5h after IPTG	stationary phase without	exp. phase before	1h after IPTG	3.5h after IPTG	stationary phase without	(1h after IPTG/ exp. before	(5h after IPTG/ exp. before	(5h after IPTG/ stationary without	(stationary IPTG/ exp. before	(1h after IPTG/ exp. before	(3.5h after IPTG/ exp. before	(3.5h after IPTG/ stationary without	(stationary IPTG/ exp. before	medium/ LB medium)
		IPTG	induction	induction	IPTG	IPTG	induction	induction	IPTG	IPTG	IPTG	IPTG	IPTG	IPTG	IPTG	IPTG	IPTG	IPTG
		Whole Cell Protein Mass (WCPM) - %																
FabB	3-Oxoacyl-[acyl-carrier-protein] synthase I	0.18	0.25	0.33	0.36	0.36	0.30	0.22	0.33	0.5	0.9	-0.1	1.0	-0.3	-0.7	-0.6	-0.1	-1.0
FabF	3-Oxoacyl-(acyl carrier protein) synthase II	0.28	0.22	0.21	0.20	0.35	0.32	0.26	0.23	-0.3	-0.4	0.1	-0.5	-0.1	-0.4	0.2	-0.6	-0.3
FabI	Enoyl-[acyl-carrier-protein] reductase [NADH] FabI	0.28	0.22	0.21	0.26	0.32	0.30	0.22	0.25	-0.3	-0.4	-0.3	-0.1	-0.1	-0.5	-0.2	-0.4	-0.2
FabZ	(3R)-Hydroxymyristoyl-[acyl-carrier-protein] dehydratase	0.12	0.14	0.11	0.10	0.14	0.07	0.08	0.06	0.2	-0.1	0.1	-0.3	-1.0	-0.8	0.4	-1.2	-0.2
	Lipopolysaccharide biosynthesis (10 proteins)	0.82	0.55	0.71	0.67	0.91	1.10	0.89	1.00	-0.6	-0.2	0.1	-0.3	0.3	0.0	-0.2	0.1	-0.2
GmhA	Phosphoheptose isomerase	0.037	0.040	0.029	0.046	0.023	0.024	0.024	0.06	0.1	-0.4	-0.7	0.3	0.1	0.1	-1.3	1.4	0.7
HldE	Bifunctional protein hldE	0.039	0.045	0.042	0.06	0.025	0.05	0.05	0.046	0.2	0.1	-0.5	0.6	1.0	1.0	0.1	0.9	0.6
HldD	ADP-L-glycero-D-manno-heptose-6-epimerase	0.31	0.11	0.15	0.18	0.20	0.49	0.26	0.34	-1.5	-1.0	-0.3	-0.8	1.3	0.4	-0.4	0.8	0.6
LpxA	Acyl-[acyl-carrier-protein]-UDP-N-acetylglucosamine O-acyltransferase	0.10	0.07	0.10	0.045	0.06	0.032	0.08	0.05	-0.5	0.0	1.2	-1.2	-0.9	0.4	0.7	-0.3	0.7
ArnA	Bifunctional polymyxin resistance protein ArnA	0.06	0.06	0.039	0.048	0.08	0.043	0.043	0.08	0.0	-0.6	-0.3	-0.3	-0.9	-0.9	-0.9	0.0	-0.4
GlmS	Glucosamine--fructose-6-phosphate aminotransferase [isomerizing]	0.14	0.11	0.19	0.12	0.27	0.22	0.22	0.16	-0.3	0.4	0.7	-0.2	-0.3	-0.3	0.5	-0.8	-0.9
GlmM	Phosphoglucosamine mutase	0.042	0.035	0.039	0.047	0.05	0.05	0.045	0.08	-0.3	-0.1	-0.3	0.2	0.0	-0.2	-0.8	0.7	-0.3
GlmU	Bifunctional protein GlmU	0.00	0.00	0.00	0.00	0.06	0.05	0.049	0.047	0.0	0.0	0.0	0.0	-0.3	-0.3	0.1	-0.4	<-5
RmlA	Glucose-1-phosphate thymidyltransferase	0.049	0.042	0.05	0.049	0.05	0.033	0.038	0.040	-0.2	0.0	0.0	0.0	-0.6	-0.4	-0.1	-0.3	0.0
RfbB	dTDP-glucose 4,6-dehydratase	0.032	0.039	0.07	0.08	0.09	0.09	0.08	0.09	0.3	1.1	-0.2	1.3	0.0	-0.2	-0.2	0.0	-1.5

Suppl. Table 5.3.5 Proteome data of hFGF-2 production in *E. coli* BL21 (DE3) using defined and complex media

Name ¹	Protein name ¹	Defind (DNB) medium				Complex (LB) medium				Log ₂ (Ratio in Defind (DNB) medium)				Log ₂ (Ratio in Complex (LB) medium)				Log ₂ (DNB
		exp. phase before IPTG	1h after IPTG induction	5h after IPTG induction	stationary phase without IPTG	exp. phase before IPTG	1h after IPTG induction	3.5h after IPTG induction	stationary phase without IPTG	(1h after IPTG) before exp.	(5h after IPTG) before exp.	(5h after IPTG) stationary without IPTG	(stationary IPTG) exp. before	(1h after IPTG) before	(3.5h after IPTG) before	(3.5h after IPTG) stationary without IPTG	(stationary IPTG) exp. before	medium/ LB medium) exp.before
		Whole Cell Protein Mass (WCPM) - %																
Synthesis of other cellular components (16 proteins)		0.86	0.88	0.81	1.02	0.71	0.74	0.72	0.96	0.0	-0.1	-0.3	0.2	0.1	0.0	-0.4	0.4	0.3
HemB	Delta-aminolevulinic acid dehydratase	0.11	0.12	0.09	0.19	0.05	0.06	0.06	0.15	0.1	-0.3	-1.1	0.8	0.3	0.3	-1.3	1.6	1.1
HemL	Glutamate-1-semialdehyde 2,1-aminomutase	0.12	0.09	0.08	0.09	0.08	0.11	0.09	0.09	-0.4	-0.6	-0.2	-0.4	0.5	0.2	0.0	0.2	0.6
IspG	4-Hydroxy-3-methylbut-2-en-1-yl diphosphate synthase	0.06	0.06	0.07	0.05	0.09	0.08	0.06	0.047	0.0	0.2	0.5	-0.3	-0.2	-0.6	0.4	-0.9	-0.6
IspE	4-Diphosphocytidyl-2-C-methyl-D-erythritol kinase	0.042	0.06	0.035	0.06	0.031	0.07	0.019	0.05	0.5	-0.3	-0.8	0.5	1.2	-0.7	-1.4	0.7	0.4
Mpl	UDP-N-acetylmuramate:L-alanyl-gamma-D-glutamyl-meso-diaminopimelate ligase	0.035	0.034	0.032	0.05	0.043	0.06	0.07	0.15	0.0	-0.1	-0.6	0.5	0.5	0.7	-1.1	1.8	-0.3
GshB	Glutathione synthetase	0.046	0.045	0.034	0.05	0.05	0.048	0.037	0.05	0.0	-0.4	-0.6	0.1	-0.1	-0.4	-0.4	0.0	-0.1
MdoG	Glucan biosynthesis protein, periplasmic	0.045	0.048	0.032	0.043	0.06	0.035	0.05	0.041	0.1	-0.5	-0.4	-0.1	-0.8	-0.3	0.3	-0.5	-0.4
SpeA	Biosynthetic arginine decarboxylase	0.08	0.09	0.07	0.11	0.15	0.17	0.14	0.08	0.2	-0.2	-0.7	0.5	0.2	-0.1	0.8	-0.9	-0.9
SpeE	Spermidine synthase	0.044	0.047	0.043	0.05	0.031	0.00	0.00	0.042	0.1	0.0	-0.2	0.2	<-5	<-5	<-5	0.4	0.5
LuxS	S-ribosylhomocysteine lyase	0.035	0.043	0.00	0.06	0.00	0.00	0.00	0.047	0.3	<-5	<-5	0.8	0.0	0.0	<-5	>5	>5
NadE	NH(3)-dependent NAD(+) synthetase	0.034	0.046	0.024	0.05	0.020	0.036	0.015	0.040	0.4	-0.5	-1.1	0.6	0.8	-0.4	-1.4	1.0	0.8
PanB	3-Methyl-2-oxobutanoate hydroxymethyltransferase	0.026	0.037	0.07	0.032	0.026	0.037	0.026	0.039	0.5	1.4	1.1	0.3	0.5	0.0	-0.6	0.6	0.0
PanC	Pantothenate synthetase	0.028	0.038	0.06	0.039	0.026	0.00	0.034	0.046	0.4	1.1	0.6	0.5	<-5	0.4	-0.4	0.8	0.1
ThiC	Phosphomethylpyrimidine synthase	0.13	0.12	0.09	0.06	0.022	0.027	0.07	0.040	-0.1	-0.5	0.6	-1.1	0.3	1.7	0.8	0.9	2.6
GlgB	1,4-Alpha-glucan branching enzyme	0.017	0.012	0.031	0.036	0.010	0.00	0.010	0.022	-0.5	0.9	-0.2	1.1	<-5	0.0	-1.1	1.1	0.8
OtsA	Alpha.alpha-trehalose-phosphate synthase [UDP-forming]	0.00	0.00	0.045	0.043	0.023	0.00	0.043	0.026	0.0	>5	0.1	>5	<-5	0.9	0.7	0.2	<-5

A-93

Suppl. Table 5.3.5 Proteome data of hFGF-2 production in *E. coli* BL21 (DE3) using defined and complex media

Name ¹	Protein name ¹	Defind (DNB) medium				Complex (LB) medium				Log ₂ (Ratio in Defind (DNB) medium)				Log ₂ (Ratio in Complex (LB) medium)				Log ₂ (DNB
		exp. phase before	1h after IPTG	5h after IPTG	stationary phase without IPTG	exp. phase before	1h after IPTG	3.5h after IPTG	stationary phase without IPTG	(1h after IPTG/ exp. before	(5h after IPTG/ exp. before	(5h after IPTG/ stationary without exp. before	(stationary IPTG/ exp. before	(1h after IPTG/ exp. before	(3.5h after IPTG/ exp. before	(3.5h after IPTG/ stationary without exp. before	(stationary IPTG/ exp. before	medium/ LB medium)
		IPTG	induction	induction	IPTG	IPTG	induction	induction	IPTG	IPTG)	IPTG)	IPTG)	IPTG)	IPTG)	IPTG)	IPTG)	IPTG)	IPTG)
(Metabolite) degradation (19 proteins)		1.67	1.46	1.14	1.64	1.52	1.51	1.33	3.45	-0.2	-0.6	-0.5	0.0	0.0	-0.2	-1.4	1.2	0.1
MalP	Maltodextrin phosphorylase	0.11	0.09	0.07	0.10	0.22	0.13	0.05	0.18	-0.3	-0.7	-0.5	-0.1	-0.8	-2.1	-1.8	-0.3	-1.0
MalQ	4-Alpha-glucanotransferase	0.13	0.09	0.06	0.12	0.40	0.28	0.19	0.21	-0.5	-1.1	-1.0	-0.1	-0.5	-1.1	-0.1	-0.9	-1.6
Pgm	Phosphoglucomutase	0.15	0.15	0.12	0.12	0.09	0.14	0.09	0.12	0.0	-0.3	0.0	-0.3	0.6	0.0	-0.4	0.4	0.7
BglX	Periplasmic beta-glucosidase precursor	0.06	0.041	0.037	0.046	0.05	0.042	0.032	0.045	-0.5	-0.7	-0.3	-0.4	-0.3	-0.6	-0.5	-0.2	0.3
GatZ	D-Tagatose-1,6-bisphosphate aldolase subunit gatZ	0.54	0.48	0.28	0.57	0.18	0.31	0.34	1.16	-0.2	-0.9	-1.0	0.1	0.8	0.9	-1.8	2.7	1.6
GatD	Galactitol-1-phosphate 5-dehydrogenase	0.14	0.13	0.10	0.14	0.07	0.11	0.10	0.60	-0.1	-0.5	-0.5	0.0	0.7	0.5	-2.6	3.1	1.0
XylA	Xylose isomerase	0.022	0.038	0.042	0.031	0.00	0.00	0.00	0.037	0.8	0.9	0.4	0.5	0.0	0.0	<-5	>5	>5
TreA	Periplasmic trehalase	0.037	0.046	0.027	0.039	0.014	0.016	0.013	0.045	0.3	-0.5	-0.5	0.1	0.2	-0.1	-1.8	1.7	1.4
TreC	Trehalose-6-phosphate hydrolase	0.05	0.026	0.08	0.09	0.11	0.10	0.10	0.07	-0.9	0.7	-0.2	0.8	-0.1	-0.1	0.5	-0.7	-1.1
MelA	Alpha-galactosidase	0.030	0.037	0.035	0.08	0.06	0.07	0.13	0.23	0.3	0.2	-1.2	1.4	0.2	1.1	-0.8	1.9	-1.0
GabT	4-Aminobutyrate aminotransferase GabT	0.16	0.09	0.14	0.047	0.00	0.00	0.022	0.09	-0.8	-0.2	1.6	-1.8	0.0	>5	-2.0	>5	>5
GabD	Succinate-semialdehyde dehydrogenase [NADP+] GabD	0.07	0.07	0.049	0.045	0.10	0.11	0.10	0.12	0.0	-0.5	0.1	-0.6	0.1	0.0	-0.3	0.3	-0.5
Prr	Gamma-aminobutyraldehyde dehydrogenase	0.034	0.038	0.043	0.03	0.020	0.00	0.00	0.20	0.2	0.3	0.3	0.0	<-5	<-5	<-5	3.3	0.8
UidA	Beta-glucuronidase	0.05	0.05	0.046	0.05	0.05	0.06	0.06	0.07	0.0	-0.1	-0.1	0.0	0.3	0.3	-0.2	0.5	0.0
CpdB	2',3'-Cyclic-nucleotide 2'-phosphodiesterase/3'-nucleotidase	0.026	0.020	0.016	0.025	0.021	0.025	0.015	0.040	-0.4	-0.7	-0.6	-0.1	0.3	-0.5	-1.4	0.9	0.3
DkgA	2,5-Diketo-D-gluconic acid reductase A	0.024	0.028	0.00	0.06	0.045	0.00	0.00	0.05	0.2	<-5	<-5	1.3	<-5	<-5	<-5	0.2	-0.9

Suppl. Table 5.3.5 Proteome data of hFGF-2 production in *E. coli* BL21 (DE3) using defined and complex media

Name ¹	Protein name ¹	Defind (DNB) medium				Complex (LB) medium				Log ₂ (Ratio in Defind (DNB) medium)				Log ₂ (Ratio in Complex (LB) medium)				Log ₂ (DNB medium/LB medium) exp.before
		exp. phase before IPTG	1h after IPTG induction	5h after IPTG induction	stationary phase without IPTG	exp. phase before IPTG	1h after IPTG induction	3.5h after IPTG induction	stationary phase without IPTG	(1h after IPTG) exp. before	(5h after IPTG) exp. before	(5h after IPTG) stationary without	(stationary without IPTG) exp. before	(1h after IPTG) exp. before	(3.5h after IPTG) exp. before	(3.5h after IPTG) stationary without	(stationary without IPTG) exp. before	
		Whole Cell Protein Mass (WCPM) - %								IPTG)		IPTG)		IPTG)		IPTG)		
NanA	N-Acetylneuraminate lyase	0.00	0.00	0.00	0.00	0.042	0.09	0.05	0.043	0.0	0.0	0.0	0.0	1.1	0.3	0.2	0.0	<-5
FadB	Multifunctional fatty acid oxidation complex subunit alpha	0.023	0.028	0.00	0.043	0.013	0.018	0.016	0.09	0.3	<-5	<-5	0.9	0.5	0.3	-2.5	2.8	0.8
FadH	2,4-Dienoyl-CoA reductase [NADPH]	0.011	0.011	0.00	0.008	0.020	0.00	0.014	0.029	0.0	<-5	<-5	-0.5	<-5	-0.5	-1.1	0.5	-0.9
Sugar transport (7 proteins)		2.05	2.00	1.43	2.92	1.37	1.77	1.37	4.17	0.0	-0.5	-1.0	0.5	0.4	0.0	-1.6	1.6	0.6
PtsI	Phosphoenolpyruvate-protein phosphotransferase	0.56	0.54	0.42	0.54	0.22	0.25	0.16	0.16	-0.1	-0.4	-0.4	-0.1	0.2	-0.5	0.0	-0.5	1.3
PtsH	Phosphocarrier protein HPr	0.33	0.45	0.30	0.37	0.10	0.13	0.13	0.12	0.4	-0.1	-0.3	0.2	0.4	0.4	0.1	0.3	1.7
Ctr	Glucose-specific enzyme IIA component of PTS	0.18	0.22	0.10	0.33	0.031	0.08	0.041	0.29	0.3	-0.8	-1.7	0.9	1.4	0.4	-2.8	3.2	2.5
ManX	PTS system mannose-specific EIIB component	0.12	0.07	0.06	0.13	0.045	0.05	0.031	0.17	-0.8	-1.0	-1.1	0.1	0.2	-0.5	-2.5	1.9	1.4
MalE	Maltose-binding periplasmic protein	0.28	0.31	0.25	0.76	0.13	0.23	0.17	1.37	0.1	-0.2	-1.6	1.4	0.8	0.4	-3.0	3.4	1.1
MalK	Maltose/maltodextrin import ATP-binding protein MalK	0.07	0.05	0.029	0.07	0.13	0.09	0.09	0.25	-0.5	-1.3	-1.3	0.0	-0.5	-0.5	-1.5	0.9	-0.9
LamB	Chain A, Maltoporin Maltose Complex	0.50	0.36	0.26	0.73	0.71	0.94	0.75	1.80	-0.5	-0.9	-1.5	0.5	0.4	0.1	-1.3	1.3	-0.5
Amino acid and peptide transport (7 proteins)		0.79	0.78	0.50	1.00	0.26	0.29	0.35	1.45	0.0	-0.7	-1.0	0.3	0.2	0.4	-2.1	2.5	1.6
GlnH	Glutamine ABC transporter periplasmic protein	0.11	0.18	0.07	0.06	0.07	0.046	0.07	0.05	0.7	-0.7	0.2	-0.9	-0.6	0.0	0.5	-0.5	0.7
ArtJ	Arginine transporter subunit	0.00	0.00	0.00	0.00	0.00	0.00	0.00	0.00	0.0	0.0	0.0	0.0	0.0	0.0	0.0	0.0	0.0
ArgT	Lysine-arginine-ornithine-binding periplasmic protein	0.08	0.07	0.11	0.12	0.027	0.06	0.07	0.12	-0.2	0.5	-0.1	0.6	1.2	1.4	-0.8	2.2	1.6
LivJ	Leucine/isoleucine/valine transporter subunit	0.26	0.31	0.19	0.55	0.05	0.09	0.10	0.12	0.3	-0.5	-1.5	1.1	0.8	1.0	-0.3	1.3	2.4

A-95

Suppl. Table 5.3.5 Proteome data of hFGF-2 production in *E. coli* BL21 (DE3) using defined and complex media

Name ¹	Protein name ¹	Defind (DNB) medium				Complex (LB) medium				Log ₂ (Ratio in Defind (DNB) medium)				Log ₂ (Ratio in Complex (LB) medium)				Log ₂ (DNB
		exp. phase before	1h after IPTG	5h after IPTG	stationary phase without	exp. phase before	1h after IPTG	3.5h after IPTG	stationary phase without	(1h after IPTG/ exp. before	(5h after IPTG/ exp. before	(5h after IPTG/ stationary without	(stationary IPTG/ exp. before	(1h after IPTG/ exp. before	(3.5h after IPTG/ exp. before	(3.5h after IPTG/ stationary without	(stationary IPTG/ exp. before	medium/ LB medium)
		IPTG	induction	induction	IPTG	IPTG	induction	induction	IPTG	IPTG)	IPTG)	IPTG)	IPTG)	IPTG)	IPTG)	IPTG)	IPTG)	IPTG)
		Whole Cell Protein Mass (WCPM) - %																
DppA	Chain A, Dipeptide Binding Protein Complex With Glycyl-L-Leucine	0.17	0.00	0.00	0.00	0.00	0.00	0.00	0.43	<-5	<-5	0.0	<-5	0.0	0.0	<-5	>5	>5
OppA	Periplasmic oligopeptide-binding protein	0.12	0.17	0.13	0.23	0.11	0.10	0.10	0.70	0.5	0.1	-0.8	0.9	-0.1	-0.1	-2.8	2.7	0.1
OppD	Oligopeptide transport ATP-binding protein OppD	0.040	0.045	0.00	0.038	0.00	0.00	0.00	0.031	0.2	<-5	<-5	-0.1	0.0	0.0	<-5	>5	>5
Other transport proteins (14 proteins)		5.45	5.51	4.93	5.66	5.58	7.53	4.56	5.04	0.0	-0.1	-0.2	0.1	0.4	-0.3	-0.1	-0.1	0.0
CusB	Copper/silver efflux system, membrane fusion protein	0.07	0.06	0.06	0.06	0.00	0.00	0.00	0.00	-0.2	-0.2	0.0	-0.2	0.0	0.0	0.0	0.0	>5
GsiB	Glutathione ABC transporter, periplasmic glutathione-binding protein GsiB	0.042	0.034	0.022	0.036	0.040	0.016	0.019	0.038	-0.3	-0.9	-0.7	-0.2	-1.3	-1.1	-1.0	-0.1	0.1
LptD	Exported protein required for envelope biosynthesis and integrity	0.06	0.08	0.047	0.10	0.08	0.08	0.044	0.06	0.4	-0.4	-1.1	0.7	0.0	-0.9	-0.4	-0.4	-0.4
FadL	Long-chain fatty acid transport protein	0.10	0.05	0.06	0.06	0.06	0.09	0.09	0.20	-1.0	-0.7	0.0	-0.7	0.6	0.6	-1.2	1.7	0.7
OmpF	Outer membrane porin 1a (Ia;b;F)	2.63	2.89	2.33	2.65	2.93	4.70	2.51	2.55	0.1	-0.2	-0.2	0.0	0.7	-0.2	0.0	-0.2	-0.2
OmpA	Outer membrane protein A	0.69	0.61	0.62	0.99	0.47	0.65	0.49	0.59	-0.2	-0.2	-0.7	0.5	0.5	0.1	-0.3	0.3	0.6
OmpA (2)	Outer membrane protein A	1.10	1.01	1.01	0.95	0.76	0.73	0.57	0.80	-0.1	-0.1	0.1	-0.2	-0.1	-0.4	-0.5	0.1	0.5
TolB	Translocation protein TolB	0.05	0.06	0.032	0.10	0.06	0.048	0.023	0.11	0.3	-0.6	-1.6	1.0	-0.3	-1.4	-2.3	0.9	-0.3
TolC	Outer membrane protein TolC	0.08	0.08	0.06	0.09	0.10	0.09	0.021	0.038	0.0	-0.4	-0.6	0.2	-0.2	-2.3	-0.9	-1.4	-0.3
OmpX	Outer membrane protein X	0.30	0.30	0.40	0.31	0.54	0.51	0.31	0.18	0.0	0.4	0.4	0.0	-0.1	-0.8	0.8	-1.6	-0.8
YbiT	Putative ATP-binding component of a transport system	0.05	0.047	0.027	0.038	0.06	0.06	0.09	0.036	-0.1	-0.9	-0.5	-0.4	0.0	0.6	1.3	-0.7	-0.3
YjjK	Uncharacterized ABC transporter ATP-binding protein YjjK	0.047	0.06	0.042	0.047	0.11	0.09	0.09	0.12	0.4	-0.2	-0.2	0.0	-0.3	-0.3	-0.4	0.1	-1.2
SecA	Preprotein translocase subunit, ATPase	0.09	0.09	0.09	0.07	0.17	0.15	0.15	0.11	0.0	0.0	0.4	-0.4	-0.2	-0.2	0.4	-0.6	-0.9

Suppl. Table 5.3.5 Proteome data of hFGF-2 production in *E. coli* BL21 (DE3) using defined and complex media

Name ¹	Protein name ¹	Defind (DNB) medium				Complex (LB) medium				Log ₂ (Ratio in Defind (DNB) medium)				Log ₂ (Ratio in Complex (LB) medium)				Log ₂ (DNB
		exp. phase before IPTG	1h after IPTG induction	5h after IPTG induction	stationary phase without IPTG	exp. phase before IPTG	1h after IPTG induction	3.5h after IPTG induction	stationary phase without IPTG	(1h after IPTG) exp. before	(5h after IPTG) exp. before	(5h after IPTG) stationary without	(stationary IPTG) exp. before	(1h after IPTG) before	(3.5h after IPTG) before	(3.5h after IPTG) without	(stationary IPTG) without	medium/ LB medium) exp.before
		Whole Cell Protein Mass (WCPM) - %																
YaeT	Outer membrane protein assembly factor yaeT	0.14	0.15	0.12	0.16	0.19	0.31	0.15	0.19	0.1	-0.2	-0.4	0.2	0.7	-0.3	-0.3	0.0	-0.4
RNA polymerases (3 proteins)		1.06	1.00	1.06	0.88	1.36	1.20	1.00	0.80	-0.1	0.0	0.3	-0.3	-0.2	-0.4	0.3	-0.8	-0.4
RpoA	DNA-directed RNA polymerase subunit alpha	0.54	0.54	0.60	0.61	0.71	0.74	0.57	0.44	0.0	0.2	0.0	0.2	0.1	-0.3	0.4	-0.7	-0.4
RpoB	DNA-directed RNA polymerase subunit beta	0.49	0.44	0.44	0.26	0.57	0.46	0.43	0.36	-0.2	-0.2	0.8	-0.9	-0.3	-0.4	0.3	-0.7	-0.2
RpoC	DNA-directed RNA polymerase subunit beta'	0.043	0.020	0.021	0.017	0.07	0.00	0.00	0.008	-1.1	-1.0	0.3	-1.3	<-5	<-5	<-5	-3.1	-0.7
RNA polymerase binding proteins (7 proteins)		0.83	0.91	0.87	0.88	1.24	1.07	1.04	0.77	0.1	0.1	0.0	0.1	-0.2	-0.3	0.4	-0.7	-0.6
RapA	RNA polymerase-associated protein rapA	0.029	0.018	0.031	0.015	0.08	0.043	0.048	0.020	-0.7	0.1	1.0	-1.0	-0.9	-0.7	1.3	-2.0	-1.5
NusA	Transcription elongation protein nusA	0.12	0.16	0.14	0.13	0.19	0.21	0.22	0.10	0.4	0.2	0.1	0.1	0.1	0.2	1.1	-0.9	-0.7
NusG	Transcription antitermination protein NusG	0.09	0.08	0.06	0.07	0.09	0.06	0.06	0.042	-0.2	-0.6	-0.2	-0.4	-0.6	-0.6	0.5	-1.1	0.0
Rho	Transcription termination factor Rho	0.37	0.38	0.40	0.34	0.62	0.55	0.42	0.29	0.0	0.1	0.2	-0.1	-0.2	-0.6	0.5	-1.1	-0.7
RpoD	RNA polymerase sigma-subunit	0.05	0.09	0.11	0.039	0.15	0.08	0.21	0.10	0.8	1.1	1.5	-0.4	-0.9	0.5	1.1	-0.6	-1.6
SspA	Stringent starvation protein A	0.08	0.09	0.08	0.12	0.07	0.08	0.05	0.11	0.2	0.0	-0.6	0.6	0.2	-0.5	-1.1	0.7	0.2
DksA	DnaK transcriptional regulator DksA	0.08	0.10	0.06	0.17	0.031	0.044	0.039	0.12	0.3	-0.4	-1.5	1.1	0.5	0.3	-1.6	2.0	1.4
Transcription factors (12 proteins)		1.78	1.84	1.74	1.79	1.65	1.69	1.68	2.03	0.0	0.0	0.0	0.0	0.0	0.0	-0.3	0.3	0.1
LacI	Lactose operon repressor	0.00	0.00	0.00	0.00	0.11	0.022	0.033	0.042	0.0	0.0	0.0	0.0	-2.3	-1.7	-0.3	-1.4	<-5
Hns	Global DNA-binding transcriptional dual regulator H-NS	0.71	0.73	0.77	0.80	0.75	0.90	0.75	0.85	0.0	0.1	-0.1	0.2	0.3	0.0	-0.2	0.2	-0.1

A-97

Suppl. Table 5.3.5 Proteome data of hFGF-2 production in *E. coli* BL21 (DE3) using defined and complex media

Name ¹	Protein name ¹	Defind (DNB) medium				Complex (LB) medium				Log ₂ (Ratio in Defind (DNB) medium)				Log ₂ (Ratio in Complex (LB) medium)				Log ₂ (DNB	
		exp. phase before IPTG	1h after IPTG	5h after IPTG	stationary phase without IPTG	exp. phase before IPTG	1h after IPTG	3.5h after IPTG	stationary phase without IPTG	(1h after IPTG/ exp. before IPTG)	(5h after IPTG/ exp. before IPTG)	(5h after IPTG/ stationary without IPTG)	(stationary without IPTG/ exp. before IPTG)	(1h after IPTG/ exp. before IPTG)	(3.5h after IPTG/ exp. before IPTG)	(3.5h after IPTG/ stationary without IPTG)	(stationary without IPTG/ exp. before IPTG)	medium/ LB medium) exp.before IPTG	
		Whole Cell Protein Mass (WCPM) - %																	
ArcA	Aerobic respiration control protein ArcA	0.09	0.07	0.07	0.08	0.08	0.08	0.08	0.14	-0.4	-0.4	-0.2	-0.2	0.0	0.0	-0.8	0.8	0.2	
KdgR	Transcriptional regulator kdgR	0.031	0.034	0.048	0.043	0.029	0.037	0.027	0.032	0.1	0.6	0.2	0.5	0.4	-0.1	-0.2	0.1	0.1	
OxyR	Hydrogen peroxide-inducible genes activator	0.038	0.05	0.039	0.043	0.029	0.06	0.046	0.037	0.4	0.0	-0.1	0.2	1.0	0.7	0.3	0.4	0.4	
BasR	Transcriptional regulatory protein BasR	0.06	0.06	0.06	0.07	0.042	0.06	0.06	0.08	0.0	0.0	-0.2	0.2	0.5	0.5	-0.4	0.9	0.5	
CspC	CspC	0.55	0.61	0.42	0.43	0.34	0.43	0.33	0.62	0.1	-0.4	0.0	-0.4	0.3	0.0	-0.9	0.9	0.7	
StpA	DNA binding protein, nucleoid-associated	0.06	0.06	0.06	0.07	0.07	0.00	0.22	0.06	0.0	0.0	-0.2	0.2	<-5	1.7	1.9	-0.2	-0.2	
PspA	Phage shock protein A	0.028	0.040	0.043	0.041	0.027	0.00	0.034	0.018	0.5	0.6	0.1	0.6	<-5	0.3	0.9	-0.6	0.1	
OmpR	Transcriptional regulatory protein ompR	0.11	0.10	0.11	0.12	0.10	0.06	0.08	0.10	-0.1	0.0	-0.1	0.1	-0.7	-0.3	-0.3	0.0	0.1	
CpxR	Transcriptional regulatory protein CpxR	0.044	0.038	0.046	0.041	0.026	0.05	0.00	0.035	-0.2	0.1	0.2	-0.1	0.9	<-5	<-5	0.4	0.8	
PhoP	Transcriptional regulatory protein phoP	0.06	0.045	0.07	0.05	0.031	0.00	0.020	0.028	-0.4	0.2	0.5	-0.3	<-5	-0.6	-0.5	-0.1	1.0	
Ribosomal proteins (5 proteins)		3.55	3.78	4.32	3.76	5.41	4.75	4.47	2.74	0.1	0.3	0.2	0.1	-0.2	-0.3	0.7	-1.0	-0.6	
RplL	50S ribosomal protein L7/L12	0.51	0.66	0.82	0.87	0.91	1.17	1.00	0.65	0.4	0.7	-0.1	0.8	0.4	0.1	0.6	-0.5	-0.8	
RplI	50S ribosomal protein L9	0.54	0.53	0.55	0.53	0.78	0.76	0.59	0.37	0.0	0.0	0.1	0.0	0.0	-0.4	0.7	-1.1	-0.5	
RpsA	30S ribosomal protein S1	1.38	1.42	1.63	1.49	1.99	2.04	1.75	1.16	0.0	0.2	0.1	0.1	0.0	-0.2	0.6	-0.8	-0.5	
RpsB	30S ribosomal protein S2	0.66	0.74	0.87	0.54	1.28	0.40	0.87	0.41	0.2	0.4	0.7	-0.3	-1.7	-0.6	1.1	-1.6	-1.0	
RpsF	30S ribosomal protein S6	0.45	0.43	0.45	0.33	0.46	0.38	0.27	0.15	-0.1	0.0	0.4	-0.4	-0.3	-0.8	0.8	-1.6	0.0	

Suppl. Table 5.3.5 Proteome data of hFGF-2 production in *E. coli* BL21 (DE3) using defined and complex media

Name ¹	Protein name ¹	Defind (DNB) medium				Complex (LB) medium				Log ₂ (Ratio in Defind (DNB) medium)				Log ₂ (Ratio in Complex (LB) medium)				Log ₂ (DNB medium/ LB medium) exp.before
		exp. phase before IPTG	1h after IPTG induction	5h after IPTG induction	stationary phase without IPTG	exp. phase before IPTG	1h after IPTG induction	3.5h after IPTG induction	stationary phase without IPTG	(1h after IPTG) exp. before	(5h after IPTG) exp. before	(5h after IPTG) without	(stationary without IPTG) exp. before	(1h after IPTG) before	(3.5h after IPTG) before	(3.5h after IPTG) without	(stationary without IPTG) exp. before	
Ribosome-associated proteins (8 proteins)		1.05	1.16	1.16	1.56	1.67	1.71	1.37	1.20	0.1	0.1	-0.4	0.6	0.0	-0.3	0.2	-0.5	-0.7
EngA	Predicted GTP-binding protein	0.039	0.036	0.032	0.027	0.035	0.00	0.023	0.023	-0.1	-0.3	0.2	-0.5	<-5	-0.6	0.0	-0.6	0.2
YcaO	UPF0142 protein ycaO	0.021	0.027	0.024	0.017	0.06	0.08	0.049	0.031	0.4	0.2	0.5	-0.3	0.4	-0.3	0.7	-1.0	-1.5
EngD (YchF)	GTP-dependent nucleic acid-binding protein EngD	0.06	0.09	0.06	0.09	0.10	0.13	0.09	0.08	0.6	0.0	-0.6	0.6	0.4	-0.2	0.2	-0.3	-0.7
TypA	GTP-binding protein typA/BipA	0.20	0.27	0.23	0.16	0.31	0.34	0.26	0.15	0.4	0.2	0.5	-0.3	0.1	-0.3	0.8	-1.0	-0.6
HflX	GTP-binding protein hflX	0.021	0.027	0.039	0.043	0.037	0.05	0.06	0.05	0.4	0.9	-0.1	1.0	0.4	0.7	0.3	0.4	-0.8
Tig	Trigger factor	0.65	0.66	0.69	0.72	0.98	1.12	0.85	0.63	0.0	0.1	-0.1	0.1	0.2	-0.2	0.4	-0.6	-0.6
Frr	Ribosome recycling factor	0.05	0.00	0.09	0.14	0.030	0.00	0.034	0.11	<-5	0.8	-0.6	1.5	<-5	0.2	-1.7	1.9	0.7
RaiA	Ribosome-associated inhibitor A	0.00	0.06	0.00	0.36	0.11	0.00	0.00	0.12	>5	0.0	<-5	>5	<-5	<-5	<-5	0.1	<-5
Aminoacyl-tRNA synthetases (23 proteins)		2.80	2.75	3.04	2.49	3.69	3.67	3.35	3.06	0.0	0.1	0.3	-0.2	0.0	-0.1	0.1	-0.3	-0.4
AlaS	Alanyl-tRNA synthetase	0.22	0.24	0.21	0.15	0.45	0.33	0.36	0.60	0.1	-0.1	0.5	-0.6	-0.4	-0.3	-0.7	0.4	-1.0
ArgS	Arginyl-tRNA synthetase	0.049	0.05	0.05	0.049	0.08	0.08	0.06	0.033	0.0	0.0	0.0	0.0	0.0	-0.4	0.9	-1.3	-0.7
AsnS	Asparaginyl tRNA synthetase	0.22	0.18	0.19	0.22	0.28	0.25	0.25	0.17	-0.3	-0.2	-0.2	0.0	-0.2	-0.2	0.6	-0.7	-0.3
AspS	Aspartyl-tRNA synthetase	0.18	0.18	0.19	0.18	0.20	0.18	0.15	0.17	0.0	0.1	0.1	0.0	-0.2	-0.4	-0.2	-0.2	-0.2
CysS	Cysteinyl-tRNA synthetase	0.12	0.08	0.08	0.09	0.09	0.16	0.14	0.09	-0.6	-0.6	-0.2	-0.4	0.8	0.6	0.6	0.0	0.4
GlnS	Glutamyl-tRNA synthetase	0.09	0.09	0.11	0.08	0.13	0.18	0.16	0.08	0.0	0.3	0.5	-0.2	0.5	0.3	1.0	-0.7	-0.5
GltX	Glutamyl-tRNA synthetase	0.10	0.09	0.09	0.09	0.10	0.10	0.07	0.16	-0.2	-0.2	0.0	-0.2	0.0	-0.5	-1.2	0.7	0.0

A-99

Suppl. Table 5.3.5 Proteome data of hFGF-2 production in *E. coli* BL21 (DE3) using defined and complex media

Name ¹	Protein name ¹	Defind (DNB) medium				Complex (LB) medium				Log ₂ (Ratio in Defind (DNB) medium)				Log ₂ (Ratio in Complex (LB) medium)				Log ₂ (DNB	
		exp. phase before IPTG	1h after IPTG	5h after IPTG	stationary phase without IPTG	exp. phase before IPTG	1h after IPTG	3.5h after IPTG	stationary phase without IPTG	(1h after IPTG/ exp. before IPTG)	(5h after IPTG/ exp. before IPTG)	(5h after IPTG/ stationary without IPTG)	(stationary without IPTG/ exp. before IPTG)	(1h after IPTG/ exp. before IPTG)	(3.5h after IPTG/ exp. before IPTG)	(3.5h after IPTG/ stationary without IPTG)	(stationary without IPTG/ exp. before IPTG)	medium/ LB medium) exp.before IPTG	
		Whole Cell Protein Mass (WCPM) - %																	
GlyQ	Glycyl-tRNA synthetase alpha subunit	0.12	0.05	0.07	0.044	0.08	0.10	0.09	0.11	-1.3	-0.8	0.7	-1.4	0.3	0.2	-0.3	0.5	0.6	
GlyS	Glycyl-tRNA synthetase beta subunit	0.15	0.12	0.13	0.09	0.21	0.24	0.18	0.09	-0.3	-0.2	0.5	-0.7	0.2	-0.2	1.0	-1.2	-0.5	
HisS	Histidyl-tRNA synthetase	0.08	0.06	0.08	0.06	0.017	0.08	0.044	0.06	-0.4	0.0	0.4	-0.4	2.2	1.4	-0.4	1.8	2.2	
IleS	Isoleucyl-tRNA synthetase	0.16	0.13	0.14	0.09	0.35	0.15	0.25	0.18	-0.3	-0.2	0.6	-0.8	-1.2	-0.5	0.5	-1.0	-1.1	
LeuS	Leucyl-tRNA synthetase	0.26	0.24	0.36	0.21	0.30	0.40	0.34	0.21	-0.1	0.5	0.8	-0.3	0.4	0.2	0.7	-0.5	-0.2	
LysS	Lysyl-tRNA synthetase	0.13	0.12	0.14	0.11	0.25	0.20	0.17	0.12	-0.1	0.1	0.3	-0.2	-0.3	-0.6	0.5	-1.1	-0.9	
MetG	Methionyl-tRNA synthetase	0.12	0.10	0.10	0.10	0.14	0.10	0.11	0.11	-0.3	-0.3	0.0	-0.3	-0.5	-0.3	0.0	-0.3	-0.2	
PheT	Phenylalanyl-tRNA synthetase subunit beta	0.17	0.20	0.19	0.18	0.15	0.14	0.13	0.11	0.2	0.2	0.1	0.1	-0.1	-0.2	0.2	-0.4	0.2	
ProS	Prolyl-tRNA synthetase	0.11	0.24	0.22	0.17	0.19	0.23	0.22	0.07	1.1	1.0	0.4	0.6	0.3	0.2	1.7	-1.4	-0.8	
SerS	Seryl-tRNA synthetase	0.11	0.11	0.10	0.09	0.14	0.14	0.11	0.10	0.0	-0.1	0.2	-0.3	0.0	-0.3	0.1	-0.5	-0.3	
ThrS	Threonyl-tRNA synthetase	0.12	0.11	0.14	0.13	0.19	0.10	0.14	0.15	-0.1	0.2	0.1	0.1	-0.9	-0.4	-0.1	-0.3	-0.7	
TyrS	Tyrosyl-tRNA synthetase	0.13	0.12	0.15	0.09	0.18	0.16	0.19	0.14	-0.1	0.2	0.7	-0.5	-0.2	0.1	0.4	-0.4	-0.5	
LysU	Lysyl-tRNA synthetase, heat inducible	0.036	0.035	0.09	0.041	0.07	0.09	0.08	0.07	0.0	1.3	1.1	0.2	0.4	0.2	0.2	0.0	-1.0	
MnmA	tRNA-Specific 2-thiouridylase mnmA	0.05	0.09	0.042	0.08	0.043	0.12	0.036	0.05	0.8	-0.3	-0.9	0.7	1.5	-0.3	-0.5	0.2	0.2	
YgfZ	tRNA-modifying protein ygfZ	0.040	0.06	0.07	0.06	0.016	0.13	0.045	0.08	0.6	0.8	0.2	0.6	3.0	1.5	-0.8	2.3	1.3	
Fmt	Methionyl-tRNA formyltransferase	0.046	0.036	0.10	0.06	0.018	0.032	0.029	0.09	-0.4	1.1	0.7	0.4	0.8	0.7	-1.6	2.3	1.4	

Suppl. Table 5.3.5 Proteome data of hFGF-2 production in *E. coli* BL21 (DE3) using defined and complex media

Name ¹	Protein name ¹	Defind (DNB) medium				Complex (LB) medium				Log ₂ (Ratio in Defind (DNB) medium)				Log ₂ (Ratio in Complex (LB) medium)				Log ₂ (DNB medium/LB medium)
		exp. phase before IPTG	1h after IPTG induction	5h after IPTG induction	stationary phase without IPTG	exp. phase before IPTG	1h after IPTG induction	3.5h after IPTG induction	stationary phase without IPTG	(1h after IPTG) exp. before IPTG	(5h after IPTG) exp. before IPTG	(5h after IPTG) stationary without IPTG	(stationary without IPTG) exp. before IPTG	(1h after IPTG) exp. before IPTG	(3.5h after IPTG) exp. before IPTG	(3.5h after IPTG) stationary without IPTG	(stationary without IPTG) exp. before IPTG	exp.before
Elongation factors (6 proteins)		4.93	6.01	5.55	6.09	6.74	8.11	7.35	6.17	0.3	0.2	-0.1	0.3	0.3	0.1	0.3	-0.1	-0.5
InfB	Initiation factor IF2-gamma	0.15	0.11	0.16	0.08	0.28	0.09	0.24	0.15	-0.4	0.1	1.0	-0.9	-1.6	-0.2	0.7	-0.9	-0.9
FusA	Elongation factor G	1.30	1.72	1.58	1.38	1.67	2.15	2.12	1.49	0.4	0.3	0.2	0.1	0.4	0.3	0.5	-0.2	-0.4
TufA	Elongation factor Tu 1	2.77	3.48	3.08	3.76	3.72	4.70	4.12	3.89	0.3	0.2	-0.3	0.4	0.3	0.1	0.1	0.1	-0.4
Tsf	Chain B, Elongation Factor Complex Ef-TuEF-Ts	0.65	0.62	0.64	0.80	0.97	1.08	0.76	0.58	-0.1	0.0	-0.3	0.3	0.2	-0.4	0.4	-0.7	-0.6
LepA	GTP-binding protein LepA	0.041	0.048	0.045	0.029	0.05	0.06	0.06	0.037	0.2	0.1	0.6	-0.5	0.3	0.3	0.7	-0.4	-0.3
PrfC	Peptide chain release factor 3	0.022	0.026	0.031	0.028	0.046	0.039	0.041	0.037	0.2	0.5	0.1	0.3	-0.2	-0.2	0.1	-0.3	-1.1
RNA degradation (3 proteins)		0.52	0.56	0.51	0.42	0.68	0.98	0.64	0.53	0.1	0.0	0.3	-0.3	0.5	-0.1	0.3	-0.4	-0.4
Pnp	Polyribonucleotide nucleotidyltransferase	0.44	0.48	0.43	0.36	0.56	0.88	0.53	0.44	0.1	0.0	0.3	-0.3	0.7	-0.1	0.3	-0.3	-0.3
Rnb	Exoribonuclease II	0.05	0.05	0.048	0.047	0.09	0.07	0.09	0.07	0.0	-0.1	0.0	-0.1	-0.4	0.0	0.4	-0.4	-0.8
RhlB	ATP-dependent RNA helicase	0.020	0.030	0.028	0.021	0.032	0.032	0.021	0.018	0.6	0.5	0.4	0.1	0.0	-0.6	0.2	-0.8	-0.7
Isomerases (5 proteins)		0.72	0.79	0.62	0.80	0.55	0.56	0.38	0.86	0.1	-0.2	-0.4	0.2	0.0	-0.5	-1.2	0.6	0.4
PpiB	Peptidyl-prolyl cis-trans isomerase B (rotamase B)	0.07	0.10	0.08	0.15	0.08	0.047	0.048	0.12	0.5	0.2	-0.9	1.1	-0.8	-0.7	-1.3	0.6	-0.2
SurA	Peptidyl-prolyl cis-trans isomerase SurA	0.09	0.09	0.08	0.09	0.07	0.10	0.10	0.11	0.0	-0.2	-0.2	0.0	0.5	0.5	-0.1	0.7	0.4
FklB	FKBP-type 22 kDa peptidyl-prolyl cis-trans isomerase	0.10	0.12	0.06	0.13	0.06	0.07	0.06	0.15	0.3	-0.7	-1.1	0.4	0.2	0.0	-1.3	1.3	0.7
FkpA	FKBP-type peptidyl-prolyl cis-trans isomerase	0.15	0.17	0.16	0.10	0.17	0.17	0.043	0.20	0.2	0.1	0.7	-0.6	0.0	-2.0	-2.2	0.2	-0.2

A-101

Appendix

Suppl. Table 5.3.5 Proteome data of hFGF-2 production in *E. coli* BL21 (DE3) using defined and complex media

Name ¹	Protein name ¹	Defind (DNB) medium				Complex (LB) medium				Log ₂ (Ratio in Defind (DNB) medium)				Log ₂ (Ratio in Complex (LB) medium)				Log ₂ (DNB
		exp. phase before	1h after IPTG	5h after IPTG	stationary phase without IPTG	exp. phase before	1h after IPTG	3.5h after IPTG	stationary phase without IPTG	(1h after IPTG/ exp. before	(5h after IPTG/ exp. before	(5h after IPTG/ stationary without exp. before	(stationary IPTG/ exp. before	(1h after IPTG/ exp. before	(3.5h after IPTG/ exp. before	(3.5h after IPTG/ stationary without exp. before	(stationary IPTG/ exp. before	medium/ LB medium)
		Whole Cell Protein Mass (WCPM) - %																
SlyD	FKBP-type peptidyl-prolyl cis-trans isomerase slyD	0.31	0.31	0.25	0.32	0.18	0.18	0.13	0.28	0.0	-0.3	-0.4	0.0	0.0	-0.5	-1.1	0.6	0.8
Chaperones (9 proteins)		1.94	2.63	5.46	1.95	2.92	5.92	7.12	2.75	0.4	1.5	1.5	0.0	1.0	1.3	1.4	-0.1	-0.6
DnaK	Molecular chaperone DnaK	0.56	0.87	2.19	0.56	0.89	2.10	2.53	0.81	0.6	2.0	2.0	0.0	1.2	1.5	1.6	-0.1	-0.7
GrpE	Heat shock protein GrpE	0.08	0.09	0.19	0.07	0.14	0.27	0.27	0.10	0.2	1.2	1.4	-0.2	0.9	0.9	1.4	-0.5	-0.8
GroL	60 kDa chaperonin (GroEL protein)	0.83	1.13	1.71	0.88	1.22	2.26	2.28	1.32	0.4	1.0	1.0	0.1	0.9	0.9	0.8	0.1	-0.6
GroS	Co-chaperonin GroES	0.11	0.14	0.26	0.13	0.15	0.36	0.54	0.14	0.3	1.2	1.0	0.2	1.3	1.8	1.9	-0.1	-0.4
HtpG	Heat shock protein 90	0.16	0.21	0.62	0.13	0.28	0.48	0.66	0.14	0.4	2.0	2.3	-0.3	0.8	1.2	2.2	-1.0	-0.8
HscA	Fe-S protein assembly chaperone HscA	0.040	0.036	0.029	0.042	0.05	0.05	0.040	0.027	-0.2	-0.5	-0.5	0.1	0.0	-0.3	0.6	-0.9	-0.3
ClpA	ATP-dependent Clp protease ATP-binding subunit	0.05	0.049	0.039	0.06	0.037	0.025	0.038	0.06	0.0	-0.4	-0.6	0.3	-0.6	0.0	-0.7	0.7	0.4
ClpB	Protein disaggregation chaperone	0.021	0.027	0.08	0.021	0.06	0.11	0.14	0.042	0.4	1.9	1.9	0.0	0.9	1.2	1.7	-0.5	-1.5
IbpA	Small heat shock protein ibpA	0.09	0.09	0.33	0.06	0.10	0.27	0.61	0.10	0.0	1.9	2.5	-0.6	1.4	2.6	2.6	0.0	-0.2
Proteases (13 proteins)		0.88	0.85	1.01	0.83	1.03	1.28	1.55	1.38	-0.1	0.2	0.3	-0.1	0.3	0.6	0.2	0.4	-0.2
DegP	Serine endoprotease	0.017	0.025	0.030	0.037	0.00	0.00	0.00	0.027	0.6	0.8	-0.3	1.1	0.0	0.0	<-5	>5	>5
PepQ	Proline dipeptidase	0.08	0.08	0.07	0.10	0.08	0.10	0.13	0.16	0.0	-0.2	-0.5	0.3	0.3	0.7	-0.3	1.0	0.0
PepD	Aminoacyl-histidine dipeptidase	0.11	0.12	0.09	0.10	0.13	0.22	0.20	0.24	0.1	-0.3	-0.2	-0.1	0.8	0.6	-0.3	0.9	-0.2
PepN	Aminopeptidase N	0.12	0.09	0.05	0.08	0.17	0.13	0.14	0.20	-0.4	-1.3	-0.7	-0.6	-0.4	-0.3	-0.5	0.2	-0.5

Suppl. Table 5.3.5 Proteome data of hFGF-2 production in *E. coli* BL21 (DE3) using defined and complex media

Name ¹	Protein name ¹	Defind (DNB) medium				Complex (LB) medium				Log ₂ (Ratio in Defind (DNB) medium)				Log ₂ (Ratio in Complex (LB) medium)				Log ₂ (DNB
		exp. phase before IPTG	1h after IPTG induction	5h after IPTG induction	stationary phase without IPTG	exp. phase before IPTG	1h after IPTG induction	3.5h after IPTG induction	stationary phase without IPTG	(1h after IPTG) exp. before	(5h after IPTG) exp. before	(5h after IPTG) stationary without	(stationary IPTG) exp. before	(1h after IPTG) exp. before	(3.5h after IPTG) exp. before	(3.5h after IPTG) stationary without	(stationary IPTG) exp. before	medium/LB medium) exp.before
		Whole Cell Protein Mass (WCPM) - %								IPTG	IPTG	IPTG	IPTG	IPTG	IPTG	IPTG	IPTG	IPTG
Dep	Dipeptidyl carboxypeptidase II	0.037	0.016	0.034	0.017	0.00	0.00	0.025	0.00	-1.2	-0.1	1.0	-1.1	0.0	>5	>5	0.0	>5
Prc	Carboxy-terminal protease	0.031	0.025	0.021	0.028	0.043	0.029	0.032	0.032	-0.3	-0.6	-0.4	-0.1	-0.6	-0.4	0.0	-0.4	-0.5
PmbA	Protein pmbA	0.039	0.030	0.033	0.034	0.041	0.045	0.08	0.10	-0.4	-0.2	0.0	-0.2	0.1	1.0	-0.3	1.3	-0.1
ClpP	ATP-dependent Clp protease proteolytic subunit	0.08	0.07	0.11	0.08	0.09	0.10	0.09	0.10	-0.2	0.5	0.5	0.0	0.2	0.0	-0.2	0.2	-0.2
HslIV	ATP-dependent protease peptidase subunit	0.030	0.05	0.14	0.035	0.06	0.09	0.14	0.032	0.7	2.2	2.0	0.2	0.6	1.2	2.1	-0.9	-1.0
HslIU	ATP-dependent protease ATP-binding subunit	0.10	0.14	0.30	0.12	0.18	0.29	0.38	0.13	0.5	1.6	1.3	0.3	0.7	1.1	1.5	-0.5	-0.8
PepB	Peptidase B	0.12	0.09	0.10	0.08	0.12	0.14	0.20	0.17	-0.4	-0.3	0.3	-0.6	0.2	0.7	0.2	0.5	0.0
PepP	Proline aminopeptidase P II	0.047	0.048	0.037	0.06	0.06	0.05	0.06	0.08	0.0	-0.3	-0.7	0.4	-0.3	0.0	-0.4	0.4	-0.4
PrlC	Oligopeptidase A	0.08	0.06	0.00	0.05	0.049	0.08	0.07	0.11	-0.4	<-5	<-5	-0.7	0.7	0.5	-0.7	1.2	0.7
Other dehydrogenases (9 proteins)		0.69	0.66	0.66	0.75	0.61	0.74	0.67	1.13	-0.1	-0.1	-0.2	0.1	0.3	0.1	-0.8	0.9	0.2
YdfG	3-Hydroxy acid dehydrogenase	0.10	0.09	0.11	0.11	0.049	0.10	0.044	0.07	-0.2	0.1	0.0	0.1	1.0	-0.2	-0.7	0.5	1.0
YqhD	Alcohol dehydrogenase, NAD(P)-dependent	0.11	0.10	0.12	0.09	0.14	0.14	0.12	0.18	-0.1	0.1	0.4	-0.3	0.0	-0.2	-0.6	0.4	-0.3
AldB	Aldehyde dehydrogenase B	0.031	0.027	0.029	0.11	0.037	0.022	0.06	0.16	-0.2	-0.1	-1.9	1.8	-0.8	0.7	-1.4	2.1	-0.3
AldA	Lactaldehyde dehydrogenase	0.10	0.10	0.09	0.10	0.047	0.10	0.12	0.36	0.0	-0.2	-0.2	0.0	1.1	1.4	-1.6	2.9	1.1
YhhX	Predicted oxidoreductase with NAD(P)-binding Rossmann-fold domain	0.046	0.044	0.023	0.038	0.033	0.06	0.044	0.049	-0.1	-1.0	-0.7	-0.3	0.9	0.4	-0.2	0.6	0.5
Ugd	UDP-Glucose 6-dehydrogenase	0.16	0.12	0.11	0.14	0.12	0.13	0.13	0.13	-0.4	-0.5	-0.3	-0.2	0.1	0.1	0.0	0.1	0.4
HdhA	7-Alpha-hydroxysteroid dehydrogenase	0.030	0.048	0.05	0.033	0.05	0.08	0.05	0.07	0.7	0.7	0.6	0.1	0.7	0.0	-0.5	0.5	-0.7

A-103

Suppl. Table 5.3.5 Proteome data of hFGF-2 production in *E. coli* BL21 (DE3) using defined and complex media

Name ¹	Protein name ¹	Defind (DNB) medium				Complex (LB) medium				Log ₂ (Ratio in Defind (DNB) medium)				Log ₂ (Ratio in Complex (LB) medium)				Log ₂ (DNB
		exp. phase before	1h after IPTG	5h after IPTG	stationary phase without IPTG	exp. phase before	1h after IPTG	3.5h after IPTG	stationary phase without IPTG	(1h after IPTG/ exp. before	(5h after IPTG/ exp. before	(5h after IPTG/ stationary without exp. before	(stationary IPTG/ exp. before	(1h after IPTG/ exp. before	(3.5h after IPTG/ exp. before	(3.5h after IPTG/ stationary without exp. before	(stationary IPTG/ exp. before	medium/ LB medium) exp.before
		Whole Cell Protein Mass (WCPM) - %																
HybC	Hydrogenase-2 large chain	0.028	0.038	0.042	0.041	0.041	0.041	0.038	0.040	0.4	0.6	0.0	0.6	0.0	-0.1	-0.1	0.0	-0.6
TrxB	Thioredoxin reductase	0.08	0.09	0.08	0.08	0.09	0.08	0.07	0.06	0.2	0.0	0.0	0.0	-0.2	-0.4	0.2	-0.6	-0.2
Oxidoreductases (8 proteins)		0.39	0.36	0.43	0.65	0.34	0.34	0.38	0.54	-0.1	0.1	-0.6	0.7	0.0	0.2	-0.5	0.7	0.2
Gor	Glutathione reductase	0.028	0.034	0.026	0.07	0.047	0.022	0.028	0.07	0.3	-0.1	-1.4	1.3	-1.1	-0.7	-1.3	0.6	-0.7
NfsA	Oxygen-insensitive NADPH nitroreductase	0.09	0.07	0.039	0.06	0.09	0.07	0.05	0.043	-0.4	-1.2	-0.6	-0.6	-0.4	-0.8	0.2	-1.1	0.0
QueF	NADPH-dependent 7-cyano-7-deazaguanine reductase	0.05	0.041	0.046	0.08	0.019	0.046	0.05	0.041	-0.3	-0.1	-0.8	0.7	1.3	1.4	0.3	1.1	1.4
NemA	N-Ethylmaleimide reductase	0.031	0.030	0.039	0.012	0.023	0.00	0.00	0.025	0.0	0.3	1.7	-1.4	<-5	<-5	<-5	0.1	0.4
SthA	Soluble pyridine nucleotide transhydrogenase	0.08	0.07	0.07	0.06	0.07	0.09	0.10	0.13	-0.2	-0.2	0.2	-0.4	0.4	0.5	-0.4	0.9	0.2
CueO	Blue copper oxidase CueO	0.033	0.028	0.016	0.034	0.025	0.030	0.029	0.049	-0.2	-1.0	-1.1	0.0	0.3	0.2	-0.8	1.0	0.4
Bfr	Bacterioferritin, iron storage and detoxification protein	0.044	0.05	0.13	0.28	0.06	0.08	0.10	0.13	0.2	1.6	-1.1	2.7	0.4	0.7	-0.4	1.1	-0.4
WrbA	Flavoprotein wrbA	0.031	0.038	0.06	0.05	0.00	0.00	0.028	0.05	0.3	1.0	0.3	0.7	0.0	>5	-0.8	>5	>5
Hydroperoxide reductases and superoxide dismutase (5 proteins)		1.26	1.45	1.17	1.92	0.83	0.88	0.75	1.83	0.2	-0.1	-0.7	0.6	0.1	-0.1	-1.3	1.1	0.6
AhpF	Alkyl hydroperoxide reductase subunit F	0.08	0.11	0.10	0.10	0.11	0.10	0.08	0.15	0.5	0.3	0.0	0.3	-0.1	-0.5	-0.9	0.4	-0.5
AhpC	Alkyl hydroperoxide reductase subunit C	0.79	0.89	0.65	1.10	0.53	0.57	0.46	1.10	0.2	-0.3	-0.8	0.5	0.1	-0.2	-1.3	1.1	0.6
Tpx	Thiol peroxidase	0.13	0.18	0.11	0.20	0.044	0.049	0.07	0.22	0.5	-0.2	-0.9	0.6	0.2	0.7	-1.7	2.3	1.6
SodB	Superoxide dismutase [Fe]	0.13	0.19	0.21	0.45	0.030	0.028	0.06	0.21	0.5	0.7	-1.1	1.8	-0.1	1.0	-1.8	2.8	2.1

Suppl. Table 5.3.5 Proteome data of hFGF-2 production in *E. coli* BL21 (DE3) using defined and complex media

Name ¹	Protein name ¹	Defind (DNB) medium				Complex (LB) medium				Log ₂ (Ratio in Defind (DNB) medium)				Log ₂ (Ratio in Complex (LB) medium)				Log ₂ (DNB medium/LB medium)
		exp. phase before IPTG	1h after IPTG induction	5h after IPTG induction	stationary phase without IPTG	exp. phase before IPTG	1h after IPTG induction	3.5h after IPTG induction	stationary phase without IPTG	(1h after IPTG) exp. before	(5h after IPTG) exp. before	(5h after IPTG) stationary without	(stationary without IPTG) exp. before	(1h after IPTG) before	(3.5h after IPTG) before	(3.5h after IPTG) stationary without	(stationary without IPTG) exp. before	exp.before
		Whole Cell Protein Mass (WCPM) - %								IPTG	IPTG	IPTG	IPTG	IPTG	IPTG	IPTG	IPTG	IPTG
KatG	Catalase/hydroperoxidase HPI(I)	0.13	0.09	0.09	0.07	0.12	0.13	0.08	0.16	-0.5	-0.5	0.4	-0.9	0.1	-0.6	-1.0	0.4	0.1
DNA protection and repair (6 proteins)		0.83	0.86	0.58	0.84	0.51	0.27	0.36	1.29	0.1	-0.5	-0.5	0.0	-0.9	-0.5	-1.8	1.3	0.7
Ssb	Single-stranded DNA-binding protein	0.046	0.045	0.037	0.047	0.024	0.00	0.044	0.06	0.0	-0.3	-0.3	0.0	<-5	0.9	-0.4	1.3	0.9
Dps	DNA starvation/stationary phase protection protein Dps	0.032	0.015	0.09	0.21	0.031	0.00	0.020	0.42	-1.1	1.5	-1.2	2.7	<-5	-0.6	-4.4	3.8	0.0
UspA	Universal stress protein A	0.07	0.06	0.05	0.15	0.09	0.07	0.08	0.16	-0.2	-0.5	-1.6	1.1	-0.4	-0.2	-1.0	0.8	-0.4
UspG	Universal stress protein G	0.06	0.041	0.09	0.10	0.10	0.00	0.00	0.00	-0.5	0.6	-0.2	0.7	<-5	<-5	0.0	<-5	-0.7
SodA	Chain A, Manganese Superoxide Dismutase	0.57	0.64	0.19	0.29	0.18	0.12	0.17	0.59	0.2	-1.6	-0.6	-1.0	-0.6	-0.1	-1.8	1.7	1.7
PolA	DNA polymerase I	0.06	0.049	0.12	0.045	0.09	0.08	0.048	0.06	-0.3	1.0	1.4	-0.4	-0.2	-0.9	-0.3	-0.6	-0.6
Unclassified proteins (7 proteins)		0.63	0.57	0.53	0.59	0.46	0.36	0.39	0.36	-0.1	-0.2	-0.2	-0.1	-0.4	-0.2	0.1	-0.4	0.5
GyrB	DNA gyrase subunit B	0.29	0.23	0.24	0.27	0.12	0.07	0.08	0.046	-0.3	-0.3	-0.2	-0.1	-0.8	-0.6	0.8	-1.4	1.3
MreB	Regulator of ftsI, penicillin binding protein 3, septation function	0.05	0.08	0.07	0.07	0.09	0.08	0.08	0.08	0.7	0.5	0.0	0.5	-0.2	-0.2	0.0	-0.2	-0.8
FtsZ	Cell division protein FtsZ	0.07	0.07	0.044	0.06	0.06	0.09	0.07	0.09	0.0	-0.7	-0.4	-0.2	0.6	0.2	-0.4	0.6	0.2
RsmC	Ribosomal RNA small subunit methyltransferase C	0.017	0.019	0.029	0.034	0.040	0.034	0.042	0.05	0.2	0.8	-0.2	1.0	-0.2	0.1	-0.3	0.3	-1.2
Can	Carbonic anhydrase	0.10	0.10	0.06	0.08	0.13	0.09	0.10	0.05	0.0	-0.7	-0.4	-0.3	-0.5	-0.4	1.0	-1.4	-0.4
FrsA	Fermentation/respiration switch protein	0.030	0.021	0.015	0.016	0.029	0.00	0.018	0.032	-0.5	-1.0	-0.1	-0.9	<-5	-0.7	-0.8	0.1	0.0
YeaG	Uncharacterized protein yeaG	0.07	0.06	0.07	0.06	0.00	0.00	0.00	0.00	-0.2	0.0	0.2	-0.2	0.0	0.0	0.0	0.0	>5

A-105

Suppl. Table 5.3.5 Proteome data of hFGF-2 production in *E. coli* BL21 (DE3) using defined and complex media

Name ¹	Protein name ¹	Defind (DNB) medium				Complex (LB) medium				Log ₂ (Ratio in Defind (DNB) medium)				Log ₂ (Ratio in Complex (LB) medium)				Log ₂ (DNB
		exp. phase before	1h after IPTG	5h after IPTG	stationary phase without IPTG	exp. phase before	1h after IPTG	3.5h after IPTG	stationary phase without IPTG	(1h after IPTG/ exp. before	(5h after IPTG/ exp. before	(5h after IPTG/ stationary without exp. before	(stationary IPTG/ exp. before	(1h after IPTG/ exp. before	(3.5h after IPTG/ exp. before	(3.5h after IPTG/ stationary without exp. before	(stationary IPTG/ exp. before	medium/ LB medium)
		IPTG	induction	induction	IPTG	IPTG	induction	induction	IPTG	IPTG	IPTG	IPTG	IPTG	IPTG	IPTG	IPTG	IPTG	IPTG
Uncharacterized proteins (13 proteins)		0.44	0.42	0.45	0.52	0.41	0.44	0.39	0.76	-0.1	0.0	-0.2	0.2	0.1	-0.1	-1.0	0.9	0.1
YhbW	Uncharacterized protein yhbW	0.028	0.028	0.019	0.027	0.049	0.041	0.036	0.047	0.0	-0.6	-0.5	-0.1	-0.3	-0.4	-0.4	-0.1	-0.8
GalF	UTP-glucose-1-phosphate uridylyltransferase	0.00	0.00	0.00	0.00	0.035	0.040	0.027	0.026	0.0	0.0	0.0	0.0	0.2	-0.4	0.1	-0.4	<-5
YbeZ	Putative ATP-binding protein in pho regulon	0.06	0.06	0.11	0.06	0.07	0.10	0.11	0.044	0.0	0.9	0.9	0.0	0.5	0.7	1.3	-0.7	-0.2
YicC	UPF0701 protein yicC	0.036	0.033	0.029	0.042	0.045	0.040	0.028	0.032	-0.1	-0.3	-0.5	0.2	-0.2	-0.7	-0.2	-0.5	-0.3
YajQ	UPF0234 protein yajQ	0.00	0.034	0.00	0.031	0.00	0.00	0.00	0.00	>5	0.0	<-5	>5	0.0	0.0	0.0	0.0	0.0
YbgI	UPF0135 protein ybgI	0.041	0.038	0.049	0.043	0.05	0.09	0.047	0.041	-0.1	0.3	0.2	0.1	0.8	-0.1	0.2	-0.3	-0.3
YjgR	Uncharacterized protein yjgR	0.016	0.011	0.037	0.012	0.012	0.00	0.00	0.024	-0.5	1.2	1.6	-0.4	<-5	<-5	<-5	1.0	0.4
YdcJ	Uncharacterized protein ydcJ	0.08	0.031	0.08	0.039	0.018	0.031	0.022	0.10	-1.4	0.0	1.0	-1.0	0.8	0.3	-2.2	2.5	2.2
YcgB	Uncharacterized protein ycgB	0.00	0.00	0.00	0.028	0.00	0.00	0.00	0.046	0.0	0.0	<-5	>5	0.0	0.0	<-5	>5	0.0
YgaU	Uncharacterized protein ygaU	0.00	0.00	0.00	0.07	0.00	0.00	0.00	0.16	0.0	0.0	<-5	>5	0.0	0.0	<-5	>5	0.0
YfbU	Hypothetical protein	0.08	0.07	0.05	0.09	0.037	0.00	0.00	0.028	-0.2	-0.7	-0.8	0.2	<-5	<-5	<-5	-0.4	1.1
LfiI	Lateral flagellar export/assembly protein LfiI	0.07	0.07	0.032	0.06	0.07	0.07	0.08	0.16	0.0	-1.1	-0.9	-0.2	0.0	0.2	-1.0	1.2	0.0
YhdH	Putative quinone oxidoreductase YhdH	0.031	0.044	0.05	0.026	0.019	0.034	0.035	0.06	0.5	0.7	0.9	-0.3	0.8	0.9	-0.8	1.7	0.7

¹ Name, protein name and Uniprot ID are according to Uniprot database (<http://www.uniprot.org/>). Functional classifications are mostly according to EcoCyc database (<http://ecocyc.org/>). The classifications are confirmed by KEGG database (<http://www.genome.jp/kegg/>).

Suppl. Table 5.3.6 Summary of proteome data of hFGF-2 production in *E. coli* BL21 (DE3) using defined and complex media

Cat. Nr.	Nr.	Name	Defind (DNB) medium				Complex (LB) medium				Log ₂ (Ratio in Defind (DNB) medium)				Log ₂ (Ratio in Complex (LB) medium)				Log ₂ (DNB medium/ LB medium) exp. before
			exp. phase before	1h after IPTG induction	5h after IPTG induction	stationary phase without IPTG	exp. phase before	1h after IPTG induction	3.5h after IPTG induction	stationary phase without IPTG	(1h after IPTG/ exp. before	(5h after IPTG/ exp. before	(5h after IPTG/ stationary without exp. before	(stationary without IPTG/ exp. before	(1h after IPTG/ exp. before	(5h after IPTG/ exp. before	(5h after IPTG/ stationary without exp. before	(stationary without IPTG/ exp. before	
			Whole Cell Protein Mass (WCPM) - %										IPTG)	IPTG)	IPTG)	IPTG)	IPTG)	IPTG)	
I		Carbohydrate Metabolism (51 proteins) Sum 1 ~ 4	13.95	13.17	10.51	13.38	12.39	14.03	12.34	19.63	-0.1	-0.4	-0.3	-0.1	0.2	0.0	-0.7	0.7	0.2
	1	Central carbon metabolism (24 proteins) Sum 1.1 ~ 1.4	6.59	6.61	5.29	7.01	7.36	7.70	6.14	8.26	0.0	-0.3	-0.4	0.1	0.1	-0.3	-0.4	0.2	-0.2
	1.1	Sub-group: Upper glycolysis (5 proteins)	1.26	1.28	0.93	1.50	0.91	0.98	0.75	1.35	0.0	-0.4	-0.7	0.3	0.1	-0.3	-0.8	0.6	0.5
	1.2	Sub-group: Lower glycolysis (to Acetyl-CoA) (11 proteins)	4.21	4.24	3.49	4.28	5.18	5.05	3.95	5.05	0.0	-0.3	-0.3	0.0	0.0	-0.4	-0.4	0.0	-0.3
	1.3	Sub-group: Glycerol metabolism (2 proteins)	0.13	0.06	0.08	0.14	0.15	0.47	0.32	0.29	-1.1	-0.7	-0.8	0.1	1.6	1.1	0.1	1.0	-0.2
	1.4	Sub-group: Pentose phosphate pathway (PPP) (6 proteins)	0.99	1.03	0.79	1.09	1.12	1.21	1.13	1.57	0.1	-0.3	-0.5	0.1	0.1	0.0	-0.5	0.5	-0.2
	2	By-product metabolism (9 proteins)	1.20	1.12	0.89	0.95	1.06	1.13	0.96	2.12	-0.1	-0.4	-0.1	-0.3	0.1	-0.1	-1.1	1.0	0.2
	3	TCA cycle (14 proteins)	5.50	4.84	3.74	4.70	3.61	4.78	4.84	8.42	-0.2	-0.6	-0.3	-0.2	0.4	0.4	-0.8	1.2	0.6
	4	Connection between glycolysis and TCA cycle (4 proteins)	0.67	0.61	0.60	0.72	0.36	0.43	0.40	0.83	-0.1	-0.2	-0.3	0.1	0.3	0.2	-1.1	1.2	0.9
II	5	Oxidative phosphorylation (7 proteins)	2.44	2.31	1.89	2.65	2.53	2.61	2.22	2.39	-0.1	-0.4	-0.5	0.1	0.0	-0.2	-0.1	-0.1	-0.1
III		Synthesis of biomass building blocks (121 proteins): Sum 6 ~ 10	18.76	17.47	16.15	18.95	10.96	11.18	10.55	16.60	-0.1	-0.2	-0.2	0.0	0.0	-0.1	-0.7	0.6	0.8
	6	Amino acid biosynthesis and metabolism (68 proteins). Sum 6.1 ~ 6.2	13.15	12.08	10.89	12.82	5.21	5.62	5.67	10.65	-0.1	-0.3	-0.2	0.0	0.1	0.1	-0.9	1.0	1.3
	6.1	Sub-group: Amino acid biosynthesis (57 proteins)	12.37	11.37	10.17	11.93	4.42	4.60	4.43	6.91	-0.1	-0.3	-0.2	-0.1	0.1	0.0	-0.6	0.6	1.5
	6.2	Sub-group: Amino acid degradation (11 proteins)	0.78	0.71	0.72	0.89	0.79	1.02	1.24	3.74	-0.1	-0.1	-0.3	0.2	0.4	0.7	-1.6	2.2	0.0
	7.1	IMP biosynthesis (for nucleotide) (7 proteins)	1.27	1.23	1.17	1.39	0.59	0.59	0.60	1.00	0.0	-0.1	-0.2	0.1	0.0	0.0	-0.7	0.8	1.1
	7.2	Nucleotide biosynthesis (start from IMP) (13 proteins)	1.53	1.64	1.48	1.87	1.90	1.83	1.59	1.88	0.1	0.0	-0.3	0.3	-0.1	-0.3	-0.2	0.0	-0.3

A-107

Suppl. Table 5.3.6 Summary of proteome data of hFGF-2 production in *E. coli* BL21 (DE3) using defined and complex media

Cat. Nr.	Nr.	Name	Defind (DNB) medium				Complex (LB) medium				Log ₂ (Ratio in Defind (DNB) medium)				Log ₂ (Ratio in Complex (LB) medium)				Log ₂ (DNB medium/ LB medium)
			exp. phase before	1h after IPTG	5h after IPTG	stationary phase without	exp. phase before	1h after IPTG	3.5h after IPTG	stationary phase without	(1h after IPTG/ exp. before	(5h after IPTG/ exp. before	(5h after IPTG/ stationary	(stationary without IPTG/ exp. before	(1h after IPTG/ exp. before	(5h after IPTG/ exp. before	(5h after IPTG/ stationary without	(stationary without IPTG/ exp. before	
			IPTG	induction	induction	IPTG	IPTG	induction	induction	IPTG	IPTG	IPTG	IPTG	IPTG	IPTG	IPTG	IPTG	IPTG	
Whole Cell Protein Mass (WCPM) - %																			
	8	Fatty acid biosynthesis (7 proteins)	1.13	1.09	1.10	1.17	1.62	1.31	1.08	1.12	-0.1	0.0	-0.1	0.1	-0.3	-0.6	-0.1	-0.5	-0.5
	9	Lipopolysaccharide biosynthesis (10 proteins)	0.82	0.55	0.71	0.67	0.91	1.10	0.89	1.00	-0.6	-0.2	0.1	-0.3	0.3	0.0	-0.2	0.1	-0.2
	10	Synthesis of other cellular components (16 proteins)	0.86	0.88	0.81	1.02	0.71	0.74	0.72	0.96	0.0	-0.1	-0.3	0.2	0.1	0.0	-0.4	0.4	0.3
IV	11	(Metabolite) degradation (19 proteins)	1.67	1.46	1.14	1.64	1.52	1.51	1.33	3.45	-0.2	-0.6	-0.5	0.0	0.0	-0.2	-1.4	1.2	0.1
V		Transportation (28 proteins): Sum 12 ~ 14	8.29	8.28	6.86	9.59	7.21	9.59	6.28	10.66	0.0	-0.3	-0.5	0.2	0.4	-0.2	-0.8	0.6	0.2
	12	Sugar transport (7 proteins)	2.05	2.00	1.43	2.92	1.37	1.77	1.37	4.17	0.0	-0.5	-1.0	0.5	0.4	0.0	-1.6	1.6	0.6
	13	Amino acid and peptide transport (7 proteins)	0.79	0.78	0.50	1.00	0.26	0.29	0.35	1.45	0.0	-0.7	-1.0	0.3	0.2	0.4	-2.1	2.5	1.6
	14	Other transport proteins (14 proteins)	5.45	5.51	4.93	5.66	5.58	7.53	4.56	5.04	0.0	-0.1	-0.2	0.1	0.4	-0.3	-0.1	-0.1	0.0
VI		Transcription and translation (66 proteins): Sum 15 ~ 22	16.51	18.02	18.25	17.88	22.43	23.18	20.91	17.31	0.1	0.1	0.0	0.1	0.0	-0.1	0.3	-0.4	-0.4
	15	RNA polymerases (3 proteins)	1.06	1.00	1.06	0.88	1.36	1.20	1.00	0.80	-0.1	0.0	0.3	-0.3	-0.2	-0.4	0.3	-0.8	-0.4
	16	RNA polymerase binding proteins (7 proteins)	0.83	0.91	0.87	0.88	1.24	1.07	1.04	0.77	0.1	0.1	0.0	0.1	-0.2	-0.3	0.4	-0.7	-0.6
	17	Transcription factors (12 proteins)	1.78	1.84	1.74	1.79	1.65	1.69	1.68	2.03	0.0	0.0	0.0	0.0	0.0	0.0	-0.3	0.3	0.1
	18	Ribosomal proteins (5 proteins)	3.55	3.78	4.32	3.76	5.41	4.75	4.47	2.74	0.1	0.3	0.2	0.1	-0.2	-0.3	0.7	-1.0	-0.6
	19	Ribosome-associated proteins (8 proteins)	1.05	1.16	1.16	1.56	1.67	1.71	1.37	1.20	0.1	0.1	-0.4	0.6	0.0	-0.3	0.2	-0.5	-0.7
	20	Aminoacyl-tRNA synthetases (23 proteins)	2.80	2.75	3.04	2.49	3.69	3.67	3.35	3.06	0.0	0.1	0.3	-0.2	0.0	-0.1	0.1	-0.3	-0.4
	21	Elongation factors (6 proteins)	4.93	6.01	5.55	6.09	6.74	8.11	7.35	6.17	0.3	0.2	-0.1	0.3	0.3	0.1	0.3	-0.1	-0.5

Suppl. Table 5.3.6 Summary of proteome data of hFGF-2 production in *E. coli* BL21 (DE3) using defined and complex media

Cat. Nr.	Nr.	Name	Defind (DNB) medium				Complex (LB) medium				Log ₂ (Ratio in Defind (DNB) medium)				Log ₂ (Ratio in Complex (LB) medium)				Log ₂ (DNB medium/ LB medium) exp. before
			exp. phase before	1h after IPTG induction	5h after IPTG induction	stationary phase without IPTG	exp. phase before	1h after IPTG induction	3.5h after IPTG induction	stationary phase without IPTG	(1h after IPTG/ exp. before	(5h after IPTG/ exp. before	(5h after IPTG/ stationary without exp. before	(stationary without exp. before	(1h after IPTG/ exp. before	(5h after IPTG/ exp. before	(5h after IPTG/ stationary without exp. before	(stationary without exp. before	
			Whole Cell Protein Mass (WCPM) - %										IPTG)	IPTG)	IPTG)	IPTG)	IPTG)	IPTG)	
	22	RNA degradation (3 proteins)	0.52	0.56	0.51	0.42	0.68	0.98	0.64	0.53	0.1	0.0	0.3	-0.3	0.5	-0.1	0.3	-0.4	-0.4
VII		Protein folding and degradation (28 proteins): Sum 23 ~ 25	3.54	4.27	7.09	3.57	4.50	7.76	9.05	4.99	0.3	1.0	1.0	0.0	0.8	1.0	0.9	0.1	-0.3
	23	Isomerases (5 proteins)	0.72	0.79	0.62	0.80	0.55	0.56	0.38	0.86	0.1	-0.2	-0.4	0.2	0.0	-0.5	-1.2	0.6	0.4
	24	Chaperones (9 proteins)	1.94	2.63	5.46	1.95	2.92	5.92	7.12	2.75	0.4	1.5	1.5	0.0	1.0	1.3	1.4	-0.1	-0.6
	25	Proteases (13 proteins)	0.88	0.85	1.01	0.83	1.03	1.28	1.55	1.38	-0.1	0.2	0.3	-0.1	0.3	0.6	0.2	0.4	-0.2
VIII		Cell redox balance (22 proteins): Sum 26.1 ~ 26.3	2.35	2.46	2.26	3.32	1.78	1.95	1.81	3.50	0.1	-0.1	-0.6	0.5	0.1	0.0	-1.0	1.0	0.4
	26.1	Other dehydrogenases (9 proteins)	0.69	0.66	0.66	0.75	0.61	0.74	0.67	1.13	-0.1	-0.1	-0.2	0.1	0.3	0.1	-0.8	0.9	0.2
	26.2	Oxidoreductases (8 proteins)	0.39	0.36	0.43	0.65	0.34	0.34	0.38	0.54	-0.1	0.1	-0.6	0.7	0.0	0.2	-0.5	0.7	0.2
	26.3	Hydroperoxide reductases and superoxide dismutase (5 proteins)	1.26	1.45	1.17	1.92	0.83	0.88	0.75	1.83	0.2	-0.1	-0.7	0.6	0.1	-0.1	-1.3	1.1	0.6
IX	27	DNA protection and repair (6 proteins)	0.83	0.86	0.58	0.84	0.51	0.27	0.36	1.29	0.1	-0.5	-0.5	0.0	-0.9	-0.5	-1.8	1.3	0.7
X	28	Unclassified proteins (7 proteins)	0.63	0.57	0.53	0.59	0.46	0.36	0.39	0.36	-0.1	-0.2	-0.2	-0.1	-0.4	-0.2	0.1	-0.4	0.5
XI	29	Uncharacterized proteins (13 proteins)	0.44	0.42	0.45	0.52	0.41	0.44	0.39	0.76	-0.1	0.0	-0.2	0.2	0.1	-0.1	-1.0	0.9	0.1

A-109

5.3.3 Suppl. Methods - Determination of NADPH turn-over involved in amino acid biosynthesis

Starting from a genome-scale reconstruction of the metabolic network of *E. coli* [1] flux balance analysis [2] was used to compute a flux distribution that maximizes growth yield in the given conditions (constraints were set as described before [1]). To determine the relative cellular NADPH production that is oxidized in amino acid metabolism, we first determined the total NADPH turnover, $NADPH_{tot}$, by summing across all reactions with non-zero flux, the flux of the reaction multiplied with the molar amount of NADPH consumed by this reaction. For $NADPH_{tot}$ we obtained a value of $12.27 \text{ mmol h}^{-1} \text{ g}^{-1} \text{ DCW}$ (Dry Cell Weight). Second, we calculated the amount of NADPH oxidized in amino acid metabolism, $NADPH_{aa}$, by performing the same calculations but only summing up reactions annotated as belonging to amino acid metabolism. For $NADPH_{aa}$ we obtained a value of $10.08 \text{ mmol h}^{-1} \text{ g}^{-1} \text{ DCW}$. To take into account reducing equivalents in terms of NADH produced during amino acid biosynthesis, we calculated the level of NADH produced during amino acid biosynthesis, $NADH_{paa}$, which is $1.84 \text{ mmol h}^{-1} \text{ g}^{-1} \text{ DCW}$. Subsequently, we determined the relative fraction of reducing equivalent consumed in amino acid metabolism through the following equation:

$$\frac{\text{Reducing Equivalent}_{aa}}{\text{Reducing Equivalent}_{tot}} = \frac{NADPH_{aa} - NADH_{paa}}{NADPH_{tot} - NADH_{paa}} = \frac{10.08 - 1.84}{12.27 - 1.84} = 79\%$$

References:

1. Feist, A. M., Henry, C. S., Reed, J. L., Krummenacker, M., Joyce, A. R., Karp, P. D., Broadbelt, L. J., Hatzimanikatis, V., and Palsson, B. O. (2007) A genome-scale metabolic reconstruction for *Escherichia coli* K-12 MG1655 that accounts for 1260 ORFs and thermodynamic information. *Mol Syst Biol* 3, 121.
2. Orth, J. D., Thiele, I., and Palsson, B. O. (2010) What is flux balance analysis? *Nat Biotechnol* 28, 245-248.

* The calculation was carried out by Dr. Christoph Kaleta: Friedrich Schiller University of Jena, School of Biology and Pharmaceutics, Department of Bioinformatics and Research Group Theoretical Systems Biology, Jena, Germany

5.4 Chemicals

Chemicals, commercial buffers, kits and other materials used in current study are listed in Suppl. Tables 5.4.1 and 5.4.2

Suppl. Table 5.4.1 Chemicals

Name	Chemical	MW:	Manufacturer	Country
Acetic acid	CH ₃ COOH	60.05	Carl Roth GmbH + Co. KG.	Germany
Acetonitrile	CH ₃ CN	41.05	Carl Roth GmbH + Co. KG.	Germany
Acrylamide and bisacrylamide stock solution	Rotiphorese® Gel 30 (37,5:1)		Carl Roth GmbH + Co. KG.	Germany
Agar	Bacto™ Agar		Becton, Dickinson and Company (BD)	USA
Agarose	Biozym LE GP Agarose		Biozym Scientific GmbH	Germany
Ammonium hydrogen carbonate	NH ₄ HCO ₃	79.06	Merck KGaA	Germany
Ammonium persulfate	(NH ₄) ₂ S ₂ O ₈	228.2	Sigma-Aldrich Laborchemikalien GmbH	Germany
Ammonium phosphate dibasic	(NH ₄) ₂ HPO ₄	132.06	Sigma-Aldrich Laborchemikalien GmbH	Germany
ammonium phosphate monobasic	NH ₄ H ₂ PO ₄	115.02	Merck KGaA	Germany
Ammonium sulfate	(NH ₄) ₂ SO ₄	132.14	Carl Roth GmbH + Co. KG.	Germany
Boric acid	H ₃ BO ₃	61.83	Merck KGaA	Germany
Bromophenol Blue	C ₁₉ H ₁₀ Br ₄ O ₅ S 3',3'',5',5''-Tetrabromophenolsulfonephthalein	669.96	Sigma-Aldrich Laborchemikalien GmbH	Germany
CHAPS	C ₃₂ H ₅₈ N ₂ O ₇ S 3-((3-Cholamidopropyl)-dimethylammonio)-1-propane-sulfonate	614.89	Biomol GmbH	Germany
Citric acid monohydrate	C ₆ H ₈ O ₇ · H ₂ O	210.14	Sigma-Aldrich Laborchemikalien GmbH	Germany
Cobalt(II) chloride hexahydrate	CoCl ₂ · 6H ₂ O	237.9	Merck KGaA	Germany
Coomassie Blue G250	C ₄₇ H ₅₀ N ₃ NaO ₇ S ₂ Coomassie Brilliant Blue G-250	854.02	Merck KGaA	Germany
Copper(II) chloride dihydrate	CuCl ₂ · 2H ₂ O	170.48	Sigma-Aldrich Laborchemikalien GmbH	Germany
DTT	C ₄ H ₁₀ O ₂ S ₂ DL-Dithiothreitol	154.25	Fermentas GmbH	Germany
Ethanol	C ₂ H ₆ O Ethanol (96%)	46.07	Merck KGaA	Germany
Fe(III) Citrate	FeC ₆ H ₅ O ₇	244.94	Sigma-Aldrich Laborchemikalien GmbH	Germany
Formic acid	HCOOH	46.03	J.T.Baker Chemical Company	USA
Glucose monohydrate	C ₆ H ₁₂ O ₆ · 2H ₂ O D-(+)-Glucose monohydrate	198.17	Sigma-Aldrich Laborchemikalien GmbH	Germany
Glycerol	C ₃ H ₈ O ₃ Glycerol (86%)	92.1	Carl Roth GmbH + Co. KG.	Germany
Glycine	C ₂ H ₅ NO ₂	75.07	Carl Roth GmbH + Co. KG.	Germany
Iodoacetamide	ICH ₂ CONH ₂	184.96	GE Healthcare	United Kingdom
IPG Buffer pH 3-10 NL			GE Healthcare	United Kingdom

Appendix

Name	Chemical	MW:	Manufacturer	Country
IPG strip pH 3-10 NL	Immobiline DryStrip pH 3-10 NL, 18 cm		GE Healthcare	United Kingdom
Magnesium sulfate heptahydrate	MgSO ₄ 7H ₂ O	246.47	Carl Roth GmbH + Co. KG.	Germany
Manganese(II) chloride tetrahydrate	MnCl ₂ 4H ₂ O	197.91	Merck KGaA	Germany
Methanol	CH ₃ OH	32.04	Carl Roth GmbH + Co. KG.	Germany
Phosphoric acid	H ₃ PO ₄ (85%)	98	Carl Roth GmbH + Co. KG.	Germany
Potassium phosphate dibasic	K ₂ HPO ₄	174.18	Carl Roth GmbH + Co. KG.	Germany
Potassium phosphate monobasic	KH ₂ PO ₄	136.09	Carl Roth GmbH + Co. KG.	Germany
SDS	NaC ₁₂ H ₂₅ SO ₄ Sodium Dodecyl Sulfate	288.38	Bio-Rad Laboratories GmbH	Germany
Sodium chloride	NaCl	58.44	Carl Roth GmbH + Co. KG.	Germany
Sodium molybdate dihydrate	Na ₂ MoO ₄ 2H ₂ O	241.95	Merck KGaA	Germany
TEMED	C ₆ H ₁₆ N ₂ N,N,N',N'-Tetramethylethylenediamine	116.2	Sigma-Aldrich Laborchemikalien GmbH	Germany
TFA	C ₂ HF ₃ O ₂ Trifluoroacetic acid	114.02	Merck KGaA	Germany
Thiourea	CH ₄ N ₂ S Thiocarbamide	76.12	Sigma-Aldrich Laborchemikalien GmbH	Germany
Titriplex III	C ₁₀ H ₁₄ N ₂ Na ₂ O ₈ 2H ₂ O Ethylenedinitrilotetraacetic acid disodium salt dihydrate	372.24	Merck KGaA	Germany
TRIS	NH ₂ C(CH ₂ OH) ₃ Tris(hydroxymethyl)aminomethane	121.14	Molekula GmbH	Germany
Tryptone	BactoTM Tryptone		Becton, Dickinson and Company (BD)	USA
Urea	NH ₂ CONH ₂ Carbamide	60.06	Sigma-Aldrich Laborchemikalien GmbH	Germany
Yeast Extract	BactoTM Yeast Extract		Becton, Dickinson and Company (BD)	USA
Zinc acetate dihydrate	Zn(CH ₃ COO) ₂ 2H ₂ O	219.51	Merck KGaA	Germany
α -Cyano-4-hydroxycinnamic acid		189.17	Sigma-Aldrich Laborchemikalien GmbH	Germany

Suppl. Table 5.4.2 Commercial buffers, kits and other materials

Chemical	Annotation	Manufacturer	Country
Acetic Acid kit	Acetate Kinase Manual Format	Megazyme International Ireland	Ireland
Benzonase	250 U/ μ L (>99% purity)	Merck KGaA	Germany
BugBuster	BugBuster [®] Protein Extraction Reagent	Novagen (Merck KGaA)	Germany
IPG Buffer pH 3-10 NL		GE Healthcare	United Kingdom
IPG strip pH 3-10 NL	Immobiline DryStrip pH 3-10 NL, 18 cm	GE Healthcare	United Kingdom
rLysozyme	27–33 KU/ μ L	Novagen (Merck KGaA)	Germany
Trypsin	Sequencing grade modified trypsin	Promega Corporation	USA
Ziptips _{C18}		Millipore Corporation	USA
PAC target	Prespotted AnchorChip target	Bruker Daltonik GmbH	Germany

5.5 List of Abbreviations

Abbreviations of identified protein are given in Suppl. Table 5.3.1 or 5.3.5.

Abbreviation	Full name
2D gel	Two-Dimensional Gel
Acetyl-CoA	Acetyl Coenzyme A
ATP	Adenosine Triphosphate
C _(CAM)	Carbamidomethyl Cysteine
cAMP	Cyclic Adenosine Monophosphate
CMPs	Central Metabolic Pathways
Cra	Catabolite repressor activator
CRP	cAMP Receptor Protein
DAB	Defined Autoinduction Broth
DCM	Cell Dry Mass
DNB	Defined Non-inducing Broth
EIICB ^{Glc}	Membrane-bound subunit of the glucosespecific PTS transporter encoded by ptsG
Exp.	Exponential
F1P	Fructose-1-Phosphate
FBP	Fructose-1,6-Bisphosphate
GFP	Green Fluorescent Protein
GlcNAc	N-Acetylglucosamine
GlcNAc-6-P	N-Acetylglucosamine-6-Phosphate
GST	Glutathion-S-Transferase
hFGF-2	Human Basic Fibroblast Growth Factor
His	Histidine
HNC	High Nitrogen Content
IEF	Isoelectric Focusing
IMP	Inosine Monophosphate
IPG	Immobiline DryStrip Gel
IPTG	Isopropyl β -D-1-Thiogalactopyranoside
LB	Luria Bertani
L-DNB	Labeling Defined Non-inducing Broth
LPS	Lipopolysaccharides
MALDI-TOF MS	Matrix-Assisted Laser Desorption Ionization Time-Of-Flight Mass Spectrometry
Met	Methionine
Met _{ox}	Oxidized Methionine
Mlc	Making Large Colonies
MW	Molecular Weight
NADH	Nicotinamide Adenine Dinucleotide
NADPH	Nicotinamide Adenine Dinucleotide Phosphate
NagC	N-Acetylglucosamine Repressor
NMR	Nuclear Magnetic Resonance
P-ArcA	Phosphorylated-ArcA
PEP	Phosphoenolpyruvate

Appendix

Abbreviation	Full name
PPP	Pentose Phosphate Pathway
PTS	Phosphotransferase System
rL-DNB	Reduced Labeling-Defined Non-inducing Broth
RNAP	RNA polymerase
RNAP	RNA Polymerase
ROS	Reactive Oxygen Species
S-DAB	Smart-Defined Autoinduction Broth
SDS-PAGE	Sodium Dodecyl Sulfate PolyAcrylamide Gel Electrophoresis
Se-Met	Selenomethionine
SL-DAB	Smart Labeling-Defined Autoinduction Broth
TAL	Transaldolase
TB	Terrific-Broth
TCA cycle	Tricarboxylic Acid Cycle
TKT	Transketolase
WCPM	Whole Cell Protein Mass

Curriculum Vitae

Personal information

First Name: Zhaopeng
Family Name: Li
Nationality: P.R. China
Sex: Male
Birth date: September 2, 1980

Working Experience

October 2008 – June 2012: Scientific assistant
Institut für Technische Chemie (Hannover, Germany).
Helmholtz Centre for Infection Research (Brunswick, Germany).
April 2006 - September 2008: Project manager
Beijing Sunbio Biotech Co., Ltd (Beijing, China)

Education

October 2008 - June 2012: PhD study of Chemistry – Life science
Leibniz Universität Hannover (Germany)
Thesis: Metabolic balance during protein production with recombinant *E. coli*.
September 2003 - June 2006: Master study of Biochemical Engineering
Beijing University of Chemical Technology (China)
Thesis: The expression of foreign protein in recombinant strains high cell density culture.
September 1999 - June 2003: Bachelor study of Bioengineering
Beijing University of Chemical Technology (China)
Thesis: Production of lipase using a strain of *Candida* sp.
September 1996 - June 1999
Beijing Bayi Middle School

Publications

PhD study of Chemistry

Institut für Technische Chemie (Hannover, Germany)

Helmholtz Centre for Infection Research (Brunswick, Germany).

Journal Articles (Peer-Reviewed)

Zhaopeng Li, Manfred Nimtz, Ursula Rinas. Optimized procedure to generate heavy isotope and selenomethionine-labeled proteins for structure determination using *Escherichia coli*-based expression systems, *Appl Microbiol Biotechnol*, 2011, 92(4), 823-833

Zhaopeng Li, Wolfgang Kessler, Joop van den Heuvel, Ursula Rinas. Simple defined autoinduction medium for high-level recombinant protein production using T7-based *Escherichia coli* expression systems, *Appl Microbiol Biotechnol*, 2011, 91(4), 1203-1213

Presentation and Poster

PEGS Europe (Hannover 2011)

Presentation:

Zhaopeng Li, Ursula Rinas. Novel defined modular media to produce recombinant proteins with *E. coli* T7 expression system

6th Conference on recombinant protein production (Vienna 2011)

Poster:

Zhaopeng Li, Manfred Nimtz, Ursula Rinas. Optimized procedure to generate heavy isotope and seleno-methionine labeled proteins for structure determination using *E. coli* based expression systems

Zhaopeng Li, Wolfgang Kessler, Joop van den Heuvel, Ursula Rinas. Simple defined autoinduction medium for recombinant protein production in *E. coli* T7 expression system